JPL NO. 9950-610

DOE/JPL 954888-80/12

DRD NO. SE-9
DRL NO. 60

DISTRIBUTION CATEGORY UC-63
DECEMBER, 1980

CONTINUOUS CZOCHRALSKI GROWTH

SILICON SHEET GROWTH DEVELOPMENT OF THE LARGE AREA SHEET TASK OF THE LOW COST SILICON SOLAR ARRAY PROJECT

FINAL REPORT

FOR PERIOD COVERING
1 OCTOBER, 1977 THROUGH 31 MARCH, 1980

PREPARED BY
C. MOODY JOHNSON

KAYEX CORPORATION
1000 MILLSTEAD WAY
ROCHESTER, NEW YORK 14624

"The JPL Low Cost Silicon Solar Array Project is sponsored by the U.S. Department of Energy and forms part of the Solar Photovoltaic Conversion Program to initiate a major effort toward the development of low cost solar arrays. This work was performed for the Jet Propulsion Laboratory, California Institute of Technology, by agreement between NASA and DOE."

ABSTRACT

The production of low-cost silicon capable of being processed into solar cells yielding efficiencies of 14% AM1 is an essential requirement of the JPL/DOE Low-Cost Solar Array (LSA) Project. Kayex has developed a process for Czochralski-type crystal growth that significantly reduces the major cost item (other than the silicon itself) involved in state of the art Czochralski growth - the quartz crucible. The new technology generated under this contract can decrease the add-on cost for silicon production from at least $51/kg (present state of the art) to $16.14/kg (CZ #3). This translates into an add-on cost of $0.25/pk watt[1] if the JPL/DOE goal of $14/kg is assumed for the polysilicon material used for the growth of crystal ingots.

Conclusions and technology status are reported for both phases of the contract which had the following objectives:

- The growth of 100 kg of silicon single crystal material of ten (10) cm in diameter or greater, utilizing one common silicon container material (one crucible).[2]
- The growth of 150 kg of silicon single crystal material of fifteen (15) cm in diameter, utilizing one common silicon container material (one crucible).[3]

The objectives of the project included:

(a) Developing a new technology concept that would allow a Hamco CG2000 crystal grower to be recharged with a new supply of polysilicon material while still under vacuum and at temperatures above the melting point of silicon.

(b) Modifying the Hamco CG2000 crystal grower to

1) accept large polysilicon charges - up to 30 kg

2) grow large crystal ingots (to 15 cm diameter and 25 kg in weight)

3) hold polysilicon material for recharging (rod or lump) while, at the same time, growing crystal ingots.

(c) Designing special equipment to

1) recharge polysilicon rods

2) recharge polysilicon lumps

3) handle and store large, hot silicon crystal ingots.

(d) Developing a new process and procedure for growing silicon crystal ingots and recharging polysilicon material without contaminating the furnace or breaking the silicon container material (crucible).

During the last two and one-half years, many continuous crystal growth runs have been performed. These runs have lasted as long as 109 hours and produced as many as ten (10) crystal ingots. Crystal sizes have reached 15 cm with weights progressing to 27 kg.

The final phase of the program culminated in two 150 kg continuous runs being achieved by the growth of six (6) 25 kg ingots from one crucible.

ACKNOWLEDGEMENTS

The author wishes to acknowledge and express his appreciation to the numerous individuals who contributed to this report.

Special thanks goes to E. Roberts, the Project's Principal Investigator, who provided valuable comments, criticism and proofing during the writing of this report. Special thanks also goes to Dr. R. L. Lane, the Project's Program Manager, who provided information necessary to write this report and valuable advice during the writing of this report. I would also like to thank B. Bezio for proof reading the final manuscript and helping to correct errors in the manuscript.

I would also like to recognize some of the individuals who were instrumental to the operation and completion of this project:

N. Sarno	-	Head Process Engineer
D. Fanale	-	Equipment Engineer
F. Merz	-	Project Engineer
D. Rakover	-	Process Engineer

TABLE OF CONTENTS

	PAGE NO.
ABSTRACT	iii
ACKNOWLEDGEMENTS	iv
1.0 INTRODUCTION	1
1.1 BACKGROUND	1
1.2 SCOPE OF WORK PERFORMED DURING CONTRACT	3
2.0 SUMMARY AND CONCLUSIONS	13
2.1 EQUIPMENT DESIGN	13
2.2 PROCESS DEVELOPMENT	27
2.2.1 STATE OF THE ART SILICON CRYSTAL GROWTH	27
2.2.2 HOT FILL EXPERIMENTS	28
2.2.3 INITIAL RECHARGING EXPERIMENTS	29
2.2.4 100 KILOGRAM CONTINUOUS RECHARGE RUNS	34
2.2.5 150 KILOGRAM CONTINUOUS RECHARGE RUNS	37
2.3 ECONOMIC ANALYSIS DEVELOPMENT	46
2.4 SOLAR CELL RESULTS AND EVALUATION	52
2.5 PROPOSED FUTURE WORK	57
3.0 GROWTH FACILITY DESIGN, CONSTRUCTION AND MODIFICATION	58
3.1 DESIGN CHANGES AND MODIFICATIONS NECESSARY FOR RECHARGING	59
3.1.1 ISOLATION VALVE	60
3.1.2 ENLARGED PULL CHAMBER	65
3.1.3 AUTOMATIC DIAMETER CONTROL (ADC) OPTICAL SYSTEM	67
3.1.4 POLY WEIGHT/RECHARGE SYSTEM	72
3.1.5 DOPANT REPLENISHING FIXTURE	77
3.2 SPECIAL EQUIPMENT FOR HANDLING OF HOT CRYSTAL INGOTS	79
3.2.1 CRYSTAL/POLY TRANSFER DEVICE	79
3.2.2 CRYSTAL/POLY STORAGE RACK	79
3.3 DESIGN CHANGES AND MODIFICATIONS FOR THE GROWTH OF LARGE DIAMETER, HIGH WEIGHT CRYSTALS	81
3.3.1 14-INCH HOT ZONE	82
3.4 SPECIAL EQUIPMENT DESIGNED FOR RECHARGING POLY SILICON	83
3.4.1 POLY ROD ATTACHMENT DEVICE	83
3.4.2 LUMP RECHARGING DEVICE	83
4.0 PROCESS RESEARCH AND DEVELOPMENT PROGRAM	87
4.1 VARIATIONS IN "STATE OF THE ART" CZOCHRALSKI CRYSTAL GROWTH PROCESS	87

TABLE OF CONTENTS (Cont'd)

	PAGE NO.
4.2 HOT FILL EXPERIMENTS	89
4.2.1 VIRGIN POLYCRYSTALLINE RODS	89
4.3 RECHARGING WITH POLYCRYSTALLINE RODS	95
4.3.1 RECHARGING PROCEDURE	95
4.3.2 ADVANTAGES AND DISADVANTAGES	95
4.3.3 STATISTICAL DATA (INCLUDING CONTINUOUS RUNS)	98
4.3.4 PLANS AND RECOMMENDATIONS	107
4.4 RECHARGING WITH POLYCRYSTALLINE LUMPS	108
4.4.1 RECHARGE PROCEDURE	108
4.4.2 ADVANTAGES AND DISADVANTAGES	108
4.4.3 STATISTICAL DATA (INCLUDING CONTINUOUS RUNS)	110
4.4.4 PLANS AND RECOMMENDATIONS	152
4.5 CRYSTAL GROWTH DEVELOPMENT	153
4.5.1 INGOT SIZE (4"-5"-6")	153
4.5.2 GROWTH RATE	155
4.5.3 CRYSTAL QUALITY	158
4.5.4 CRUCIBLE PERFORMANCE	176
5.0 CHARACTERIZATION DATA AND ANALYSIS	202
5.1 SOLAR CELL DATA	202
5.1.1 SINGLE CRYSTAL VS. POLYCRYSTALLINE SILICON	203
5.1.2 SOLAR CELL EFFICIENCY PERFORMANCE AS A FUNCTION OF TOTAL AMOUNT GROWN DURING A CONTINUOUS RECHARGE RUN	230
5.1.3 SOLAR CELL EFFICIENCY PERFORMANCE AS A FUNCTION OF GROWTH TIME INTO A CONTINUOUS RECHARGE RUN	230
5.1.4 SOLAR CELL EFFICIENCY PERFORMANCE AS A FUNCTION OF CRYSTAL LOCATION	232
5.2 IMPURITY ANALYSIS DATA	237
5.2.1 CRYSTAL INGOTS	247
5.2.2 CRUCIBLE SAMPLES	248
5.2.3 PLANS AND RECOMMENDATIONS	248
6.0 ECONOMIC ANALYSIS AND MODEL	249
6.1 SUMMARY OF COST PROJECTIONS	250
6.2 COST COMPONENTS OF CONVENTIONAL CZ GROWTH VS. CZ NO. 3*	266
7.0 REFERENCES	275
APPENDIX A STRUCTURE LOSS IN CZ SILICON CRYSTAL GROWTH	A-1
APPENDIX B COMPARISON OF LUMP VS. ROD RECHARGING	B-1

ILLUSTRATIONS

FIGURE NO.		PAGE NO.
1	OLD CG2000	14
2	REDESIGNED CG2000 FOR JPL PROJECT	15
3	FLOW DIAGRAM OF CONTINUOUS CZ	16
4	ADC OPTICAL SYSTEM	18
5	POLY ATTACHING DEVICE	20
6	DOPANT FIXTURE	21
7	CRYSTAL/POLY TRANSFER DEVICE SCHEMATIC	22
8	CRYSTAL/POLY TRANSFER DEVICE WITH CRYSTAL	23
9	TRANSFER DEVICE - LOADING STORAGE RACK	24
10	SCHEMATIC - LUMP RECHARGE DEVICE	25
11	PHOTOGRAPH - LUMP RECHARGE DEVICE	26
12	JPL CONTINUOUS GROWTH FACILITY	32
13	150 MM DIAMETER CRYSTAL RUN NO. 51	39
14	CRYSTAL FROM RUN NO. 63	40
15	CRYSTALS FROM RUN NO. 70	43
16	CRYSTALS FROM RUN NO. 72	45
17	COST EFFECTS - MULTIPLE CRYSTAL GROWTH FROM ONE CRUCIBLE	49
18	HAMCO/JPL FACILITY - INITIAL INSTALLATION	61
19	SCHEMATIC - CRYSTAL GROWER RECHARGE MODE WITH ROD	62
20a	DRAWING - VALVE PLATE ASSEMBLY (ISOLATION VALVE)	63
20b	DRAWING - VALVE PLATE ASSEMBLY (ISOLATION VALVE)	64
21	ISOLATION VALVE - ON GROWER	65
22	ENLARGED PULL CHAMBER	66
23	ADC OPTICAL SYSTEM	68
24	ADC OPTICAL SYSTEM	69
25	ADC OPTICAL SYSTEM	70
26	ADC OPTICAL SYSTEM	71
27	POLYSILICON ROD READY FOR RECHARGING	74
28	POLYSILICON ROD AFTER RECHARGING	75
29	DRAWING - POLY WEIGHT/RECHARGE DEVICE	76
30	SCHEMATIC - CRYSTAL/POLY STORAGE RACK	80
31	SEED LIFT MECHANISM	81a
32	SCHEMATIC - POLY CHUNK RECHARGE SYSTEM - RECHARGE MODE	85
33	CRYSTAL WEIGHT AND LENGTH VS. TIME - RUN NO. 5	91

ILLUSTRATIONS (Cont'd)

FIGURE NO.		PAGE NO.
34	22 KG CRYSTAL GROWN BY HOT FILLING TECHNIQUE - RUN NO. 5	92
35	POWER CONSUMPTION - RUN NO. 5	93
36	CRYSTAL INGOTS GROWN DURING RUN NO. 60	133
37	CRYSTAL INGOTS GROWN DURING RUN NO. 62	135
38	GRAPH - KILOGRAMS GROWN VS. TIME (RUN NO. 62)	137
39	INGOT DIAMETER PROGRESSION - 4"-5"-6"	156
40	RGA CHART SECTION - RUN NO. 70	164
41	CARBON MONOXIDE CONCENTRATION VS. TIME - RUN NO. 8	167
42	CARBON MONOXIDE CONCENTRATION VS. TIME - RUN NO. 9	168
43	CARBON MONOXIDE CONCENTRATION VS. TIME - RUN NO. 14	169
44	CRUCIBLE DEVITRIFICATION - 18 HOUR RUN	177
45	CRUCIBLE DEVITRIFICATION - SEVERE	178
46	CRUCIBLE DEVITRIFICATION - TYPICAL RECHARGE RUN	179
47	SEVERE CRUCIBLE DEVITRIFICATION	184
48	SEVERE CRUCIBLE DEVITRIFICATION (CLOSE-UP)	184
49	CRUCIBLE USED FOR RUN NO. 47 (OUTSIDE SURFACE)	186
50	CRUCIBLE USED FOR RUN NO. 47 (INSIDE SURFACE)	187
51	CRUCIBLE USED FOR RUN NO. 49	188
52	CRUCIBLE USED FOR RUN NO. 2*	189
53	SOLAR EFFICIENCY VS. KILOGRAMS GROWN - RUN NO. 30	222
54	SOLAR EFFICIENCY VS. KILOGRAMS GROWN - RUN NO. 47	223
55	SOLAR EFFICIENCY VS. KILOGRAMS GROWN - RUN NO. 49	224
56	SOLAR EFFICIENCY VS. KILOGRAMS GROWN - RUN NO. 55	225
57	SOLAR EFFICIENCY VS. KILOGRAMS GROWN _ RUN NO. 2*	226
58	SOLAR EFFICIENCY VS. KILOGRAMS GROWN - RUN NO. 60	227
59	SOLAR EFFICIENCY VS. KILOGRAMS GROWN - RUN NO. 62	228
60	ADD-ON COST VS. GROWTH RATE - CZ NO. 1	261

TABLES

TABLE NO.		PAGE NO.
1	CUMULATIVE RECHARGE RUNS - PRESENTED AT THE 15TH PROJECT INTEGRATION MEETING APRIL 1, 1980	6
2	CZ GROWTH METHODS - CZ NO. 1 AND CZ NO. 2	7
3	SOLAR CELL RESULTS FOR CONTINUOUS RUNS	9
4	COMPOSITE OF RECHARCE AND INGOT GROWTH TIMES FOR 100 KG RUNS	38
5	RUN NO. 63	41
6	SAMICS ANALYSIS OF FOUR METHODS OF CONTINUOUS CZ (DECEMBER, 1978)	48
7	CONDENSED SOLAR CELL EFFICIENCY RESULTS	55, 56
8	SUMMARY OF TWO-MELT RUN (NO. 9)	100
9	SUMMARY OF THREE-MELT RUN (NO. 11)	101
10	SUMMARY - RUNS NO. 19, 21 AND 22	106
11	SUMMARY OF INGOT PRODUCTION - RUN NO. 30	111
12	RUN NO. 30 - SUMMARY	112
13	RECHARGE AND INGOT GROWTH TIME (RUN NO. 30)	114
14	RECHARGE INFORMATION - RUN NO. 41	116
15	RUN NO. 41 - SUMMARY	118
16	RUN NO. 47 - SUMMARY	118
17	RECHARGE AND INGOT GROWTH TIME - RUN NO. 47	119
18	RUN NO. 49 - SUMMARY	122
19	RECHARGE AND INGOT GROWTH TIME - RUN NO. 49	123
20	RUNS NO. 55 AND 2* - SUMMARY	126
21	RECHARGE AND INGOT GROWTH TIME - RUN NO. 55	128
22	RECHARGE AND INGOT GROWTH TIME - RUN NO. 2*	129
23	SUMMARY OF RUNS NO. 60 AND NO. 62	132
24	RECHARGE AND INGOT GROWTH TIME - RUN NO. 60	138
25	RECHARGE AND INGOT GROWTH TIME - RUN NO. 62	139
26	COMPOSITE RECHARGE AND INGOT GROWTH TIME	141
27	RUN NO. 63 - SUMMARY	143
28	RUN NO. 70 - SUMMARY	146
29	RECHARGE AND INGOT GROWTH TIME - RUN NO. 70	147

TABLES (Cont'd)

TABLE NO.		PAGE NO.
30	RUN NO. 72 - SUMMARY	150
31	RECHARGE AND INGOT GROWTH TIME - RUN NO. 72	151
32	IMPURITY LEVELS OF QUARTZ VS. SAND CRUCIBLE	180
33	FUSED QUARTZ CRUCIBLE IMPURITIES	191
34	IMPURITY CONCENTRATIONS (CRUCIBLE SAMPLES, ETC.)	194
35	IMPURITY CONCENTRATIONS (COMPLETE)	195 - 197
36	IMPURITY ANALYSIS RESULTS PERFORMED BY QUARTZ PRODUCTS INC.	198
37	SOLAR CELL ELECTRICAL DATA	204 - 221
38	RESISTIVITY DATA	234, 235
39	DIFFUSION LENGTH MEASUREMENTS - RUN NO. 30	236
40	IMPURITY ANALYSIS DATA	238
41	IMPURITY ANALYSIS DATA - RUN NO. 30	239, 240
42	IMPURITY ANALYSIS DATA - RUN NO. 47	241, 242
43	IMPURITY ANALYSIS DATA - RUN NO. 49	243, 244
44	IMPURITY ANALYSIS DATA - RUN NO. 55	245, 246
45	CZ GROWTH METHODS	252
46	CZ GROWTH METHODS - CZ NO. 1 & CZ NO. 2	255
47	SAMICS/IPEG INPUT DATA AND COST CALCULATION FOR CZ NO. 1 AND CZ NO. 2	256, 257
48	PROCESS CYCLE TIMES - CZ NO. 1 & CZ NO. 2	259
49	COST UPDATE FOR CZ NO. 2*	263
50	CZ NO. 3* GROWTH METHOD	265
51	SUMMARY OF COST PROJECTIONS	267
52	SAMICS/IPEG COST COMPONENTS OF CONVENTIONAL BATCH CZ GROWTH	268
53	SAMICS/IPEG COST COMPONENTS OF CONTINUOUS CZ GROWTH	269
54	DETAILED SAMICS/IPEG COST ANALYSIS BATCH #1 AND BATCH #2	271, 272
55	DETAILED SAMICS/IPEG COST ANALYSIS CZ #3 (IDEAL) AND CZ #3 CONSERVATIVE	273, 274

1.0 INTRODUCTION

This report presents the conclusions from two phases of work by the Kayex Corporation for the Jet Propulsion Laboratory under Contract 954888. Phase I began in October, 1977, the Phase I extension in April, 1979, and Phase II in January, 1980.

This contract was a part of the JPL/DOE Low-Cost Solar Array (LSA) Project, and had the objective of decreasing the cost of completed solar cell arrays to $2000 per peak kilowatt by 1982 and to $500 per peak kilowatt by 1986, based on 1975 dollars.

Kayex's efforts were directed toward a continuous Czochralski process capable of producing silicon suitable for use as low-cost solar cells.

1.1 Background

Kayex Corporation began producing Czochralski type crystal growing equipment at Rochester, New York in the late 1960's and has expanded its production capacity in the 1970's to meet the increased market required by the semiconductor industry.

Kayex has steadily increased its share of the market for crystal growing equipment. It is currently considered to be the leading domestic manufacturer of crystal growing furnaces.[4]

Based upon the Hamco Division's knowledge of crystal growing furnaces and silicon growth technologies, a proposal was submitted to JPL in 1976 to develop a method to produce low-cost silicon for solar cell fabrication based on Czochralski type crystal growth. This initial proposal was not accepted by JPL. However, a new proposal was submitted by Kayex Corporation in 1977 and was accepted.

The original contract No. 954888 was scheduled to run from October, 1977

through March of 1979 (18 months). The goals of this program were:

- Continuous growth of 100 kg of single crystal from one common container (one crucible)
- Resistivity of 1 to 3 ohm-cm P-type, in all material
- Dislocation density below $10^4/cm^2$
- Growth rate of 10 cm/hr
- Diameter of 10 cm or greater
- After-growth yield of 90%

A proposal for the continuation of the Project (contract No. 954888) for a period of nine months was submitted to JPL on January 31, 1979. JPL approved the continuation with the following goals:

- Qualify the equipment for 100 kg production type operation
- Improve quality/yield of produced ingot
- Develop a more accurate cost analysis for continuous Czochralski growth

A supplemental agreement was reached for Phase II of contract No. 954888 lasting three months starting January 1, 1980 with completion scheduled for March 31, 1980. The goals of Phase II were:

- Continuous growth of 150 kg or more of single crystal
- Optimize a production procedure for growing six (6) ingots each of twenty-five (25) kg in weight from a single crucible at a growth rate of ten (10) cm per hour.

As a result of a unified effort on the part of the Hamco Division of Kayex Corporation and the Corporate Technology Center, which was formed in November of 1979,from the Hamco Research and Development group, the program's technical goals and milestones have been reached with the exception of a growth rate of 10 cm per hour for 15 cm diameter crystals. This goal is presently being developed under JPL project No. 955270.

1.2 Scope of Work Performed During Contract

The objective of Phase I of this program was to demonstrate the growth of at least 100 kg of single crystal ingot from one melt container (crucible) by the Czochralski (CZ) method.

The normal commercial procedure for Czochralski type crystal growth is to grow one crystal from one crucible, replacing the old crucible with a new one each time a crystal is grown.

Although a number of methods of accomplishing continuous CZ growth could have been devised, it was very important that the chosen method would be suitable for a production environment and that it would be attractive in terms of safety, reliability and cost. In a production-type process, variables should be well-controlled and equipment should not require operators with great skill or technical ability. Therefore, Kayex's approach to the continuous growth process relied on conventional CZ technology combined with new equipment designs which allowed repeated alternate cycles of crystal growth and hot melt replenishment by methods which would be suitable for use in a high volume production facility.

The production of several crystals (up to 100 kg total) from one melt container (crucible) by the Czochralski (CZ) method required equipment and process modifications not commonly used in the semiconductor device industry. These modifications were required for the purpose of permitting a method of silicon replenishment without cooling the residual melt and container or contaminating the silicon.

In order to accomplish continuous CZ growth based on the method proposed by Kayex, it was necessary to design a crystal grower with the capability of:

- Continuous high temperature operation of the furnace section and continuous purging with argon at a vacuum of 20 torr.

- Isolating the top portion of the crystal grower from the lower furnace section
- Supporting a polycrystalline rod or hopper (lump material) to be used to refill (recharge) the hot crucible before starting another growth cycle.

These three requirements were met by redesigning and modifying a Hamco Model CG2000 crystal grower with a special chamber for the storage of a supply of polycrystalline silicon and a vacuum-tight isolation valve to permit retrieval of crystals and melt replenishment without contamination.

This new grower design, along with low cost objectives for grown silicon, necessitated additional modifications to the new grower and special crystal handling equipment.

- The newly designed isolation valve necessitated a redesign of the Automatic Diameter Control (ADC) optical system.
- The growth of large crystal ingots (greater than 4" diameter) required a modified bead chain/cable mechanism.
- The furnace section was redesigned to accommodate a 14" crucible and corresponding hot zone (12" standard).
- A dopant fixture was designed to allow dopant replenishment to the melt during a recharge cycle without contaminating the melt.
- A special crystal/poly transfer device and a storage rack were designed to handle large, hot crystal ingots.
- A hopper was designed and developed which has successfully demonstrated the recharging of lump poly silicon.

The first crystal growth test runs were performed in January, 1978 followed by successful hot-filling and crystal growth runs being demonstrated in February, 1978. By the end of June, 1978, all grower modifications and special

equipment had been completed except for the 14-inch hot zone, the lump recharge system and melt level control via weight. Moreover, the process development program was on schedule. Two recharges (three melts and ingot growth cycles from the same crucible) had been demonstrated with encouraging results (Run No. 11). See Table 1.

By the end of June, 1978, a SAMICS IPEG cost analysis had been completed based upon data obtained from the initial continuous recharge runs (Run No. 9 and Run No. 11). This data indicated that the final add-on cost for silicon was $19.40/kg in 1975 dollars ($27.16 1980 dollars). This SAMICS/IPEG cost analysis was referred to as CZ No. 1.CZ No. 1 was based on the assumption that five (5) 20 kg crystals were to be grown from one 12 inch diameter crucible - See Table 2.

At this time, a SAMICS/IPEG cost analysis was also projected for continuous CZ growth using a 14 inch diameter crucible (CZ No. 2)- See Table 2. This projection indicated that larger diameter crystals grown from larger size melts could potentially bring the add-on cost of silicon down to $15.07/kg in 1975 dollars ($21.10 1980 dollars).

The large furnace chamber (designed to accommodate a 14 inch hot zone was put into operation initially with the standard 12 inch hot zone in October, 1978. The 12 inch hot zone was used to compare the new furnace tank's performance with previous experience. Subsequently, some modifications had to be made to the hot zone as a result of considerably larger heat losses. Due to these modifications and the lack of practical knowledge of the thermal conditions created by the new furnace tank, it was decided to postpone 14 inch development work until the growth of 100 kg from a 12 inch crucible was demonstrated.

This was finally demonstrated the week of January 29 to February 1, 1979 (Run No. 30) - See Table 1. In the interim, the lump recharge device had been

CONTINUOUS CZ GROWTH SUMMARY

DATE	RUN NO.	TOTAL PULLED (KG)	NO. OF INGOTS	DIAMETER (CM)	AVG PULL RATE (CM/HR)	RUN TIME (HR)	THROUGH-PUT (KG/HR)	MONO-CRYSTAL (%)	AM-1 EFFICIENCY, %		
									RUN AVG	MONO-CRYSTAL	POLY CRYSTAL
2/78	5	22	1	11	9.1	18	0.82	100	-	-	-
4/78	9	27	3	11	8.7	39	0.70	85	11.5	11.6	11.4
6/78	11	43	4	11	9.1	44	0.97	88	11.8	11.9	11.2
10/78	19	57	6	13	8.9	64	0.89	56	11.8	-	-
11/78	21	53	5	13	8.4	44	1.21	62	-	-	-
12/78	22	46	5	13	9.0	50	0.93	91	-	-	-
1/79	30	99	6	13	8.7	79	1.25	27	11.2	13.3	9.8
6/79	47	60	5	13	6.8	52	1.17	88	13.0	13.0	-
7/79	49	108	9	13	7.0	86	1.26	85	13.8	13.8	-
10/79	55	101	10	13	7.2	91	1.11	75	12.0	13.0	9.7
10/79	2	100	9	13	7.7	109	0.92	64	12.3	12.7	10.6
12/79	60	100	8	13	7.6	85	1.18	61	12.0	13.0	11.0
1/80	62	103	9	13	7.9	97	1.06	89	12.9	13.2	11.2
2/80	70	152	6	15	6.9	99	1.53	44	-	-	-
3/80	72	151	6	15	7.0	94	1.61	17	-	-	-

TABLE 1

SAMICS ANALYSIS OF
TWO METHODS OF CONTINUOUS CZ

CONDITIONS	CZ NO. 1 1979	CZ NO. 2 1980
CRUCIBLE SIZE, DIA. X HT. (IN.)	12 x 9	14 x 10.5
CRYSTAL DIAMETER (CM)	10	12.5
GROWTH RATE (CM/HR)	10	10
NO. CRYSTALS/CRUCIBLE	5	4
TOTAL POLY MELTED (KG)	105	144
TOTAL INGOT PULLED (KG)	100	134
PULLED YIELD (%)	95	93
USABLE AFTER GRINDING (KG)	87	117
USABLE INGOT YIELD (%)	83	81
TOTAL CYCLE TIME (HR)	75.4	75.1
THROUGHPUT (KG/HR), (M^2/HR)	1.12	1.56
ADD-ON COST, 1975 ($/$M^2$), (1980$/M^2)	19.40 (27.16)	15.07 (21.10)

TABLE 2

designed, built and tested for reliability with excellent results. The lump recharging device was used along with the poly rod recharging system during Run No. 30. It worked well and helped to speed up the recharging process.

As in previous continuous runs, structure loss proved a problem during Run No. 30. A discussion of possible crystal structure loss mechanisms is included in Appendix A. Of the three structure loss mechanisms discussed in Appendix A, it was felt that one or more forms of melt contamination was the cause of structure loss problems during long continuous CZ growth runs. Therefore, after Run No. 30, a great deal of emphasis was placed on starting each continuous run with a clean furnace environment and maintaining a clean argon environment throughout the entire continuous run.

In February, 1979, the furnace was converted to the 14 inch hot zone. Two successful runs were demonstrated in March by growing 25 kg ingots from 30 kg melts. A 100 kg run was also attempted utilizing the 14 inch crucible and hot zone, but was unsuccessful due to a seed failure.

On March 31, 1979, the original Phase I of the 954888 contract was finished. However, a nine month extension had been granted to Kayex by JPL for the purpose of:

- Qualifying the equipment for 100 kg production type operation
- Improving quality/yield of produced ingot
- Developing a more accurate cost analysis of continuous Czochralski growth.

During the first three months of the contract extension, April 1, 1979 through June 30, 1979, improved quality/yield of produced ingot was realized with continuous Runs No. 41, yielding 66% single crystal, and No. 47, yielding 88% single material.

It was now evident that continuous Czochralski growth - as developed by

SOLAR CELL ANALYSIS

DATA TAKEN AT AMO (CONVERTED TO AM1)

Run No.	Ingot No.	Sample Description	Resistivity ohm-cm	N Avg AMO	N Avg. AM1
30	1	Top - OD	2.30	11.4	13.7
30	1	Middle - OD	1.86	11.5	13.8
30	1	Bottom - Dislocated	1.82	8.4*	10.1
30	2	Middle - Poly	1.72	7.8	9.4 9.7
30	2	Bottom - Poly	2.94	8.7	10.4
30	3	Top - OD	2.47	11.1	13.3
30	3	Bottom - Poly	2.78	8.2	9.8
30	4	Top - OD	2.34	11.3	13.6
30	4	Middle - Poly	3.12	8.7	9.2 10.4
30	4	Bottom - Poly	1.95	8.6	10.3
30	5	Top - OD	2.20	11.1	13.3
30	5	Bottom - Poly	2.48	7.8	9.4
30	6	Top - OD	2.16	10.6	12.7
30	6	Middle - Poly	2.97	7.4	8.9
30	6	Bottom - Poly	1.90	9.0	10.8
47	1	Top - OD	Not Completed	11.4	13.7
47	3	Top - OD (Thin wafer 7 mils)		9.8	11.8
47	3	Bottom - OD		11.4	13.7
49	1	Top - OD	2.67	11.6	13.9
49	1	Bottom - Single	1.95	11.5	13.8
49	6	Top - OD	1.80	11.6	13.9
49	9	Top - OD	2.06	11.5	13.8
49	9	Bottom - Single	1.73	11.1	13.3

Table 3

Kayex - was feasible. Previous solar cell efficiency results indicated that polycrystalline material was less efficient than single crystal silicon. It was important to prove that a high percentage of single crystal material could be grown using the (recharge) system for continuous growth and so impact on the solar cell efficiency.

Following Run No. 47, the furnace was converted to the 14 inch hot zone for the remainder of the contract. Some minor modifications were made to the hot zone prior to a successful one hundred kilogram continuous run being performed (Run No. 49)- See Table 1. This continuous run was the most successful continuous run to date, resulting in 108 kg of silicon crystal being grown from one 14 inch diameter crucible, yielding 84.8% high quality crystal. Moreover, during continuous Run No. 49, two of the largest crystals grown to date were produced - crystal No. 1, 22.4 kg (100% single crystal), and the last crystal, No. 9, 20.5 kg (82% single crystal).

By the time Run No. 49 was performed, recharging had progressed to the point where all recharging was done with lump material (no rod). The advantages of lump recharging outweighed the advantages of rod recharging - refer to Appendix B. The hopper designed for use during the 954888 contract allows for a maximum lump charge of slightly over 18 kg.

Following Run No. 49, a meaningful analysis of solar cell efficiency results was compiled from Runs No. 30, No. 47, and No. 49. These results indicated that efficiencies of single crystal material do not decrease significantly from the beginning of a continuous run to the end. Refer to Table 3.

During September, 1979, another milestone was approached when two 5.9 inch diameter crystals were grown during process parameter test runs, indicating that 150 mm diameter crystals could be grown utilizing a Hamco CG2000 RC crystal grower.

Two more 100 kg continuous runs were successfully completed during October, 1979, increasing the total of 100 kg continuous runs performed to four under the nine month extension to the 954888 contract. Furthermore, one of these 100 kg runs (Run No. 2*) (see Table 1) was performed in a standard Hamco CG 2000 RC crystal grower using process techniques and special crystal handling equipment developed under this project.

In December of 1979, and the first week of January, 1980, the last two 100 kg continuous runs were completed - Run No. 60 and Run No. 62 (refer to Table 1). Again, solar cell efficiencies did not deteriorate significantly throughout the entire run.

The culmination of all the efforts of the Hamco Research and Development Department, which had recently been formed into a new division - the Corporate Technology Center, was now directed toward the second phase of the 954888 project. This phase required the growth of six 150 mm diameter, twenty-five (25) kg ingots from one crucible. After several process parameter test runs, this task was finally accomplished the week of February 25, 1980 (refer to Table 1). A total of 152 kg of silicon crystals (6) was grown from one 14 inch diameter crucible. A second 150 kg continuous run commenced the week of March 17, 1980 resulted in 151 kg of silicon crystals (6) being grown from one 14 inch crucible. This run - Run No. 72 (Table 1)- was completed shortly before the 15th Project Integration Meeting on April 1, 1980 and prior to the final completion of DOE/JPL Contract No. 954888.

The economic analyses describing CZ1, CZ2*, and CZ3* are contained in Section 6.0 of the final report.

CZ1, CZ2, CZ3, and CZ4 Projected December, 1978

CZ2* Projected September, 1979

CZ3* Projected April, 1980

The individual technical tasks in the Phase I and Phase II program have been completed; the resulting technological and economic data for the continuous Czochralski type crystal growth as developed by the Corporate Technology Center provides a firm basis for the future work aimed at commercialization.

2.0 SUMMARY AND CONCLUSIONS

2.1 Equipment Design

The process for CZ growth of multiple crystal ingots from one crucible proposed by Kayex was dependent on the ability to remove a grown crystal from the grower and hot fill (recharge) the fused quartz crucible without contaminating the melt or allowing the furnace to cool down.

To accomplish the grown crystal removal and subsequent recharging, it was necessary to isolate the furnace section of the crystal grower from the upper portion (pull chamber) of the grower (refer to Figure 1 and Figure 2). In isolating the furnace tank from the pull chamber, a vacuum-tight seal had to be maintained so that the pull chamber could be brought to atmospheric pressure while the furnace tank was still under vacuum. Once the pull chamber was at atmospheric pressure, the door could be opened and the grown crystal removed. A new supply of virgin poly silicon (rod or lumps) could then be placed in the pull chamber, the door closed, the pull chamber purged of air with clean, inert argon and finally pumped down to a vacuum equal to the furnace tank, thus enabling the operator to open the isolation valve and proceed with the recharge cycle. Separate vacuum systems for the furnace tank and pull chamber were necessary to accomplish this cycle. A flow diagram of a continuous CZ cycle is included (Figure 7), page 16.

To meet the economic goals of the project, it was felt that time and cost savings would be accomplished if a supply of polysilicon material (rod or lump) could be contained in the pull chamber while a crystal was being grown This would allow the operator to recharge the crucible, then grow the next crystal, eliminating one cycle of opening the pull

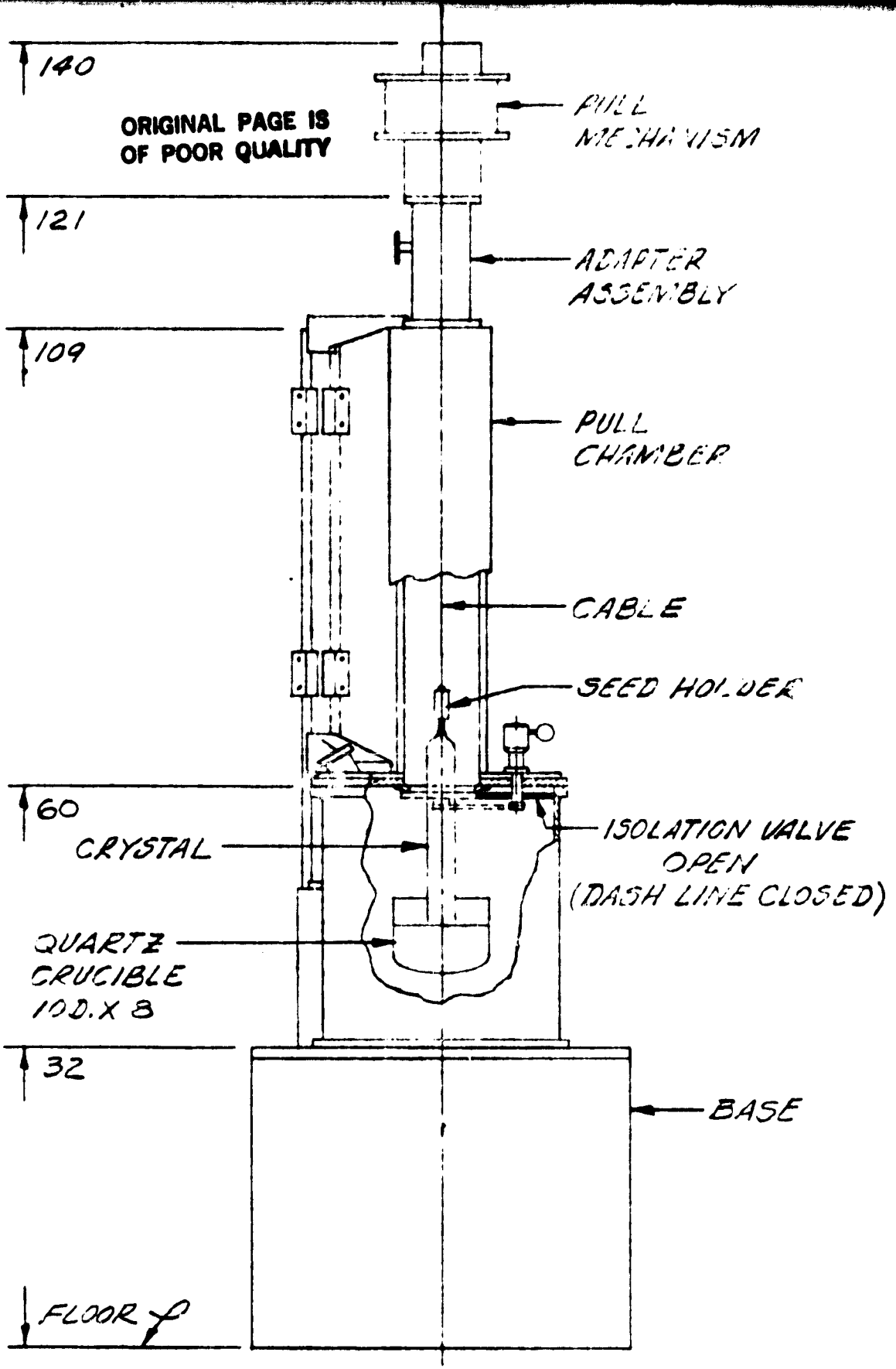

FRONT VIEW
SINGLE CZOCHRALSKI
GROWTH FACILITY

Figure 1

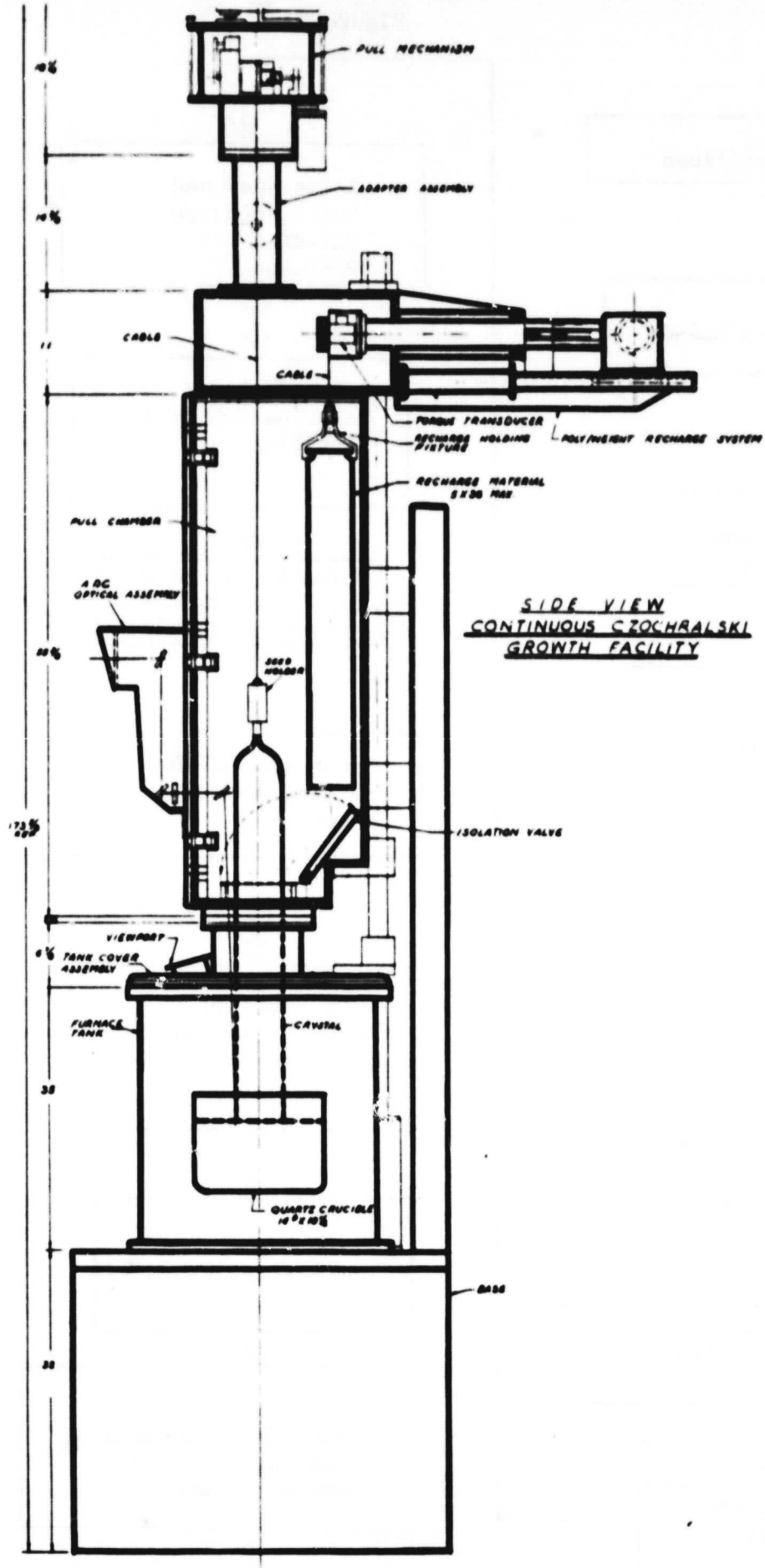
PULL MECHANISM
ADAPTER ASSEMBLY
CABLE
CABLE
TORQUE TRANSDUCER
RECHARGE HOLDING FIXTURE
POLYWEIGHT RECHARGE SYSTEM
RECHARGE MATERIAL 5 X 30 MAX
PULL CHAMBER
ADC OPTICAL ASSEMBLY
SEED HOLDER
ISOLATION VALVE
VIEWPORT
TANK COVER ASSEMBLY
FURNACE TANK
CRYSTAL
QUARTZ CRUCIBLE
BASE
SIDE VIEW
CONTINUOUS CZOCHRALSKI
GROWTH FACILITY

FIGURE 2

FLOW CHART FOR CONTINUOUS CZ GROWTH

Figure 3

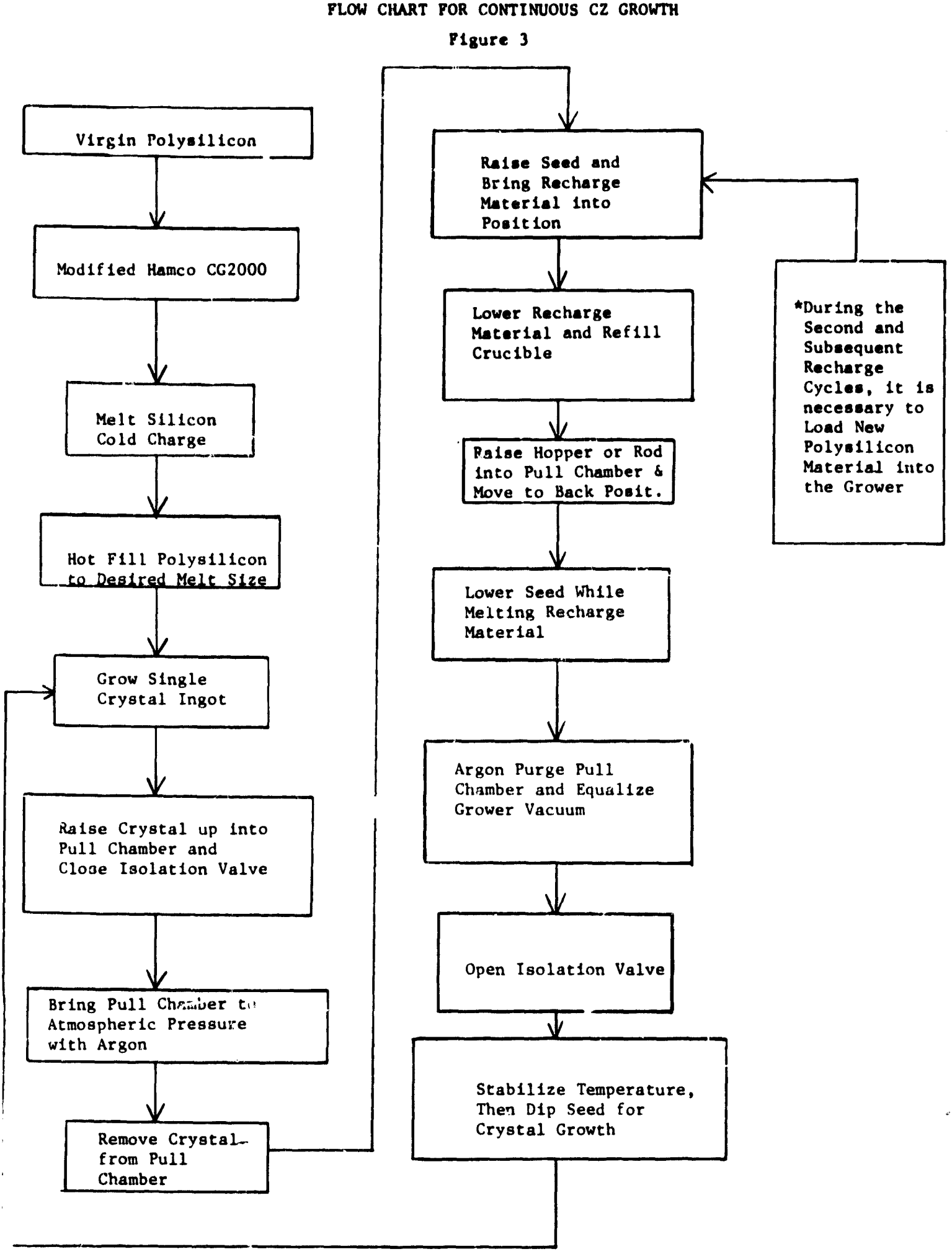

chamber door. Therefore, a polyweight Recharge System was designed with its own cable system to hold a supply of polysilicon material for recharging - details are explained in Section 3.1.2.

The newly designed isolation valve was not compatible with the old automatic diameter control optical system (ADC). An ADC optical system utilizing appropriate lenses for sighting through the valve throat was designed and built for the new grower (Figure 4). It was also necessary to see the new flapper type isolation valve relative to the grown crystal and polysilicon material to be used for recharging. Therefore, a larger viewport window was designed into the pull chamber door for this purpose. The pull chamber had to be modified further (enlarged) to provide space for storage of polysilicon (Figure 2).

The growth of large crystals (4" diameter) from large melts (20 kg to 45 kg) was highly cost effective and was included as part of the 954888 contract proposal. This objective could be accomplished by increasing the capacity of the melt container (crucible). A 14 inch diameter crucible was calculated to be the optimum size for the project goals. However, a newly designed 14 inch hot zone required a larger furnace tank than the standard CG 2000 equipment. The newly designed furnace tank was capable of accommodating either the 12 inch or 14 inch hot zone. With the increase in melt size and the corresponding size and weight of the crystals grown, the need for a stronger bead chain seed lift device became necessary. The seed lift pull mechanism was modified to utilize a stainless steel cable. Mechanical and electrical modifications were also included to permit weight measurement of ingots up to 50 kilograms.

Two problems had to be solved when it was decided to recharge using

ORIGINAL PAGE IS
OF POOR QUALITY

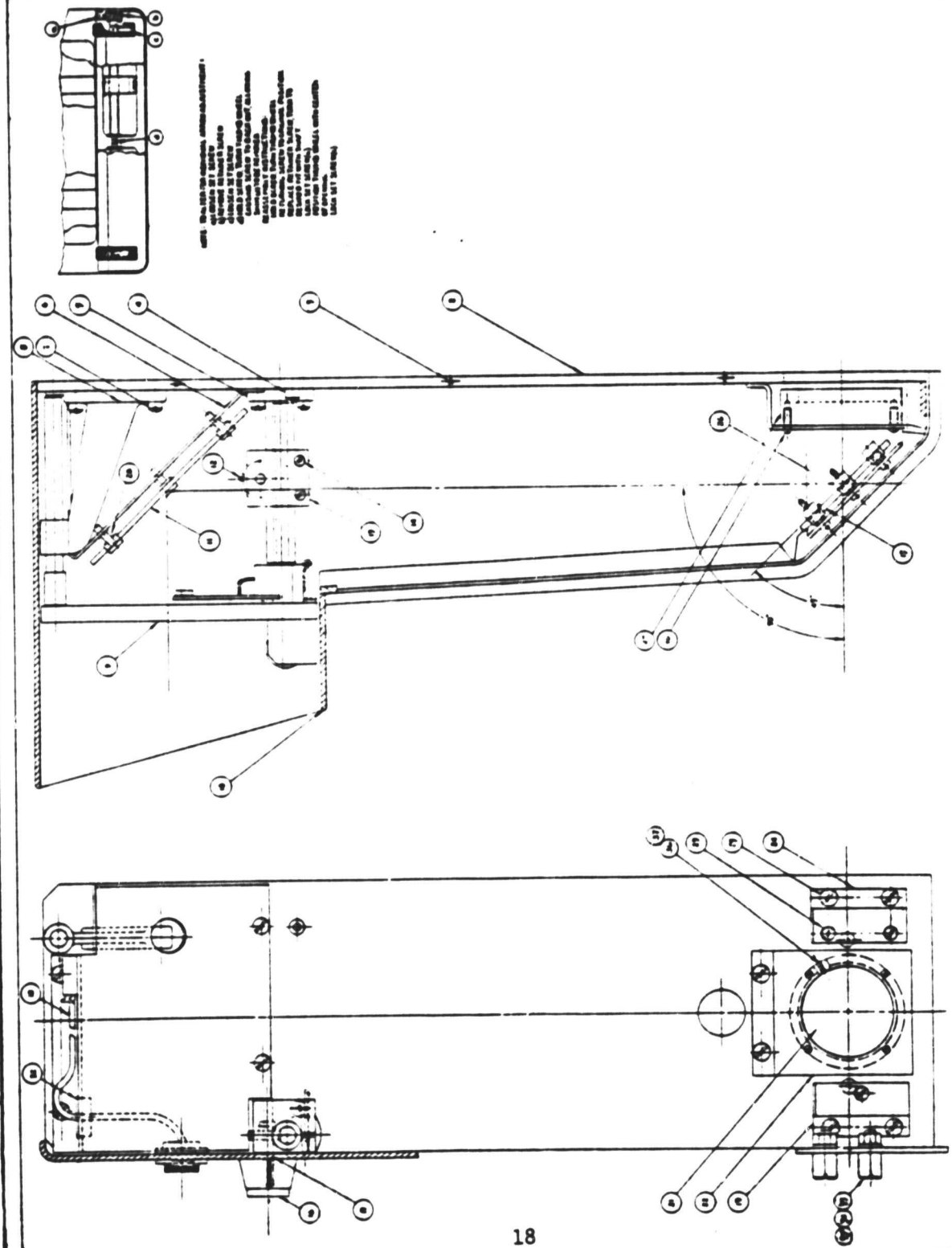

FIGURE 4 ADC OPTICAL SYSTEM

polysilicon rods:

1). A method of attaching the rods to the support cable had to be developed.

2). A method of adding dopant to the crucible while it was hot and under vacuum required development.

The first problem was solved by designing a poly attaching device (Figure 5). This clamp type of design required notching of the poly silicon rod. The second problem was solved by designing a dopant fixture (Figure 6) that would allow for insertion of dopant pellets, incorporation of a vacuum interlock system and rotating capabilities such that it could be positioned over the crucible (melt). The dopant pellets could then be released and the fixture rotated out of the way so that the next crystal could be grown. The dopant fixture was designed to fit into the furnace tank cover.

Finally, since the continuous CZ process did not allow for the prolonged cooling of grown crystals in the crystal grower, it was necessary to design and build special crystal handling and storage devices (Figures 7 and 8) which could accommodate large, hot crystals and large poly silicon rods. Figure 9 shows a crystal being held by the crystal/poly transfer device ready to be placed into the crystal/poly storage rack.

Minor mechanical and electrical modifications were made to the Hamco CG 2000 crystal grower in conjunction with the previously mentioned design changes and modifications. These modifications will not be discussed here.

A major design and process study was necessary to recharge lump poly silicon. A lump recharging system was developed incorporating a self-dumping hopper design (Figures 10 and 11). The hopper used during the 954888 project allowed for a maximum recharge capability of 18 kilograms of poly silicon lumps. More details can be found in Section 3.4.2.

ITEM NO.	PART NO.	DESCRIPTION	QTY
1	021-0065-201	HOOK - RC HOLDING FIXTURE	2
2	024-0079-201	ROD - RC HOLDING FIXTURE	1
3	027-[illegible]-101	WASHER - RC HOLDING FIXTURE	1
4	026 0001-438	NUT - 1"-8 STD. 3.5	1

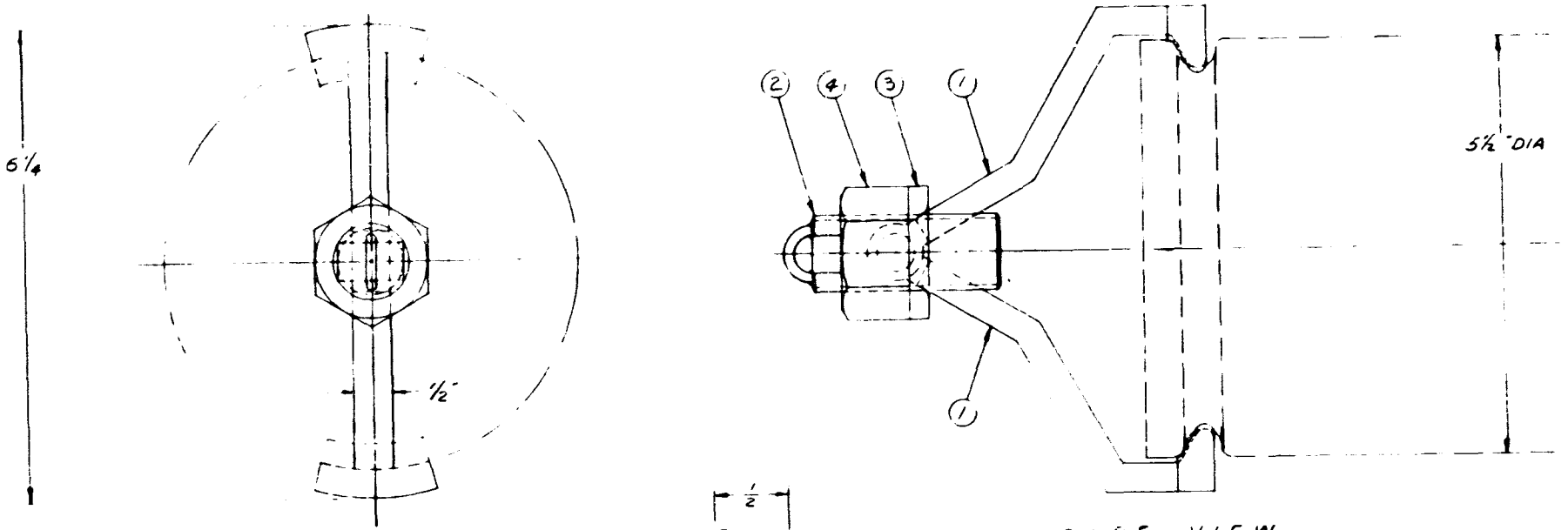

PLAN VIEW

SIDE VIEW

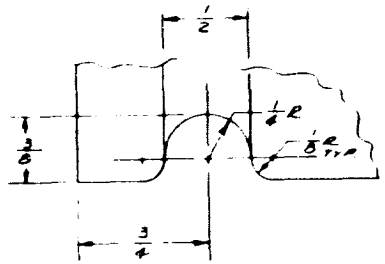

GROOVE DETAIL FOR ALL RECHARGE MATERIAL
SCALE: 2×

POLY ATTACHMENT DEVICE

FIGURE 5

HAMCO DIV. OF THE KAVEX CORP.
ROCHESTER, N. Y.

CWJ 10/4/77 316 S.S
FULL
500-0101-2 C 1-0058-201

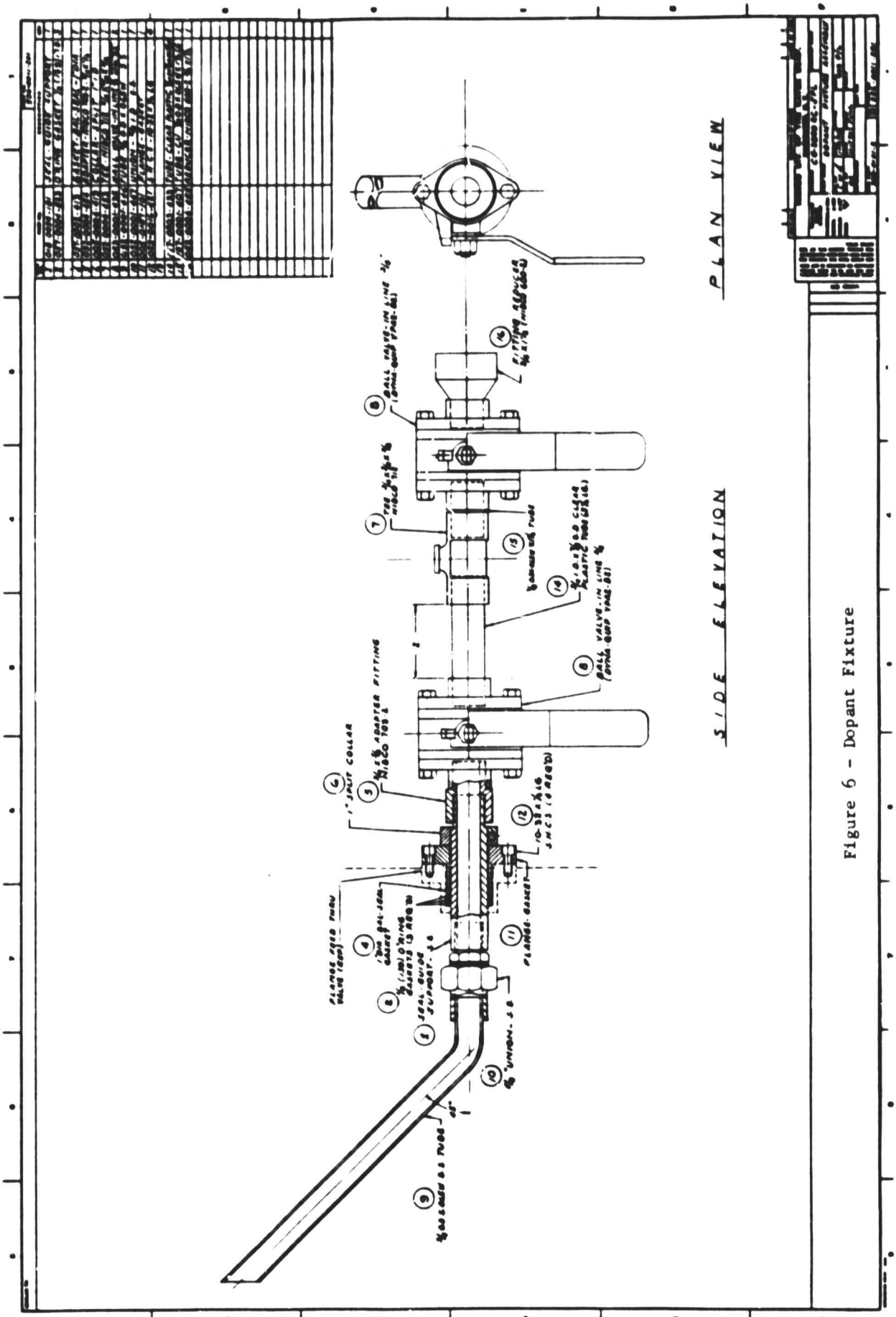

Figure 6 - Dopant Fixture

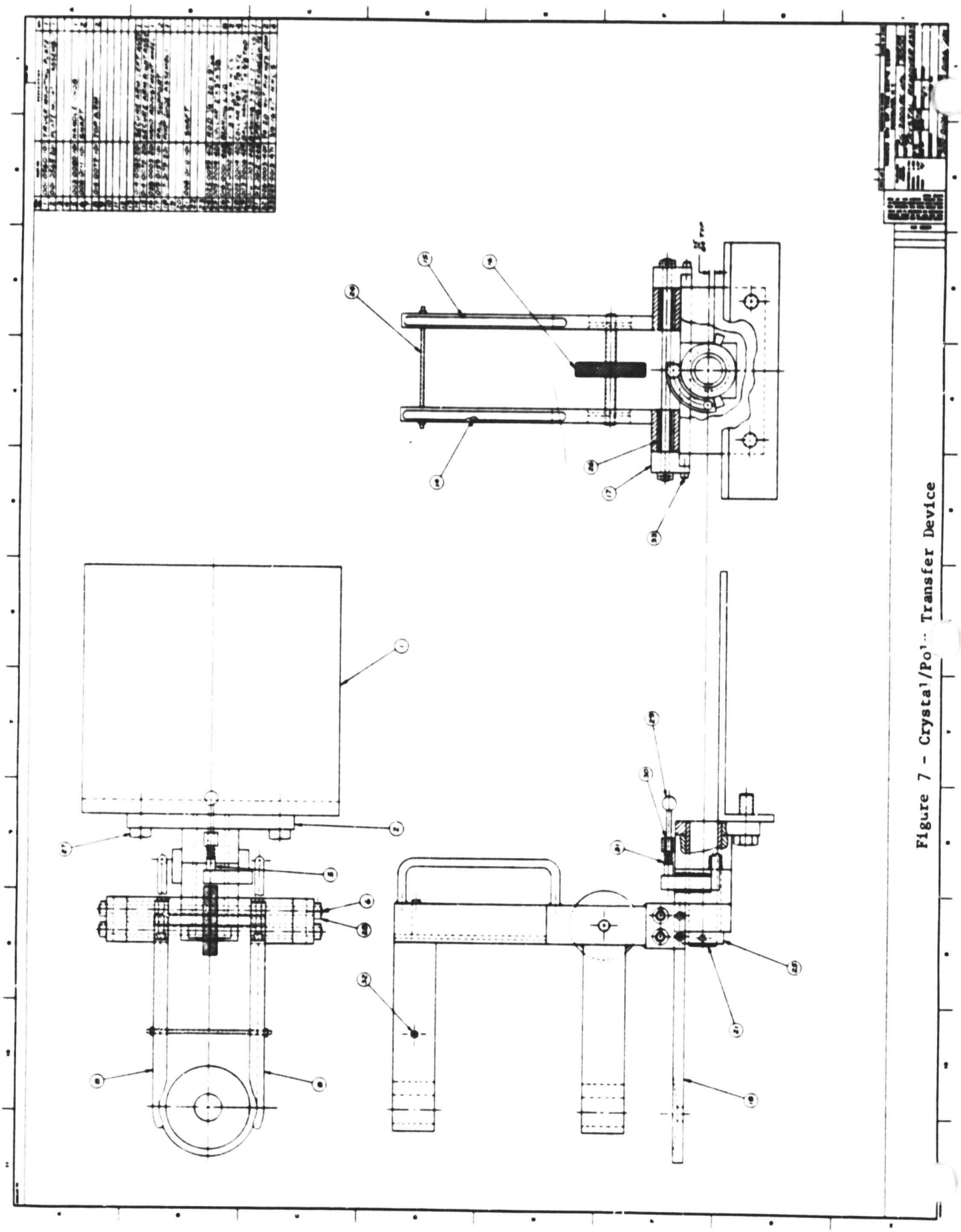

Figure 7 - Crystal/Po[illegible] Transfer Device

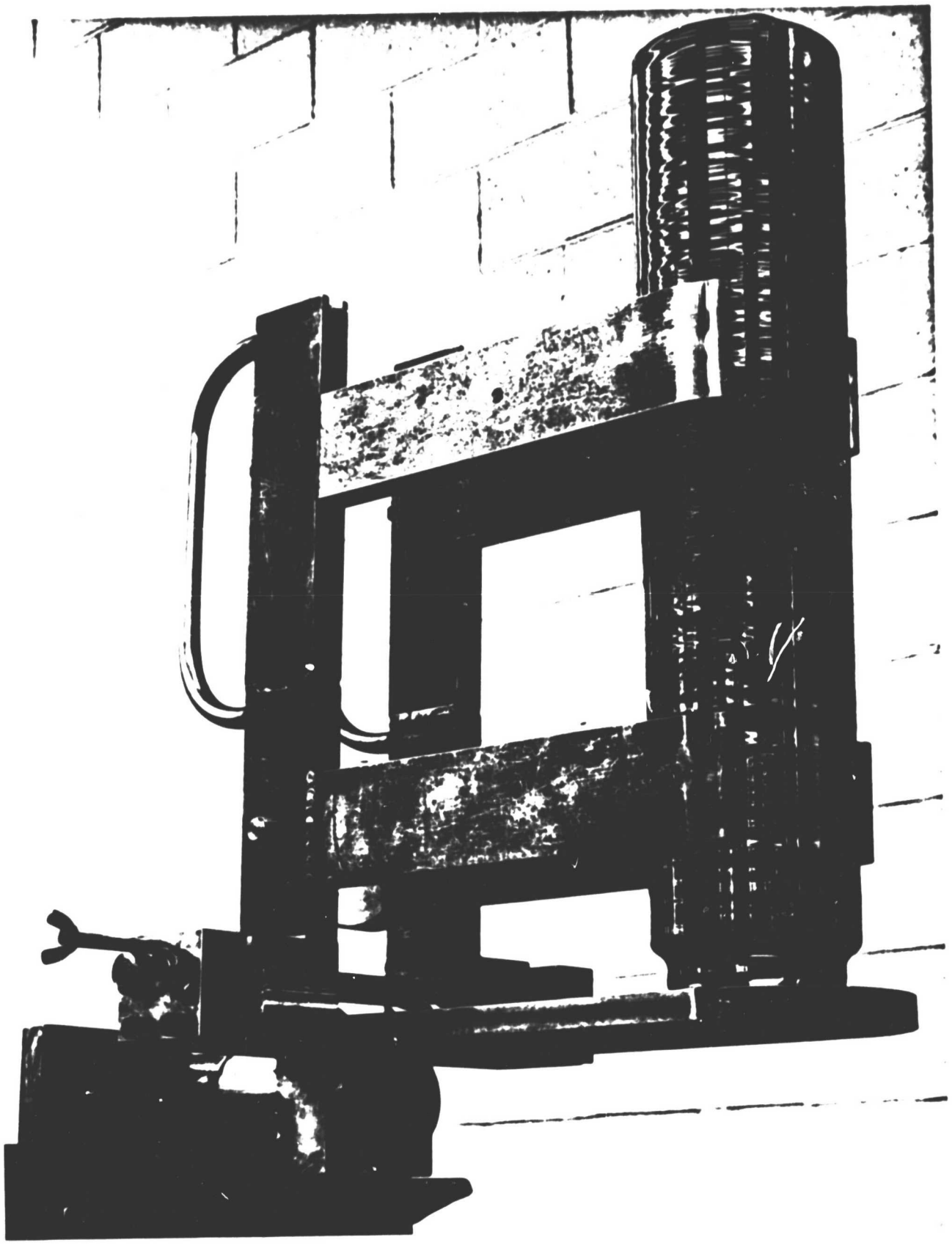

FIGURE 8
CRYSTAL/POLY TRANSFER DEVICE

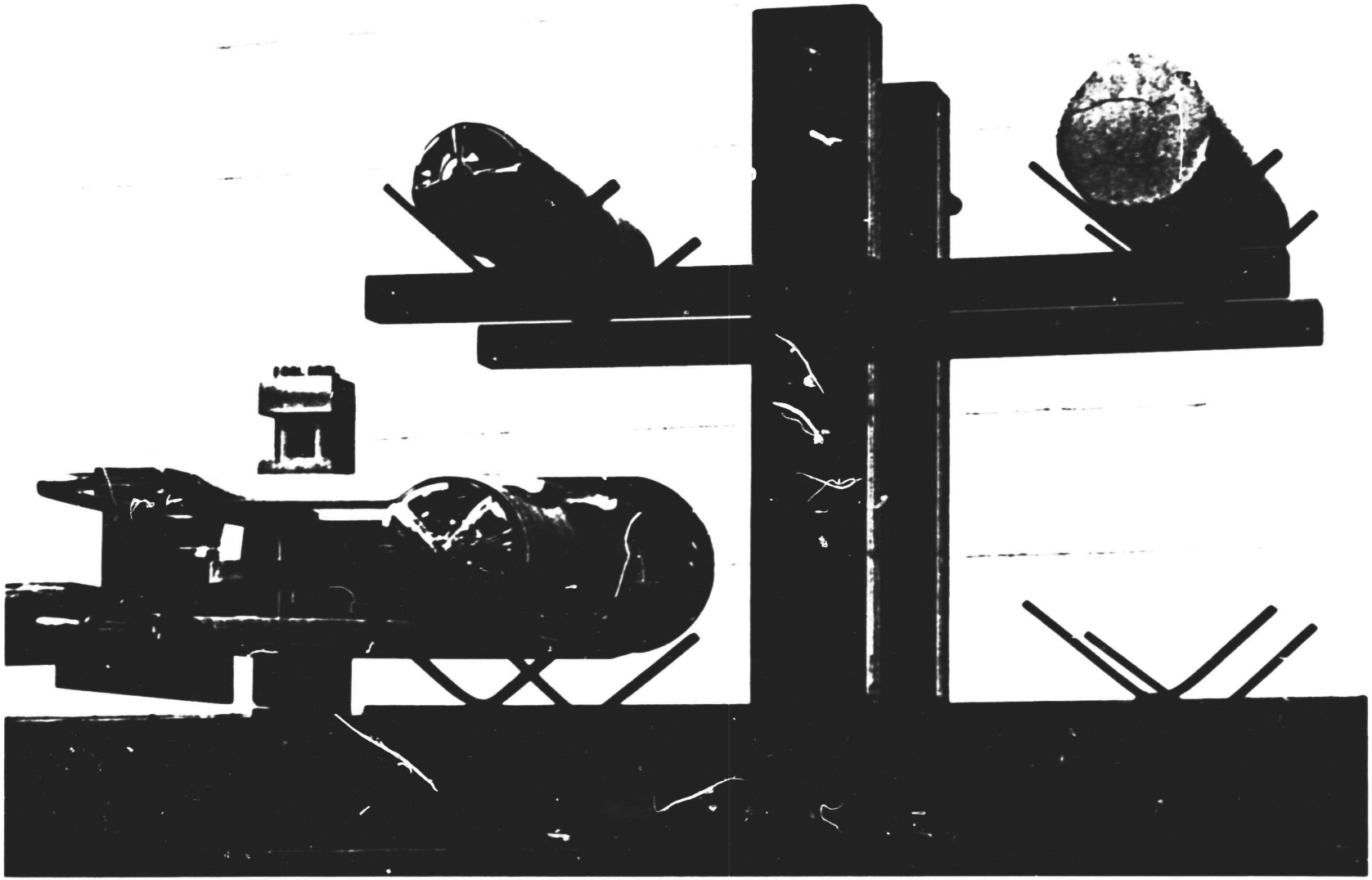

FIGURE 9 - PLACING CRYSTAL ON COOLING RACK

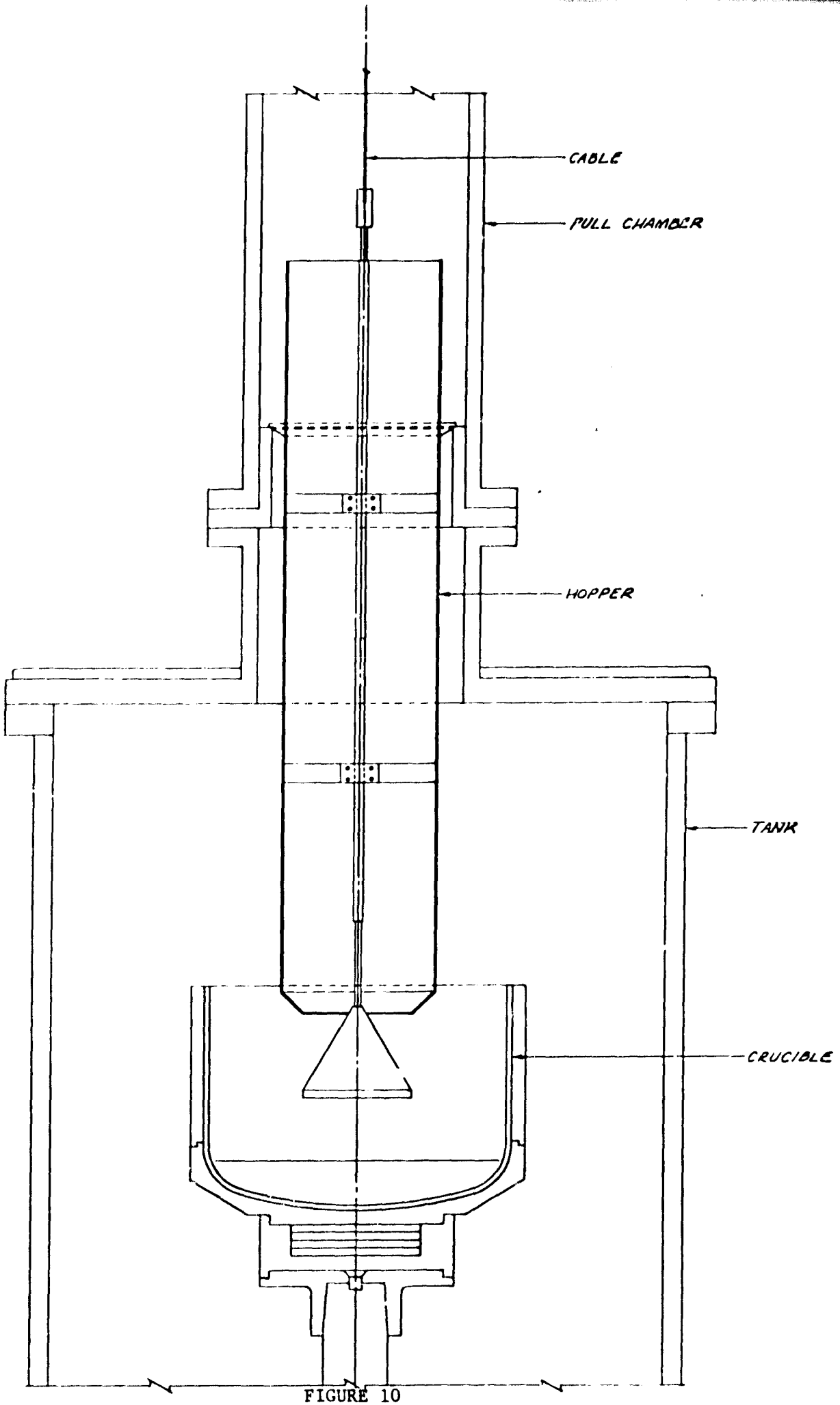

FIGURE 10

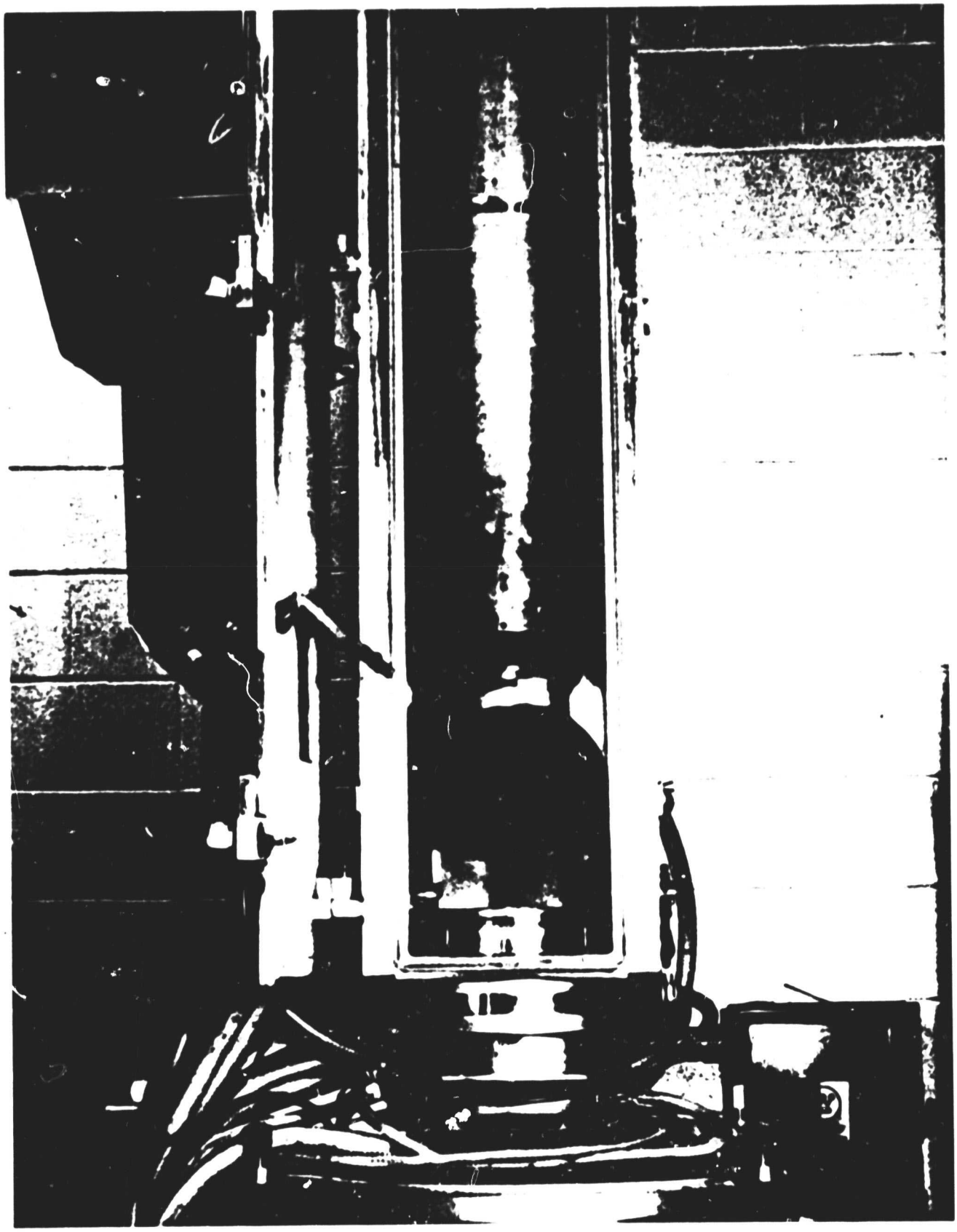

FIGURE 11

2.2 Process Development

The intent of Kayex Corporation in submitting a proposal to the Jet Propulsion Laboratory to develop a method of producing low cost silicon suitable for solar cell fabrication was twofold:

a) Kayex's expertise was in the field of Czochralski type crystal growth. It was felt that this method of silicon production held the highest probability for successful completion of the JPL cost goals within the required time frame.

b) The technology of Czochralski type crystal growth of silicon was presently highly developed and could be used in the development of the continuous growth method proposed by Kayex.

2.2.1 State of the Art Silicon Crystal Growth [5]

A large majority of present day silicon crystal growth involves the controlled freezing of molten silicon onto a single crystal silicon seed. Czochralski improved the original system by continuously withdrawing the seed from the melt. Teal and Little further improved the Czochralski method of crystal growth as it relates to silicon and germanium. The Teal-Little concept is the predominant method used for silicon crystal growth today.

Much can be said about the intricacies of Czochralski type silicon crystal growth. However, the most important facet involving the cost of the silicon produced was the present practice of growing only one crystal from one melt container (crucible). The crucibles are normally made of high purity fused quartz and break when the furnace is cooled down to remove the grown crystal and clean the furnace. Therefore, one crucible is required for each crystal grown. Kayex's primary approach centered around the cost of these fused quartz crucibles which is relatively high. Cost savings for silicon produced could be realized by growing more than one

crystal from the same crucible.

In order to grow more than one crystal from the same crucible, a process had to be developed to remove the grown crystal and refill the crucible without contaminating the furnace or allowing the crucible to cool down. Kayex's concept was to redesign a standard crystal grower to include a vacuum tight isolation valve that could effectively separate the upper chamber (pull chamber) of the crystal grower from the lower chamber (furnace tank) which must be constantly kept at high temperature and argon purged vacuum - refer to Sections 2.1 and 3.1.

2.2.2 Hot Fill Experiments

January, 1978 saw the first test runs performed in the modified CG2000 crystal grower to be used during contract No. 954888. Although several modifications had not been completed (Poly Weight/Recharge System and Dopant Fixture), the isolation valve, ADC optical system and modified (strengthened) cable mechanism were completed and installed on the grower. Three successful state of the art test runs followed to establish that control systems were working and adjusted properly. Development of hot fill methods then began.

Testing of the vacuum system and isolation valve commenced at this point with satisfactory results. Two crystals were grown from each of two 18 kilogram melts and removed from the furnace while still hot. A minor problem involving control of pressures and gas flow in the pull chamber and furnace tank was remedied by installing a secondary vacuum pump to the pull chamber.

The first melt-down of silicon in a crucible fills it to about 50% of its capacity if lump silicon is used, due to the packing factor of the poly. In order to achieve the highest efficiency, more silicon had to

be added to fill the crucible to its capacity before the first crystal is started. Hot filling techniques would also be used during recharge cycles that were subsequently developed.

Initially, hot fill experiments were conducted by securing a poly rod to the seed lift mechanism by means of the poly attachment device (Figure 5). When the poly/weight recharge device became available, the poly rods were supported by the cable on the poly/weight recharge device.

During February, 1978, the first two hot fill runs were performed. The first attempt was unsuccessful due to the failure of the seed lift cable. Modifications were then made to the poly attaching device. The next attempt satisfactorily demonstrated the hot-filling concept by first cold-filling a 12 inch diameter crucible with 18 kg of poly silicon and then hot-filling an additional 7 kg. A 22 kg high quality crystal was grown from this 25 kg melt.

Work then progressed on further modifications to the crystal grower and special handling equipment so that process development could continue into the next stage - recharging. This equipment included a dopant fixture, (Figure 6), a crystal/poly transfer device (Figures 7 and 8), and a crystal/poly storage rack (Figure 9).

It should be noted that hot-filling was accomplished with poly silicon rods only. Hot-filling was not demonstrated using poly silicon lumps until January, 1979 following the design and development of a prototype model.

2.2.3 Initial Recharging Experiments

With the installation of the dopant fixture, the ability to add dope pellets to the hot melt without contaminating the furnace was realized. In order to produce P-type silicon with the proper resistivity to produce

suitably efficient solar cells, boron doping of the virgin poly silicon had to be accomplished. Since there was no practical way to incorporate this into the melting of the poly rod, it had to be accomplished in a separate procedure - necessitating the design and development of the dopant fixture.

Completion of the crystal/poly transfer device allowed for handling of large, hot crystals so that recharging could be performed a short time after the growth cycle was completed.

The first run demonstrating recharge capability was performed April 17 and 18, 1978. A 14 kg crystal was grown from an 18 kg melt with no initial hot fill. With only one operator available, the recharge cycle was delayed to the following morning. At that time, 12 kg was melted off a 13.2 kg poly rod at the rate of 6 kg/hr. Dopant was added, the seed was replaced, and the second crystal was grown. The second crystal lost structure after about 10 inches of crystal had been grown (6.3 kg) due to a particle of silicon monoxide that fell into the melt. The growth cycle was stopped, the second crystal removed, and the melt reseeded for the growth of a third crystal. This crystal was also twinned by a particle of silicon monoxide after 12 inches had been grown (6.8 kg). This first attempt at recharging to develop the continuous CZ growth method proved to be relatively successful. Even though hot fill experiments had proved that the recharging cycle could be done, the run proved that the continuous CZ concept as out lined by Kayex was feasible.

Delays had been experienced in the completion of the poly weight/recharge system which was now scheduled to be installed on the grower in June, 1978. Therefore, prior to the poly weight/recharge system becoming fully operational, a two-recharge run was planned. This run - Run No. 11 -

resulted in 42.5 kilograms of single crystal material being grown from one crucible by melting a total of 48.7 kilograms in three successive melts, for a cumulative pulled yield of 87%. The 10 cm diameter grown crystal material was approximately 80% zero dislocation structure. Run No. 11 lasted forty four hours resulting in an average throughput of 0.97 kg/hr.

Progress had been made toward the goal of producing 100 kg of silicon crystal from one crucible. The problem of structure loss, although occurring later into the run, was still an area of major concern.

Crucible devitrification - originally considered to be a potential problem during long continuous runs - did not appear to be a problem during Run No. 11 - the longest continuous run up to that time (44 hours).

In July of 1978, an evaluation of a low cost crucible made from impure sand proved to be negative. Refer to Section 4.5.4 for more details. The recharge device continued to give problems in operation, both electrically and in vacuum integrity. However, by the end of July, the recharge mechanism appeared to be in full working order and ready to be used for recharge runs. The grower can be seen on page 32, Figure 12.

During the next several months, a great deal of difficulty was encountered in achieving the desired goal of growing 100 kg of silicon from one crucible. Equipment problems, mechanical problems, and operator error (new operators were being trained during this time) resulted in aborted runs and less than satisfactory results on completed runs.

In August, 1978, the grower was almost completely dismantled. The new larger furnace tank was installed, allowing for the use of a 14 inch hot zone, the recharge mechanism was reworked to try and eliminate the vacuum problems encountered with its use and two ports were added to the

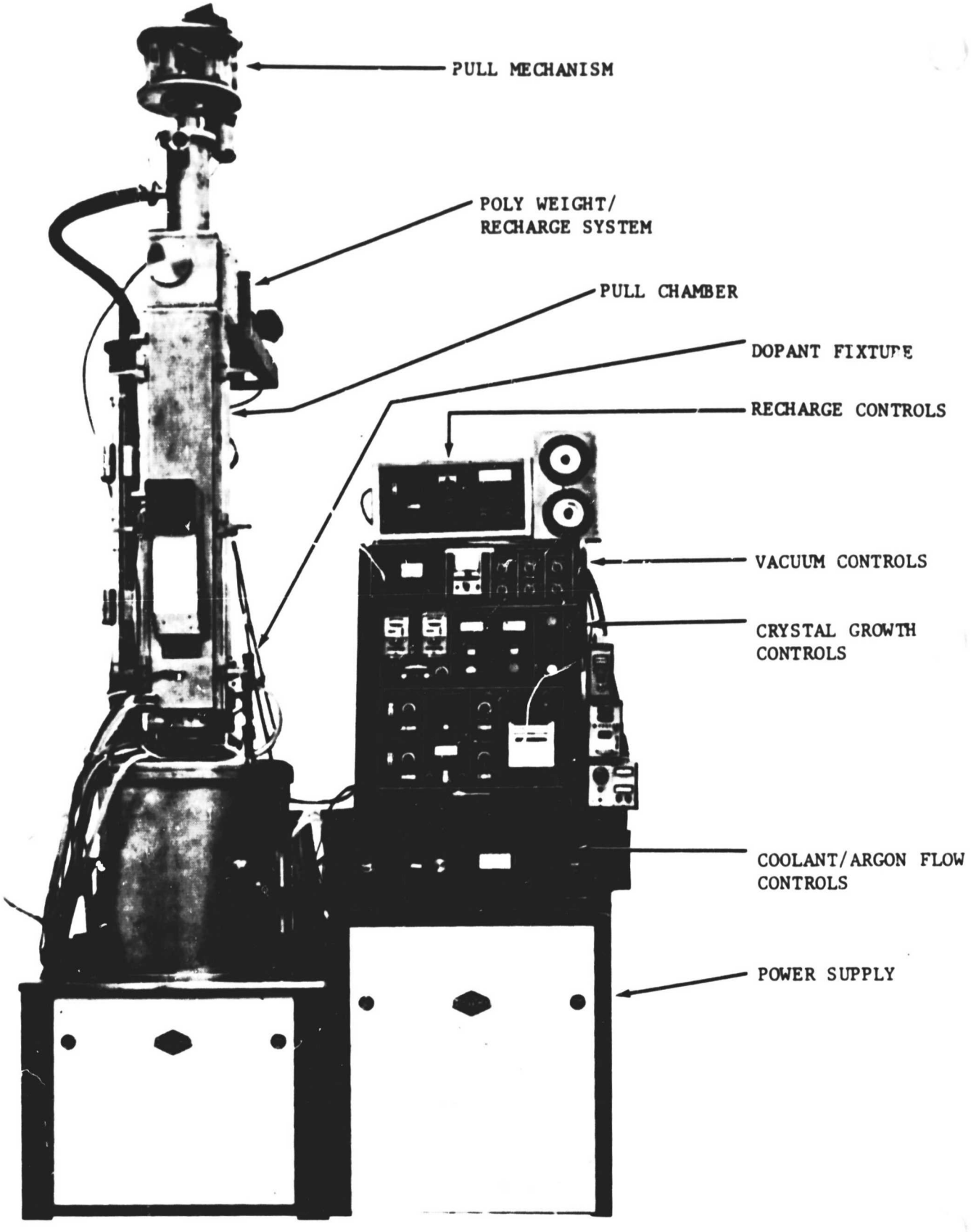

FIGURE 12

JPL CONTINUOUS CZ GROWTH FACILITY

pull chamber for the purpose of temperature profile measurements.

Two other problems were encountered during this period - microscopic (pin hole) water leaks in some of the weld areas of the grower and thermal expansion fracture of poly rods used for recharging. The microscopic water leaks were attributed to an improperly constructed furnace top plate that was finally replaced with a new top plate in June of 1979, following numerous attempts to correct the problems associated with the old top plate. The problem of poly rods fracturing during the recharging cycle was minimized by requiring the rods to be lowered into the furnace chamber at a slower rate, decreasing the thermal shock on the rod.

The work on the grower was completed in September and, in October, 1978, the grower with the large furnace chamber was put into operation initially with the standard 12 inch hot zone in order to compare its performance with previous experience. Some modifications were made to the hot zone as a result of considerably larger radiative heat losses.

During the next three months, several short (one-ingot) runs were performed and four continuous runs were attempted. The largest continuous run lasted 64 hours and produced 57 kilograms of ingot. Four recharge cycles were performed during this run.

The major problem in achieving the 100 kg goal was difficulty in maintaining high quality (single crystal) ingot growth for long periods of time. (Refer to Appendix A).

Recharging of lump poly silicon was demonstrated for the first time in January, 1979, immediately before the first 100 kg continuous run - Run No. 30. 5.4 kilograms of poly silicon chunks were hot filled (dumped) into

a small charge (6.7 kg) and a high quality crystal grown. Refer to Sections 3.4.2 and 4.4 for more information on the lump recharger and the related process development.

2.2.4 100 Kilogram Continuous Recharge Runs

On Monday, January 29, 1979, the first 100 kilogram continuous run was started (Run No. 30). Structure loss problems occurred early into the run, however. It had been decided before the run was started that the effort would be made to grow 100 kilograms of crystal ingot regardless of the overall crystal quality. The run was completed Thursday, February 1, after seventy-nine (79) hours of continuous run time. Six ingots were grown ranging in size from 15.5 kg to 17.7 kg for a total of 99.1 kilograms. (See Table 1). Even though the percentage of high quality crystal was low, it had finally been demonstrated that 100 kg of silicon crystal ingots could be grown from one crucible.

The lump recharge device used in combination with poly rod for recharging proved to be successful and indicated that recharging times could be decreased by using the lump recharge method. The crucible appeared to be in relatively good condition at the end of the run with devitrification no worse than that experienced on earlier, shorter runs.

Following Run No. 30, the furnace was converted to the 14-inch hot zone and preliminary thermal characteristic test runs were performed. Two successful runs were demonstrated by growing 25 kg ingots from 30 kg melts. Also, a 100 kg run was attempted, utilizing the 14-inch crucible/hot zone. This run was prematurely terminated due to excessive silicon monoxide accumulation on the viewports and a seed failure.

At this time, April, 1979, it was felt that problems associated with the

grower could be solved more easily if the grower were converted back to the 12-inch hot zone. An intensive effort was made over the next three months to find the source of the structure loss problems. Areas where vacuum grease might contaminate the grower atmosphere were identified and corrected. Extensive leak checking of the grower was performed including all vacuum lines and argon lines. Machine alignments and calibrations were checked and corrected as necessary. The seed lift assembly was rebuilt and the pull chamber door was machined to eliminate air leaks found in the sealing area. Several runs were made during this period of time, including one attempt at growing 100 kg. Although much was learned about the condition of the grower and several parameters of the growth process, results continued to be less than satisfactory. The discovery of further microscopic pin hole water leaks in weld areas around the furnace tank viewports necessitated the replacement of the furnace tank cover plate (June, 1979).

Structure loss problems on the subsequent run resulted in a decision to remove the recharge mechanism. It was felt that, since the recharge mechanism had exhibited vacuum problems in the past, a further variable could be eliminated by removing the recharge mechanism and starting with a grower as close to a standard production CG2000 RC as possible. The next run showed marked improvement in the cleanliness of the furnace atmosphere, crucible walls and furnace interior.

The pull chamber was again checked for vacuum grease. Two areas were located and cleaned. Vacuum seals were inspected and replaced where necessary in preparation for the next scheduled 100 kg run on June 26, 1979. This run was to be performed with the JPL project technical monitor present. One result of this run (Run No. 47) was the largest percentage of single crystal to date (Table 1). Five crystals were grown, totalling 60.2 kilograms, of which 88% was single crystal. Of the 60.2 kg grown, nearly 70% was disloca-

tion-free. Severe crucible devitrification and deformation was observed towards the end of the fifth growth cycle. This condition necessitated termination of the run prior to attaining the 100 kg goal. However, the large percentage of high quality crystal indicated that the efforts of the last few months were rewarded.

The ongoing study and development of the lump recharging process had now reached the stage where it was possible to recharge 15 kg of lump silicon into a 12-inch crucible in one recharge cycle using a two step method. All recharging for Run No. 47 was done using the lump recharge method.

With six months remaining on the 954888 contract extension, the furnace was converted to the 14-inch hot zone. Five more 100 kg continuous runs were still required by the end of the contract.

The second run attempted after the grower was converted to the 14-inch hot zone was very successful and met most of the goals of Phase I of the project. Several hot zone modifications were made prior to Run No. 49.

Run No. 49 (Table 1) commenced on Monday, July 17, 1979. A total of 108 kg of silicon crystals were grown in eighty-five (85) hours. Moreover, 85% of the silicon grown was single crystal. It had finally been demonstrated that at least 100 kg of silicon could be grown from one crucible, yielding a high percentage of single crystal material.

A direct result of the work performed on the crystal grower during the three month period from April, 1979 through June, 1979 and the subsequent success led to the reaffirmation that a satisfactory percentage of high quality crystal. Production requires a clean growth environment.

Two more 100 kg continuous runs were completed in October, 1979. Four of the six 100 kg runs required under the 954888 project extension had now been completed. During this time, continued data was accumulated concerning cycle times and materials usage. From this data, cost updates were formu-

lated - refer to Section 2.3. A composite of recharge and ingot growth times for all 100 kg runs is presented in Table 4, page 38.

2.2.5 150 Kilogram Continuous Recharge Runs

Whereas Phase I of the 954888 contract called for the growth of 100 kg of silicon crystal ingots greater than four inches in diameter, Phase II required the growth of 150 kg of silicon crystal ingots 150 mm in diameter.

Runs No. 51 and 52 had indicated that the growth of 150 mm diameter crystals during a continuous run were highly probable (Figure 13). However, the production of 50% more silicon from the same crucible was a significant challenge. Calculations showed that 150 mm diameter crystals would produce 38.7% more silicon per inch of crystal than 125 mm diameter crystals, but the time factor involved necessitated a minimum of crystal growth cycles during the continuous run. Ideally, a total of six 25 kg crystals would be grown to meet the 150 kg goal. It would no longer be possible to grow nine or ten crystals within the time frame allotted for the continuous run. Potential structure loss problems, for whatever reason, had to be minimized and continuous growth procedures previously developed had to be optimized.

Test runs to set the parameters for 150 mm diameter crystal growth began immediately following Run No. 62, the second week of January, 1980. Run No. 63 resulted in a 150 mm diameter crystal being grown entirely dislocation-free. (See Figure 14). The crystal weighed 25.5 kg with the complete run lasting thirteen hours, resulting in a growth rate of 1.96 kg/hr. Refer to Table 5, page 41.

Following a second successful test run, the first attempt at growing 150 kg was begun the week of January 28, 1980. A mechanical problem involving a failure of a coupling on the seed lift mechanism precluded a successful run being completed.

The first three weeks of February involved an intensive effort to:

COMPOSITE OF RECHARGE AND INGOT GROWTH TIMES FOR 100 KG RUNS

RUN NO.	RECHARGE TIME(1) HRS	%	GROWTH PREPARATION(2) HRS	%	STRAIGHT GROWTH & TAPER HRS	%	TOTAL RUN TIME HRS
30	18.9	(23.9)	20.9	(26.5)	39.2	(49.6)	79
47	8.8	(17.1)	11.9	(23.1)	30.9	(59.9)	51.6
49	16.4	(19.2)	20.3	(23.7)	48.8	(57.1)	85.5
55	12.9	(14.2)	33.5	(36.8)	44.6	(49)	91
2*	19	(17.4)	38.3	(35.1)	51.7	(47.4)	109
60	12.8	(15.1)	21.4	(25.2)	50.8	(59.8)	85
62	13.0	(13.4)	32.6	(33.6)	51.4	(53)	97

(1) Recharge Time includes:
- Removal of grown crystal
- Insertion of hopper
- Dump hopper charge
- Melt down
- Seed preparation up to seeding the melt

(2) Growth Preparation includes:
- Stabilize Temperature
- Growing Seed
- Crown Growth
- Melt Backs

TABLE 4

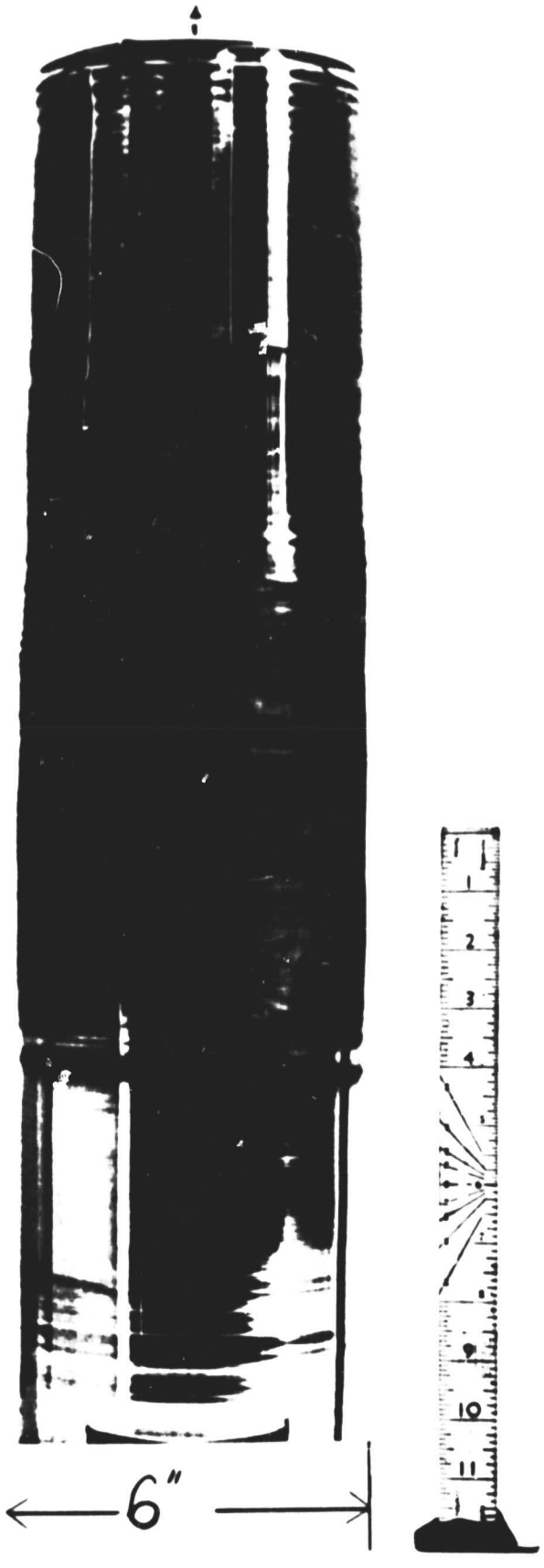

FIGURE 13
15 CM DIAMETER CRYSTAL - RUN NO. 51

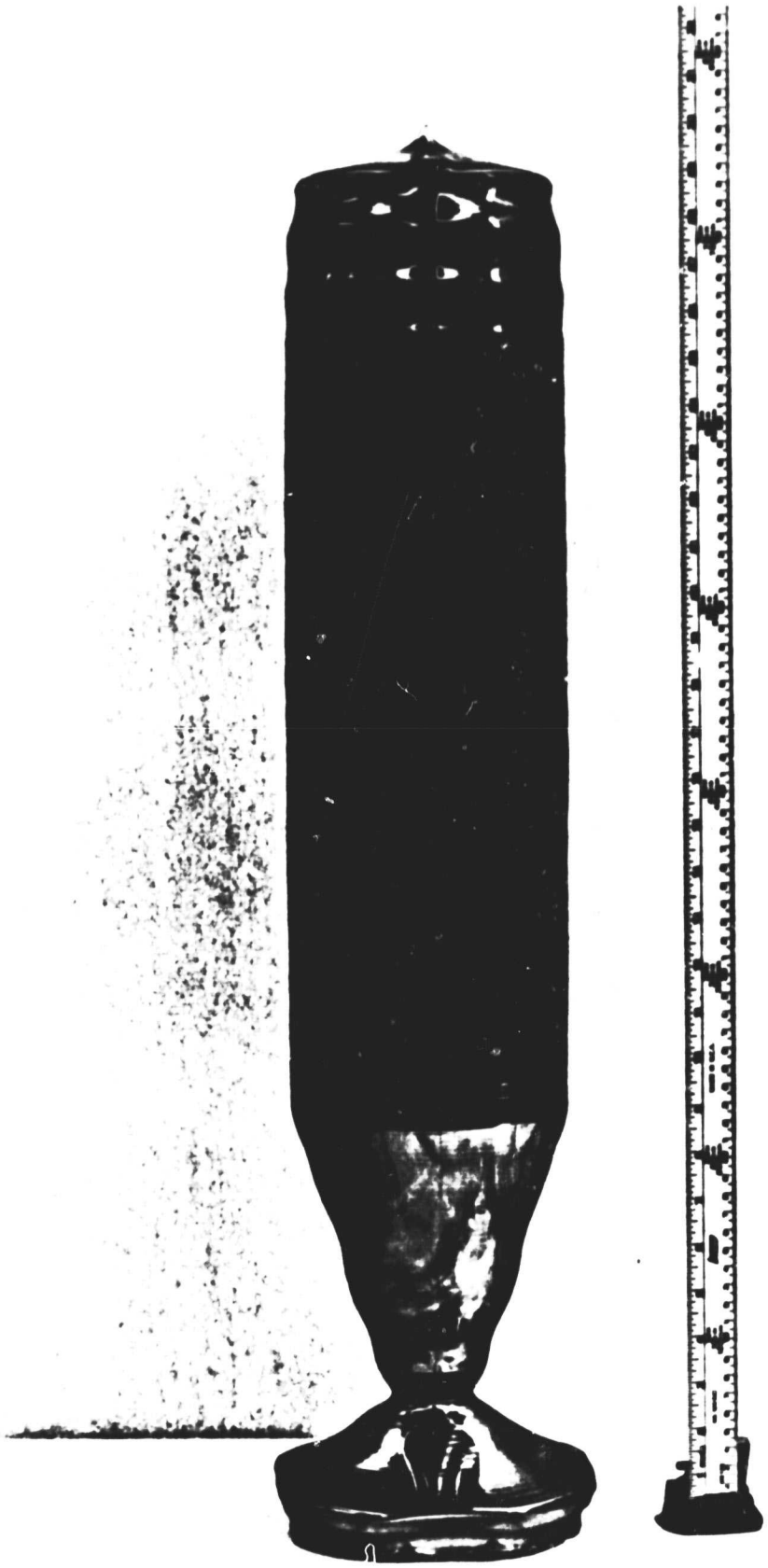

FIGURE 14
15 CM DIAMETER CRYSTAL - RUN NO. 63

RESULTS OF RUN NO. 63

Crystal Ingot Diameter	152 mm
Initial Melt Charge	28 kg
Crucible Diameter	14"
Total Ingot Pulled	25.5 kg
Pulled Yield	91.1%
Total Monocrystal (all OD)	100% (all OD)
Number of Ingots	1
Overall Throughput	1.96 kg/hr
Straight Growth Throughput	3.3 kg/hr
Total Run Time	13 hours

TABLE 5

- Reset the growth parameters for 150 mm diameter growth
- Perform required and preventative maintenance on the grower
- Initiate a limited training period for the operators involved in the continuous growth runs

Four test runs were performed during this period.

On February 25, the second attempt at growing 150 kg from one crucible was initiated. Run No. 70 was successful resulting in 151.5 kg of crystal ingots being grown from a total melt of 154.4 kg (98.1% pulled yield). Six crystals were grown over a total run time of ninety nine (99) hours. The crystals ranged in weight from 24.8 kg to 25.9 kg. Growing 150 mm diameter ingots resulted in a significant increase in the overall throughput (1.53 kg/hr).

The group of six crystals grown during Run No. 70 can be seen in Figure 15, page 43. Details of the run can be found in section 4.5.

It had now been demonstrated that 150 kg of silicon crystal could be grown from one 14-inch diameter crucible. It had also been demonstrated that 150 mm diameter crystals could be grown from a crucible over an extended period of time as part of a continuous run. The percentage of high quality crystal was less than expected due to the occurrence of a microscopic water leak in the furnace tank cover following the growth of the second crystal. Up to that time, 100% of the crystal grown was single crystal.

The last required 150 kg continuous run was scheduled for the middle of March. The weld leak was repaired, preventative maintenace was performed, and preparations made for the next 150 kg run. Our supply of virgin polysilicon was nearly exhausted with barely enough for this 150 kg run. Therefore, there was no alternative but to continue this run regardless of the overall quality of the crystal produced.

Although slightly over 150 kg was grown, the percent of single crystal

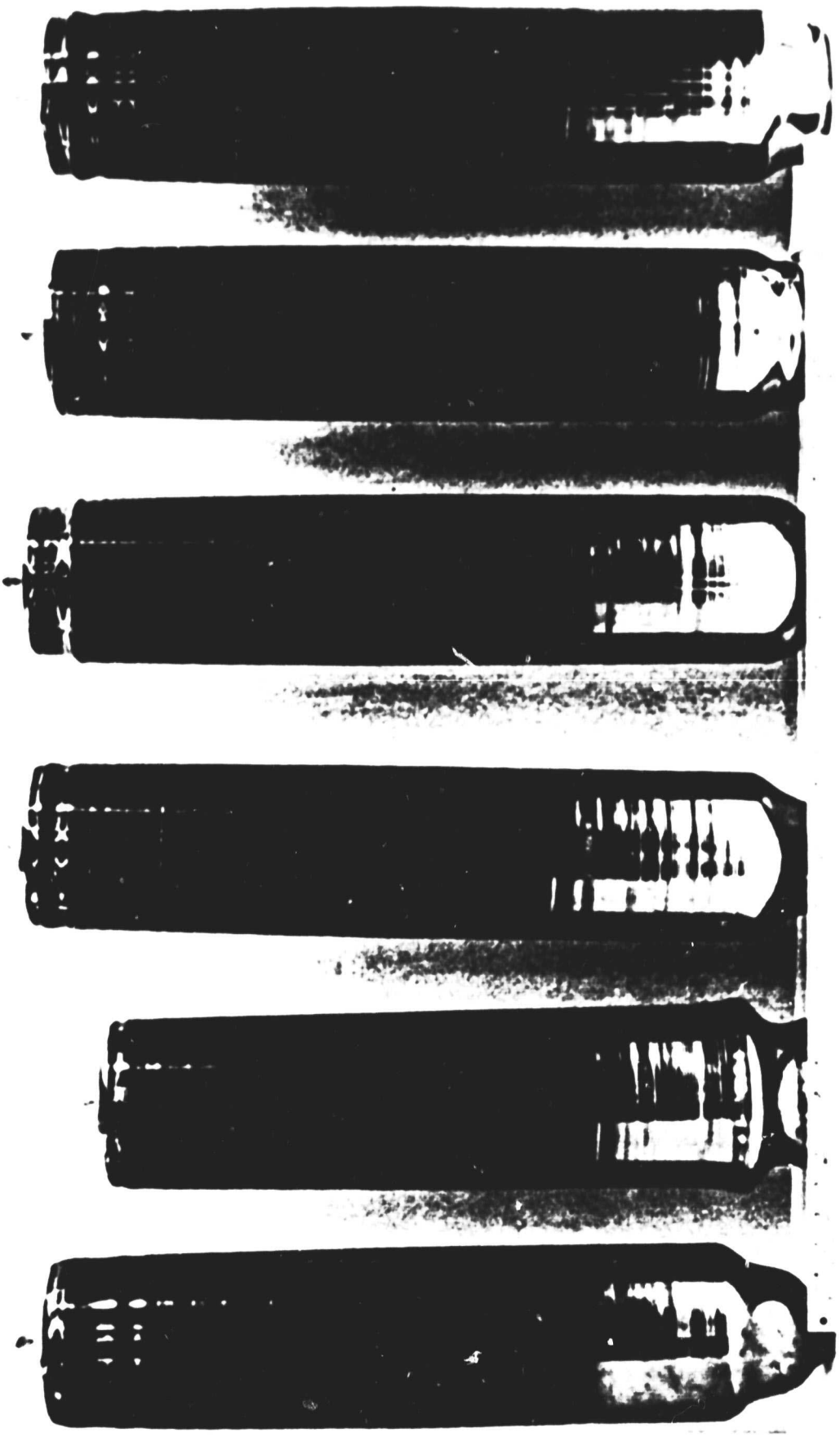

RUN NO. /0 - 150 KG

FIGURE 15

material was very low (17.2%). The six crystals grown during this run can be seen in Figure 16, page 45 and details of the run are included in section 4.5.

Another 150 kg continuous run had been demonstrated and useful data and information had been collected concerning time cycles. However, loss of single crystal structure was a major problem. Throughout the entire run the residual gas analyzer which had been experimented with since January, indicated that the furnace atmosphere was not clean. Indications were that air was getting into the furnace. This condition was visibly evidenced by greater than normal amounts of silicon monoxide being produced in the furnace. After the run was completed, the cause found to be in the argon line near the argon source.

The Kayex method of continuous growth of silicon crystal for the purpose of producing low cost silicon for the JPL "Low Cost Solar Array Project" had now progressed to the growth of 150 kg of 150 mm diameter crystals from one melt container. The process had been developed such that it could be readily transferred into a production type setting. No significant degradation of solar cell efficiencies were found to occur in single crystal silicon produced throughout the continuous run - refer to section 5.0, and cost projections based on actual run time cycles had surpassed the 1982 goals. Even though structure loss problems were at times unacceptable, large percentages of single crystal silicon were produced on many occasions and causes of structure loss problems were many times a result of an unclean furnace environment, a condition that could be corrected. Moreover, crystals with greater than 80% single crystal were produced near the end of continuous runs after eighty and ninety hours of continuous run time.

Continued proces development is needed in the areas of structure loss causes and parameters, and accelerated growth rates. However, it is the concerted opinion of those associated with the 954888 project that it was a relative success.

RUN NO. 72 - 150 KG

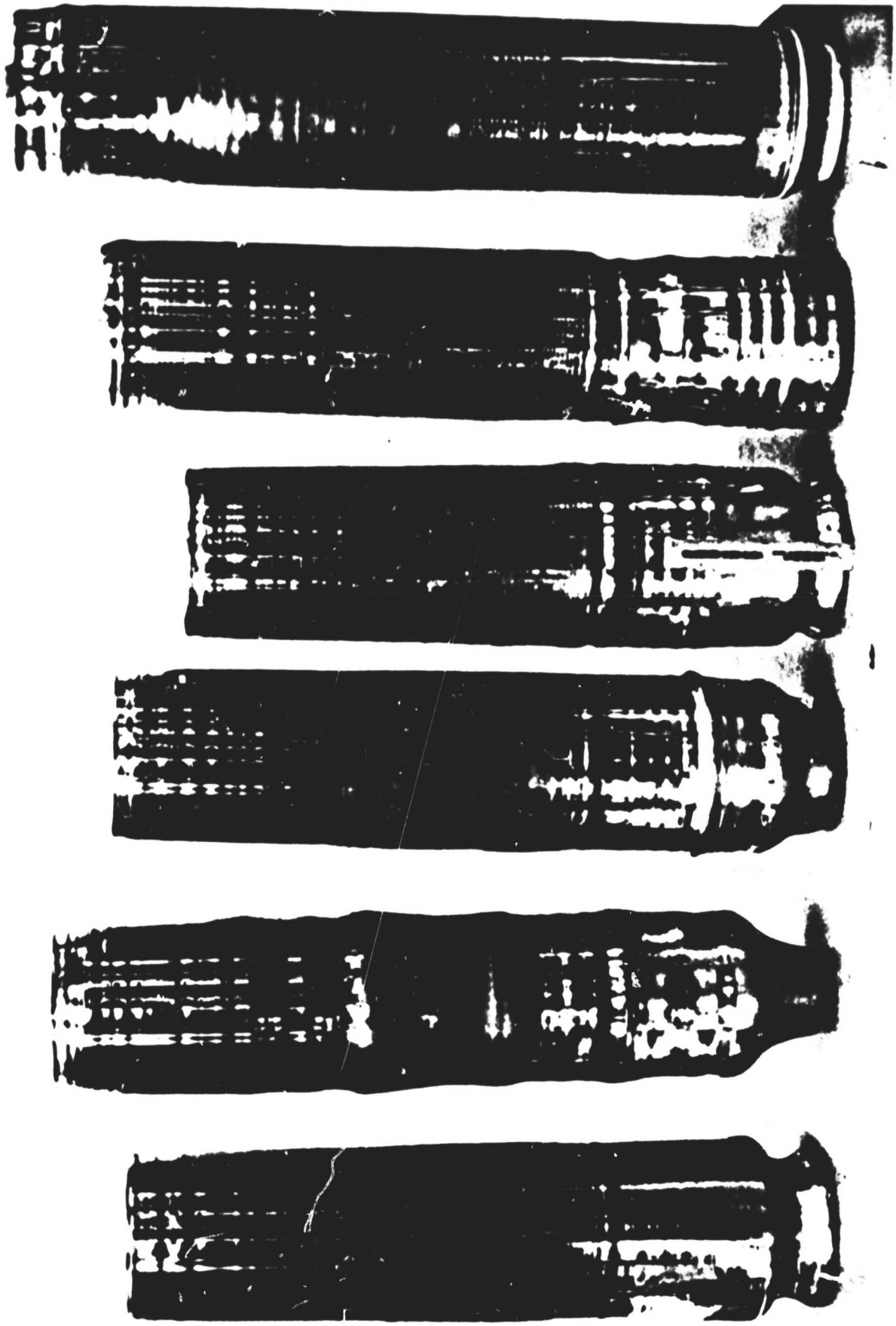

FIGURE 16

2.3 Economic Analysis Development

The 954888 contract proposal's development was directed toward a continuous Czochralski process capable of producing silicon suitable for use as low-cost solar cells that would meet the JPL cost goals of $\leq$ \$2000 (\$2800*) per peak kilowatt for completed arrays by 1982 and $\leq$ \$500 (\$700) per peak kilowatt by 1986.

The original economic model developed was based on:

1) Time-cycle data to obtain throughput information and

2) cost estimates for each cost item for crystal growth.

The results were to be expressed primarily as kilograms per hour (kg/hr) throughput and as add-on cost per kilogram (\$/kg) of crystal grown. From these figures, other calculations could be made (with certain assumptions relating to slicing), such as cost per meter^2 (\$/m^2) for crystal growth and number of crystal growers required in a production facility to produce silicon sheet at a given rate.

A state of the art "batch method" for production of silicon was formulated as a base line condition. The batch method produced one 10 cm diameter crystal per crucible and resulted in an add-on cost of \$33.09 (\$46.33)/kg. The throughput for this method was 0.93 kg/hr when a 14.4 kg crystal was grown from a 12" x 9" high crucible. The growth of a 12.5 cm diameter crystal instead of a 10 cm diameter crystal using the batch method improved the throughput to 1.1 kg/hr but did not improve the add-on cost in the same proportion \$30.00 (\$42.00)/kg.

Cost calculations indicated that the fused quartz crucible used as the melt container were a major cost item of the batch method. Subsequent updated cost calculations [6] for conventional Czochralski ingot growth resulted in

*Original cost calculations were performed using 1975 dollars as a base level. Figures in parentheses ( ) are based on 1980 dollars. (1980 dollars = 1975 dollars x 1.4).

crucible costs amounting to 48% of the cost of producing the silicon. Therefore, the growth of multiple ingots from one crucible with periodic melt replenishment appeared to be the most cost effective method of silicon production.

Section 6.0 contains a complete and thorough analysis of economic advantages and data associated with the Kayex method of continuous CZ crystal growth.

Periodic updates of cost projections have been included in 954888 reports throughout the two and one-half year contract. The December, 1978 quarterly progress report [7] included a SAMICS analysis of four methods of continuous CZ growth. These cost analyses were projections, and were based on the information and data generated by the project up to that time. This analysis chart is located on page 48, Table 6.

In addition to the cost analysis of the different continuous CZ growth methods, an analysis was performed relating the effects of growing one crystal and multiple crystals from one crucible on the CZ add-on cost. The major cost saving occurs as the progression is made from the growth of one crystal to the growth of the second crystal. This cost saving ranges from 22% to 28% depending on the continuous CZ method used. When a third crystal is grown, the add-on cost is further reduced from 9% to 11%. The cost reduction curves continue to flatten out as more crystals are grown (see Figure 17). Therefore, there is a point at which the growth of more crystals has little impact on reducing the add-on cost. Furthermore, the cost of yield losses due to the additional risk of crucible failure or low quality ingots at some point surpasses the cost reduction of growing more crystals from the same crucible.

Other factors significantly affecting the add-on cost of continuous CZ crystal growth are crystal diameter and growth rate. An increase in diameter correspondingly increases the weight per centimeter of crystal grown while an increase in the growth rate increases the number of centimeters grown per unit

SAMICS ANALYSIS OF
FOUR METHODS OF CONTINUOUS CZ

CONDITIONS	CZ NO. 1 1979	CZ NO. 2 1980	CZ NO. 3 1982	CZ NO. 4 1986
CRUCIBLE SIZE, DIA. x HT. (IN)	12 x 9	14 x 10.5	14 x 11.5	15 x 12
CRYSTAL DIAMETER (CM)	10	12.5	15.2	17.8
GROWTH RATE (CM/HR)	10	10	10	11
NO. CRYSTALS/CRUCIBLE	5	4	4	5
TOTAL POLY MELTED (KG)	105	144	170	260
TOTAL INGOT PULLED (KG)	100	134	160	250
PULLED YIELD (%)	95	93	94	96
USABLE AFTER GRINDING (KG)	87	117	140	219
USABLE INGOT YIELD (%)	83	81	82	84
TOTAL CYCLE TIME (HR)	75.4	75.1	75	80
THROUGHPUT (KG/HR), (M^2/HR)	1.12	1.56	1.86	2.74
ADD-ON COST, 1975 \$/M^2	19.40	15.07	12.97	8.56
ADD-ON COST, 1980 \$/M^2	(27.16)	(21.10)	(18.16)	(11.98)

TABLE 6

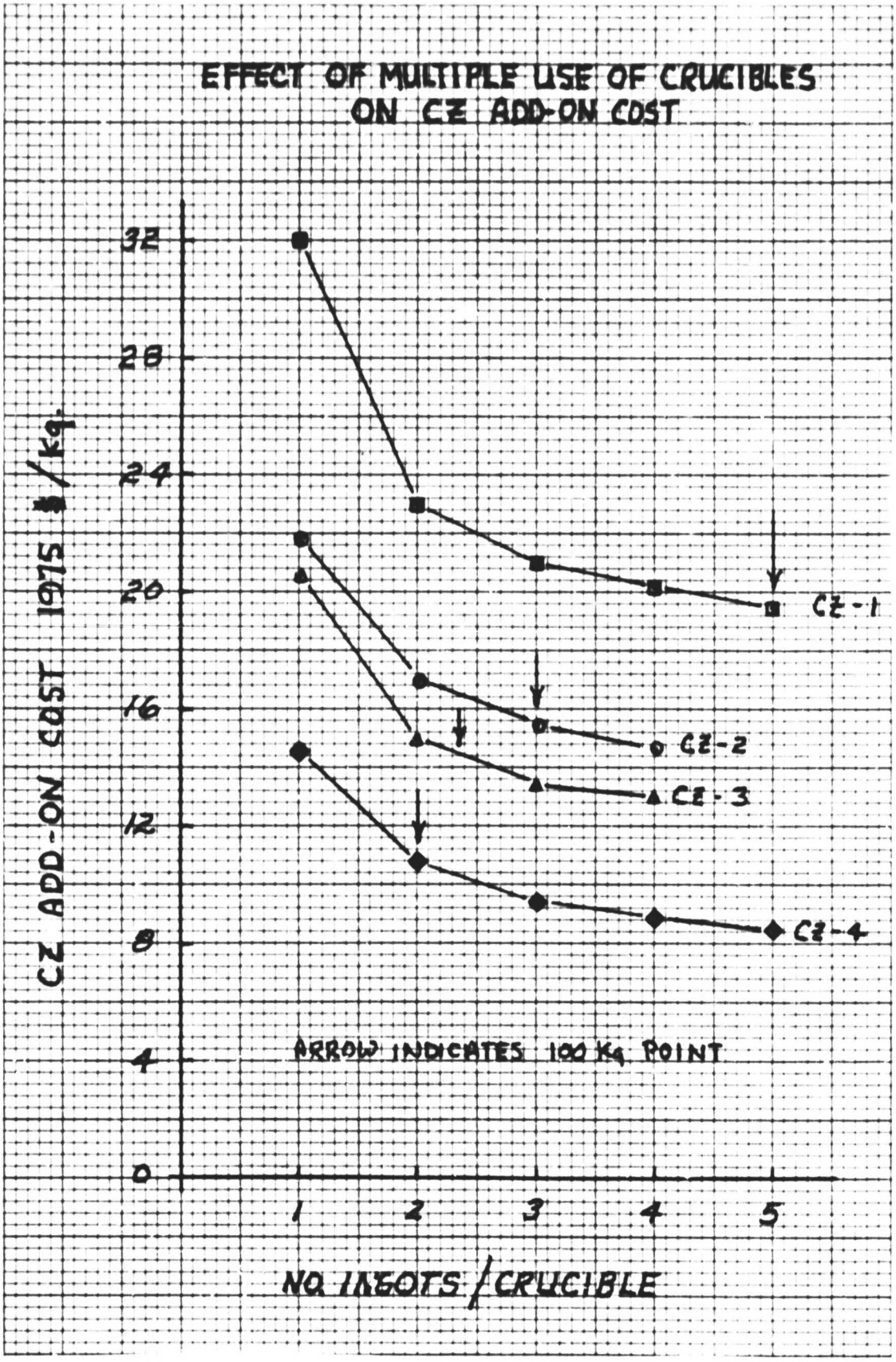
EFFECT OF MULTIPLE USE OF CRUCIBLES
ON CZ ADD-ON COST
CZ ADD-ON COST 1975 $/Kg.
32
28
24
20
16
12
8
4
0
CZ-1
CZ-2
CZ-3
CZ-4
ARROW INDICATES 100 Kg POINT
1
2
3
4
5
NO INGOTS / CRUCIBLE

FIGURE 17

time. Both factors affect the throughput for a continuous CZ growth run. Evidence of these effects can be seen in Table 6.

Finally, a cost analysis has been performed based on the most recent data produced by Phase II of the 954888 project. All computations have been completed using present 1980 costs. The Cont. #3*(page 51) cost projections are based on the best observed process parameters experienced to date. The Cont. #3* projects the cost factors if six (6) crystal ingots are grown from one 14-inch diameter crucible. Each crystal is twenty-five kilograms (25 kg) in weight for a total of 150 kg of silicon produced. The crystals are 15 cm in diameter and are grown at a rate of 10 cm/hr. Therefore, under optimum conditions, a throughput of 2.09 kg/hr can be realized leading to an add-on cost for silicon of $16.14 per kilogram. Assuming that the future cost of polysilicon will be $14/kg, the total cost of the silicon ingot prior to being cut into wafers and processed into solar cells would be $36.30. This figure, when converted to cost in dollars per peak watt ($/Wp) results in an add-on cost of $0.254/Wp.

Details of Cont. #3* cost projections, other cost projections and economic model information can be found in section 6.0 of this report, starting on page 249. In order to better relate the progress made by Kayex in terms of cost reduction, a cost analysis was performed for two batch type operations using time cycles and cost data consistent with that used for Cont. #3*. It is assumed that these cost analyses would be representative of a 1980 state-of-the-art production facility growing one crystal per crucible. Batch #1 process assumes an 18 kg melt using a 12-inch diameter crucible with a 70% after ground yield. A 10 cm diameter crystal is grown at a rate of 7.6 cm/hr. The resultant throughput under these conditions is 0.73 kg/hr. The add-on cost is $51.12/kg.

If a 14-inch x 10-1/2 inch crucible is used to grow one crystal (Batch #2), another set of cost values are generated. The assumptions for Batch #2 are:

a) 30 kg melt with 75.3% after ground yield

b) a 12.5 cm diameter crystal

c) a growth rate of 7.6 cm/hr

A 31% increase in throughput is realized by Batch #2 (0.95 kg/hr). The add-on cost is decreased by approximately 17% to $42.19/kg. Refer to pages 267 through 272 for the time cycles and SAMICS/IPEG Input Data cost calculations for Batch #1 and Batch #2.

From the preceding add-on costs, it can be readily seen that Cont. #3 allows for a 68% cost reduction from Batch #1 and a 62% cost reduction from Batch #2.

The comparison for Batch #1, Batch #2, and Cont. #3* expressed in dollars per peak watt ($/Wp) is shown below. The availability of $14/kg polysilicon material is assumed in each calculation.

Batch #1	Batch #2	Cont. #3*
$0.49/Wp	$0.43/Wp	$0.25/Wp

The statistical data presented in this section was prepared using the SAMICS/IPEG guidelines provided by the Jet Propulsion Laboratory. These guidelines have been used in conjunction with the best approximations that could be determined from actual crystal growth runs. The results indicate that significant cost saving can be realized toward the LSA project goal by growing multiple silicon crystal ingots from one fused quartz crucible using the equipment and methods developed by Kayex Corporation.

2.4 Solar Cell Results and Evaluation

Solar cells have been produced for many years using silicon as a base material. However, the cost of these solar cells has been high in relation to other means of electricity production.

The "Low Cost Silicon Solar Array Project" has included a design goal for array efficiency greater than 10%. Due to array design requirements, packing factors of cells and hardware and other variables involved in module and array manufacture, a cell efficiency considerably greater than a 10% terrestrial efficiency is required. Kayex's objective was to produce silicon of a quality sufficient to fabricate solar cells with a terrestrial efficiency $\geq$ 14%.

Solar cell efficiency results are reported according to two testing methods. The standard testing method is referred to as "Air Mass 0" (AM0). This testing method is based on the solar spectrum in outer space. The second method of testing solar cell efficiency is referred to as "Air Mass 1" (AM1). This testing method is based on the solar spectrum at the earth's surface for optimum conditions at sea level, sun at its zenith. "Air Mass" is defined as the secant of the sun's angle relative to the zenith, measured at sea level.

All solar cell efficiency data and results obtained under the 954888 contract were tested under AM0 conditions. AM1 results were arrived at by using a conversion factor based on the AM0 values.

During the first two years of the project, a conversion factor of 1.4:1 (AM1:AM0) was used as indicated by JPL. All reports written through December, 1979 used the 1.4:1 conversion factor. Continued information concerning the relationship between AM1 and AM0 resulted in a revision of the conversion factor to 1.2:1 (AM1:AM0). All results included in this report will use the 1.2:1 conversion factor.

Table 7 is a condensation of all solar cell efficiency results accumulated

during the 954888 contract. Included in the table are average values for AM0, AM1 (converted) and fill factors (CFF). All cells tested were fabricated according to standard state-of-the-art techniques. Each cell was 2 cm x 2 cm in size and had a standard antireflective coating applied. All cells reported in Table 7 were processed and tested by a well-established solar cell manufacturer recommended by JPL.

Several conclusions can be made based on the information presented in Table 7:

- Taking into account the standard deviation for efficiency results for cells made from the same wafer, efficiencies do not tend to significantly decrease as a continuous run progresses to the end (first crystal to last crystal). Run No. 62 average efficiency values (not including polycrystalline material) actually shows an increase.
- Polycrystalline material from continuous runs fabricated into solar cells averages 15% to 25% lower in efficiency than single crystal material.
- Many cells from continuous runs were equal to or surpassed the efficiency results of the high quality control samples provided by the testing lab.

It is impossible to develop any correlation between the solar cell efficiency and the position in the crystal the wafer came from (Top, Middle, Bottom). Some results show a decrease from top to bottom and some show an increase based on the data from Table 7. It is our observation that most variations in efficiency results are a factor of the fabrication, processing and testing of the solar cells. This can be evidenced by the deviations from the mean for four cells fabricated from the same wafer. Deviations have ranged from 0% to as high as 13% with the average being 2% to 4% in single crystal material. Polycrystalline material tends to exhibit a higher average deviation.

Details concerning solar cell data can be found in Section 5.1, starting on page 202.

These solar cell efficiency results exhibit factual knowledge concerning

the effects of continuous CZ crystal growth on the quality of material produced. It can therefore be concluded that the Hamco CG2000 RC crystal grower can produce multiple silicon crystal ingots from one fused quartz crucible suitable for the production of high efficiency solar cells.

2.5 Proposed Future Work

The continuous Czochralski growth method developed under the 954888 project is now ready for conversion to a production type operation.

Future development recommendations would be put into two classifications:

Specific recommendations for further cost reductions are:

1). Cost reductions through increased throughputs and decreased labor costs.

2). Continued improvements in high quality crystal yields.

- Accelerated growth rates
- Larger crystal size - both diameter and total weight
- Accelerated melt and recharge
- Automation of growth process - microprocessor control
- Further process development work is needed to more precisely identify structure loss mechanisms and develop equipment and process modifications that will eliminate or minimize the cause.

3.0 Growth Facility Design, Construction and Modification

The production of several crystals from one container by the Czochralski (CZ) method required equipment and process modifications not commonly used in the semiconductor device industry. In general, these modifications are required for the purpose of permitting some method of silicon replenishment without freezing the residual melt and container or contaminating the silicon.

Although a number of methods of accomplishing continuous CZ growth can be devised, it is very important that the chosen method be suitable for a production environment and that it is attractive in terms of safety, reliability, and cost. In a production-type process, variables should be well controlled and equipment should not require operators with great skill or technical ability.

It is the purpose of this project to develop equipment and process to achieve low-cost continuous CZ production of silicon single crystal ingot by repeated refilling (recharging) of the vitreous silica crucible and subsequent crystal growth cycles.

The equipment used was a Hamco CG 2000 Production Crystal Grower. Certain modifications* were made to the grower to enable periodic replenishment of silicon into the crucible and removal of grown crystals.

*The following design changes and modifications were developed prior to, and in anticipation of, awarding of the 954888 contract:

1). Vacuum-tight isolation valve.

2). Enlarged Pull Chamber

3). Modified Bead Chain/Cable Mechanism.

The Optical Diameter Control System was an upscaling of a modified commercially available Optical Diameter Control System developed by Kayex in 1968. The 14-Inch Hot Zone was an upscale of a preexisting hot zone.

3.1 Design Changes and Modifications Necessary for Recharging.

Since the vitreous silica crucible is always destroyed by fracture during the cooling-off cycle due to the thermal expansion difference between silicon and silica, it was necessary to provide a means to refill the crucible while maintaining it at high temperature. Furthermore, it was necessary to continuously maintain an inert atmosphere surrounding the molten silicon and the graphite furnace parts, to prevent oxidation. A pressure range of about 25 mbar minimizes the deposits of silicon monoxide which tend to collect on the cooler surfaces of the furnace. The monoxide, formed by the reaction between the molten silicon and the silica crucible, sometimes falls from surfaces to land in the melt causing loss of zero-dislocation crystal structure, twinning or polycrystalline growth. Therefore, the following criteria were established for the design of the furnace modifications:

1. The recharge operation must permit the crucible to remain at or above the melting point of silicon.
2. The hot zone must be always protected by vacuum or low argon pressure.
3. Polysilicon insertion and crystal removal must be performed in a safe reliable way without contamination of the silicon or the hot zone environment.

A new CG 2000 production crystal grower was constructed with special modifications to the chambers to make it suitable for recharging. The pull chamber was enlarged to permit polysilicon to be stored within the furnace in a ready condition for recharging. (The initial effort utilized polysilicon rods for recharging. A subsequent design was suitable for niblet or nugget silicon - Section 3.4).

Other initial modifications to the chambers included a vacuum-tight isolation valve, larger view ports, a larger pull length capacity and a

larger growth chamber suitable for 14-inch diameter crucibles -(Section 3.3). Subsequently, additional modifications to the crystal growth facility were made, including a recharge mechanism, a larger capacity cable-pull mechanism, an automatic diameter control optical system suitable for 12.5 cm diameter crystals, and a dopant replenishing fixture.

Peripheral equipment to accommodate recharging included a crystal-poly transfer device for loading raw material and retrieving grown crystals, and a special vacuum pumping manifold to control furnace pressure during the crystal retrieval process - Section 3.2.

Figure 18 is a photograph of the JPL continuous CZ facility after installation in the room specially prepared and designated for the project.

Figure 2, page 15 and Figure 19 on page 62 are schematic illustrations of the growth chambers with modifications showing both the crystal growth and the recharge modes of operation.

Figure 12, page 32 is a later photograph after additional modifications had been completed.

3.1.1 Isolation Valve.

A "flapper"-type isolation valve was designed for simplicity, reliability and ease of cleaning. It is water cooled, relying on an O Ring seal. A manually operated external lever actuates the valve. The isolation valve allows the operator to maintain a vacuum in the furnace while the pull chamber door is opened for removal of crystals. The performance of the valve over many runs has been excellent. The water-cooled O Ring has not been degraded at all by pulling hot crystals through the valve. Figures 20(a), 20(b) and 21 show details of the new isolation valve.

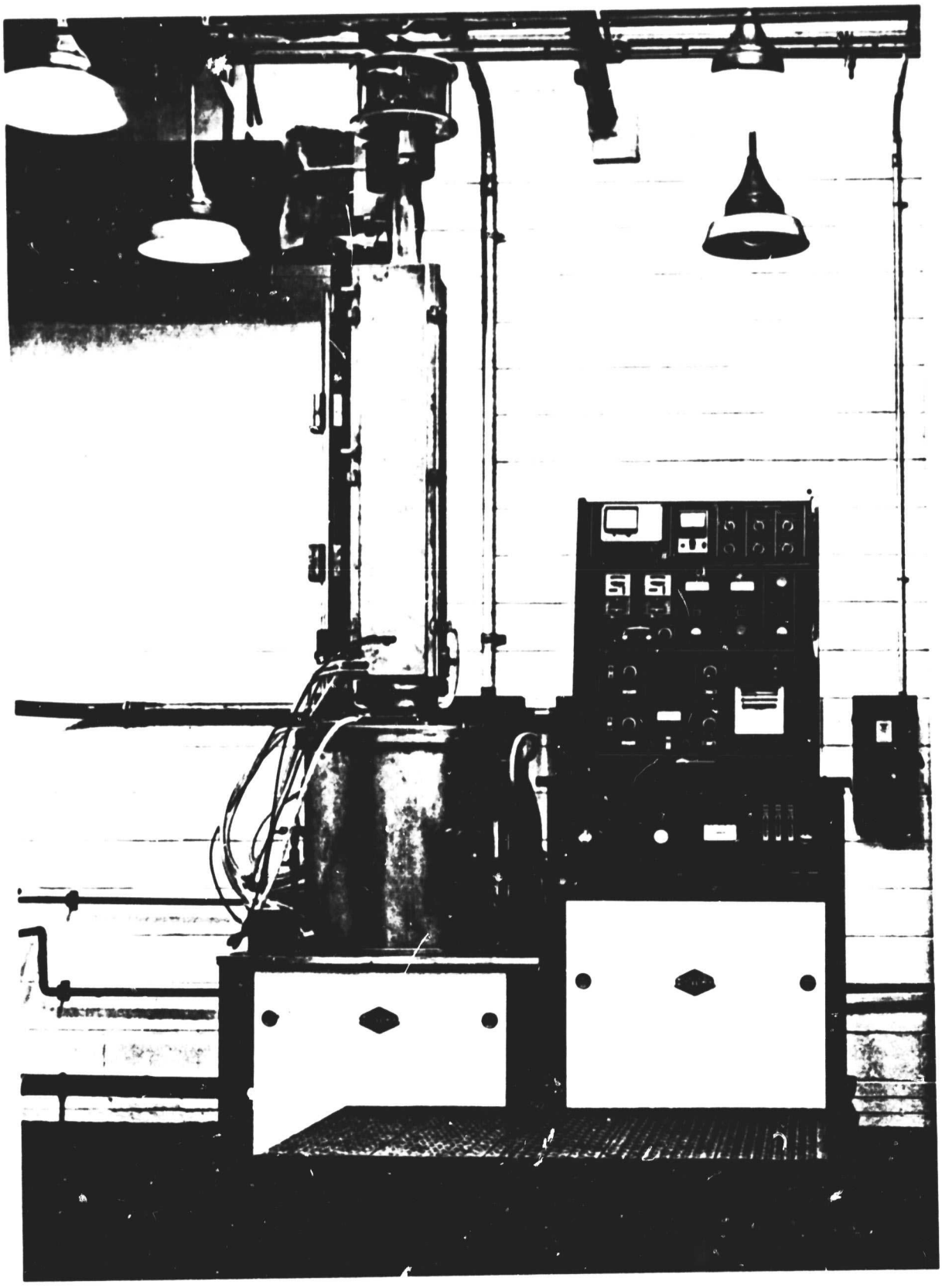

FIGURE 18
HAMCO/JPL FACILITY

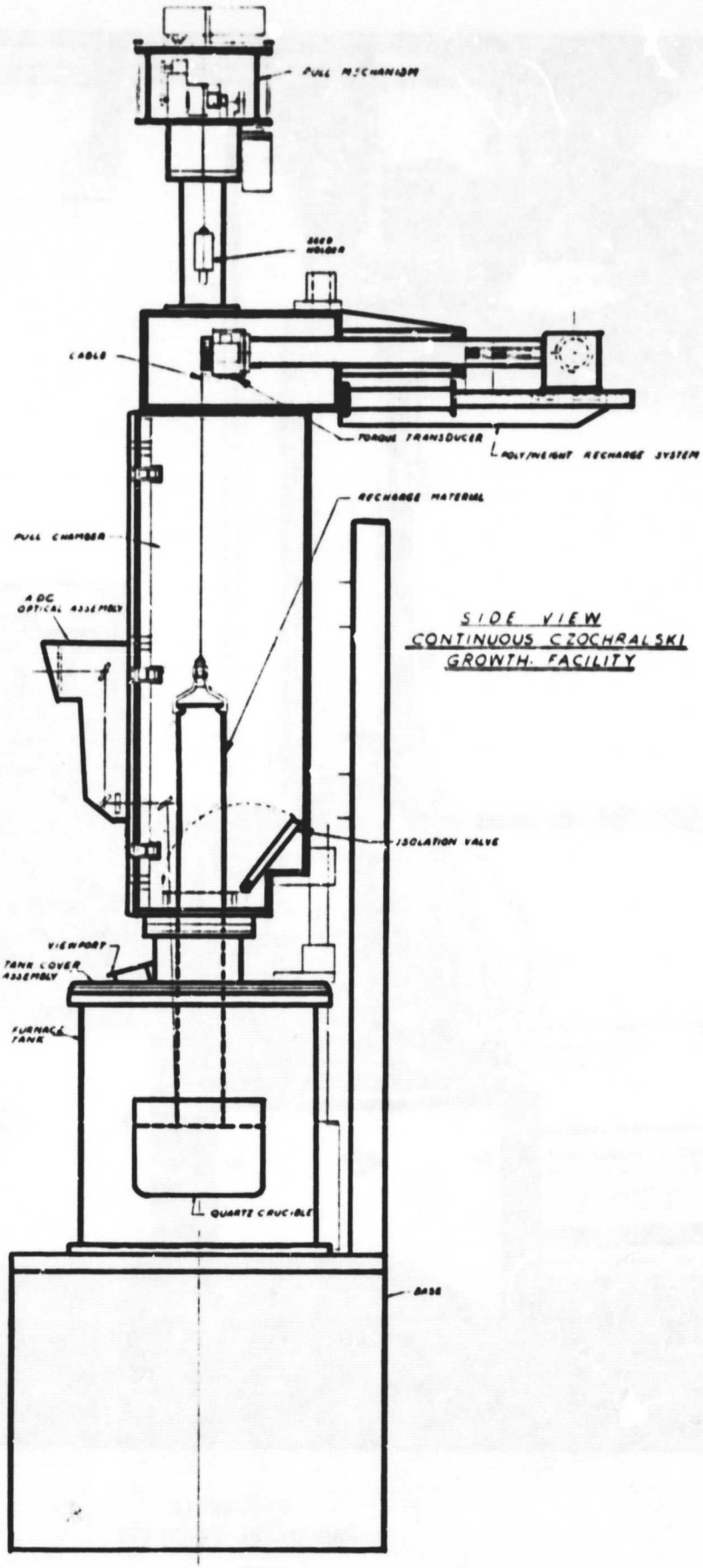

FIGURE 19 - RECHARGE MODE

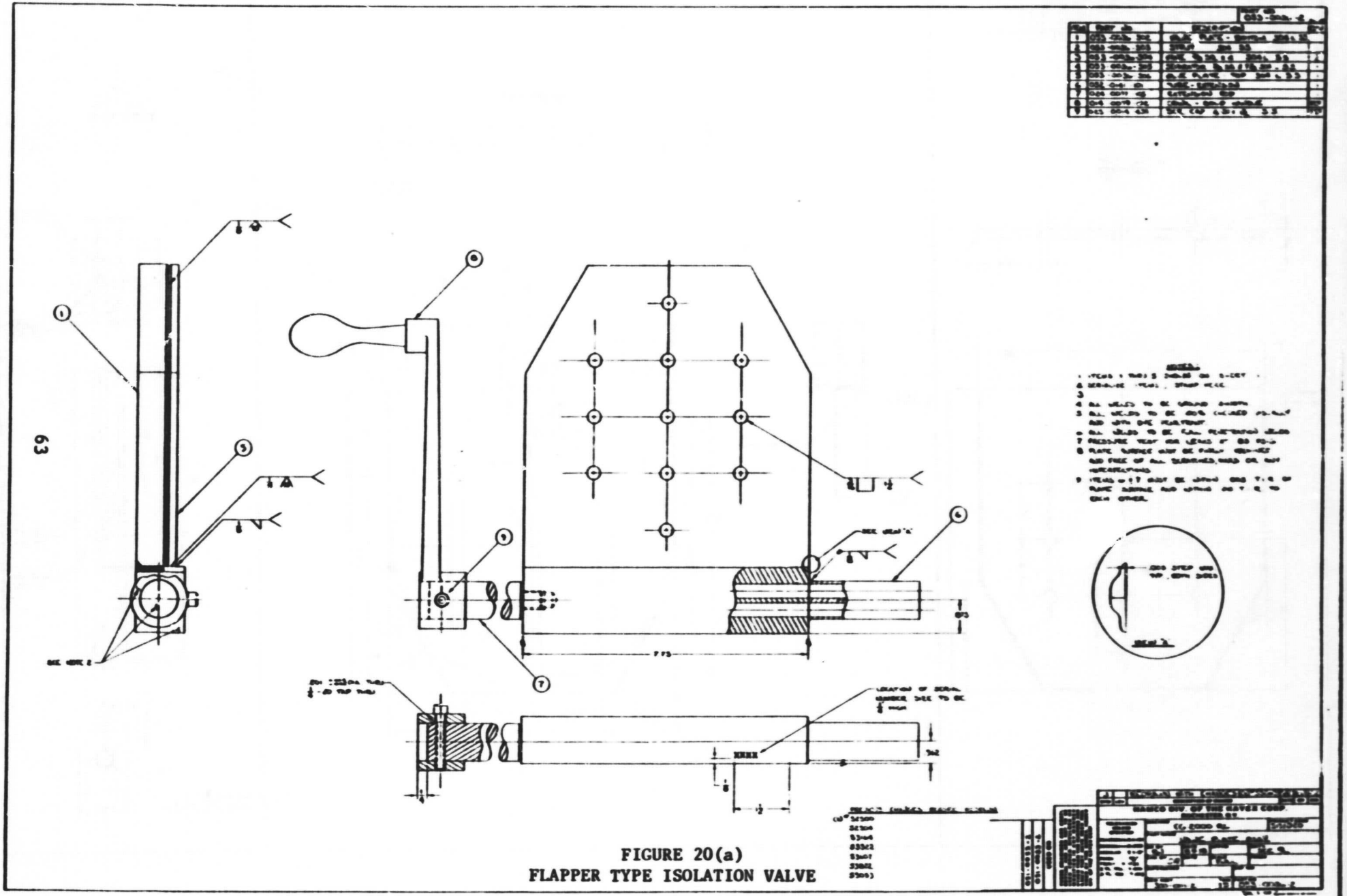

FIGURE 20(a)
FLAPPER TYPE ISOLATION VALVE

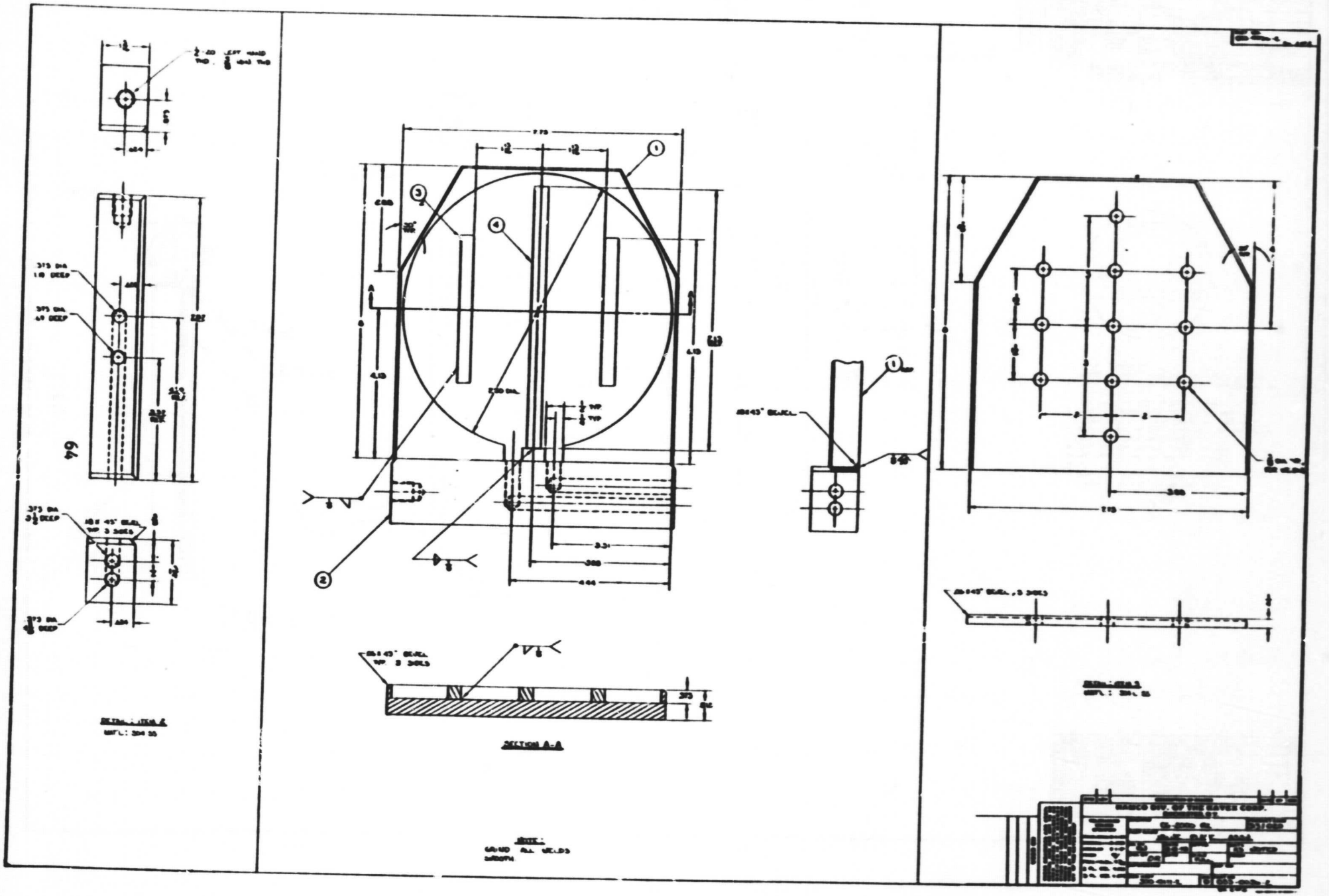

FIGURE 20(b)

FLAPPER TYPE [illegible]LATION VALVE

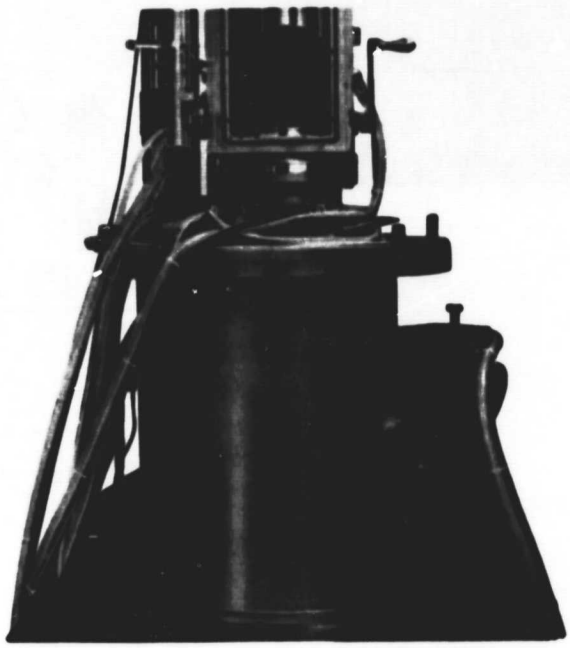

Flapper Type Isolation Valve
Figure 21

3.1.2 Enlarged Pull Chamber

The crystal grower is equipped with an enlarged pull chamber to provide space for storage of poly silicon inside the furnace (see Figure 22).

The pull chamber was fabricated from 304L stainless steel and is water cooled.

The three piece pull chamber assembly, which includes the vacuum tight isolation valve, is bolted to the furnace tank. A 20.32 x 106.68 cm (8" x 42") door on the pull chamber provides easy access for crystal removal and chamber cleaning.

An enlarged viewport was designed into the pull chamber door to allow the operator to see when the crystal had cleared the isolation valve and to allow for a periscope projection system (ADC) which projects an image of the melt. The pull chamber was designed to be operated under purged inert atmosphere or vacuum.

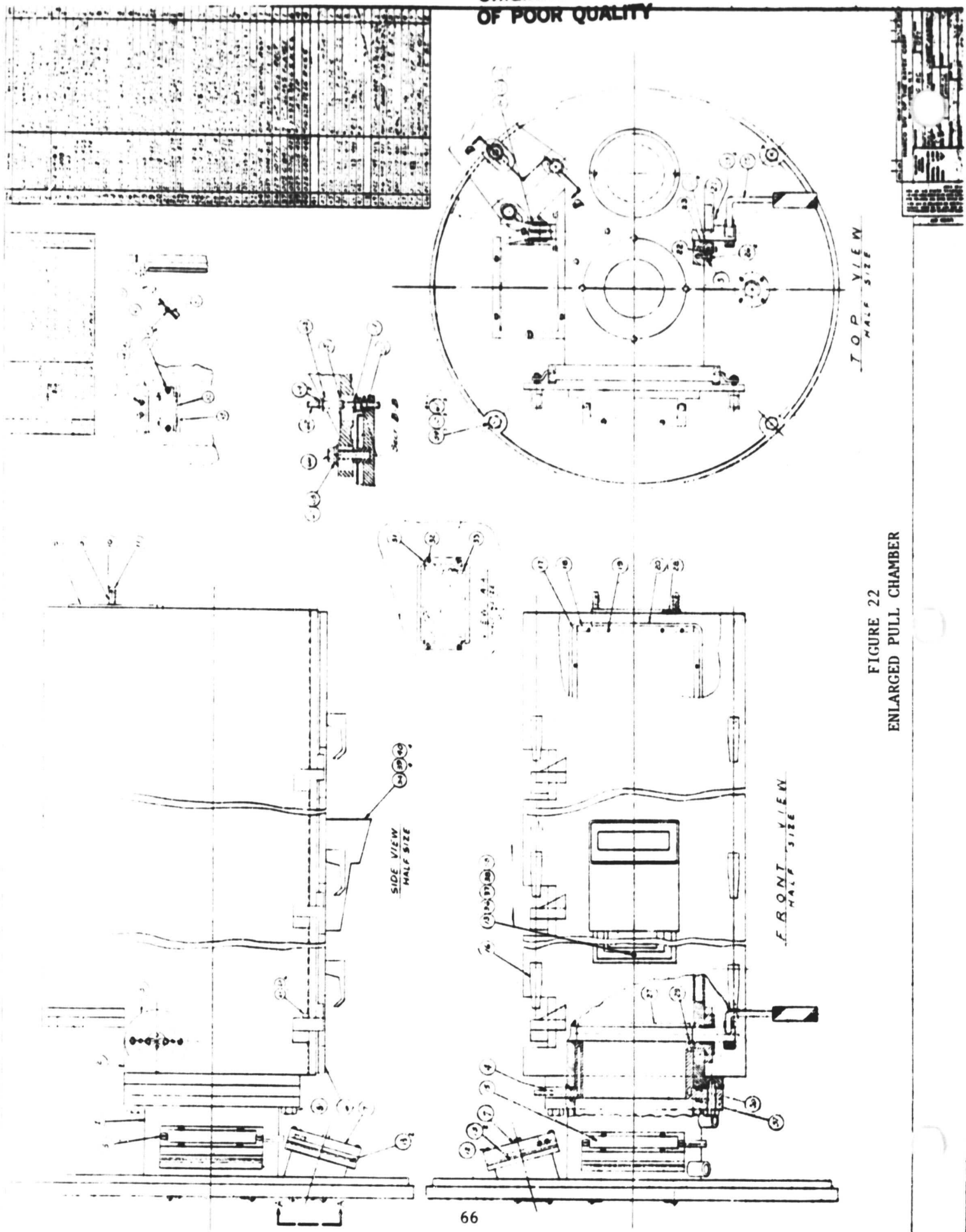

FIGURE 22
ENLARGED PULL CHAMBER

3.1.3 Automatic Diameter Control (ADC) Optical System

A standard ADC optical system normally used for the CG 2000 was not suitable for use on the CG 2000 with modified throat and vacuum isolation valve.

A redesigned optical system utilizing appropriate lenses for sighting through the valve throat or through a separate view port was required. This system was optically and mechanically different from the existing CG 2000 system, but would interface with the same electronic controls.

The design of this unit was made similar in principle to a standard CG 2000, but incorporated a larger focal length lens. A 53 mm, 13 inch focal length lens was chosen which would display the image of the growth interface with exactly a 2:1 reduction for convenience in determining crystal diameter.

Also, a pull chamber door modification was required, relating to the port through which the ADC system sights. A small round port was removed and a larger rectangular port was designed. The larger port allowed for some adjustment of the optical system and also allowed the operator to visually verify that the crystal clears the valve prior to closure of the valve and subsequent crystal removal. (See Figures 23 - 26).

The ADC control operates through a dual photocell detector system. The signal processing of the detector is capable of eliminating false signals created by faceting flats or crystal orbiting by outputing through a three mode process control system. The ADC system is not affected by normal variations in furnace temperature. The ADC system is capable of maintaining a crystal diameter tolerance of $\pm$ 1.27 mm.

ORIGINAL PAGE IS
OF POOR QUALITY

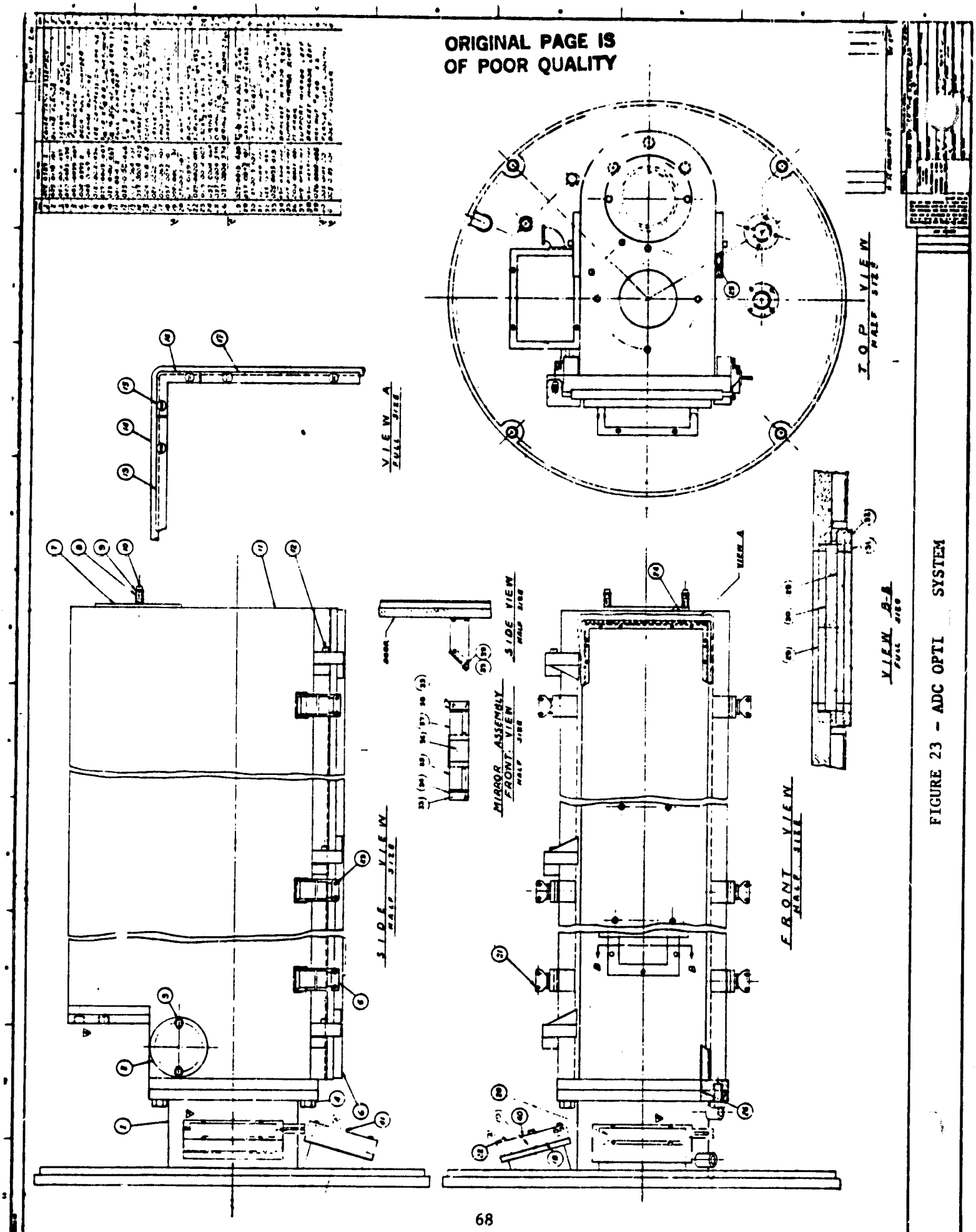

FIGURE 23 - ADC OPTI SYSTEM

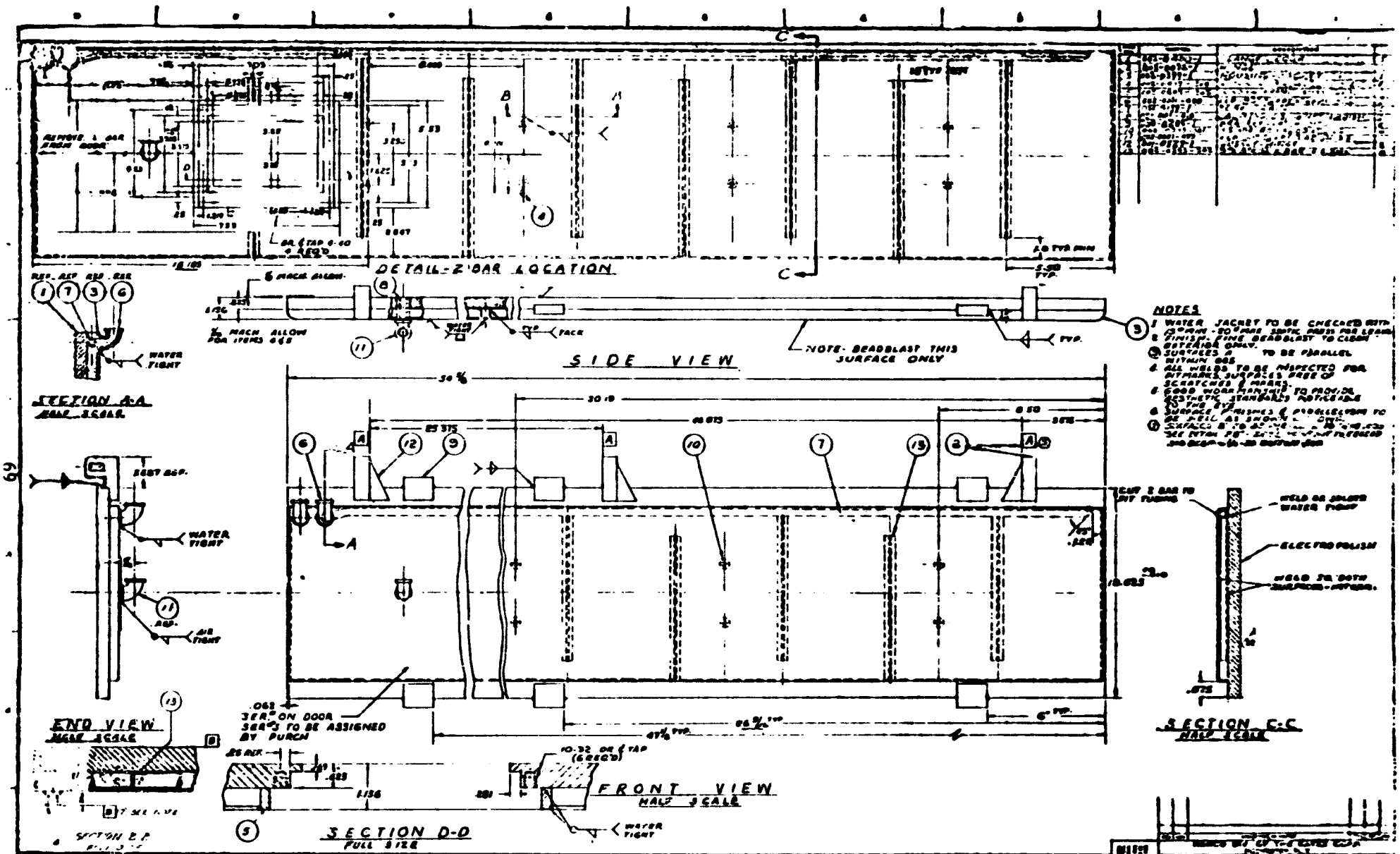

FIGURE 24 - ADC OPTICAL SYSTEM

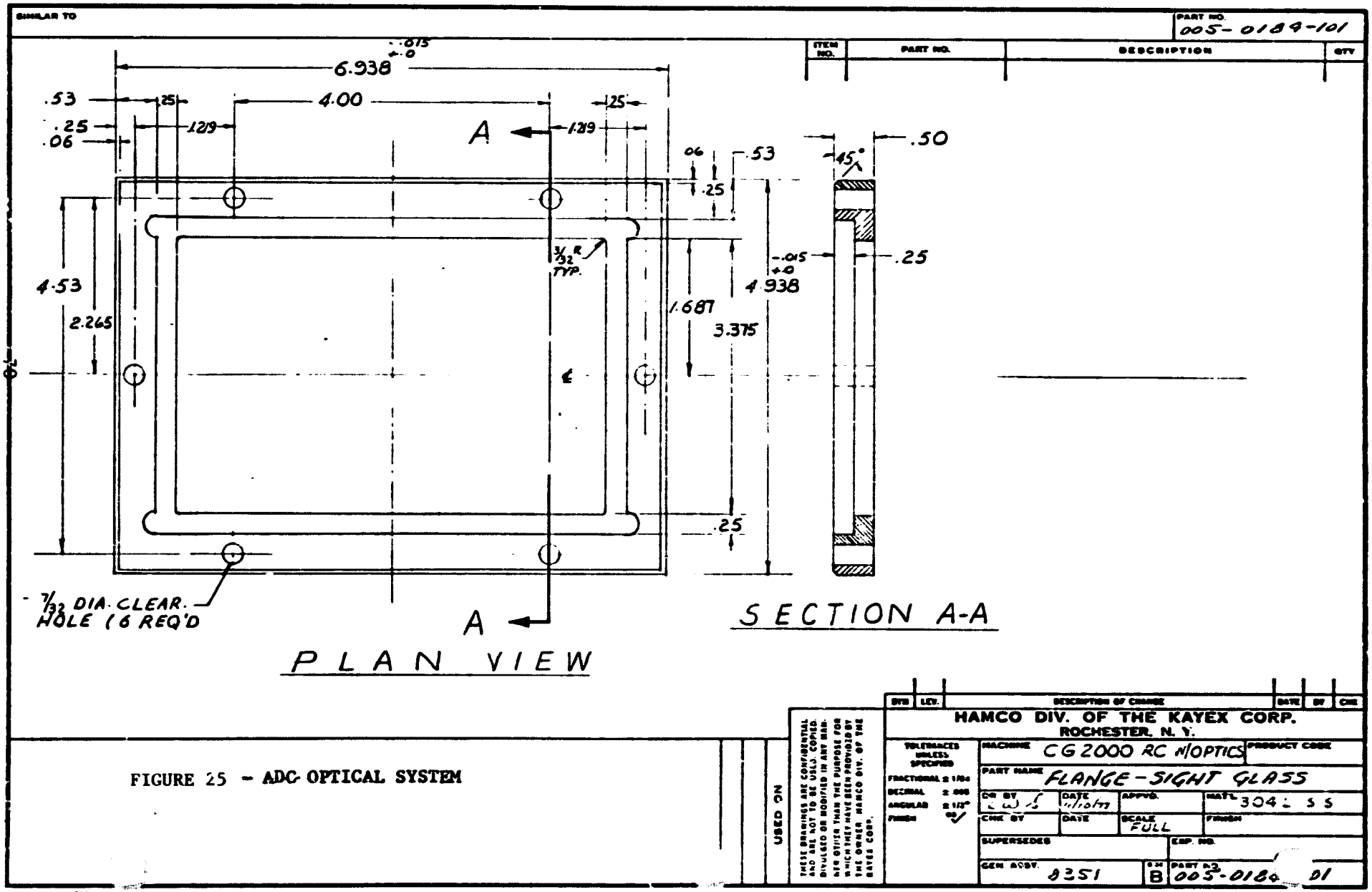

FIGURE 25 - ADC OPTICAL SYSTEM

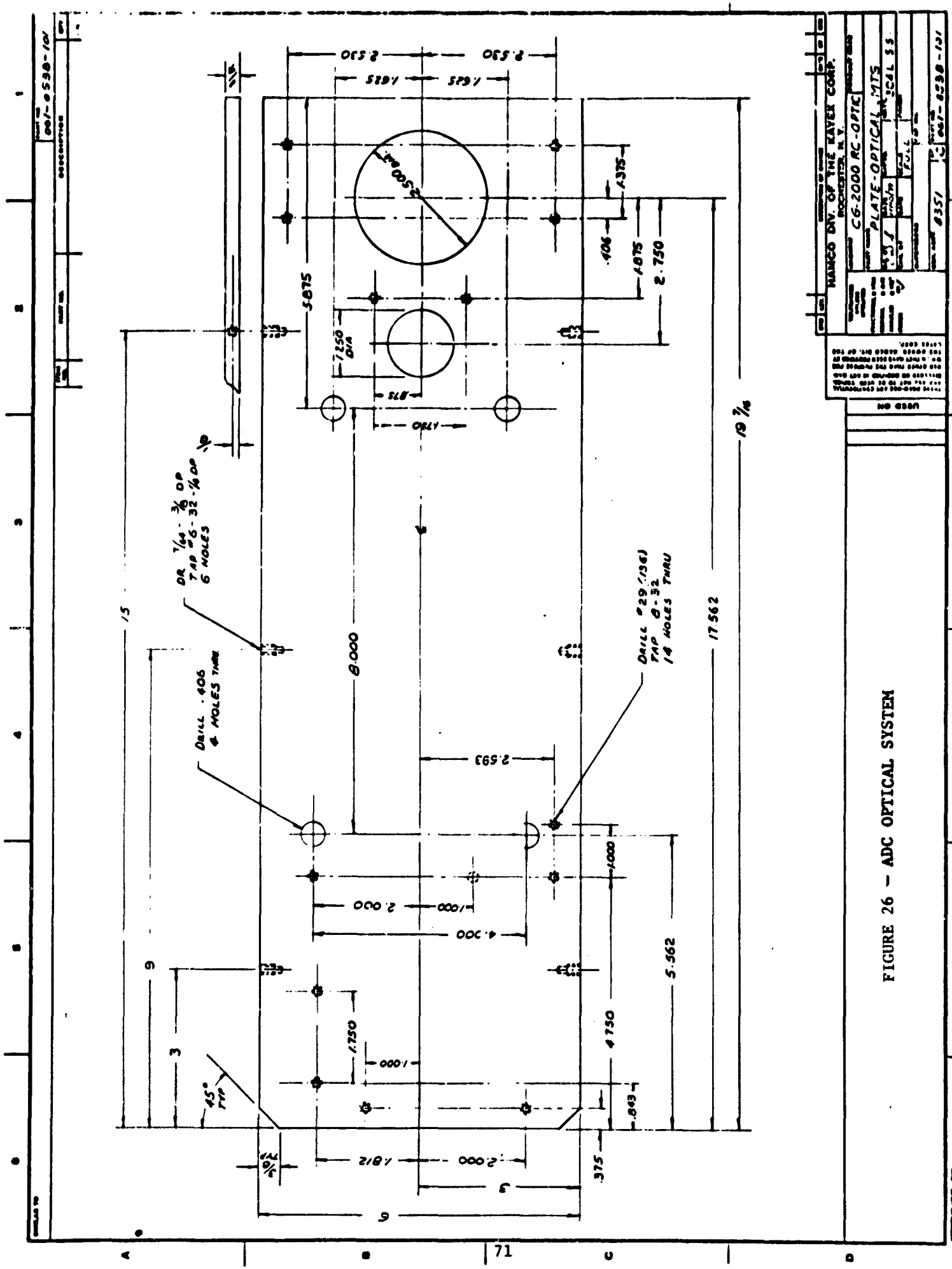

FIGURE 26 – ADC OPTICAL SYSTEM

3.1.4 Poly Weight/Recharge System

The key factor in continuous CZ growth is the reliable and controlled addition of polysilicon to the hot crucible.

The first approach on this project was to develop process and equipment for handling polysilicon that is in rod form. Rods of 30 - 40 kg are available in the industry now.

The continuous method incorporates the growth of large crystals (using presently well-established methods) with a subsequent crucible recharge after each crystal. A separate mechanism capable of lowering the poly into the crucible while simultaneously weighing the rod allows for a more efficient and controllable process.

The modified CG 2000 used throughout the project had an enlarged pull chamber which made it possible to contain both a billet of poly silicon of up to about 60 kilograms, as well as a crystal 5 inches in diameter by 40 inches long (See Figure 2, page 15).

The poly billet is supported on a cable/winch mechanism at the rear of the pull chamber, behind the growing crystal. The mechanism allows the poly to be moved forward directly over the crucible and lowered for the hot fill or recharge process (Figure 19). The seed is raised up out of the pull chamber into the spool piece so as not to interfere with the process. Thus, one cycle of back-fill, opening the chamber, and pump-down is avoided each time the crucible is re-filled.

A weight measurement device was designed as part of the mechanism that raises or lowers the poly billet at any point during recharge. As the billet is being melted, it is lowered slowly. Melt-back continues until the proper amount of poly has been added to the crucible.

After the crucible is refilled, the unmelted poly is raised into the pull chamber and moved back into the rear position to make room for

normal crystal growth. Figures 27 and 28 show a poly rod before and after recharging. The weight measurement device consists of mechanical fixturing and a strain transducer. Appropriate circuitry is provided to allow display of the weight on a digital meter in grams. After consideration of a number of alternatives, the concept of a torque sensing transducer fixed to the end of a horizontal shaft (Figure 29 was the preferred route). The shaft rotates for raising or lowering the poly and translates horizontally to move the poly over the crucible. A commercially available torque sensing strain-gauge transducer was purchased and included in the design.

The POLY WEIGHT/RECHARGE DEVICE is a removable, independent unit positioned between the pull chamber and the pull mechanism support. This minimized rework cost to the pull chamber, increased the recharge capacity of the furnace and simplified the modification procedure.

The control circuitry for the Poly Weight/Recharge Device provides for (1) continuous weighing of the poly so that accurate measure of the amount remaining (and therefore the amount melted off) is always available, and (2) automatic shut-down of the lowering motor when the desired amount of silicon has been melted. A tachometer feedback DC-PM motor raises and lowers the poly while the lateral movement is produced by a hydraulic cylinder operating off of the main hydraulic pump.

The recharge mechanism required that a slot be machined in the top of the pull chamber to allow the recharge cable to be moved backward and forward. Additionally, a chamber overpressure relief valve had to be relocated, as the recharge mechanism covered the original valve.

The controls for the poly weight/recharge mechanism allows the operator to manually move the poly rod horizontally (hydraulic drive) and verically (DC motor) either at high speed or at a controlled rate. A DC-PM motor with a tachometer feedback system is used to control the

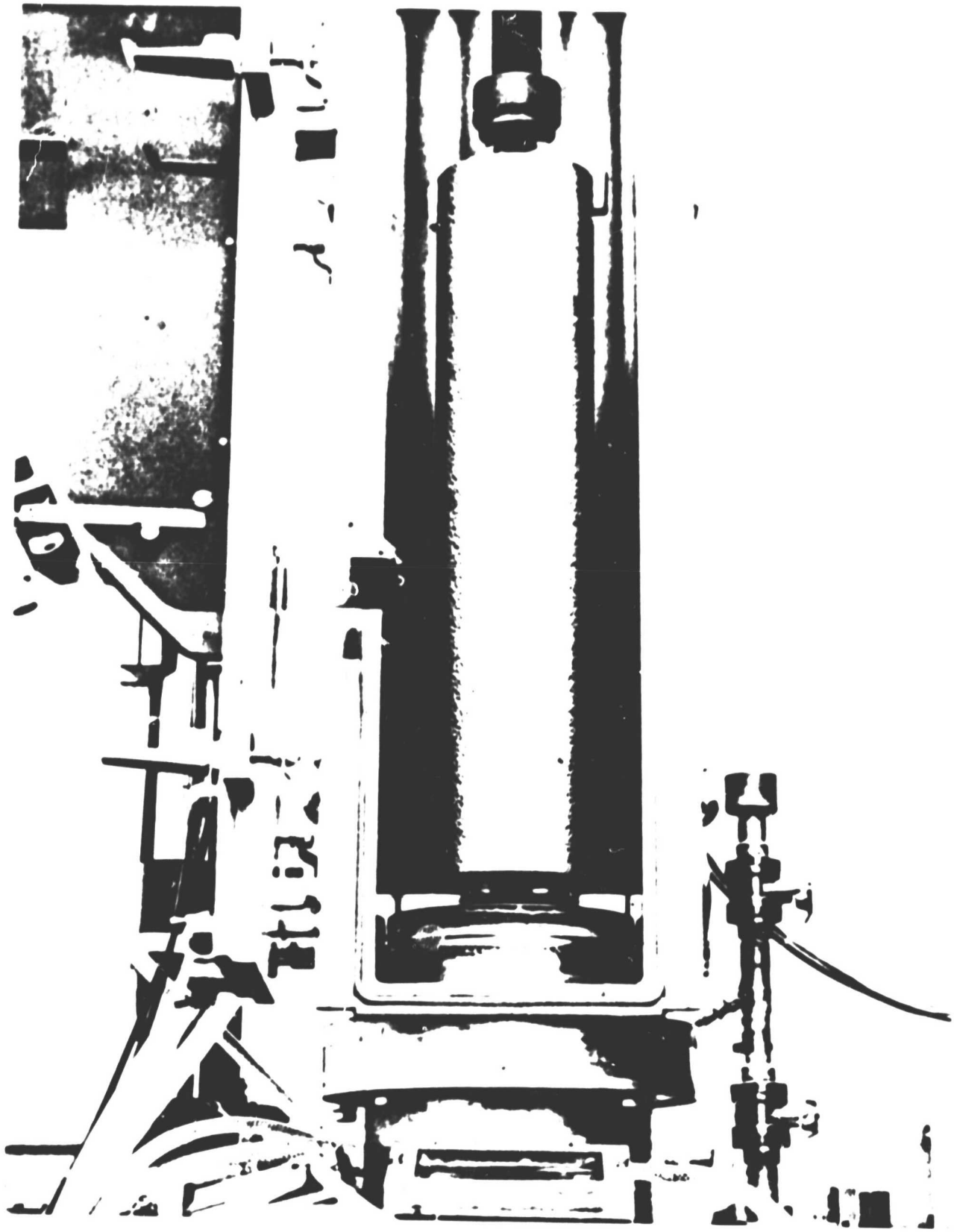

FIGURE 27
POLYSILICON ROD READY FOR RECHARGING

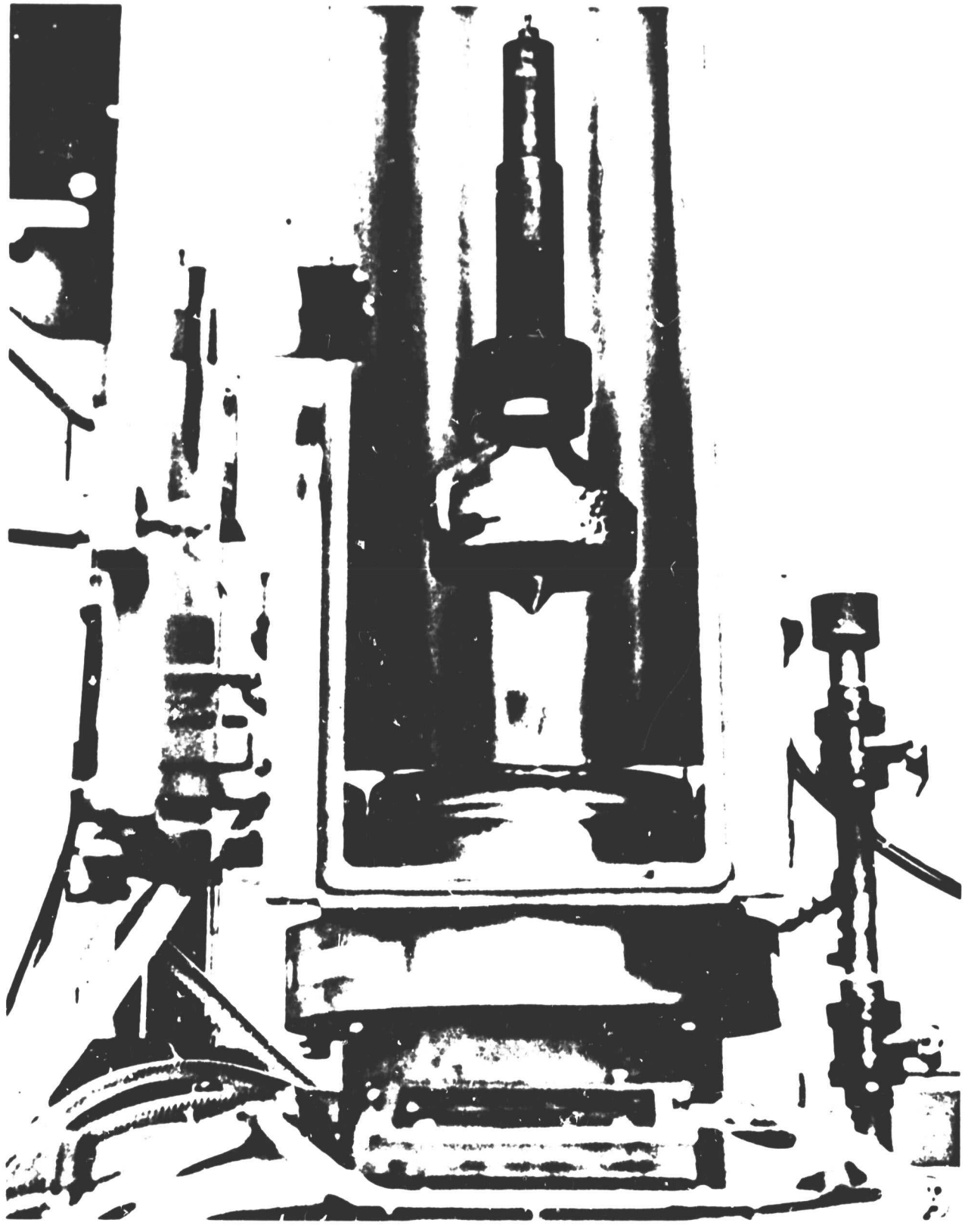

FIGURE 28
POLYSILICON ROD AFTER RECHARGING

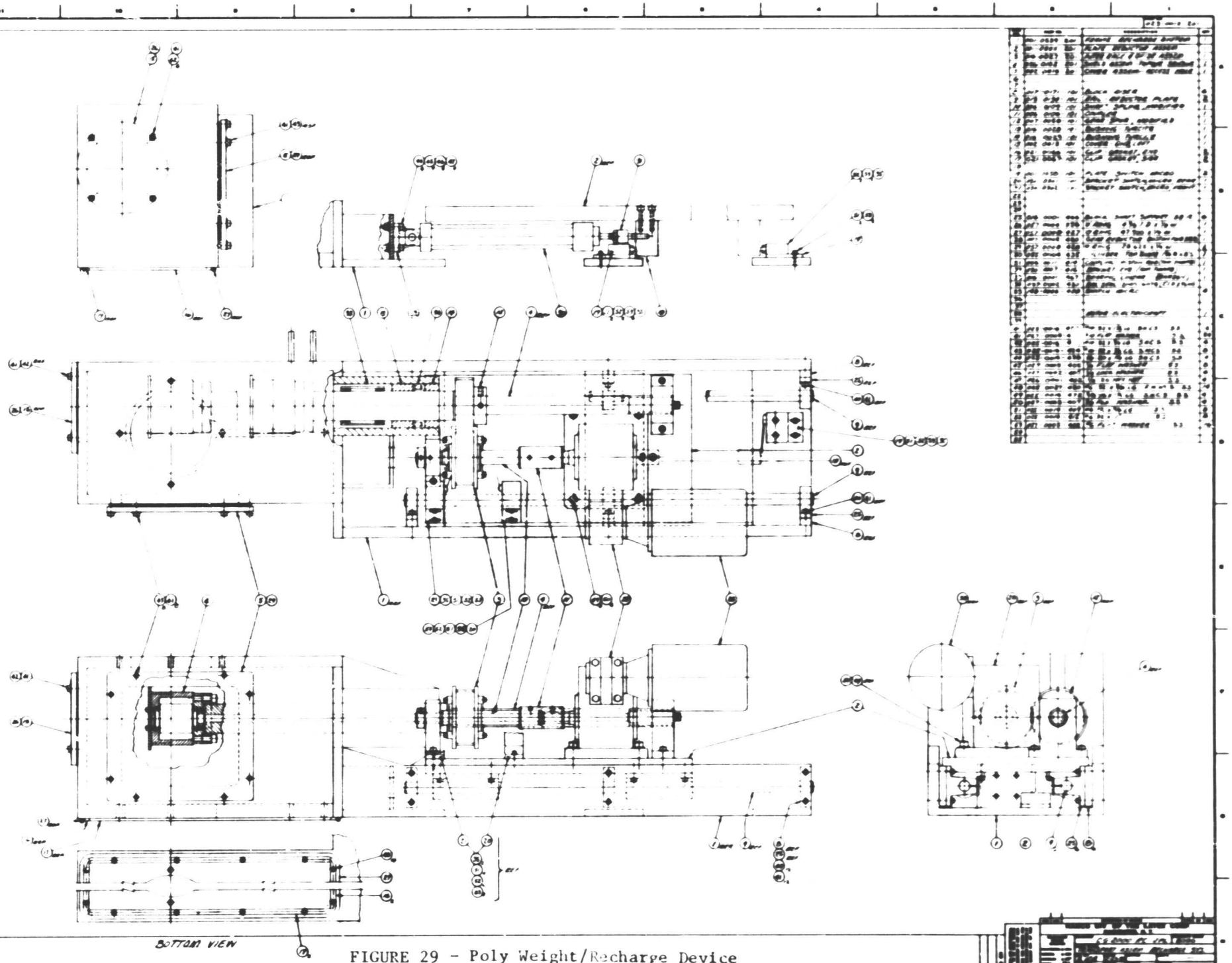

FIGURE 29 - Poly Weight/Recharge Device

melt-off rate. This is quite critical to the process. The rate of lowering is measured with a digital meter calibrated in inches per hour.

A torque-sensing strain gauge is used to measure the weight of the poly rod. This is calibrated in kilograms and reads to the nearest 0.01 kg. The poly rods used during the project weighed about 20 kg. In actual practice, the weight system is set at the desired melt-off amount, and when the indicated weight reaches zero, the melt-off is terminated by stopping the motor.

The device (Figure 12) permits the charge of poly silicon to be added to the hot crucible in a controlled manner. It allows a display of the amount of poly left unmelted, melts back at a predetermined rate and stops at a preset value when a poly rod is being fed.

3.1.5 Dopant Replenishing Fixture

After a single crystal ingot has been grown, dopant material as well as polysilicon must be added in the recharge step. This required a separate fixture with a vacuum interlock chamber and appropriate valve to allow dopant pellets to be added to the crucible without permitting air to enter the furnace chamber.

A separate opening into the chamber was preferred rather than the use of a view port.

The dopant fixture (Figure 6, Page 21) consists of two vacuum valves with an air-lock chamber between which can be evacuated using the secondary pumping system. With the lower valve closed, dopant pellets can be added through the upper valve. After the upper valve is closed and the air-lock evacuated, the lower valve is opened, allowing the pellets to drop into the crucible.

Dopant pellets will slide down a tube into the crucible. The tube is retracted away from the crucible at other times.

Dopant can be added in premeasured amounts at any time during melt-down or melt replenishment.

3.2 Special Equipment for Handling of Hot Crystal Ingots

3.2.1 Crystal/Poly Transfer Device

A device which would positively support ingots of up to six inches diameter by 42 inches long was required. The maximum weight of such an ingot is about 50 kg or about 110 lbs, and therefore a rugged structure, separately moveable in relation to the crystal grower, was required. Hot crystals and poly rods must be safely and reliably transferred from and to the growth facility.

The transfer device was built (Figures 7 & 8) for this purpose. This design employs a clamping support for holding the crystal mounted on a commercially available manual lift hoist. The crystal/poly can be rotated to a horizontal position for placing on the cooling or storage rack (Figure 9). The rack design is shown in Figure 30.

3.2.2 Crystal/Poly Storage Rack

Crystal/Poly Rack - A moveable rack was designed and constructed to hold crystals or poly. (Figure 30). This was convenient for multiple recharge runs. The crystal/poly transfer device has been designed to facilitate placing crystals on the rack or removing poly from it.

a. Poly-Load Method

The ingot is secured by the transfer device, moved into place inside the CG 2000 pull chamber, and attached to the cable. A winch mechanism inside the grower is operated until the ingot is completely supported by the cable. The transfer device can then be moved out of the way.

b. Crystal-removal Method

After the pull chamber door is opened, the device is moved up

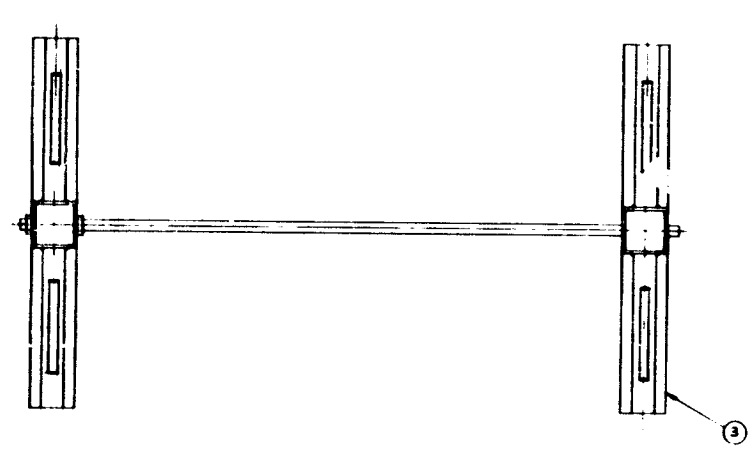

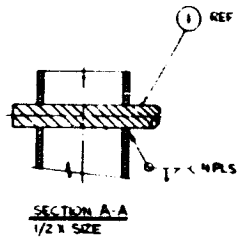

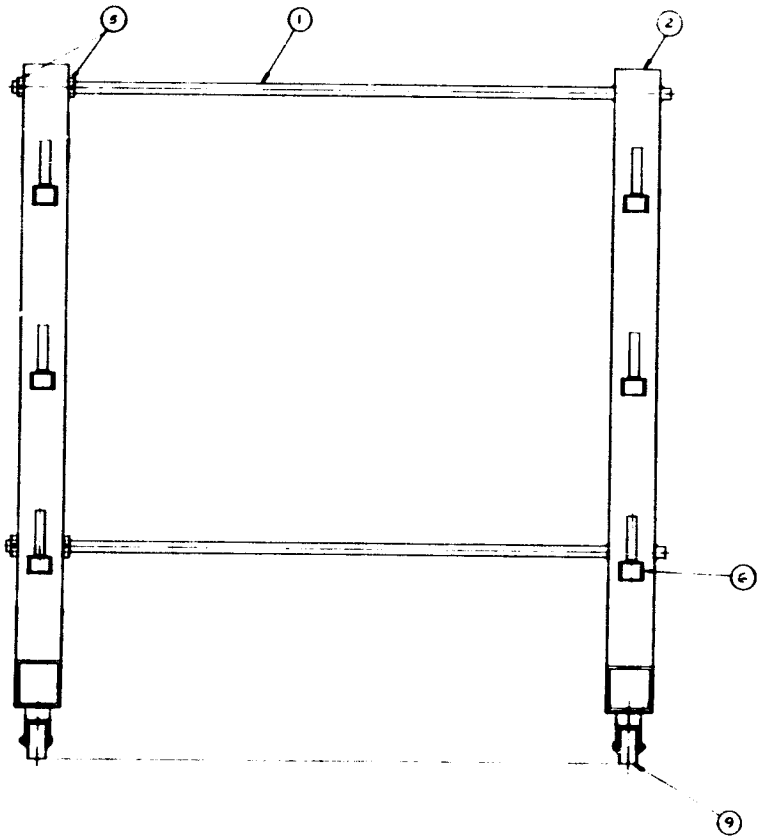

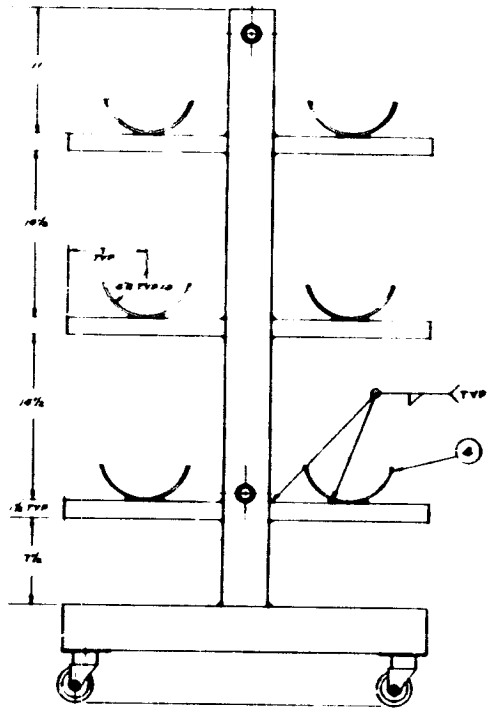

FIGURE 30 - Crystal ly Storage Rack

to the grower and inserted into the pull chamber. A clamping/support mechanism positively contains the ingot. The crystal is lowered until the weight is completely removed from the cable. At this point, the seed may be cut or the whole seed chuck may be removed from the cable and a new seed attached. The crystal is wheeled away from the crystal grower and transferred to the cooling fixture.

3.3 Design Changes and Modifications for the Growth of Large Diameter, High Weight Crystals.

The Hamco standard bead chain pull mechanism required certain modifications for the purpose of this project.

The standard seed lift (pulling) mechanism utilized a stainless steel bead chain. In order to increase the capacity of the unit to 40 kilograms and to permit accurate weighing of the growing crystal, the device was strengthened and the bead chain was replaced with a polystrand stainless steel cable.

This included increasing the size of the main drive shaft and bearing and improving the method of attaching the main gear to the shaft. A device to measure weight of the growing crystal (or melting poly) was also added having a 40 kg readout capacity.

The present cable seed lift mechanism utilizes a 122.47 kilogram test strength stainless steel polystrand cable. The cable is wound on a traveling, horizontal reel capable of maintaining accurate alignment. Seed rotation is accomplished by rotation of the entire seed lift mechanism on a precision preloaded bearing spindle - Figure (31).

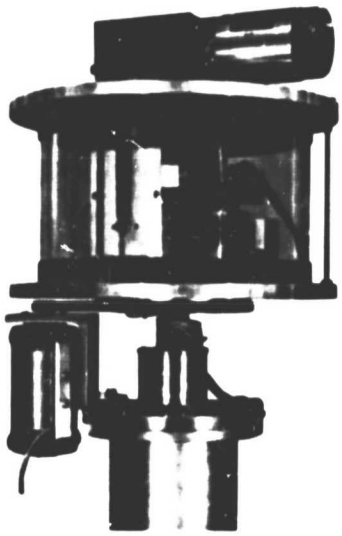

FIGURE 31
SEED LIFT MECHANISM

The internal mechanism is under reduced pressure during vacuum operations. The cable assembly is bolted to the top of the upper pull chamber extension and can easily be removed for repairs or maintenance. The cable and seed chuck can be used as a plumb bob for alignment of the crystal seed with respect to the center of crucible rotation and the melt surface. A digital readout of the crystal length and weight can be continuously displayed on the control panel. The cable mechanism tolerates orbital motion of the grown crystal without loss of structure.

3.3.2 14-Inch Hot Zone

In order to assure that the goal of 20 kg crystals could be achieved, furnace internal graphite parts to accommodate a 14 inch diameter crucible were designed and built.

In deriving the program plan, it was believed that the 14-inch hot zone could be retrofitted to the JPL crystal grower without major changes to the chamber. However, after a more careful study of the problem, it was concluded that the size of the chamber was insufficient to safely accommodate the hot zone, especially in the case of a molten silicon spill.

Since a 14-inch crucible can hold up to 40 - 45 kilograms of silicon, it was imperative that a reliable insulating spill tray be incorporated into the furnace design to contain the molten silicon in the case of a crucible failure. It was found that an adequate spill tray required considerably more space than anticipated and that the furnace chamber must increase in height a total of seven inches. Since the project cost estimate did not include funding for a new furnace tank, and a 7-inch tank extension would cost almost as much as a new tank, the Company decided to purchase a new replacement tank for the

JPL grower using Kayex funds.

The 14-inch hot zone is considered to be very important in meeting JPL cost goals as it makes the growth of larger diameter crystal economically more attractive and results in a significant reduction in the crystal growth add-on cost.

Due to the fact that the inside height of the growth chambers would be 7 inches higher than a standard furnace the electrodes needed to be redesigned, along with the crucible shaft and pedestal assembly.

3.4 Special Equipment Designed for Recharging Poly Silicon

3.4.1 Poly Rod Attachment Device

A convenient and reliable method of attaching heavy poly rods was required. A clamping device to securely hold poly rods of up to 50 kg was designed and built to attach to the cable of the poly weight/recharge device. In order to evaluate it and to proceed with hot-filling experiments, the poly was initially suspended from the seed lift mechanism for lowering into the crucible.

The poly attachment device (Figure 5, page 20), fabricated of molybdenum was found to perform adequately for recharging with poly rods up to 5 inches in diameter. Two notches are required to be cut in the rod to accept the teeth of the clamp. Poly can be melted off to a point where only about one kilogram remains unmelted.

Design changes were later implemented to this device to protect the cable and clamp from the intense heat of melt-down. It was fabricated completely of molybdenum and had a longer support to keep the cable away from the high temperature region.

3.4.2 Lump Recharging Device

The modified CG 2000 to be used throughout the project has an enlarged pull chamber which will accommodate a lump/recharge device of up to 30 kilograms capacity as well as a crystal 5 inches in diameter by 40 inches long.

The lump recharging device is based on a self-dumping hopper design that can be seen in Figure 10, 11, and 12. Chunks of silicon are loaded into the hopper when it is in the furnace pull chamber. The isolation valve is closed and the pull chamber is at atmospheric pressure. It is necessary to keep the bottom funnel portion of the hopper closed (tight to the bottom opening) so that silicon will not fall through the bottom opening while loading the hopper. This is accomplished by raising the hopper enough to keep its weight on the funnel. When the hopper is loaded with the desired amount of silicon, it is raised to a sufficient height for the isolation valve to be opened. Before the isolation valve can be opened, however, it is necessary to equalize the vacuum in both the pull chamber and furnace sections of the grower. This is accomplished by first purging the pull chamber of air by pumping in argon and simultaneously pulling a vacuum on the pull chamber. Once the pull chamber has been purged and the vacuum pressure equalized, the isolation valve is opened and the hopper can be lowered to discharge the silicon into the crucible.

During the loading and purging cycles, the residual melt has been partially frozen on the surface to prevent splashing when the silicon is discharged into the crucible. Also, the crucible has been brought to a position that will minimize the distance the silicon will fall and, at the same time, prevent the silicon from piling up beyond the bottom of the funnel.

The discharge of the silicon is accomplished by stopping the hopper travel with the use of a support ring that rests on the flange of the isolation valve. The rod and funnel portion of the hopper is allowed to travel further, thus creating an opening between the funnel and stationary portion of the hopper. When the desired amount of silicon has been

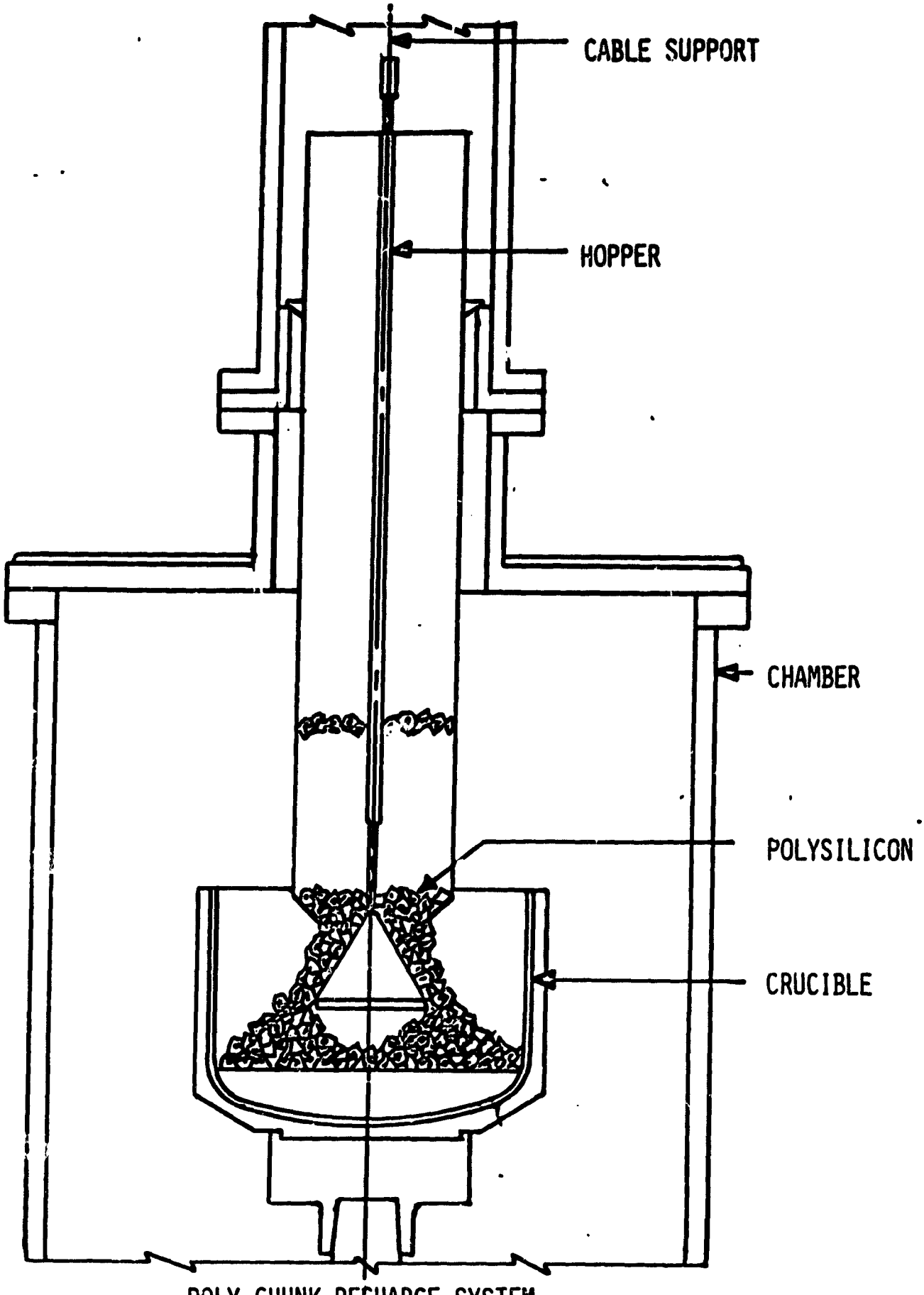

POLY CHUNK RECHARGE SYSTEM

FIGURE 32

discharged, the rod and funnel are raised, closing the opening. Once the funnel contacts the stationary portion of the hopper, the entire hopper can be raised into the pull chamber past the isolation valve. At this point, you can either prepare for another recharge cycle, if necessary, or move the hopper back out of the way and lower the seed to grow another crystal.

4.0 PROCESS RESEARCH AND DEVELOPMENT PROGRAM

4.1 Variations in "State of the Art" Czochralski crystal growth process:

(a). Multiple Ingot Growth from one melt container (crucible). Present "State of the Art" Czochralski crystal growth allows for the growth of one crystal from one melt container.

The Kayex continuous Czochralski growth method involved the development of process parameters, new equipment, and equipment modification that allowed for the growth of multiple crystal ingots from one melt container by periodic melt replenishment.

(b). Recharging capability (rod or lump).

In order to grow multiple ingots from one crucible, it was necessary to develop a process for refilling the crucible with virgin polysilicon material. The refilling or "recharging" had to be accomplished without allowing the crucible and residual melt to cool down to a point where the residual melt would freeze extensively. It was also necessary to maintain an argon purged 20 torr atmosphere when recharging the crucible to prevent contamination of the silicon melt. Recharging capability was developed for polysilicon material in both rod and lump form. Details of the recharging development effort can be found in sections 4.2, 4.3, and 4.4.

(c). Diameter 10 cm or greater.

"State of the Art" Czochralski crystal growth has progressed to 10 cm (4 inch) diameter crystal size. The 954888 project proposal and subsequent development work stressed the economic advantages of growing silicon crystals larger than 10 cm diameter. At the completion of the contract 15 cm diameter crystals were routinely being grown.

(d). 14-Inch Hot Zone.

Standard size hot zones presently in production use for Czochralski type growth of silicon range from 8-inch to 12-inch. The 954688 project included the development of a 14-inch hot zone capable of containing a 14-inch by 11-inch crucible. The 14-inch crucible could theoretically hold in excess of 40 kg of liquid silicon, where as a 12-inch crucible normally is filled with a maximum of 20 kg in silicon production facilities. The 14-inch crucible afforded the cost advantages of growing larger crystals during each growth cycle.

C-2

4.2 Hot Fill Experiments

Since the growth chambers on the CG 2000 being used for the project were significantly different from a standard grower, and the ADC System had been redesigned, it was necessary to make some test runs to determine that state-of-the-art crystals could be grown and that the isolation valve worked satisfactorily.

The first run was a 10 kilogram melt in a 10-inch diameter crucible. No trouble was experienced in achieving zero-dislocation structure, and control systems performed similarly to the standard CG 2000 on the 10 cm. diameter crystal.

Two 18-kilogram runs were then performed. During each of these runs, two crystal removal cycles were performed successfully. All crystals were 12.5 cm. diameter and 7 - 8 Kg. in size. One of the crystals was pulled through the isolation valve while still at yellow heat (900 - 1000°) without damage to the valve seat or the valve.

Following the two 18 Kg runs, it was concluded that the grower was fully operational and preparations were made to start experiments in hot-filling a crucible.

4.2.1 Virgin Polycrystalline Rods

The first melt-down of silicon in a crucible fills it to only about 50% of its capacity if lump silicon is used due to the packing factor of the poly. In order to achieve the highest efficiency, more silicon should be added to fill the crucible to its capacity, even before the first crystal is started.

Initially, this process was conducted by hanging the poly attachment device on the pull mechanism cable. Although this method was not as efficient, it established the feasibility of the proposed method without waiting for completion of the recharge system.

Polysilicon (semiconductor grade) is readily available in rod form, and the initial recharge procedure which was used on the program was to slowly lower the poly rod feed stock into the hot crucible, melting it off until the desired amount of liquid was obtained in the crucible.

Two attempts were made to hot-fill a 12-inch crucible to a total charge of 25 Kg. The additional poly was attached to the pull mechanism by using the poly attachment device and was then lowered into the crucible after completely melting the 18 Kg of cold charge poly.

The first attempt was a failure because the cable failed (apparently due to overheating) and the complete rod and poly attachment device fell into the melt.

A longer attachment device was then fabricated which allowed the cable to remain in the cooler portion of the furnace, and this performed satisfactorily. Following the testing of the longer attachment device, a 12-inch crucible was loaded in the usual manner with 18 kilograms of silicon. Because of the packing factor of lump material, 18 kg is the present limit of this crucible, which when fully melted, leaves about 4 inches of freeboard.

From an 8 kilogram rod of poly, over 7 Kg was melted, leaving less than 1 Kg left on the device. The hot-fill device was then removed from the cable and the seed attached in its place.

From this melt, a 22 kilogram, 87 cm long, zero-dislocation crystal was grown at a diameter of 11.4 cm. Average growth rate was 7.3 cm/hr. Figure 33 is a plot of crystal weight and length increase during the run. Figure 34 shows the crystal grown during this run (Run No. 5).

Power consumption during the run was monitored (Figure 35) and time cycles were recorded.

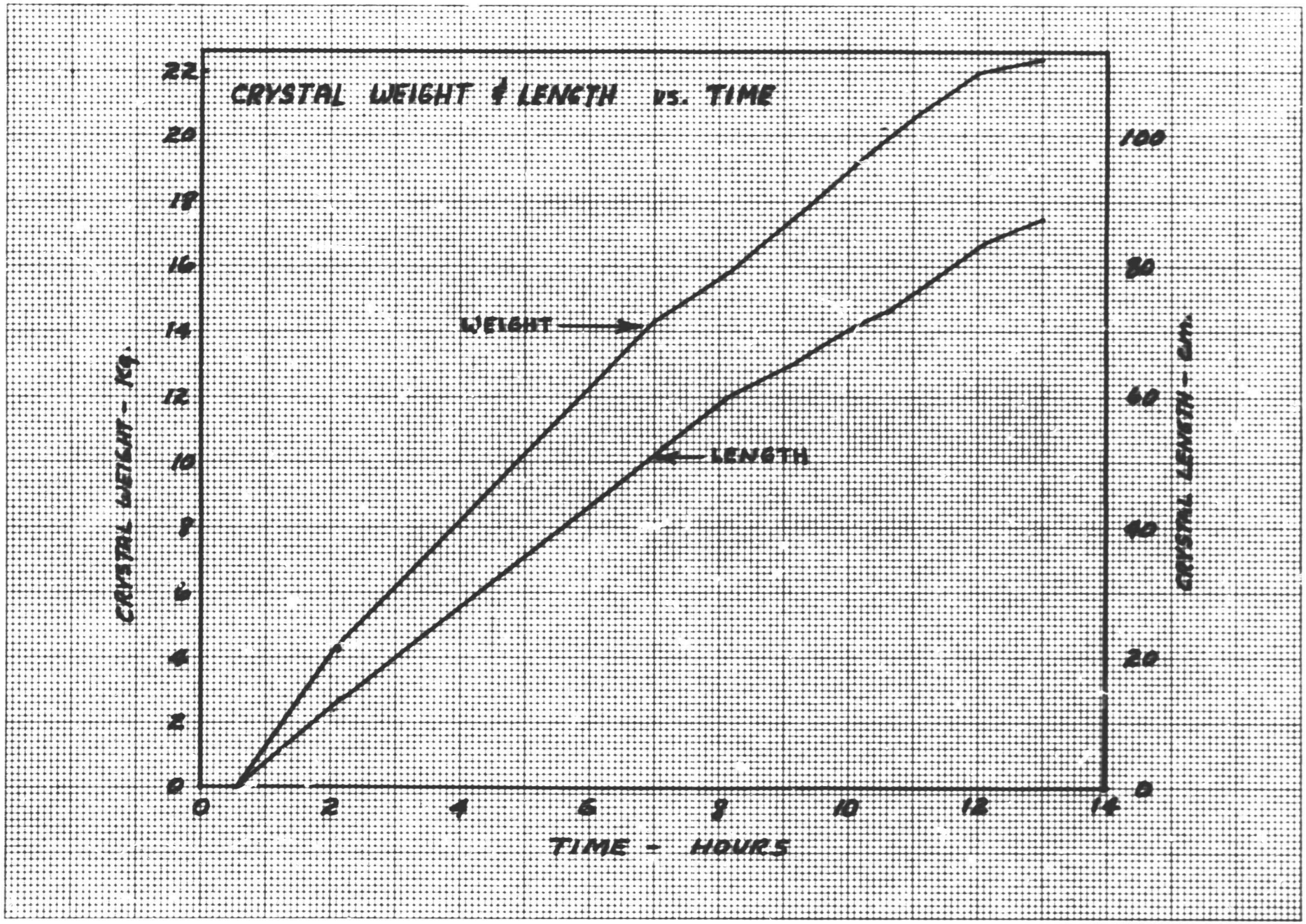

Figure 33

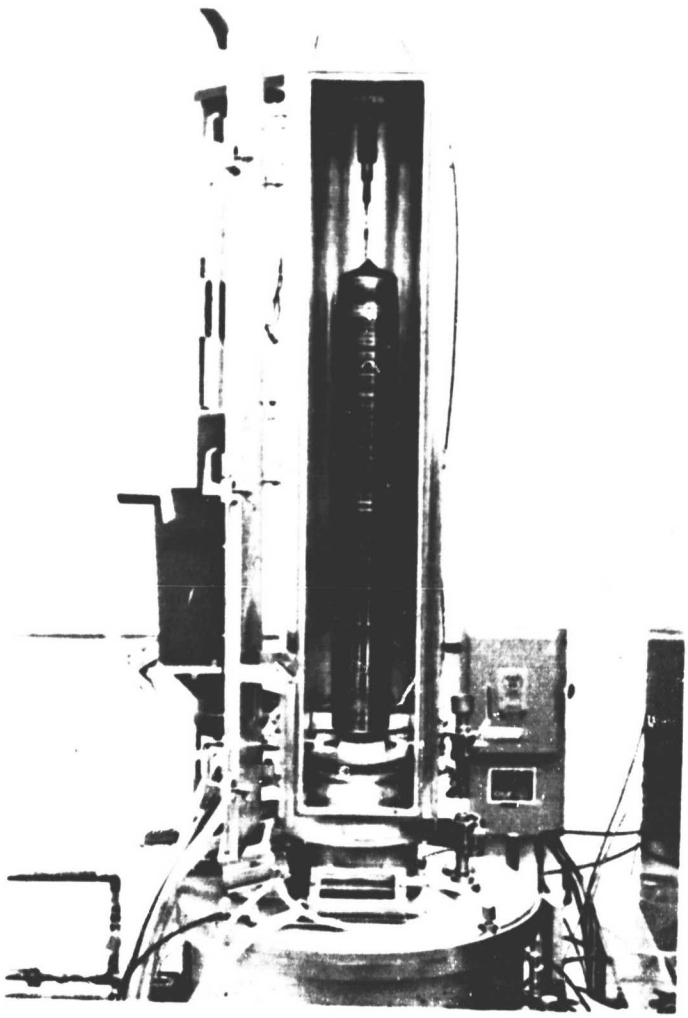

A 22 kg crystal grown by hot filling technique

Figure 34

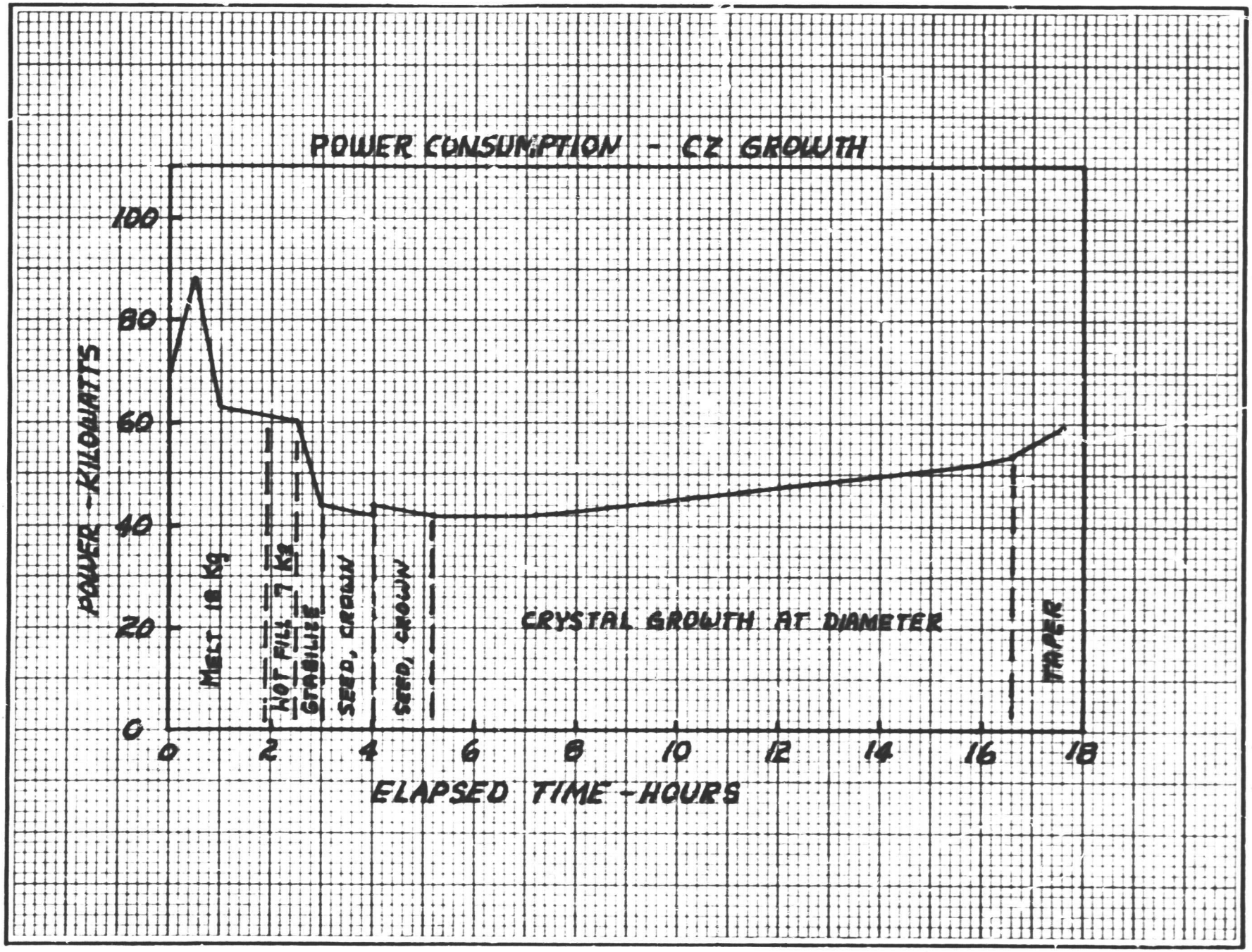
POWER CONSUMPTION - CZ GROWTH
POWER - KILOWATTS
100
80
60
40
20
0
0
2
4
6
8
10
12
14
16
18
ELAPSED TIME - HOURS
MELT IN kg
HOT FILL 7 kg
GRADUATE
SEED, CROWN
SEED, CROWN
CRYSTAL GROWTH AT DIAMETER
TAPER

Figure 35

The crystal run, as performed, corresponds to the first growth cycle in continuous CZ and therefore, the economic model (see section 6.1) can be compared easily with the data from the run. Time cycles and power levels were found to compare quite closely with the model. The throughput of the run was 1.1 Kg per hour including furnace set-up and clean-up time.

Poly silicon was added to the melt during the hot-fill cycle at a melt-back rate of 10.7 Kg/hr. The total hot-fill cycle including back fill and pump down of the pull chamber took 65 minutes.

The following conclusions were consistent with the results and data generated by the hot fill experiments:

1). Hot-filling with poly rod feed material was feasible.

2). A crucible could be filled to a larger capacity than with cold fill techniques.

3). The assumptions in the economic model relating to the cycle time, power consumption, and growth rate were realistic, and in some areas conservative.

4). Continuous CZ as defined depended now only upon the ability of the crucible to survive the long term exposure to molten silicon and to the ability of the crystal grower to perform without malfunction.

4.3 Recharging with Polycrystalline Rods

4.3.1 Recharging Procedure.

Poly rod feed stock can be stored in the rear of the pull chamber. When a crystal growth cycle is complete, the valve is closed and the pull chamber is brought up to atmospheric pressure by introducing argon. After removal of the crystal, the pull chamber is closed and returned to low argon pressure by pumping down and purging. After the valve is opened, the poly rod is moved forward, lowered into the hot zone and the crucible is filled. (At this time, the seed is positioned above the recharge mechanism). After recharging, the remaining poly is retracted and the seed is lowered into the furnace to start a new crystal.

After the second crystal is grown and removed from the furnace, a new poly rod can be placed on the recharge cable, if required.

Illustrations of the crystal growth cycle and recharging cycle can be found on page 15 , Figure 2 and page 62 , Figure 19.

4.3.2 Advantages and Disadvantages

Due to the availability of large semiconductor grade polysilicon rods, it was expedient to attempt initial hot fill and recharging experiments with these polysilicon rods. These early experiments revealed certain problem areas associated with the use of these polysilicon rods.

(a). Five inch diameter poly rods are not crack-free. Therefore, sufficient thermal shock can fracture a rod. If this occurs during the recharge cycle, the possibility of large chunks of poly rod falling into the crucible exists. These poly rod chunks might break the crucible causing a silicon spill which would force the run to be aborted and could result in damage

to the graphite piece parts in the crystal grower. For that reason it became necessary to include a significant amount of time during a recharge cycle to slowly heat up the poly rod prior to its being melted. Futhermore, experience with poly rods which had previously been partially used for recharging indicated that the probability of these pieces fracturing was considerably greater than new polyrods used for the first time.

(b). The thermodynamics of the furnace design make it necessary to maintain elevated heater temperatures (considerably above crystal growth temperatures) when melting a poly rod during a recharge cycle. These elevated temperatures maintain the center of the melt at a temperature sufficiently high enough to melt the poly rod at a reasonable rate, but also tend to increase the devitrification of the fused quartz crucible. This accelerated devitrification decreases the useful life of the crucible and may also contribute to structure loss problems.

(c). Another disadvantage associated with the use of polysilicon rods stems from the method used to hold the rods.

The poly attachment device, shown in Figure 5, page 20. requires the poly rod to be notched at one end so that the claws of the attachment device can be inserted into the rod, secured and allow the weight of the rod to rest on the claws. The process of notching the rod created a possible contamination problem which required each poly rod to be cleaned (etched) prior to its use for recharging. When niblet size lump polysilicon was available, no special etching was needed. The niblets could be loaded into the recharge hopper directly from the bag.

Furthermore, at least one kilogram of rod could not be recharged because of the holding method (poly attachment device) used. However, this material could be used later for the initial cold charge.

The primary advantage associated with the poly rod method of recharging was the ability to melt the rod without the rod coming in contact with possible sources of contamination.

Another current advantage of the poly rod involves the availability of greater than 25 kg rods allowing a single recharge cycle when growing 25 kg crystal ingots.

4.3.3 Statistical Data (Including Continuous Runs)

The first run demonstrating recharge capability was performed 4/17/78. The crucible was cold packed with 18 kg of lump poly with the appropriate amount of dopant. It was melted in the normal way and a 14 kg crystal was grown, 11 cm diameter (78% yield).

The valve was then closed and the crystal prepared for removal. Since it was late in the day, it was decided to wait until the following morning to recharge. The remaining 4 kg of silicon was thus held molten for 9 hours overnight.

The next day, a 13.2 kg poly rod was placed on the cable and lowered into the crucible at the rate of 6 kg/hr. 12 kg total was melted off to bring the total melt back to 18 kg.

Dopant was added, the seed was replaced, and growth was started again. After about 10 inches of crystal had been grown (6300 g), the crystal lost structure due to a particle of silicon monoxide which fell into the melt. The crystal was withdrawn and the melt reseeded.

A second crystal was grown which again was twinned by a particle of silicon monoxide after 12 inches had been grown (6800 g).

At this time, the machine had been running for 39 hours. It was shut down leaving 2900 grams in the crucible.

The following day the inside of the furnace was checked to see where the greatest amount of monoxide had deposited. In general, the furnace was clean with the exception of the area around the left view port.

It was determined that gas flow to the left side view port was excessive and that too much cooling effect and/or turbulence had caused the deposits. Since the front view port was of identical configuration, the side view port was plumbed and regulated in a manner identical

to the front one.

In summary, three crystals were grown from the crucible:

Crystal #1	14,000 g
Crystal #2	6,300 g
Crystal #3	6,800 g
Total grown	27,100 G

Total poly melted:

Cold fill	18,000 g
Recharge	13,200 g
	31,200 g

Pulled yield = 27,100/31,200 = 86.9%

The crucible survived very well although some devitrification was observed, the greatest amount being at the bottom. From a total wall thickness of 5 to 8 millimeters, approximately 10% of the thickness was devitrified. Devitrification was only observed on surfaces that were in intimate contact with the graphite supports.

Run No. 11 begun June 12 1978,was the first attempt at a three-melt run utilizing a basic 18 kg melt and two recharge cycles. Two excellent 10 cm diameter crystals were grown from the first two melts, each weighing about 15 kg. Structure loss problems occurred after the second recharge cycle so that two crystals were pulled from the third melt, each being dislocated after about 6 kg had been grown.

A summary of the data from run Nos. 9 and 11 is included in Tables 8 and 9.

Process problems, primarily the loss of zero-dislocation structure, appeared to result from excessive silicon monoxide build-up around one view port. This situation occurred severely in run No. 9 and to a lesser extent in run No. 11. Gas flows in the chamber were adjusted slightly

CRYSTAL NO.	MELTED WEIGHT (kg)	PULLED WEIGHT (kg)	CUMULATIVE MELTED WEIGHT (kg)	CUMULATIVE PULLED WEIGHT (kg)	YIELD %	CUMULATIVE YIELD %
1	18.0	14.0	18.0	14.0	77.8%	77.8%
2*	13.2	13.1	31.2	27.1	76.2%	86.9%

*Two crystals were grown from this melt, due to loss of zero dislocation structure.

Crucible diameter x height	12" x 9" (30.5 cm x 22.9 cm)
Crystal diameter	4.4" (11.2 cm)
Total run time	39 hours
Average growth rate	3.42"/hr (8.69 cm/hr)
Throughput	0.695 kg/hr

SUMMARY OF TWO-MELT RUN (NO. 9)

TABLE 8

CRYSTAL NO.	MELTED WEIGHT (kg)	PULLED WEIGHT (kg)	CUMULATIVE MELTED WEIGHT (kg)	CUMULATIVE PULLED WEIGHT (kg)	YIELD %	CUMULATIVE YIELD %
1	18	14.91	18.0	14.91	82.8	82.8
2	15	15.38	33.0	30.29	95.4	91.8
3*	15	12.25	48.7	42.54	68.0	87.3

*Two crystals were grown from this melt, due to loss of zero-dislocation structure. The crystals were approximately 65% dislocation-free.

Crucible diameter x height	12" x 9" (30.5 cm x 22.9 cm)
Crystal diameter	4.2" (10.7 cm)
Total run time	44 hours
Average growth rate	3.6"/hr (9.1 cm/hr)(1.9 kg/hr)
Throughput, average	0.97 kg/hr

SUMMARY OF THREE-MELT RUN (NO.11)

TABLE 9

between the two runs, resulting in the improvement. The cause of the build-up of monoxide was determined later to be a pin-hole leak in a weld which allowed water vapor to enter the chamber.

Attempts to fill 12-inch crucibles to a capacity larger than 18-20 kg, although successful, put an excessive load on the upper crucible support. This support is a cylinder of graphite resting on the lower crucible support which conforms to the bottom radius of the crucible. The upper support had been slotted vertically to take advantage of the elasticity of the graphite during cool-down to prevent breakage of the parts which is certain to occur without the slot.

The forces on the crucible during the run, combined with the high temperature, cause a continuous and permanent spreading effect on the upper crucible support so that after a small number of 25 kg melts, the support spreads sufficiently to allow the crucible to bulge out, and it must therefore, be discarded. The upper support was redesigned with a graphite plate across the slot to provide support for the crucible. The plate was pinned with graphite pins to support the crucible during the run. During cool-down, the pins shear to relieve stresses, thereby preventing graphite breakage.

Following the relative success of Runs No. 9 and No. 11, further recharge runs were attempted. All of these were aborted prematurely for various reasons. The first (Run No. 13) was to be a three-recharge run but was aborted after the first crystal was grown because the upper graphite crucible support failed. This allowed the crucible to distort severly which jeopardized the furnace and hot zone.

A second run was aborted because a poly rod fractured during the recharge cycle. The rod had been partially melted off in a previous run. It was believed that strains had been set up in the rod during

the first recharge which were of too high a magnitude to survive the thermal shock of rapidly lowering the rod into the hot zone. Partially used rods apparently cause a breakage risk factor which may be eliminated by controlled slow heat-up.

The third attempt at a recharge run was aborted due to excessive silicon monoxide deposits on the furnace interior, precluding normal ingot growth. It was finally determined that a microscopic water leak had opened up in the pull chamber due to a weld failure.

At this point in the process development program, there had been no crucible failures although devitrification had been moderate to severe in some cases. Initially, all recharging was done with poly rods. Figures 27 and 28 illustrate a typical rod before and after recharging. Later, as it was necessary to recycle the silicon, recharging was also performed with ingots from previous runs.

Up to this time, all crystal growth runs had been performed in the JPL grower using a standard CG 2000 furnace tank. During the month of September, 1978, the installation of the larger furnace tank was completed. The seven inch longer furnace tank allowed for the implementat on of a 14-inch hot zone when the new furnace tank had proved to be mechanically and thermally acceptable.

After vacuum leak checking, thermal tests were performed. A standard 12-inch hot zone was placed in the larger chamber to obtain comparative data with earlier runs in the smaller chamber.

It was found that power input was too high in relation to actual temperature. In fact, on the first crystal growth run, melt-down time was much longer than expected. The normal melt down time for 20 kg had been about 2 hours, and the new chamber system required 3-1/2 hours.

This situation was improved by heat shielding and insulation in the

lower portion of the furnace. A reflecting shield under the heater and additional base plate insulation reduced melt down time back to normal. Apparently the reflectivity of the chamber top and bottom were reduced significantly when the larger chamber was used.

Therefore, it was decided to postpone 14-inch development work until the growth of 100 kg from a 12-inch crucible was demonstrated. The additional shielding and insulation corrected the 12-inch hot zone problem, and several zero dislocation crystal runs were successfully completed with the larger chamber.

Efforts focused upon striving to achieve the growth of 100 kg of ingot from one 12-inch crucible.

The longest recharge run to date was made during this period. Run No. 19 was started October 31, 1978. It lasted 64 hours and produced 57 kilograms of ingot material. Thirty-two kilograms (56.4%) of the ingot was zero dislocation.

The ingots were 12.7 cm diameter and were grown at an average pull speed of 8.9 cm/hr. The run was terminated due to the inability to achieve zero dislocation crystals.

Six ingots were pulled with an average size of about 10 kg each. The ingot size was small because of the structure loss problem.

At this point, it was not clear why the crystals lost structure although there were a number of theories and observations which related to structure loss (refer to appendix A), most of which point to the presence of foreign particles in the melt.

All crystals turned to polycrystalline growth shortly (within one hour) after dislocating.

Run No. 21 produced 53.4 kg of ingot and lasted 44 hours. 62% of the pulled material was zero dislocation.

This run was terminated for two reasons: the crucible appeared to be degrading severely, and excessive silicon monoxide build-up on the crucible and viewports made the growth of high quality material impossible.

At least a portion of the oxide build-up may have been related to the excessive degradation of the crucible. It was devitrified extensively and had reacted sufficiently with the silicon to expose bubbles which were originally below the surface of the quartz. This excessive reaction would produce copious quantities of silicon monoxide.

The reason for the severe degradation of this crucible in such a short time was not understood. Since it is well established that impurities, especially alkali metals and halides, accelerate devitrification, it might be surmised that the crucible in question had been contaminated, either during manufacture or during handling.

Run No. 22 was started within a few hours after No. 21 was terminated. Run No. 22 lasted 50 hours and had promise of being one of the best runs to date. However, during the third recharge cycle, the cable holding the recharge rod failed, dropping the rod into the hot zone and destroying it. The run produced 46.3 kolograms, of which 90.5% was zero dislocation. Severe crucible degradation such as that experienced on Run 21 was not repeated; in fact, the crucible condition was good after the 50 hours with only mild devitrification.

Table 10 summarizes Runs No. 19, No. 21, and No. 22.

Following the completion of Runs 21 and 22 an experimental prototype of a lump recharging device was fabricated. The next continuous recharge run attempted (Run No. 30) incorporated the use of this device in addition

CONTINUOUS CZ GROWTH SUMMARY

Runs No. 19, 21, & 22

RUN NO.	TOTAL MELTED (kg)	TOTAL PULLED (kg)	NO. CRYSTALS	DIAM. (cm)	AVG. PULL SPEED (cm/hr)	RUN TIME (hr)	THROUGHPUT (kg/hr)	PULLED YIELD (%)	ZERO DISLOC. (%)
19	63.9	57.2	6	13.3	8.9	64	0.89	90	56
21	55.0	53.4	5	13.3	8.4	44	1.21	97	62
22	52.4	46.3	5	13.3	9.0	50	.93	88	91

TABLE 10

to the poly rod method of recharging. Therefore, this discussion will be included in Section 4.4.3.

4.3.4 Plans and Recommendations

The use of the poly rod method of recharging was discontinued in favor of the lump recharging system shortly after Run No. 30 was completed and fully analyzed. It was felt the disadvantages associated with the poly rod method of recharging were significant. It was also felt that the advantages associated with the lump recharge method outweighed the advantages of the poly rod method.

The following recommendations should be considered for improvements to the poly rod method of recharging:

a). Crackfree 5-inch diameter poly rods are needed to insure less risk of thermal shock breakage.

b). A means of melting the rods without prolonged increase in residual melt temperature would benefit the life of the fused quartz crucible and significantly decrease the amount of crucible devitrification.

4.4 Recharging with Polycrystalline Lumps

4.4.1 Recharge procedure

A preliminary concept for lump recharging was developed which utilizes a self-dumping hopper. The hopper is loaded with silicon and lowered (using the recharge device) into the crucible. The residual melt is partially frozen to prevent splashing and the silicon is released into the crucible.

Additional loads can be added to the crucible when a majority of the first load has melted. Illustrations of the hopper can be seen on pages 25, 26, and 85 Figure 10, Figure 11, and Figure 32.

A more detailed description of the lump recharging procedure can be found in section 3.4.2 page 83.

It appears that particle size for optimum operation will be about 1 inch maximum for the present hopper design. It is not known what the minimum particle size will be, and no powdered material has been available for such a test.

4.4.2 Advantages and Disadvantages

The major advantage associated with the lump recharging method is the elimination of the potential thermal cracking problems characteristic of the poly rods used for recharging.

The lump method of recharging does not allow the crucible to remain at a temperature considerably higher than the melting point of silicon for long periods of time. The melt down is similar to a cold charge melt down where the total silicon charge is contained in the crucible maintaining the liquid silicon at or near the melting point. This decreases the rate of devitrification and prolongs the life of the crucible.

The lump method of recharging eliminates the time necessary to

slowly heat up the poly rod and makes recharging easier and more convenient due to the fact that the hopper can remain in the furnace during the entire run. To refill the hopper is simply a matter of loading with bagged silicon while the hopper remains in the furnace pull chamber.

The present lump recharging method has several disadvantages also.

The possibility of melt contamination is present due to the silicon lumps contacting the interior of the hopper. However, this possible source of contamination has not been indicated in impurity analyses of silicon ingot material grown following lump recharging. Furthermore, solar cell efficiency results have not been lowered by the use of lump recharged silicon.

Lump size is somewhat critical. If the silicon chunks are too large, they can get stuck in the opening between the lower cone and hopper body creating a jamming effect which can prevent the total hopper charge from dropping into the crucible.

If a significant amount of fines are included in the hopper charge, a condition exists whereby these fines can be blown around the furnace collecting on the crucible walls or other parts of the hot zone.

Care should be taken to screen lump material within the size requirements of the present hopper design.

Finally, the potential for crucible chipping or breakage exists whenever solid pieces of silicon are dropped into the crucible. During the past year and a half that the lump recharging method has been used, these potential hazzards have not been experienced.

4.4.3 Statistical Data (Including Continuous Runs)

A number of preparatory runs were made prior to the next attempt at 100 kg to assure that the equipment was working properly and that the new recharge hopper was reliable. Several hot fill runs were performed successfully with the hopper.

Run No. 30 was the most successful recharge run up to that time. It lasted 79 hours and produced 99.1 kg of silicon ingot. Six ingots were grown from six successive melts.

The melt size ranged from 23.7 to 17.6 kg. The melt size was deliberately reduced each cycle to minimize the crucible etching that occurs rapidly at the melt surafce.

Table 11 is a summary of the ingots produced in the run.

Table 12 includes additional information from the run, such as yields and throughput. It is apparent that the yield of high quality zero dislocation material was low. In fact, more difficulty than normal was experienced on the first ingot in the run in achieving zero dislocation.

Since the raw material was virgin semiconductor grade polysilicon, it was unlikely that impurity build-up in the melt could have been the cause of the structure problem.

The crucible appeared to be in good condition at the end of the run with devitrification no worse than that experienced in earlier, shorter runs.

It was significant at that time, that polysilicon in both lump and rod form was used during the run. The typical procedure used was to add 5 kilograms of lump silicon to the depleted melt with the hopper, followed by a rod melt-back. The rod was placed in the furnace and lowered slowly into the crucible while the lump material was melting.

SUMMARY OF INGOT PRODUCTION FROM RUN NO. 30

MELT NO.	KG ADDED (POLYSILICON)	MELT SIZE	INGOT SIZE	CUMULATIVE MELTED	CUMULATIVE INGOT	RESIDUAL MELT
1	23.7 LUMP	23.7	15.54	23.7	15.5	7.9
2	12.1 ROD	20.0	17.7	35.8	33.2	2.3
3	5.0 LUMP 11.7 ROD	19.0	16.0	52.5	49.2	2.9
4	5.0 LUMP 11.0 ROD	18.9	17.0	68.5	66.2	1.9
5	6.2 LUMP 10.4 ROD	18.5	16.7	85.1	82.9	1.8
6	15.8 LUMP	17.6	16.2	100.9	99.1	1.4

TABLE 11

SUMMARY OF RUN NO. 30

CRYSTAL INGOT DIAMETER	13.3 CM
AVERAGE GROWTH RATE	8.7 CM/HR
RUN TIME	79 HRS
THROUGHPUT	1.2 KG/HR
PULLED YIELD	99%
ZERO DISLOCATION	27%
TOTAL INGOT PULLED	99.1 KG

TABLE 12

Using this procedure, the recharge rod was heated more slowly than earlier runs and was less likely to fracture due to thermal shock.

The time required to recharge was a significant portion of the total time (Table 13) and the actual ingot growth time was exactly one half of the total run time. The last recharge was completely lump silicon. 15.8 kg of polysilicon material was dumped into the crucible and completely melted in two hours. The first recharge cycle, in which only rod material was used, took four hours and only 12.1 kg of material was melted. The extra time was required to heat the rod up to the proper temperature to melt off.

It is interesting to note that only 50% of the total time was devoted to actual crystal growth at full diameter. About one fourth of the run time was used for the recharge operation. The balance was used in neck growth, crown growth, and final crystal taper.

Although the throughput of 1.2 kg/hr as predicted in the economic model [1] was achieved, it was apparent that, not only increased growth rate should be attempted, but that faster recharging would be very effective in reducing the cost of crystal growth.

The yield of zero dislocation material from Run No. 30 was disappointing. The growth of high quality ingot material was difficult to achieve throughout the run. Several attempts had to be made on the first ingot to achieve a zero dislocation structure. This problem became worse as the run progressed, with all subsequent crystals dislocating part way through the growth cycle.

It is not clear why the dislocation problem was encountered, especially on the first ingot, because that operation was essentially the same as the state of art crystal growth process being used for semiconductor materials.

RECHARGE AND INGOT GROWTH TIME (RUN 30)

MELT NO.	RECHARGE TIME (HR)[1]	COMMENTS	CRYSTAL GROWTH TIME (HR)[3]
1	3.5[2]	6.5 KG LUMP HOT FILLED	5.5
2	4.0	ROD MATERIAL, ONLY 12.1 KG	7.5
3	3.0	5.0 KG LUMP PLUS 11.7 KG ROD	7.0
4	3.4	5.0 KG LUMP PLUS 11.0 KG ROD	7.0
5	3.0	6.2 KG LUMP PLUS 10.4 KG ROD	6.5
6	2.0	15.8 KG LUMP	5.7
	TOTAL 18.9 HR		39.2 HR

(1) RECHARGE TIME INCLUDES: REMOVAL OF GROWN CRYSTAL
INSERTION OF POLY
HOT FILL
MELT DOWN
SEED PREPARATION UP TO SEEDING THE MELT

(2) INCLUDES COLD FILL AND HOT FILL TIME ON FIRST MELT

(3) AT 125 MM DIAMETER

TABLE 13

The exceptions to the standard process were: (1) hot filling to about 25 kg in a 12-inch diameter crucible and (2) the growth of 130 mm diameter ingots.

During the developmental testing of the recharge hopper and the lump recharging method a minor disadvantage of the lump recharge method was observed. This involved the tendency of fine particles of silicon to scatter and attach to the crucible wall or to fall in other parts of the hot zone. This problem was due to the relatively large quantity of fine particles in the recharge material, most of which was prepared by hand methods from previously grown ingots. Commercial "nugget" or "niblet" polysilicon contained very few fine particles, and thus the problem was minimized when commercial lump material was used. Solar grade silicon, if in granular or lump form, would preferably have fine particles removed. Of course, a small quantity of fines would be generated in shipping, handling and feeding lump material and therefore this problem should be considered in production equipment design.

The lump recharge process was subsequently improved by sifting out the smaller fines of silicon produced by crushing.

During Run No. 41, two recharge cycles were attempted using between 9 and 10 kilograms of lump silicon per cycle. (Refer to Table 14).

Up to this time, a maximum of 6.5 kilograms of silicon lumps had been used per recharging cycle with the usual amount being 5.0 kilograms.

All recharge cycles were successful. The results proved that it was possible to recharge approximately 10 kilograms of silicon chunks into a 12" crucible containing approximately 3 kilograms of residual melt or approximately 13 kilograms of residual melt. The results further indicated that the amount of time necessary to melt a large amount of silicon (10 kilograms) when recharging was nearly the same as melting a small amount

RECHARGE INFORMATION - RUN NO. 41

MELT NO.	AMOUNT OF SILICON RECHARGED (KG)	RESIDUAL MELT (KG)	AMOUNT OF TIME NECESSARY TO MELT RECHARGED MATERIAL (MIN)	MELT RATE (KG/HR)
1	4.8 (Hot Fill)	16.8	30	9.6
2	9.68	2.8	40	14.5
	9.2	12.48	30	18.4
3	6.0	10	40	9.0
	4.0	16	30	8.0

TABLE 14

of silicon (4 kilograms). The results also indicated that melt time would be faster with a relatively large residual melt.

The results of Run No. 41 are shown in Table 15. A total of three crystals were grown. The run started out well with an 18.76 kilogram crystal grown, 22½" of 23" grown was OD. However, the run progressively deteriorated.

The problem of structure loss coupled with marginal crucible devitrification resulted in the termination of the run following the growth of the third crystal.

In June, 1979, during Run No. 47, the ability to recharge more than 10 kg of lump silicon per recharge cycle was realized. During one recharge cycle in Run No. 47, the hopper was filled with 15 kg of lump silicon. It was not possible to dump all 15 kg at once into a 12" crucible with a normal amount of residual melt. Therefore, a two step dumping procedure was attempted with satisfactory results. The first step was to lower the hopper and dump the silicon lumps according to the normal procedure. By monitoring the weight, it was possible to stop dumping the lumps after a certain weight of silicon had been dumped by raising the hopper and closing the opening. After the silicon dumped during the first step was nearly melted, the hopper was again lowered and the remainder of the silicon released. During this recharge cycle, 7.8 kg was dumped during step one and 7.2 kg was dumped during step two. The total melt size after this recharge cycle amounted to 23.5 kg in a 12" crucible. The results were successful. This new procedure allowed for the recharge of up to 15 kg without opening the pull chamber door and reloading the hopper.

Tables 16 and 17 summarize the results of the 60 kilogram (Run No. 47). Crystal size was similar to Run No. 30. However, the average growth rate was lower. It was felt that conservative pull speeds would increase the

SUMMARY OF RUN NO. 41

Crystal Ingot Diameter	12.7 cm
Average Growth Rate	7.6 cm/hr
Run Time	42-1/2 hrs
Throughput	1.15 kg/hr
Pulled Yield	97%
Zero Dislocation	66%
Total Ingot Pulled	48.71 kg

TABLE 15

SUMMARY OF RUN NO. 47

Crystal Ingot Diameter	12.7 cm to 13.5 cm
Average Growth Rate	6.8 cm/hr
Run Time	51.6 hrs
Throughput	1.17 kg/hr
Pulled Yield	92.5%
High Quality Crystal	88.3%
Total Ingot Pulled	60.2 kg

TABLE 16

RECHARGE AND INGOT GROWTH TIME (RUN 47)

MELT NO.	RECHARGE TIME (HR)(1)	COMMENTS	CRYSTAL GROWTH TIME (HR)(3)
1	2.5(2)	5.0 kg lump hot filled	3.5
2	1.8	10.0 kg lump	7.0
3	2.0	15.0 kg lump by two step method	10.2
4	2.5	10.0 kg lump, cycle 1 8.0 kg lump, cycle 2	.8 then melt back 2.0
5	No Recharge		7.4
Total	8.3 Hr		30.9 HR

(1) Recharge Time includes: Removal of grown crystal
Insertion of hopper
Dump hopper charge
Melt down
Seed preparation up to seeding the melt

(2) Includes cold fill and hot fill time on first melt.

(3) At growth diameter 127 mm to 135 mm.

NOTE: Total Run Time = 51.6 hours; 11.9 hours were devoted to neck, crown growth, and melt backs.

TABLE 17

yield of high quality crystal until thermal gradient parameters could be optimized in the furnace. Even with the slower growth rate, the overall throughput was nearly the same as Run No. 30. This was possible due to the decreased time used in recharging procedures.

The percentage of time devoted to actual crystal growth at full diameter was higher on this run, 60% as opposed to 50% during Run No. 30. The amount of run time used for recharging was lowered from 25% in Run No. 30 to 17% in Run No. 47. The remainder of the run time was used for neck growth, crown growth, and melt backs of crowns or crystals that may have lost structure early into the run.

The yield of high quality material improved dramatically with this Run (88.3%). It was felt that if the crucible had not failed due to excessive devitrification, the run may have continued to the 100 kg goal with good results.

It was not known why the crucible failed, but the possibility existed that new carbon parts installed prior to this run were either of poor quality or insufficiently baked out. The possibility of an inferior crucible was also considered.

A decision was made after the 5th crystal had been grown to terminate the run at this point due to the dangerous condition of the crucible (large inward bulges). Pieces of quartz were observed floating in the melt after the 5th crystal was grown.

During the month of July, 1979, the furnace hot zone assembly was converted from a 12" hot zone to a 14" hot zone. The first run attempted with the 14" parts indicated that thermal parameters were poor and that modifications were necessary.

Following these modifications, another attempt was made at a 100kg run.

Run No. 49 resulted in 108 kg of silicon crystal being grown from one 14" diameter crucible yielding 84.8% high quality single crystal. Two of the largest crystals grown to date during a continuous run were realized (22.4 kg and 20.5 kg).

Tables 18 and 19 summarize the results of the 108 kg run (Run No. 49). The crystal size was similar to other continuous runs (No. 30 and No. 47). However, the average growth rate was lower than Run No. 30, but slightly higher than Run No. 47. Again, it was felt that conservative pull speeds would increase the yield of high quality crystal. Since this was our first run after hot zone modifications had been made to the 14 inch set up (following Run No. 48), it was felt that conservative pull speeds (growth rate) were justified. However, the throughput was actually higher (1.26 kg/hr) than either Run No. 30 or Run No. 47.

The percentage of time devoted to actual crystal growth at full diameter was 57%. The amount of run time used for recharging amount to 19%. Therefore, 24% of the run time was devoted to neck growth, crown growth, and melt backs of crowns or crystals that lost structure early into a growth cycle.

The yield of high quality material was encouraging (84.8%) as it was in Run No. 47.

After crystal #2 (22.4 kg) was grown, the total recharge amounted to 22.2 kg using two separate cycles. After crystal #6 was grown, the two step method of recharging was attempted with the hopper completely filled. A total of 18.2 kg was dumped by the two step method. The results also tend to further confirm previous results indicating that the amount of silicon recharged is not a significant factor in the amount of time necessary to melt the lump silicon, e.g. 5 kg requires approximately 30

SUMMARY OF RUN NO. 49

Crystal Ingot Diameter	13.3 cm
Average Growth Rate	7.00 cm/hr
Run Time	85.5 hr
Throughput	1.26 kg/hr
Pulled Yield	94.3%
High Quality Crystal	84.8%
Total Ingot Pulled	108.0 kg

TABLE 18

RECHARGE AND INGOT GROWTH TIME (RUN 49)

MELT NO.	RECHARGE TIME (HR)[1]	COMMENTS	CRYSTAL GROWTH TIME (HR)[2]
1	2.0	30.0 kg Cold Charge	4.0
2	2.0	9.26 kg Lump	10.5
3	2.1	13.23 kg Lump Cycle 1 8.95 kg Lump Cycle 2	2.5
4	2.5	6.78 kg Lump	2.3
5	No Recharge		2.5
6	No Recharge		4.5
7	2.2	18.2 kg Lump by Two Step Method	7.0
8	2.6	14.52 kg Lump	6.0
9	3.0[3]	13.51 kg Lump	9.5
Total	16.4 Hr	84.45 kg Lump	48.8 Hr
		30.0 kg Cold Charge	
		114.45 kg Total	

(1) Recharge Time includes:
Removal of grown crystal
Insertion of hopper
Dump hopper charge
Melt down
Seed preparation up to seeding the melt

(2) At growth diameter 133 mm

(3) Seed broke after crystal was pulled and valve closed. This required renotching the seed and replacing in the furnace.

TABLE 19

minutes to melt while 10 kg also requires approximately 30 minutes to melt.

An optical pyrometer was fitted to the grower in July to replace the standard thermocouple for temperature control. The optical pyrometer significantly decreases the possibility of air leaks from this sealing area. It also eliminates the possibility of thermocouple breakage when removing the thermocouple during the cleaning of the furnace.

Several modifications were made to the 14" hot zone in August to further improve the thermal parameters and efficiency of the furnace. A lower heat shield that fits underneath the heater was received and used for Run No. 50. It was felt that this lower heat shield would increase the thermal efficiency of the furnace and at the same time improve thermal gradients through the growth zone.

To further increase thermal efficiency and improve other thermal parameters, addition of grafoil to the inside diameter of the insulating heat pack cylinder was attempted. While the results were encouraging, the ability to permanently attach the grafoil to the insulating heat pack was not feasible. Therefore, the vendors of the heat packs were contacted to see if they could provide us with a cemented-on grafoil heat pack.

With the improvements to the thermal efficiency of the hot zone, power consumption at dip temperature was decreased from 60 kilowatts to 48 kilowatts with the 12-inch hot zone. Power consumption for the 14-inch hot zone has been decreased from 70 kilowatts to 60 kilowatts.

Improvements were made to the recharging process during August with the design and fabrication of a movable mirror to replace the standard stationary one used for diameter control.

This moveable mirror eliminated the problem of having to remove the stationary mirror (used in conjunction with the optical system used for diameter control) when lowering the hopper. This was necessitated because of a dimensional conflict between the stationary mirror and the hopper

support ring.

Two more 100 kg continuous recharge runs were completed during October. They are identified as Run No. 55 and Run No. 2*. The table of results on page 126 presents the data for these two runs. Run No.55 was performed on the original grower used for this project with a 14 inch hot zone. Run No. 2* was performed on a new CG 2000 grower that was used in conjunction with the JPL 955270 project.

This grower was not fitted with a special recharge mechanism; therefore, the seed lift cable was used when recharging. Using continuous growth techniques developed under this contract and crystal handling equipment also developed and built under this contract, it was possible to perform this continuous recharge run with this standard production grower.

Run # 55 started out poorly with a diameter control problem. Due to the diameter control problem, the first three crystals had ranged in diameter from 12.7 cm to 16.0 cm. It is interesting to note, however, that the second crystal grown during this run maintained zero dislocation structure for 14 inches while the diameter was slowly increasing from 14.0 cm to 16.0 cm at the bottom. A total of 15-1/4 inches were grown weighing 16.4 kg before the crystal was removed from the melt.

After the diameter control problem was corrected, five crystals were grown weighing a total of 53.4 kg yielding 94.6% high quality monocrystalline material and 86.5% zero dislocation material. During the growth of the eighth crystal, a very small pin hole water leak developed in a weld area of the spectator view port. From that point on, it was impossible to maintain monocrystalline structure for any length of time and polycrystalline material was grown for a large proportion of the last two crystals. This condition decreased the yield of high quality crystal from 92.5% after the eighth crystal was grown to 74.6% when the run was completed following

SUMMARY OF RUN NO. 55 AND RUN NO. 2*

	No. 55	No. 2*
Crystal Ingot Diameter	12.7 - 16.0 cm	12.7 cm
Initial Melt Charge	30 kg	18 kg
Crucible Diameter	35.5 cm (14 in)	30.5 cm (12 in)
Total Silicon Melted	106.1 kg	104.5 kg
Total Ingot Pulled	100.6 kg	100.3 kg
Pulled Yield	94.8%	96%
Total Mono Crystal	75.1 kg (74.6%)	63.9 kg (63.7%)
Number of Ingots	10	9
Throughput	1.11 kg/hr	0.93 kg/hr
Total Run Time	91 hours	108 hours
Recharge Material	100% lump	100% lump

TABLE 20

the tenth crystal.

Tables 21 and 22 break down Run No. 55 and Run No. 2* as a function of the time cycles for recharging and straight growth of each crystal ingot grown. The time between the end of the recharge cycle and the beginning of straight growth on the crystal amounts to the time devoted to what we refer to as growth preparation. Growth preparation is comprised of (1) stabilizing the melt temperature after melt down, (2) growing of the seed neck, (3) crown growth, and (4) melt backs of crowns or short ingots that have lost structure. Ideally, this process cycle should not take more than two to two-and-one-half hours per ingot growth cycle. Therefore, if ten crystals are grown, growth preparation should not require more than twenty (20) to twenty-five (25) hours. A total of thirty-three-and-one-half (33.5) hours (36.8%) of the run time was devoted to growth preparation during Run No. 55. If only twenty hours were needed for growth preparation, the total run time would have decreased to seventy-seven-and-one-half (77.5) hours, resulting in a throughput of nearly 1.3 kg/hr. Moreover, if you look at continuous runs from the point of view of number of crystals grown, it becomes very evident that the fewer crystals grown to accomplish the total 100 kg goal, the better the throughput and corresponding costs.

Run No. 2*, although not a typical run (mechanical problems), also resulted in an excess amount of time being devoted to the growth preparation cycle. Over thirty-eight (38.3) hours (35.1%) of the total run time was devoted to growth preparation. Since only nine crystals were grown, ideally it could have required only eighteen (18) hours for growth preparation. This would decrease the total run time to eighty-nine hours and possibly improve the percentage of monocrystalline material.

RECHARGE AND INGOT GROWTH TIME (RUN 55)

Melt No.	Recharge Time (Hr)[1]	Comments	Crystal Growth Time (Hr)[2]
1	1.8 (10:30 - 12:15 pm)	30.0 kg cold charge	1.7 (5.6 kg) (2:15 - 3:55 pm) (3.3 kg/hr)
2	1 (3:55 - 4:55 pm)	4.4 kg lump (one melt back)	5.8 (16.4 kg) (9:05 - 2:55 am) (2.83 kg/hr)
3	1.8 (2:55 - 4:40 am)	16.2 kg lump	1.3 (3.1 kg) (6:20 - 7:40 am) (2.38 kg/hr)
4	0	None (one melt back)	3.8 (10.0 kg) (10:50 - 2:40 am) (2.63 kg/hr)
5	2.7 (2:40 - 5:25 pm) (Quartz in melt) ~ 1 hr	10 kg lump (one melt back)	6.0 (13.2 kg) (9:30 - 3:30 am) (2.2 kg/hr)
6	1.8 (3:30 - 5:20 am)	16.5 kg lump (one melt back)	2.0 (4.6 kg) (9:30 - 11:30 am) (2.3 kg/hr)
7	0	None (one melt back)	5.8 (12.1 kg) (6:30 - 11:00 pm) (2.09 kg/hr) (Taper 11:00 - 12:20 am)
8	1.8 (12:20 - 2:10 am)	15.5 kg lump one melt back (crown)	5.7 (13.5 kg) (5:10 - 10:50 am) (2.39 kg/hr)
9	2.0 (10:50 - 12:50 pm)	12.4 kg lump one melt back (crown)	6.3 (12.1 kg) (3:30 - 9:50 pm) (1.92 kg/hr)
10	0	None	6.2 (10 kg) (11:20 - 5:30 am) (1.61 kg/hr)
	Total 12.9 Hr	106.1 kg	44.6 Hr

TABLE 21

(1) Recharge Time inclues:
- Removal of grown crystal
- Insertion of hopper
- Dump hopper charge
- Melt down
- Seed preparation up to seeding the melt

(2) At growth diameter 127 mm to 160 mm

NOTE: Total Run Time = 91 hours
12.9 hrs was devoted to the recharging procedure inc. initial melt down of 30 kg cold charge.
44.6 hrs was devoted to straight growth at diameter.
33.5 hrs or 36.8% of the run time was used for Growth Preparation: (1) Stabilize Temperature, (2) Growing Seed, (3) Crown Growth, (4) Melt Backs

RECHARGE AND INGOT GROWTH TIME (RUN NO. 2*)

Melt No.	Recharge Time (Hr)[1]	Comments	Crystal Growth Time (Hr)[2]	
1	2.1 (8:15 - 10:20 am)	18.0 kg cold charge (12" hot zone)	5.5 (11:40 - 5:10 pm)	(13.7 kg) (2.49 kg/hr)
2	2.3 (5:10 - 7:30 pm)	15.7 kg lump (several melt backs) ingots (2) & crowns	4.7 (5:40 - 10:20 am)	(9.9 kg) (2.11 kg/hr)
3	2.8 (10:20 - 1:10 pm)	10.4 kg lump (replaced cruc. lift belt) melt backs	6.6 (6:15 - 12:50 am)	(13.8 kg) (2.09 kg/hr)
4	3.3 (12:50 - 3:10 am)	13.8 kg lump (replaced broken cable)	3.5 (6:10 - 9:40 am)	(9.0 kg) (2.57 kg/hr)
5	2.3 (9:40 - 11:55 am)	8.0 kg lump (maint. on cruc. shaft)	6.7 (1:30 - 8:10 pm)	(12.5 kg) (1.87 kg/hr)
6	1.8 (8:10 - 9:55 pm)	12.3 kg lump	1.3 (10:45 - 12:05 am)	(3.0 kg) (2.31 kg/hr)
7	0	None melt backs (2)	4.3 (3:30 - 7:50 am) with taper	(7.1 kg) (1.65 kg/hr)
8	2.3 (7:50 - 10:07 am)	9.4 kg lump (quartz in melt) melt backs (2) (seed & crystal fell into melt ~ 2 kg)	9.3 (6:55 - 4:10 am)	(15.4 kg) (1.66 kg/hr)
9	2.1 (4:10 - 6:20 am)	16.8 kg lump (lost structure twice on crown)	9.8 (10:50 - 8:40 pm)	(15.9 kg) (1.62 kg/hr)
Total	19.0 hr	104.4 kg	51.7 hr	

(1) Recharge Time includes: Removal of grown crystal
Insertion of hopper
Dump hopper charge
Melt down
Seed preparation up to seeding the melt

(2) At growth diameter 127 mm

NOTE: Total Run Time = 109 hours
19 hours was devoted to the recharging procedure inc. initial melt down of 18 kg cold charge.
51.7 hours was devoted to straight growth at diameter
38.3 hours or 35.1% of the run time was used for Growth Preparation: (1) Stabilize Temperature, (2) Growing Seed, (3) Crown Growth, (4) Melt Backs.

TABLE 22

It should be noted that all runs attempted on the 954888 crystal grower since June 15, 1979, (following Run No. 44) were performed without the recharge mechanism attached to the grower.

A 100 kilogram continuous run was attempted November 12 using the original recharge mechanism designed for this project. The results were less than satisfactory and the run was terminated after fifty two (52) kilograms had been grown. Structure loss problems occurred early into the run and continued to get worse as the run progressed.

As a result of Run No. 58 and previous experiences with the originally designed recharge mechanism, it was felt that the originally designed recharge mechanism could cause distortion and sealing problems to occur, especially in the pull chamber door. Since it was possible to accomplish continuous recharge runs without the recharge mechanism, it was decided, with JPL approval, to remove the recharge mechanism for the next run. The entire pull chamber was changed when it was discovered that the door on the original pull chamber was warped.

Following the required machine repair and maintenance, and a one crystal growth run, a 100 kilogram continuous recharge run was attempted on December 10.

The results were much better than Run No. 58. Therefore, after preventative maintenance was performed on the grower, a test run (Run No. 61) yeilding very good results, convinced us to attempt the sixth one-hundred kilogram continuous run with purified parts on January 7, 1980.

Table 23 summarizes Run No. 60 and Run No. 62. Run No. 60 produced 100.4 kg of crystal. Eight crystals were grown, yeilding 60.8 kg of monocrystalline silicon. An air leak developed early in the run which eventually caused a serious structure loss problem after the fifth crystal had been grown. Figure 36 shows a composite of the eight crystals grown during Run No. 60. The discoloration on the second crystal indicates that an air leak was present at this time. Crystals 5, 7, and 8 also show the discoloration patterns characteristic of an air leak. Crystal No. 4 exhibits this discoloration to a lesser degree. Starting with crystal 5, circular ring patterns are also visible on the crystals. This pattern usually means that the air leak is a periodic leak - not continuously the same. When the run was completed, an air leak was found in the feed through shaft which operates the seed lift. When the shaft was rotated, the vacuum increased and decreased periodically. If the shaft rotation was stopped at a certain point, the leak would seal and the grower vacuum would decrease to the required limits. (Even though it was possible to grow high quality crystal when the air leak was present, it was felt that excessive silicon monoxide buildup occurred along with severe devitrification of the crucible as the run progressed, making it impossible to maintain structure for any length of time during a growth cycle). This can be evidenced by the last three crystals grown. Crystals #7 and #8 lost structure on the crown and contained only 18% and 10% high quality crystal respectively. This, of course, decreased the overall percentage of high quality crystal from 98.6% after 55.7 kg had been grown to 60.6% at the end of the run.

Run No. 62 resulted in the highest percentage of monocrystalline silicon being grown to date. A total of 103.0 kg was pulled, of which 89.3 was monocrystalline. Moreover, 72.2 kg were of "OD" quality.

SUMMARY OF RUN NO. 60 AND RUN NO. 62

	NO. 60	NO. 62
Crystal Ingot Diameter	12.2 - 13.2 cm	11.7 - 12.7 cm
Initial Melt Charge	30 kg	30 kg
Crucible Diameter	35.5 cm (14 in.)	35.5 cm (14 in.)
Total Silicon Melted	108.7 kg	104.5 kg
Total Ingot Pulled	100.4 kg	103.0 kg
Pulled Yield	92.4%	98.6%
Total Mono Crystal	60.8 kg (60.6%)	89.3 kg (86.7%)
Number of Ingots	8	9
Throughput	1.18 kg/hr	1.06 kg/hr
Total Run Time	85 hours	97 hours
Recharge Material	100% lump	100% lump

TABLE 23

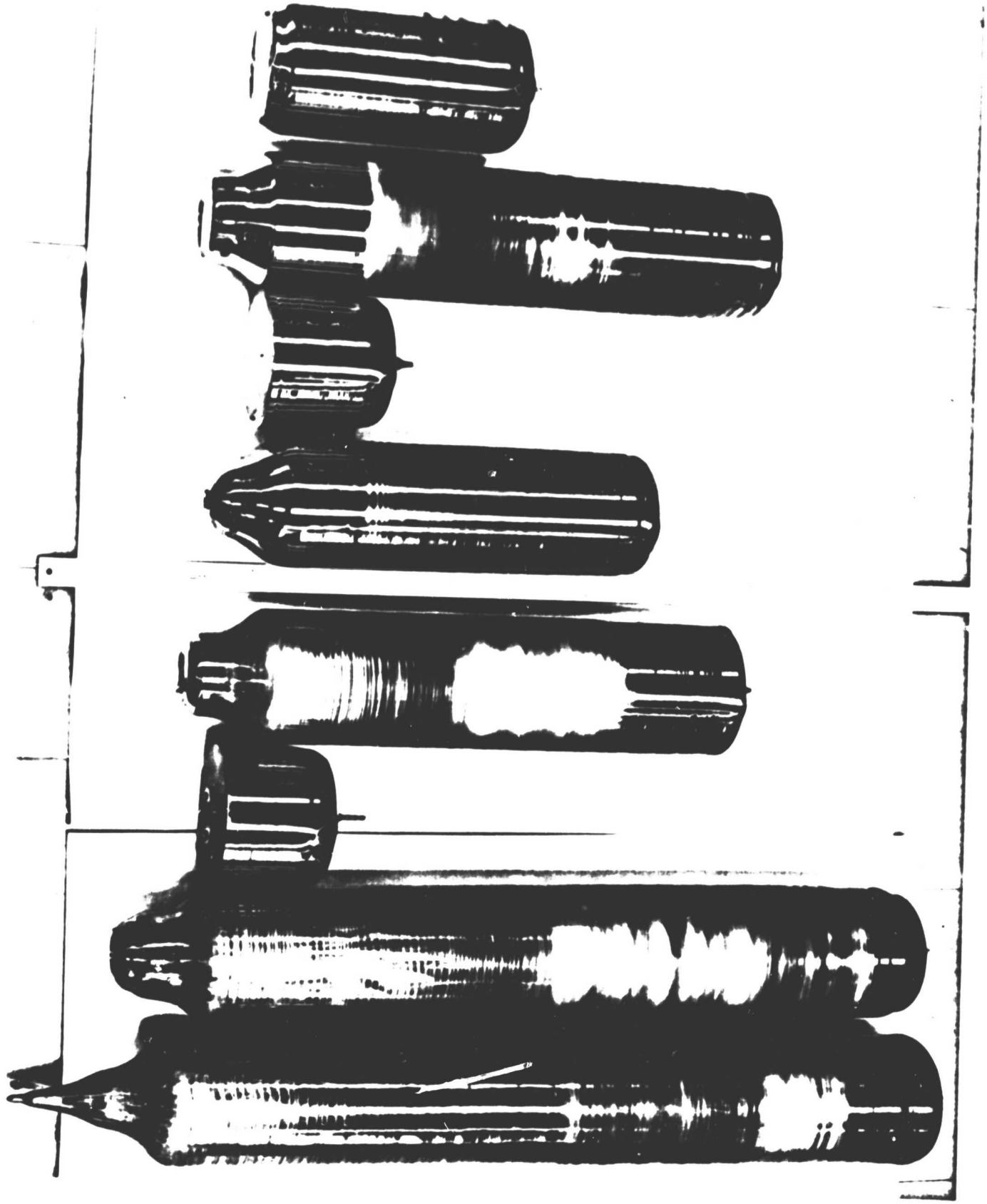

RUN NO. 60

Figure 36

Figure 37 shows the group of nine crystals grown during Run No. 62. The first crystal resulted in a 20.4 kg crystal being grown, which was 90% "OD" and the remainder single crystal. At this point, a potential problem was noticed. The crucible had sagged such that one side was in contact with the graphite upper support while the other side showed a gap of 1/4" to 1/2" from the upper support. A thick layer of silicon monoxide formed on the top lip of the crucible where the gap occurred. When the crucible was raised up into the cold part of the furnace as the crystal was grown, the oxide cracked and broke apart. From time to time during the run, pieces of silicon monoxide were noticed falling from the top rim of the crucible into the melt.

The capability of growing "OD" was demonstrated on eight of the nine crystals grown. The sixth crystal was the only crystal that did not contain at least 50% "OD" material. Moreover, the eighth crystal was 85% single crystal while the last crystal was "OD" for 15 of the total 27 inches.

The fact that it was possible to grow a high percentage of monocrystalline material at the end of the run tends to indicate that the structure loss problems that were encountered during the run were not consistent or predictable and may have been caused by pieces of the oxide layer falling into the melt. However, it is known from experience that, as the crucible goes higher up into the colder regions of the upper furnace chamber, the oxide tends to crack and peel, increasing the possibility of some coming loose and falling into the melt. An example of this can be seen on the bottom of the straight growth portion of crystal #6 (2.9 kg). Pieces of the oxide were flaking off and falling into the melt during the first four inches of this growth cycle. A large piece actually stuck to the outside of the crystal at the bottom - observe rough area on sixth

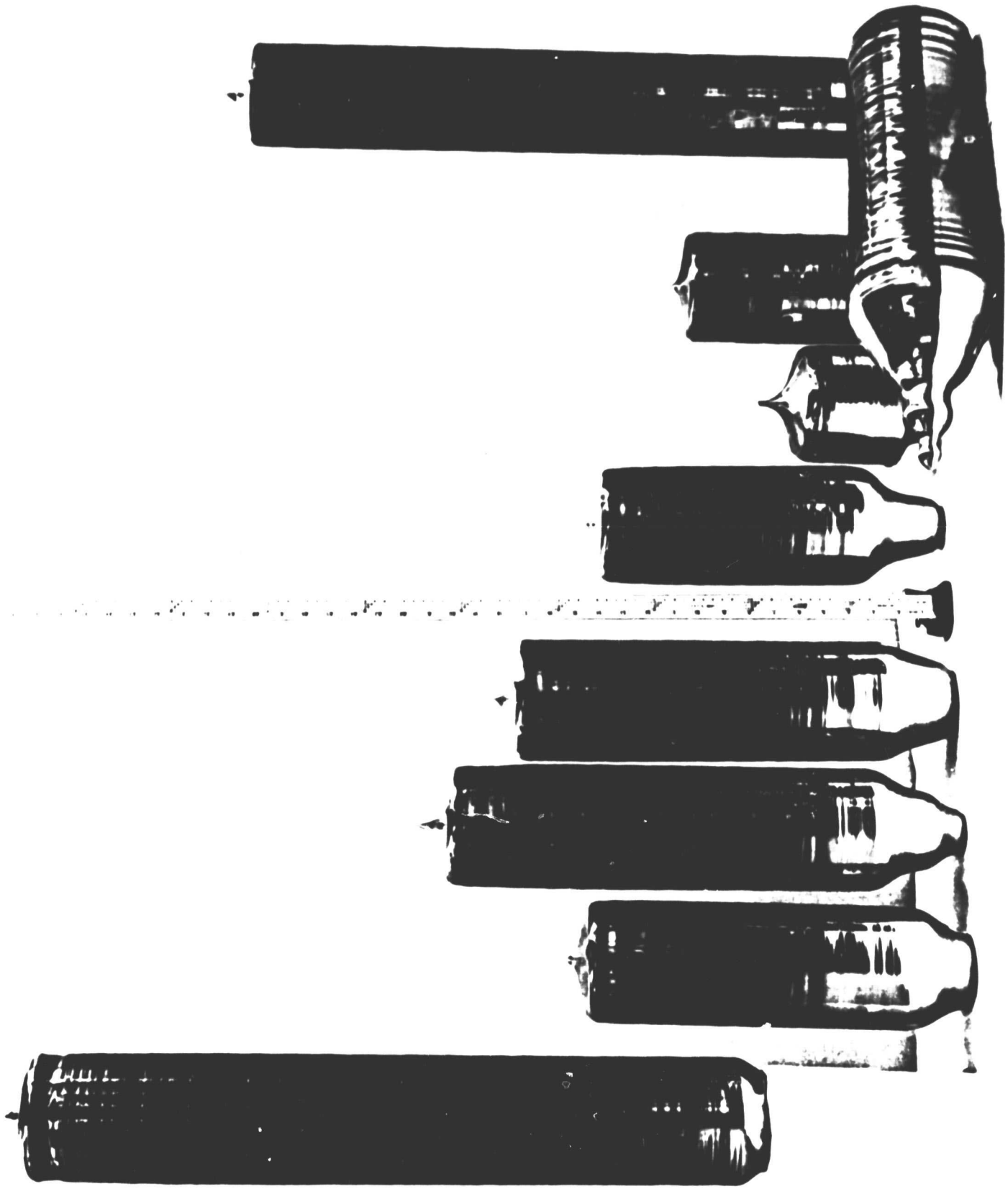

RUN NO. 62
Figure 37

crystal at the bottom. Refer to Figure 37, page 135.

It is felt that, if a crucible fits the upper support properly - tight to the inside diameter, the upper crucible walls stay hotter and therefore, drastically reduce the amount of oxide buildup on the upper portions of the crucible walls.

If Figure 36 and Figure 37 are compared, the discoloration of the crystals in Figure 36 becomes apparent. The crystals in Figure 37 are clean in comparison to those in Figure 36.

The graph in Figure 38 relates the number of kilograms pulled during Run No. 62 as a function of run time. As can be seen, up until the time that severe structure loss problems occurred (during the growing of the fifth crystal), the growth rate was satisfactory (2.09 kg/hr - 2.38 kg/hr) and the throughput was also satisfactory - 1.26 kg/hr. After the fifth crystal was grown, the thoughput fell sharply, concluding at 1.06 kg/hr. Sixty-five (65) kilograms had been grown after fifty-one hours of run time, yielding 80.2% "OD" material.

Tables 24 and 25 further break down the run time cycles into three categories (Recharge Time, Crystal Growth Time and Growth Preparation Time). A comparison between Run No. 60 and Run No. 62 indicates that the Recharge Time and Crystal Growth Time are nearly the same during both runs even though one more crystal was grown during Run No. 62. The major difference occurs in the area of Growth Preparation, where 21.4 hours was devoted during Run No. 60 while 32.6 hours were devoted during Run No. 62.

Table 26 presents a composite of the time cycles for all 100 kg runs completed to date. Runs No. 30, 47, and 2* were performed using 12 inch crucibles and corresponding hot zones. Recharge times have improved

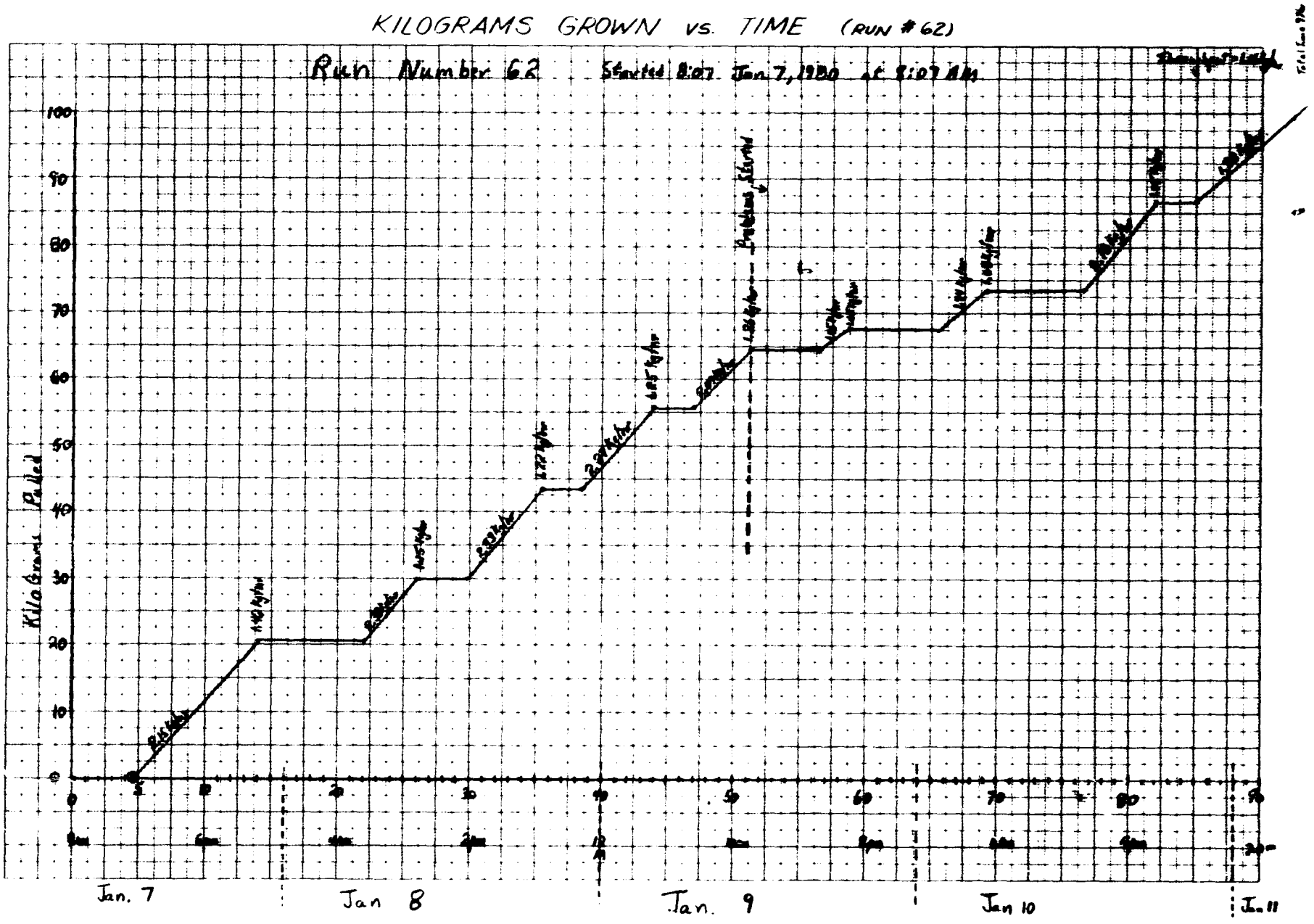
KILOGRAMS GROWN vs. TIME (RUN # 62)
Run Number 62
Started 8:07 Jan 7, 1980 at 8:07 AM
Kilograms Pulled
Jan. 7
Jan 8
Jan. 9
Jan 10
Jan 11

Figure 38

RECHARGE AND INGOT GROWTH TIME (RUN NO. 60)

Melt No.	Recharge Time (Hr)(1)	Comments	Crystal Growth Time (Hr)(2)	
1	2.0 (8:15 - 10:15am)	30.0 kg cold charge	5.0 (12:55 - 5:55pm)	(10.9 kg) (2.18 kg/hr)
2	1.8 (5:55 - 7:45pm)	10.0 kg lump	8.8 (9:05 - 4:55am)	(16.1 kg) (1.83 kg/hr)
3	2.5 (4:55 - 7:25am)	15.8 kg lump	1.3 (8:45 - 10:05am)	(3.4 kg) (2.62 kg/hr)
4	0	None (Replaced cable & coupling)	3.7 (12:55 - 3:35pm)	(7.2 kg) (1.95 kg/hr)
5	2.0 (3:35 - 5:35pm)	10.9 kg lump	7.6 (7:05 - 2:40am)	(15.0 kg) (1.97 kg/hr)
6	1.8 (2:40 - 4:30am)	16.8 kg lump 1) Rewired seed holder (5:45am) 2) Lost on crown (7:30am) 3) Lost on crown (9:30am) 4) Lost 1" on crystal (11:00am)	1.2 (10:55 - 12:05pm)	(3.1 kg) (2.58 kg/hr)
7	0	None (Replaced broken cable)	11.0 (4:40 - 3:40am)	(22.5 kg) (2.05 kg/hr)
8	2.7 (3:40 - 6:20am)	26.5 kg lump (Two dump cycles) Lost structure on crown (7:30am)	12.2 (9:30 - 9:45pm)	(22.2 kg) (1.82 kg/hr)
	Total 12.8 hr	108.7 kg	50.8 hr	

(1) Recharge time includes:
Removal of grown crystal
Insertion of hopper
Dump hopper charge
Melt down
Seed preparation up to seeding the melt

(2) At growth diameter 122mm - 132mm

NOTE: Total run time = 85 hours
12.8 hrs (15.1%) was devoted to the recharging procedure including initial melt down of 30 kg cold charge. 50.8 hrs (59.8%) was devoted to straight growth at diameter. 21.4 hrs (25.2%) of the run time was used for Growth Preparation: (1) Stabilize temperature (2) Growing Seed (3) Crown Growth (4) Melt Backs

TABLE 24

RECHARGE AND INGOT GROWTH TIME (RUN NO. 62)

Melt No.	Recharge Time (Hr)(1)	Comments	Crystal Growth Time (Hr)(2)	
1	1.5 (8:05 - 9:35am)	30.0 kg cold charge	9.5 (12:15 - 9:45pm)	(20.4 kg) (2.15 kg/hr)
2	2.7 (9:45 - 12:25am)	20.1 kg lump 1) Quartz on seed (2 dumps) 2) Lost structure at 1" - melt back 2:40am 3) Lost structure on shoulder 4:00am	4.2 (6:00 - 10:10am)	(9.5 kg) (2.26 kg/hr)
3	2.0 (10:10 - 12:10pm)	9.5 kg lump	5.6 (1:50 - 7:25pm)	(13.4 kg) (2.39 kg/hr)
4	1.8 (7:25 - 9:15pm)	13.4 kg lump	5.6 (10:25 - 4:00am)	(12.5 kg) (2.23 kg/hr)
5	1.5 (4:00 - 5:30am)	12.5 kg lump	4.5 (7:00 - 11:30am)	(8.9 kg) (1.98 kg/hr)
6	1.7 (11:30 - 1:10pm)	9.0 kg lump 1) Lost structure on crown (2:25pm)	1.7 (4:45 - 6:25pm)	(2.9 kg) (1.71 kg/hr)
7	0 (Put new seed on) (6:25 - 7:30pm)	None 1) Lost structure on crown (8:40pm) 2) Change seed was 1,1,1 (9:30pm) 3) Change seed to 1,0,0 (10:10pm) 4) Lost structure on crown (11:10pm)	3.3 (1:20 - 4:40am)	(6.8 kg) (2.06 kg/hr)
8	1.8 (4:40 - 6:30am)	10.5 kg lump 1) Lost structure on crown (8:00am) 2) Lost structure at about 2" meltback (10:20am)	5.2 (12:40 - 5:50pm)	(12.0 kg) (2.31 kg/hr)
9	0 (5:50 - 7:45pm) Waited for pictures to be taken	None	11.8 (9:10 - 9:00am)	(16.6 kg) (1.41 kg/hr)
Totals	13.0 hrs	104.5 kg	51.4 hrs	

(1) Recharge Time includes:
Removal of grown crystal
Insertion of hopper
Dump hopper charge
Melt down
Seed preparation up to seeding the melt

(2) At growth diameter 117mm - 127 mm

NOTE: Total run time = 97 hours
13.0 hrs (13.4%) was devoted to the recharging procedure including initial melt down of 30 kg cold charge. 51.4 hrs (53%) was devoted to

TABLE 25

straight growth at diameter. 32.6 hrs (33.6%) of the run time was used for Growth Preparation: (1) Stabilize Temperature, (2) Growing Seed, (3) Crown Growth, (4) Melt Backs.

TABLE 25 (Cont'd)

COMPOSITE OF RECHARGE AND INGOT GROWTH TIMES FOR 100 KG RUNS

RUN NO.	RECHARGE TIME(1)		GROWTH PREPARATION(2)		STRAIGHT GROWTH & TAPER		TOTAL RUN TIME
	HRS	%	HRS	%	HRS	%	HRS
30	18.9	(23.9)	20.9	(26.5)	39.2	(49.6)	79
47	8.8	(17.1)	11.9	(23.1)	30.9	(59.9)	51.6
49	16.4	(19.2)	20.3	(23.7)	48.8	(57.1)	85.5
55	12.9	(14.2)	33.5	(36.8)	44.6	(49)	91
2*	19	(17.4)	38.3	(35.1)	51.7	(47.4)	109
60	12.8	(15.1)	21.4	(25.2)	50.8	(59.8)	85
62	13.0	(13.4)	32.6	(33.5)	51.4	(53)	97

(1) Recharge Time includes:
- Removal of grown crystal
- Insertion of hopper
- Dump hopper charge
- Melt down
- Seed preparation up to seeding the melt

(2) Growth Preparation includes:
- Stabilize Temperature
- Growing Seed
- Crown Growth
- Melt Backs

TABLE 26

while straight growth times have stabilized at about 50% of the run time. The largest variation is experienced in Growth Preparation, usually due to mechanical problems and structure loss problems.

Run No. 62 marked the completion of Phase I of the 954888 project. Based upon the results of the six 100 kg continuous recharge runs performed under the 954888 contract extension, it was felt that the crystal grower and its component parts were capable of growing at least 100 kg of silicon from one crucible at any time. However, a leak-free system must be maintained throughout the run in order to grow a high percentage of monocrystalline or zero dislocation material.

Table 1, page 6, summarizes the six one-hundred kilogram continuous runs performed under the Phase I extension of this contract. They were accomplished between June 26, 1979, and January 11, 1980.

Phase II of the 954888 project had already begun. The growth of 150 kg of 150 mm diameter crystal was the ultimate objective.

During the month of January, our first scheduled attempts at growing 150 mm diameter crystals were initiated. It was necessary to develop growth parameters, investigate furnace capabilities and limitations, and institute a learning curve for grower operators.

Therefore, on January 16, the first scheduled attempt at growing a 150 mm diameter crystal was begun. The results are shown in Table No. 27. The crystal grown during Run No. 63 can be seen in Figure 14.

Run No 63 was very successful for a first attempt at growing 150 mm diameter crystals. The diameter control was good, and the growth rates were acceptable for this stage of development.

RESULTS OF RUN NO. 63

Crystal Ingot Diameter	152 mm
Initial Melt Charge	28 kg
Crucible Diameter	14"
Total Ingot Pulled	25.5 kg
Pulled Yield	91.1%
Total Monocrystal (all OD)	100% (all OD)
Number of Ingots	1
Overall Throughput	1.96 kg/hr
Straight Growth Throughput	3.3 kg/hr
Total Run Time	13 hours

TABLE 27

Based on the success of Run No. 63, the decision was made to attempt the first 150 kg run after performing the necessary preventative maintenance on the grower and the successful performance of a test run. The test run - Run No. 64 - was very successful resulting in an 18.4 kg crystal being grown from a 19.8 kg charge, dislocation-free for its entire length. It is interesting to note that the material used to grow this crystal was reclaimed from frozen silicon remaining in a crucible used during other growth runs. The results of Runs No. 63 and 64, therefore, led to the 150 kg attempt - Run No. 65.

Run No. 65 was started January 28, 1980. However, a freak mechanical problem (loose set screw) prevented a successful attempt at a 150 kg run.

Initially, the problem was thought to be the Automatic Diameter Control, but later it was learned that a loose set screw on a seed lift mechanism coupling was the cause of all the diameter control problem.

After four process and control runs were completed, another attempt at the 150 kg continuous run was made on February 25. This continuous run was relatively successful, with the first two crystals being 100% monocrystalline. However, a microscopic water leak occurred after the second crystal was grown that resulted in loss of monocrystalline growth after only 20% of the crystal was grown for the succeeding four crystals (Figure 15, Page 43).

A total of 151.5 kg of silicon was grown from a total melt of 154.4 kg. A total of six crystal ingots were grown, varying between 24.8 kg and 25.9 kg. The first two crystals grown resulted in approximately 50 kg of monocrystalline ingot (42.6 kg being dislocation-free).

This run was the first 150 kg run to be completed in phase II of the project. The pulling of 150 mm diameter crystals resulted in a sub-

stantial increase in the throughput rate. The overall throughput for the run (Run No. 70) was 1.53 kg/hr. Previous overall throughputs for 100 kg continuous runs had ranged from 0.92 kg/hr to 1.26 kg/hr. Moreover, the straight growth throughput for the 150 mm diameter continuous growth run averaged 2.60 kg/hr for all six crystals.

Since a problem occurred following the growth of the second crystal, it might be significant to analyze the throughputs for the first two crystals. Overall throughput for the first two crystals was 1.63 kg/hr with straight growth throughputs of 2.69 kg/hr for crystal No. 1 and 2.99 kg/hr for crystal No. 2. (All straight values include taper).

Table 28 provides a summary of Run No. 70. Table 29 is a detailed breakdown of the run time cycles and is divided into three categories (Recharge Time, Crystal Growth Time and Growth Preparation Time).

It had now been demonstrated that the continuous recharge method of Czochralski crystal growth could be applied to large diameter (150 mm) crystals. It had also been demonstrated that 150 kg of crystal ingot could be grown from one melt container (crucible) using a modified Hamco CG 2000 RC crystal grower with special equipment and techniques developed under the 954888 contract. However, the periodic structure loss problem reoccurred during Run No. 70 culminating in a less than satisfactory yield of monocrystalline silicon being grown. The structure loss problem was identified and can be solved. Moreover, 100 kg continuous recharge runs of equal time duration have produced much higher yields when this type of structure loss problem did not occur.

Therefore, on March 18, 1980, a second 150 kg run was begun with the purpose of improving the yield of high quality crystal. Our supply of virgin poly silicon was barely sufficient to complete this run. Due to the limited supply of poly, it was imperative that Run No. 72 be continued to the 150 kg goal regardless of the crystal quality results.

RESULTS OF RUN NO. 70

CRYSTAL INGOT DIAMETER	150 mm
INITIAL MELT CHARGE	30 kg
CRUCIBLE DIAMETER	14"
TOTAL SILICON MELTED	154.4 kg
TOTAL INGOT PULLED	151.5 kg
PULLED YIELD	98.1%
TOTAL MONO CRYSTAL	67.3 kg (44.4%)
NUMBER OF INGOTS	6
OVERALL THROUGHPUT	1.53 kg/hr
STRAIGHT GROWTH THROUGHPUT (INCLUDES TAPER)	2.60 kg/hr
TOTAL RUN TIME	99 hours
RECHARGE MATERIAL	100% lump

TABLE 28

RECHARGE AND INGOT GROWTH TIME (RUN NO. 70)

Melt No.	Recharge Time (Hr)[1]	Comments	Crystal Growth Time (Hr)[2]	
1	2.0 (7:45-9:45 am)	30.0 kg cold charge	9.4 (12:20-9:45 pm)	(25.3 kg) (2.69 kg/hr)
2	2.5 (9:45-12:15 am)	24.8 kg lump (2 cycles) Lost OD structure at 2" of Straight Growth - Meltback after 4" went poly (4:15 am)	8.3 (6:20-2:35 pm)	(24.8 kg) (2.99 kg/hr)
3	2.0 (2:35-4:35 pm)	24.3 kg lump (2 cycles) 1) Replaced cable 2) Lost structure on crown 2 times (8:45 pm)	9.0 (9:00-6:00 am)	(25.2 kg) (2.80 kg/hr)
4	2.3 (6:00-8:20 am)	24.5 kg lump (2 cycles) 1) Lost structure on crown 5 times (2:30 pm)	10.5 (3:30-2:00 am)	(25.2 kg) (2.4 kg/hr)
5	2.5 (2:00-4:25 am)	27.9 kg lump (2 cycles) 1) Lost structure on crown twice (6:30 am)	10.8 (6:45-5:35 pm)	(25.1 kg) (2.32 kg/hr)
6	2.7 (5:35-8:15 pm)	24.6 kg lump (2 cycles) 1) Crucible rotation motor malfunction - replaced with motor matic. 2) Lost structure on crown (10:00 pm) 3) 1.5" crystal left melt when wall freeze was eliminated (10:30 pm) 4) Lost structure on crown again (11:30 pm)	10.2 (12:30-10:45 am)	(25.9 kg) (2.54 kg/hr)
	14.0 hrs	156.1 kg	58.2 hrs	

1) Recharge Time includes:

Removal of grown crystal
Insertion of Hopper
Dump Hopper charge
Melt Down
Seed Preparation up to Seeding the Melt

2) At growth diameter (includes Taper)

NOTE: Total Run Time = 99 hours
14.0 hrs (14.1%) was devoted to the recharging procedure including initial meltdown of 30 kg cold charge.
58.2 hrs (58.8%) was devoted to straight growth at diameter. Includes taper.

TABLE 29

26.8 hrs (27.1%) of the run time was used for Growth Preparation:
1) Stabilize temperature
2) Growing Seed
3) Crown Growth
4) Meltbacks

Table 29 (Cont'd)

Structure loss problems occurred early into the run as evidenced by the total amount of monocrystalline material grown (Table 30). The first crystal lost monocrystalline structure after 8-1/2 inches of growth. The second crystal grown lost monocrystalline structure after 8 inches of growth with the remaining four crystals losing monocrystalline structure between 1 and 4 inches of growth.

The residual gas analyzer was operating during this run and indicated that an abnormally high concentration of air was present in the furnace environment. During the run, attempts were made to locate possible air leaks with no apparent success. If sufficient virgin poly silicon would have been available for another attempt at growing 150 kg, Run No. 72 would been aborted.

A total of 150.6 kg of silicon was grown from a total melt of 153.6 kg. Six crystal ingots were grown varying in size from 24.2 kg to 27.2 kg.

This run was the second and last 150 kg run to be completed under Phase II of the 954888 contract. The overall throughput again showed the advantage of growing 150 mm diameter crystals (1.61 kg/hr). Both the overall throughput and the straight growth throughput (2.74 kg/hr) were improvements on Run No. 70. It is felt that if structure loss problems can be solved or at least minimized, throughputs can be significantly increased. Structure loss problems and considerations are discussed in Section 4.5.3. By the completion of the 954888 contract, structure loss characteristics had been well defined with effective means to eliminate the problem being developed.

Table 30 provides a summary of Run No. 72. Table 31 breaks down the run further into run time cycles.

Results of Run No. 72

Crystal Ingot Diameter	150 mm
Initial Melt Charge	30 kg
Crucible Diameter	14 inches
Total Silicon Melted	153.6 kg
Total Ingot Pulled	150.6 kg
Pulled Yield	98.1%
Total Mono Crystal	25.9 kg (.7.2%)
Number of Ingots	6
Overall Throughput	1 61 kg/hr
Straight Growth Throughput (Includes Taper)	2.74 kg/hr
Total Run Time	93.6 hrs.
Recharge Material	100% lump

Table 30

Table 31

Recharge and Ingot Growth Time (Run No. 72)

Melt No.	Recharge Time (Hr)[1]	Comments	Crystal Growth Time (Hr)[2]	
1 A	2.0 (6:30 - 8:30 am)	1.2 30.0 kg cold charge	8.7 2:40 - 10:03 - 11:20 pm 9:40 - 5:00 - 6:25 pm	24.8 kg 2.85 kg/hr
1 B	2.3 (6:25 - 8:45 pm)	4.0 24.8 kg lump (2cycles) (1) over heated on melt down to get cracks of crucible melt.	8.4 12:45 - 8:20 - 9:10 am	24.7 kg 2.94 kg/hr
2	2.7 (9:10 - 11:50 am)	5.6 24.2 kg lump (2 cycles) (1) lost structure on crown 3 times, includes two melt backs 3:55 pm	9.9 5:25 - 1:15 - 3:20 am	24.9 kg 2.52 kg/hr
3	3.0 (3:20 - 6:20 am)	4.2 24.7 kg lump (2 cycles) (1) fuse blow on PC pump, had to bring grower to atmosphere. (2) lost structure on crown 9:05 am.	8.4 10:35 - 6:20 - 7:00 pm	24.7 kg 2.94 kg/hr
4	4.3 (7:00 - 11:20 pm)	3.9 24.1 kg lump (2 cycles) (1) lost structure about 1" 1:40 am	9.0 3:15 - 12:00 - 12:15pm	24.2 kg 2.69 kg/hr
5	2.6 (12:15 - 2:50 pm)	2.9 25.2 kg lump (2 cycles) (1) Lost structure on crown but continued	10.5 5:40 - 3:50 - 4:10 am	27.2 kg 2.59 kg/hr
Total	16.9(Hrs)	153.6 kg 21.8 hrs.	54.9 Hrs. (includes tapers)	

(1) Recharge time includes: Removal of grown crystal, insertion of hopper, dump hopper charge, melt down, seed preparation up to seeding the melt.

(2) At growth diameter - 150 mm (includes tapers)

Note: Total run time = 93.6 hrs. 16.9 hrs (18.1%) was devoted to the recharging procedure including initial melt down of 30 kg cold charge. 54.9 hrs (58.7%) was devoted to straight growth at diameter and tapers. 21.8 hrs (23.3%) of the run time was used for growth preparation. (1) Stabilize temperature, (2) Growing Seed, (3) Crown Growth, (4) Melt Backs.

4.4.4 Plans and Recommendations

The lump recharging method has proven to be an acceptable method for recharging silicon during continuous crystal growth. Two potential problems associated with this form of recharging have not been noticeable in impurity analysis results and observations made during recharging.

Contamination of the silicon crystal from the hopper has not been indicated by mass spectrometer analyses of representative silicon samples.

There has not been one crucible failure caused by dropping chunks of silicon into a fused quartz crucible during recharging or hot filling.

The following recommendations should be considered for improvements to the lump method of recharging:

a. If niblet size (maximum 1 inch) lump silicon is not available it becomes necessary to crush the silicon and screen out the fines. This operation requires the chunk silicon to be cleaned (etched) and dried before it is acceptable for use.

   A redesigned hopper might allow for larger size lump silicon to be used.

b. A larger hopper would enable the recharging of more silicon per cycle which is necessary when growing 25 kg and larger crystals.

c. The present method of loading the hopper could be improved. At present, bags full of lump silicon are simply dumped directly into the hopper. The possibility exists for chunks to fall out of the bag outside the hopper. A transfer device from the storage bags to the hopper would improve the efficiency of loading the hopper and eliminate the chunks from falling outside the hopper.

4.5 Crystal Growth Development

Crystal growth development has been concentrated in two areas:

a). The growth of large diameter crystals

b). Faster growth speeds.

Both areas of development directly affect the throughput (kg/hr) of silicon produced during CZ crystal growth. The higher the throughput associated with the CZ growth of silicon, the lower the cost of the silicon produced. Therefore, the throughput has a direct bearing on the final cost of silicon solar cells and consequently the cost of electricity produced from silicon solar cells.

Several problems associated with standard furnace design, thermodynamics of the CZ growth process and furnace hot zone, and hot filling (replacement of the melt) were considered in order to meet the objectives of the project.

Due to the new technology developed under this contract and the lack of detailed information or studies pertaining to the continuous recharge method of CZ crystal growth proposed by Kayex Inc. unforeseen problems such as structure loss (loss of monocrystalline crystal structure), crucible devitrification and thermal cracking of polycrystalline silicon rods required substantial amounts of time and effort.

4.5.1 Ingot Size (4" - 5" - 6")

In 1977, when Kayex Inc. proposed the continuous recharge method for production of low cost silicon for solar cells, the normal silicon crystal ingot grown by production facilities was either 3-inch or 4-inch diameter. The following conversion can be made based on the density of solid silicon:

- For a 3-inch diameter crystal each inch (length) grown represents 275 gm of silicon.

- For a 4-inch diameter crystal each inch (length) grown represents 480 gm of silicon.

It is readily seen that an increase in the growth of silicon crystals from 3-inch diameter to 4-inch diameter produces 205 gm more silicon per inch of growth length or a 74.5% increase in production for the same length of crystal.

If one compares the standard 4-inch diameter crystal to a 5-inch and 6-inch diameter crystal the following statistics are generated:

- 5-inch diameter crystal yields 750 gm for each inch of length. When compared to a 4-inch diameter crystal the increase amounts to 270 gm per inch of crystal length or a 56.3% increase in production for the same length of crystal.

- 6-inch diameter crystal yields 1083 gm/inch or an increase of 603 gm per inch of crystal length. This computes to a 125.6% increase in production for the same length of crystal.

The following chart presents the mass of silicon produced for each inch (and cm) of crystal length based on crystal diameter.

Crystal Diameter	Mass (wt) inch of crystal	Mass (wt) cm of crystal
3-inch	275 gm/in	107 gm/cm
4-inch	480 gm/in	189 gm/cm
5-inch	750 gm/in	295 gm/cm
6-inch	1083 gm/in	426 gm/cm

Theoretically, economic considerations as evidenced by throughput (kg/hr) definitely favor large diameter crystals.

Figure 39 illustrates the progression from 4-inch diameter crystals to 5-inch diameter crystals and finally to 6-inch diameter crystals (Phase II). During the initial stages of crystal growth development crystals between 4.0 and 4.5 inch (11 cm) diameter were grown (Table 1). At this time it was necessary to make sure that the modified (CG 2000 crystal grower was operating correctly and prove that hot filling and recharging procedures were feasible. However, most of the crystals grown during this contract were approximately 5-inch (13 cm) in diameter (Table 1). 6-inch (15 cm) diameter crystals were not routinely attempted until the beginning of Phase II in January, 1980.

In each case, whether it was 4-inch, 5-inch, or 6-inch diameter, it has been possible to grow high quality dislocation free crystals.

4.5.2 Growth Rate

Thermodynamic fundamentals involving the heat of formation (latent heat of fusion) when liquid silicon undergoes a change in state has always been a limiting factor to the growth rate of silicon crystals. The amount of heat produced by the phase change of liquid silicon crystallization is considerable and tends to limit the ability to increase growth rates by transferring more heat to the melt per unit time as the growth rate increases. It is possible to increase growth rates by decreasing the melt temperature, but limits are reached when proper thermal gradients with the melt - both lateral and longitudinal - are not maintained. Silicon crystallization (wall freeze) can occur on the crucible walls at the top surface of the melt if the crucible walls are not hot enough to prevent the liquid silicon from solidifying. Spontaneous nucleation can occur on the melt surface and

FIGURE 39

constitutional super cooling of the melt at the growth interface can cause loss of monocrystalline structure. Therefore, as growth rates increase, these thermodynamic considerations have to be dealt with.

In order to improve upon normal equilibrium growth rates, a means of removing the latent heat of fusion before it can sufficiently increase the melt temperature at the growth interface must be devised. This can be accomplished without adversely affecting the thermal gradients in the melt by increasing the heat lost by radiation from the crystal and the heat lost by conduction from the crystal. The modified Hamco CG 2000 was designed with this in mind. The upper protion of the water cooled furance tank was designed to allow for a high degree of radiative heat loss from the crystal, while the argon flow patterns were intended to provide a maximum degree of conductive heat loss.

The growth of silicon crystal ingots during the project has reached speeds of 5-inches/hr. for a four inch diameter crystal. One of the project goals was to maintain an average growth rate of 4-inches/hr. during continuous recharge runs. Although this growth rate was demonstrated on the growth of selected crystals during continuous recharge runs, the maximum overall growth rate accomplished during a 100 kg continuous run was 8.7 cm/hr (3.43 inches/hr). The crystal diameter during this run was 13 cm (5.1 inches).

Structure loss problems periodically encountered during the crystal growth development program resulted in polycrystalline growth which impacted on the increased growth rate program. Polycrystalline silicon crystal growth is much more difficult to control at elevated growth rates than monocrystalline growth. The average growth rates for all continuous recharge runs is contained in Table 1 page

It is interesting to note that 15 cm diameter crystals have been grown at rates similar to 12.7 cm diameter crystals. The crystal grown during Run No. 63 was grown at an average growth rate of 7.9 cm/hr (3.1 in/hr).

The economics of faster growth rates are self explanatory. There is a direct linear relationship between growth rate and throughput. If the growth rate doubles, the amount of silicon produced also doubles. The maximum cost savings can be realized however, when increased growth rates and increased crystal diameters are combined.

Normal commercial growth rates for 4-inch diameter silicon crystals are very near to 3 inches/hour. There are many theories that state that growth rates must decrease as the crystal diameter increases. Assuming that all growth conditions are precisely the same, the thermodynamics of silicon crystal growth would definitely support the above theories. However, variations in growth conditions and grower modifications can in fact increase growth rates. Based on information, data, and observations recorded during this project, it is felt that with improvements in the radiative and conductive heat loss from the crystal, improvements can be realized toward faster growth rates for both 12.7 cm and 15 cm diameter crystals.

4.5.3 Crystal Quality

The American Society for Testing and Materials manual defines high quality silicon crystal as monocrystalline silicon with dislocation densities less than $500/cm^2$. This in turn would indicate that the silicon would be free of grain boundaries, twin boundaries, lineage and slip lines.

One objective of the JPL 954888 project was to produce silicon material capable of producing 14% AM 1 efficient solar cells. If this efficiency criteria could have been met by growing polycrystalline silicon

crystals then the need for growing monocrystalline material would not have been necessary. However, based on solar cell efficiency data generated by this project and other JPL projects [8] polycrystalline silicon normally yields solar cell efficiencies from 8% to 10% depending on the grain size and other imperfections in the samples tested.

Therefore, due to the primary objective of producing low cost silicon material for the production of solar cells (not semiconductor devices) our definition of high quality material related directly to the ability of the material produced to yield solar cell efficiencies in the area of 13% to 14% AM 1.

Resistivity criteria dictated that the silicon be p-type (Boron Doped) with a resistivity between 1.5 and 3.0 ohm - cm. The recommended crystallographic orientation was 1-0-0 and it was felt that monocrystalline material would be required.

As previously stated, solar cell efficiency data has substantiated the original contention that monocrystalline material is needed to produce solar cell efficiencies in the 13% to 14% AM 1 areas desired. However, the data also indicates that material commonly referred to as "OD" - zero dislocation (less than 500 dislocations/cm^2) is not necessary for producing the high efficiency solar cells required. The limiting factor appears to be polycrystalline growth as opposed to monocrystalline growth.

It has been stated earlier in this report that the ability to maintain monocrystalline growth throughout the complete continuous recharge run created some problems. This section will try to deal with these problems.

An explanation of probable causes of structure loss in silicon crystal growth is contained in Appendix A.

(a). Furnace Atmosphere:

It is well established that melt contamination can cause structure loss in silicon crystals. This melt contamination may be attributed to

any number of impurities, whether in the form of a gas, solid, or liquid. The following areas of possible melt contamination were evaluated and acted upon during the course of the crystal growth development program:

1). Raw material (silicon)

2). Etching Procedure (cleaning of silicon)

3). Purity of carbon parts in the furnace

4). Volatile Matter (grease, etc.)

5). Argon Purity

6). Air Leaks

7). Water Leaks

There was little work done on identifying possible contaminants from virgin silicon or recycled silicon. Only a few samples were sent out for impurity analysis. It was necessary to rely on our vendors to provide us with high quality raw materials.

The etching facilities being utilized were not as good as standard production etching facilities. Improved procedures for etching, rinsing, drying, and handling the silicon were instituted. Very little investigation was done to determine the purity of the silicon prepared in this way. However, this was not relevant to virgin polysilicon used for continuous runs. The objective was to arrive at an acceptable procedure for the equipment that was available and then attempt to make it as reproducible as possible.

Possible contamination from carbon parts has been a constant concern throughout this contract. It has been demonstrated in the past that a melt down attempted under hard vacuum (no argon flow for cleansing the melt surface) can result in a high carbon content scum to be formed on the melt surface. It is essential that the carbon parts in the furnace be of high quality. These parts must be free of volatile materials and be dense enough to eliminate

outgassing that would force carbon particles into the furnace atmosphere where they might be blown into the crucible and come into contact with the melt. Another possible detrimental effect of poor quality carbon is possible devitrification of the crucible wherever it comes into contact with the carbon parts (upper and lower supports).

Satisfactory bakeouts are always necessary for carbon parts, especially new ones. However, these bakeouts may still not eliminate problems caused by poor quality carbon parts.

An area of possible contamination that we felt we had significant control of was the area of volatile matter being introduced into the furnace atmosphere from a source not directly related to or needed to grow crystals, for example, vacuum grease on O rings and other types of seals used to make the furnace air tight. The types of materials being used were investigated and found to be detrimental to the crystal growth process. A silicone base vacuum grease was substituted for the vacuum grease being used. However, it was later learned that silicon vacuum grease will oxidize at temperatures above 450°F. Silicon dioxide powder results from oxidation along with highly volatile methyl groups.

During the months of May and June, 1979, a considerable amount of time was spent identifying areas of volatile matter contamination, removing the possible contaminants and making sure that each area was still air tight. By the time Run No. 47 was attempted, it was felt that this area of possible contamination had been eliminated.

The relationship between argon and silicon monoxide flow patterns in the furnace were considered. Of interest was what causes silicon monoxide to be deposited on the crystal as it is being grown: was this monoxide detrimental to crystal growth and could the flow patterns in the furnace be altered to eliminate this monoxide coating without adversely affecting

the thermal condition of the furnace? Areas to be considered were:

1). Amount of argon flow - furnace vacuum and valve settings.

2). The height of the crystal at which the monoxide starts to deposit.

3). The effects of the crucible starting position in relation to the heater.

4). Exhaust mechanisms and methods.

It was determined that monoxide on the grown crystal was not a cause of structure loss unless the monoxide was contaminated by other substances which could cause loss of structure. The silicon monoxide formation was a normal reaction during the melt down and crystal growth process. However, with the use of a Residual Gas Analyzer it was determined that temperature conditions of the melt and vacuum conditions within the furnace have a direct bearing on the degree of silicon monoxide produced. Sources of oxygen from outside the furnace, however, will significantly contribute to the amount of silicon monoxide produced.

A Residual Gas Analyzer was received in January, 1980, on a test basis. It was connected to the grower and initial tests were begun. The purpose in testing the equipment was to monitor crystal growth atmosphere during the growth and recharge cycles and to investigate if any atmosphere degradation occurred during these cycles.

Initial test results from the RGA system indicated that the system had the ability to sample the exhaust gases from the grower by pumping them through a pressure reduction system to a chamber where the analyzer head could measure the partial pressures of the gases present.

It was planned to monitor continuous runs in addition to single crystal growth runs, etc. Therefore, a more detailed analysis of the RGA's capabilities and its relationship to the crystal growth process could be determined. Our results indicate that the equipment was capable of:

1). Scanning a mass range acceptable to required needs.

2). Monitoring a single amu peak and indicating changes in the peak height.

3). Responding to vacuum changes in the furnace.

4). Responding to changes in concentrations of specific amu's - as indicating by relative partial pressure - within a satisfactory time period.

A specific example of the capabilities and possible uses of a Residual Gas Analyzer is contained in the following paragraph:

During this continuous run (No. 70), we continuously monitored the exhaust gases from the grower with the residual gas analyzer previously mentioned. Most of the time we were monitoring the top of the 28 AMU peak so that we could see changes in the concentration of nitrogen and/or carbon monoxide. Occasionally, a scan in the 2 to 60 AMU range was made to analyze for the presence of other elements and compounds or to further identify the composition of the gases when the 28 peak increased. During the raising of the second crystal into the pull chamber, the RGA indicated a dramatic increase in the 28 peak (Figure 40). Subsequent scans through the 2 to 60 AMU mass range did not indicate an increase in the 14 AMU peak. Therefore, we concluded the dramatic increase in the 28 peak was due to carbon monoxide and not air (nitrogen). After the run was completed and the grower was inspected following cool down, a microscopic pin hole water leak was found on the top plate of the furnace where the dopant fixture is situated. Therefore, all data and results indicate that a microscopic water leak occurred for a period of time from the end of the growth of the second crystal through the subsequent recharging and up to the start of the third crystal.

As previously mentioned, we were unable to maintain monocrystalline growth on any crystal following the growth of the second crystal.

In addition to the information and data gathered during continuous recharge runs, a brief study was undertaken in March, 1980, to correlate the

Run No. 70 RGA Chart

(Partial)

Figure 40

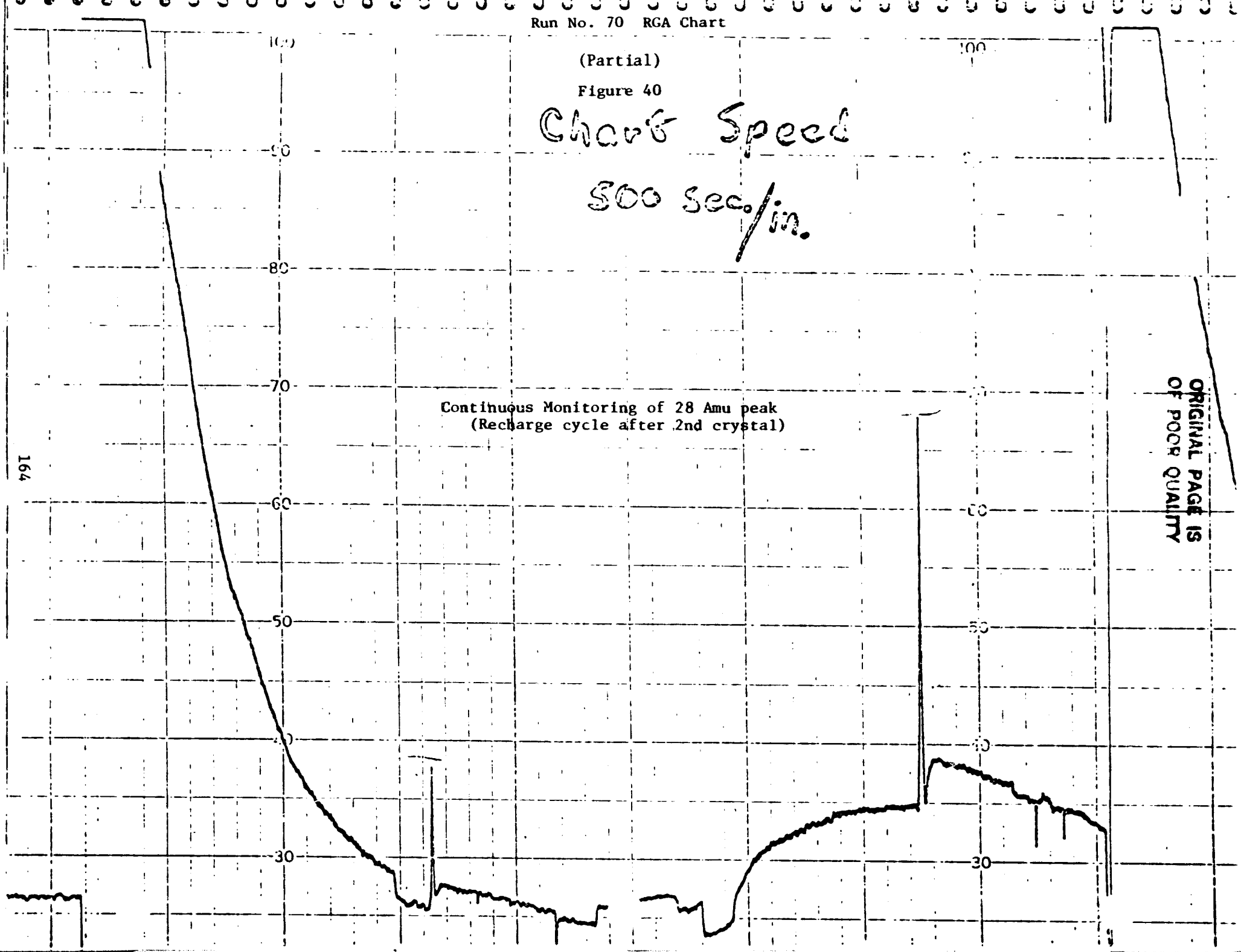

relationship between carbon monoxide production (amu-28) within the crystal grower and the crystal growth cycle.

Extensive research had previously been performed regarding the relationships between furnace temperature, furnace pressure (vacuum levels) and the production of carbon monoxide (CO), carbon dioxide (CO_2), Silicon monoxide (SiO), Silicon dioxide (SiO_2) and Silicon Carbide (SiC).[9] This research was performed in conjunction with the heat exchanger method (HEM) of silicon production. This research indicated that at certain temperature pressure levels, CO and SiO are produced by the interaction of the fused quartz crucible and the graphite furnace parts that come in contact with the crucible. The gaseous CO that is produced by this reaction is capable of being transported to the silicon melt where it may react with the liquid silicon-depending on temperature and pressure to form SiC. If a sufficient concentration of SiC is allowed to build up in the silicon melt, SiC precipitation can cause constitutional super cooling at the crystal growth interface resulting in structure loss.

The data presented in the HEM report seemed to indicate that the SiO production would occur in a similar fashion as CO production and would also be formed by the reaction between liquid silicon and the fused quartz crucible ($Si + SiO_2 \longrightarrow 2SiO$).

It was not possible to measure the partial pressure of SiO using the RGA due to the fact that it condenses to a solid at a temperature above the temperature of the exhaust gases of the crystal grower. Therefore, our data is based solely on the CO concentrations observed in the crystal grower exhaust gases. However, it should be noted that visual observation of SiO concentration within the furnace did show a direct relationship with the concentration of CO recorded by the RGA.

The studies were performed during normal crystal growth cycles involv-

ing the following general procedures:

1). Melt Down

2). Temperature Stabilization

3). Seed Dip and Neck Growth

4). Crown growth

5). Straight Body Growth at Diameter

Figures 41, 42, and 43 illustrate the relative concentrations of CO as a function of time during a complete growth cycle. In each case, the maximum CO concentration occurred during the meltdown cycle generally when the furnace temperature was at its highest level and a large majority of the silicon had been melted. However, it was also observed that decreases in pressure levels in the grower tended to increase the CO concentration.

Normal crystal growth pressures were 20 torr of argon. Severe changes in argon pressures were not attempted because the RGA studies were done in conjunction with and were not the primary objective of the growth run. Decreasing the argon pressure in the crystal grower would have the effect of lowering the overall concentration of argon in the furnace atmosphere in relation to other gaseous species present, however, the data still indicates that a significant, measurable increase in CO concentration was brought about by a decrease in argon pressure from 20 torr to 15 torr.

The CO concentration in all three crystal growth cycles represented by Figures 41, 42, and 43 tends to be the same:

1). A sharp increase during the meltdown cycle.

2). A sharp decrease during melt stabilization when the furnace temperature is rapidly decreasing to the proper growth temperature.

3). A gradual slow decrease in the CO concentration as the straight body section of the crystal is grown.

The sharp increase and decrease in the CO concentration during the

46 0700

28amu - Green - CO

44 amu - Blue - CO_2

Run No. 8

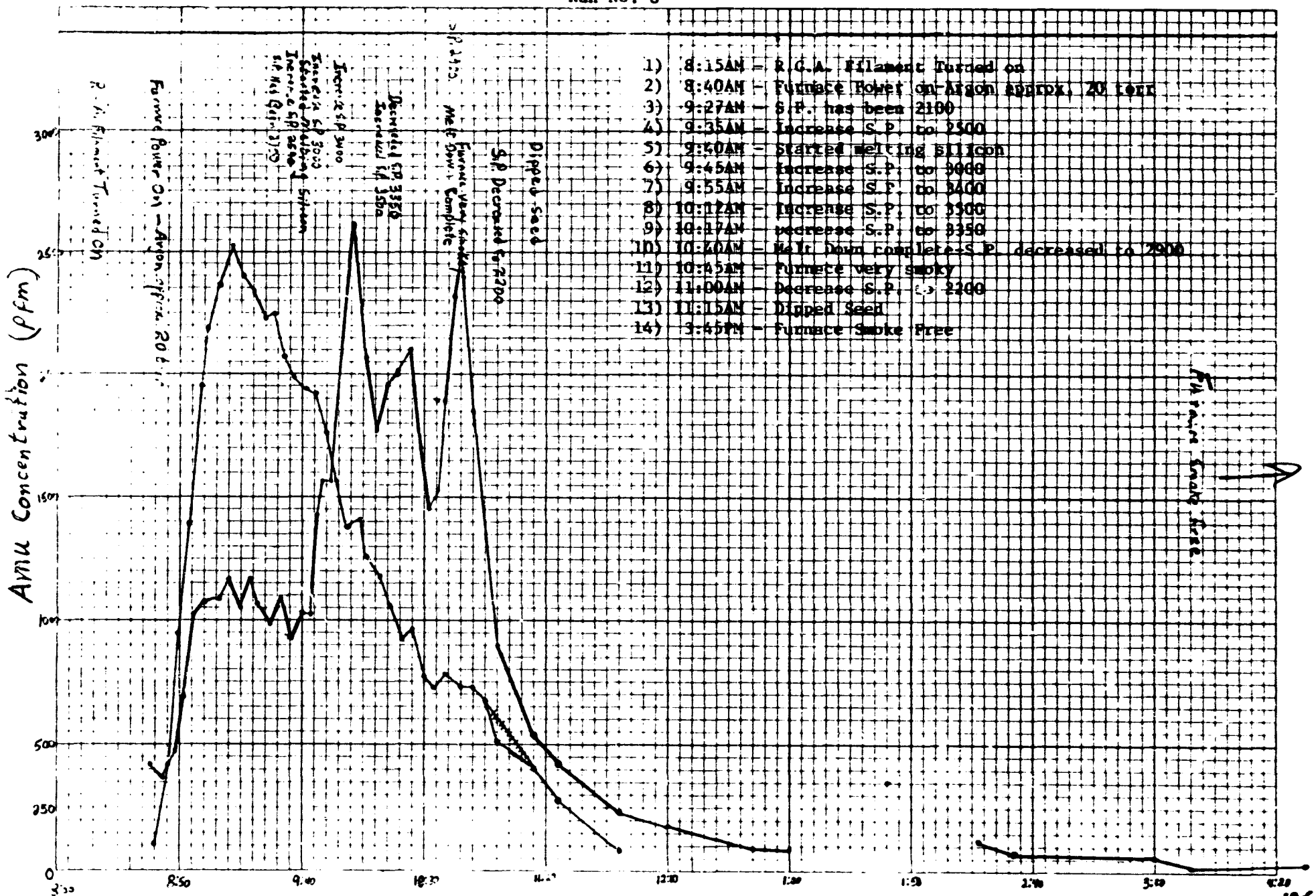

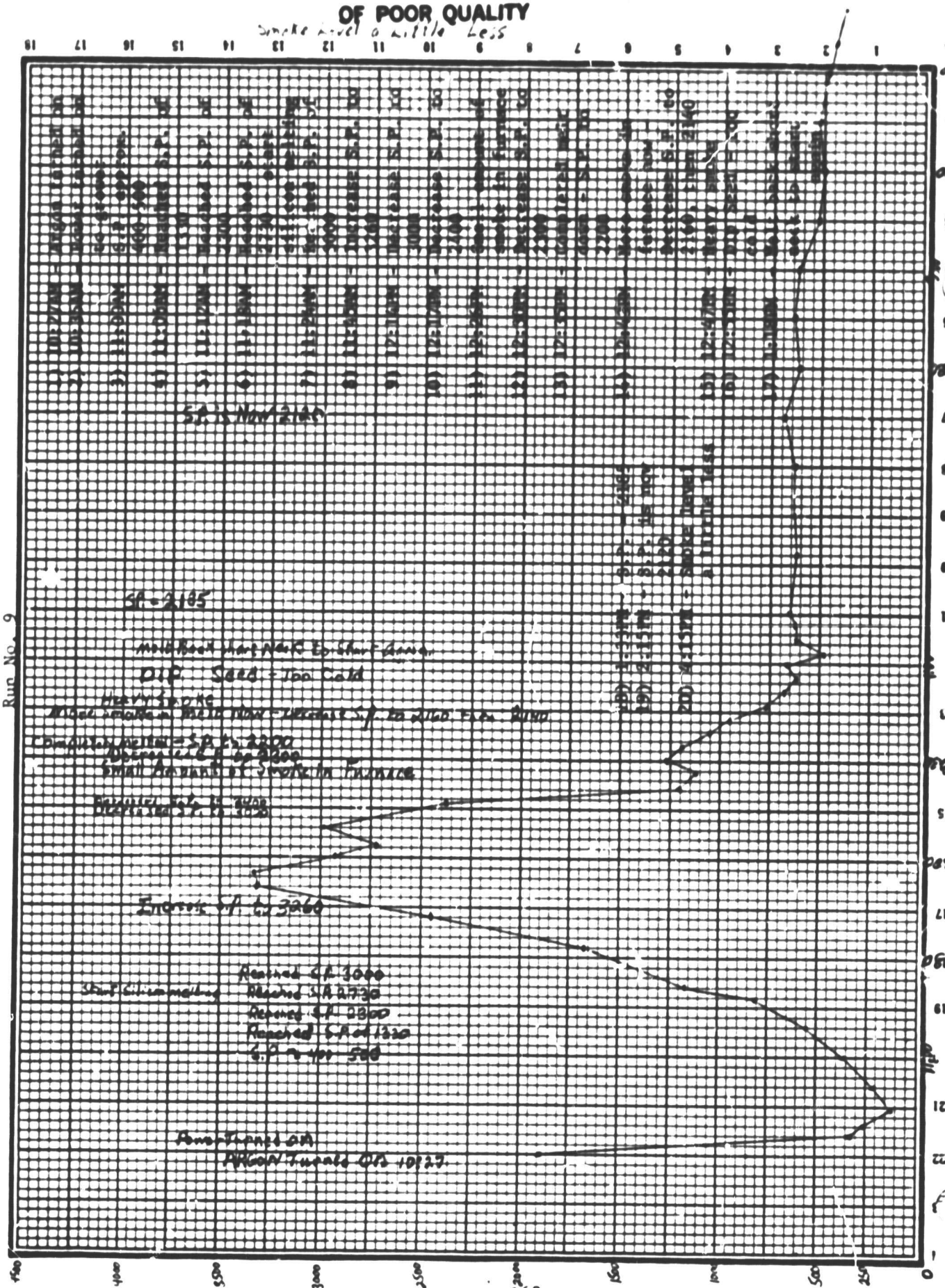

Run # 14
Std Graphite Parts
Concentration (ppm)
4000
3500
3000
2500
2000
1500
1000
500
0
8:30
9:00
10:00
11:00
12:00
1:00
2:00
2:30

Figure 43

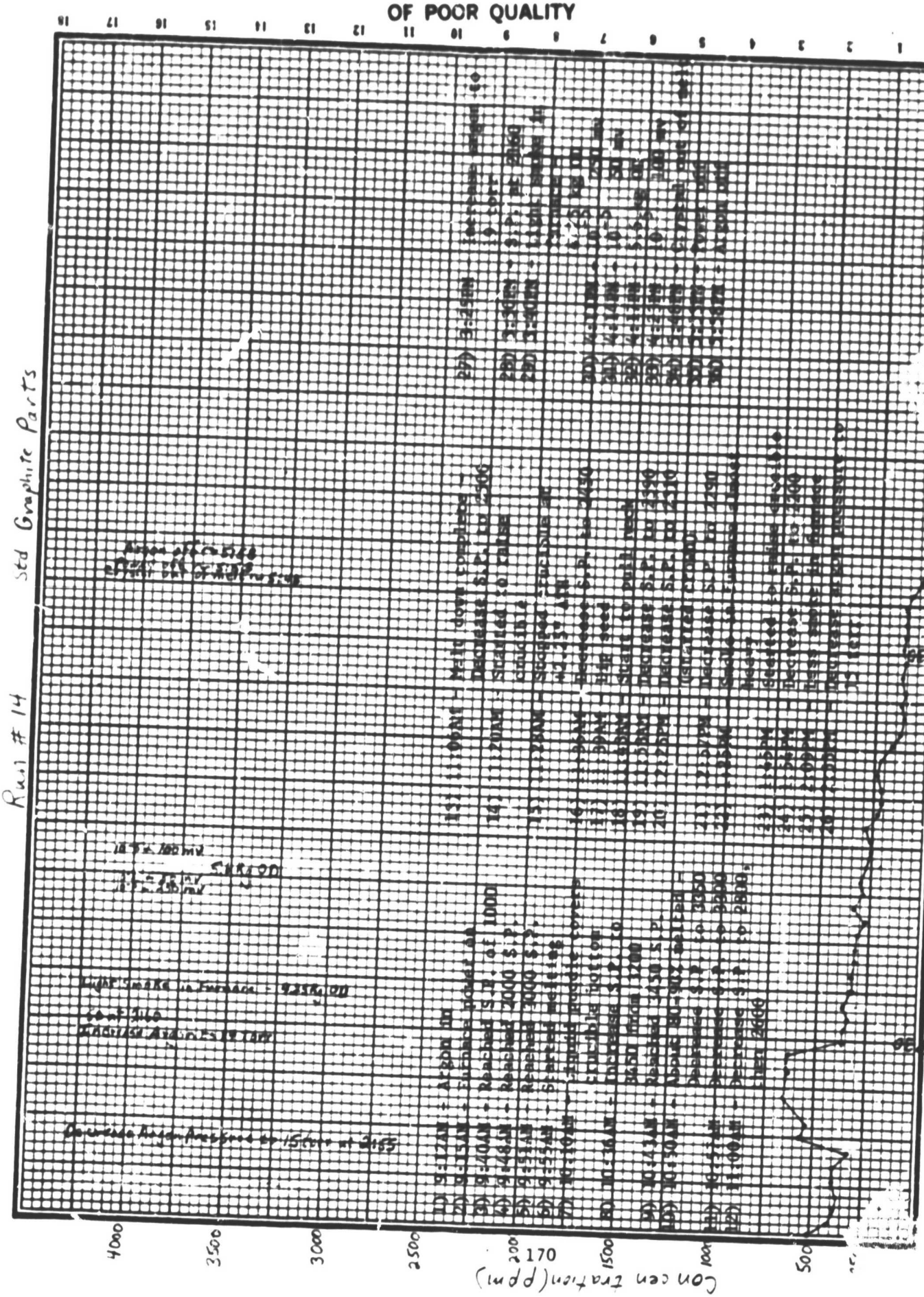

Figure 43 (Cont'd)

melt down and stabilization cycles can be attributed to the rapid increase and decrease in the furnace temperature. However, the slow decrease in CO concentration during the straight growth cannot be attributed to furnace temperature or pressure - the temperature is actually increased during the middle and later stages of the straight growth cycle. Therefore, another factor must be considered in order to explain the slow decrease in CO concentration during the straight growth cycle. The answer is found in the need to maintain a constant melt level in relation to the furnace's resistance heater. It is necessary to maintain this constant melt level to maintain thermal equilibrium during the growth process.

As the crystal is grown, the level of the liquid silicon (melt) decreases inside the crucible. The fused quartz crucible and its outer supporting parts are raised in relation to the stationary heater to maintain the silicon liquid level at the same starting position in relation to the heater. As the graphite parts are raised they leave the hot zone (heater zone) of the furnace decreasing the temperature below the reaction temperature of Carbon (C) and Silicon dioxide (SiO) to produce CO.

Observations of SiO concentration taken during normal crystal growth indicate that the highest concentrations are observed at the end of the melt down cycle. The concentrations are negligible until a majority of the silicon is melted and then they tend to decrease as the stabilization cycle is completed and the straight growth progresses. If another source of oxygen other than the fused quartz crucible is present in the furnace then SiO and CO concentration are directly affected.

Although the level of CO concentrations has been indicated on the graphs in Figures 41, 42 and 43, neither the method for calculating these values nor the values themselves have been varified by an authoritative source. However, they can be used to interpret relative CO concentrations

and may be factual concentrations.

The CO concentrations associated with these crystal growth runs did not appear to affect the crystal structure of the crystals grown. It is of great interest what concentration level of CO would be detrimental to single crystal growth. However, the RGA was obtained on a trial basis and was returned to its vendor following these initial studies.

A Residual Gas Analyzer could be a useful tool for determining if a crystal grower has an atmosphere conducive to high quality crystal growth. It can also be used to monitor the grower atmosphere during growth cycles to indicate when the grower's gaseous environment has changed.

Whenever a known microscopic water leak has developed within the crystal grower the furnace atmosphere has been affected such that the ability to grow monocrystalline material has been precluded. Evidence of this can be readily seen in the discussion regarding Run No. 70.

Small air leaks although detrimental to continuous recharge crystal growth have not resulted in an immediate structure loss problem.

Based upon the fact that it was possible to grow monocrystalline material with an air leak present, a theory that impurities entering the furnace in conjunction with an air leak are not in themselves causing a structure loss problem was proposed. It appears to be the excessive silicon monoxide and silicon dioxide that are formed when a supply of oxygen is available (air leak) along with the accelerated crucible devitrification that may be the major cause of structure loss.

Observations taken during Run No. 60 and Run No. 62 caused us to question the primary cause of structure loss during continuous runs. It is still felt that a leak-free system is imperative for growing high quality crystals over an extended period of time. However, even with a

tight, leak-free system, the possibility exists that silicon monoxide or silicon dioxide may build up on the upper portion of the crucible wall and, from time to time, fall into the melt and result in loss of monocrystalline structure.

(b). Furnace Thermal Conditions

Thermal perturbations have been known to cause the loss of monocrystalline structure during crystal growth. However, gradual thermal changes (non-equilibrium) beyond the normal range during crystal growth have not seemed to be a problem. Several crystals have been grown when the crucible lift was not functioning with no loss of monocrystalline structure. However, extreme temperature changes or fluctuations such as power loss, severe cooling water temperature change or severe instantaneous argon flow rates have caused structure loss problems.

The possibility exists that thermal perturbations while causing significant changes in growth rates may cause solid particles to be forced off the walls of the crucible which in turn is the cause of structure loss problems.

In addition to thermal perturbations as a cause of structure loss, improper thermal gradients are of even more importance in the growth of monocrystalline silicon crystals. Radial thermal gradients must be properly controlled to maintain the silicon in the liquid state at the crucible walls and across the surface of the melt. This allows optimum solidification at the growth interface. The vertical thermal gradient in the melt must also be condusive to correct melt solidification at the growth interface while inhibiting spontaneous nucleation or solidification within the melt.

Any problems that may have been associated with thermal considerations was corrected early into the crystal growth program for both 12-inch and 14-inch hot zones.

(c). Mechanical Considerations

The crystal growth process is capable of withstanding moderate mechanical shock or vibration without the loss of monocrystalline structure. Moreover, regular continuous melt vibration is not uncommon during crystal growth and has not been a structure loss problem. The structure loss problem arises when excessive external or internal shock or vibration occurs. This type of shock or vibration may be initiated by several sources such as:

1). 1). Seed Lift cable jerk or excessive vibration.

2). Crucible shaft jerk or sticking.

3). Loose graphite supporting parts or failure of these parts (cracking).

4). Rubbing of moveable hot zone parts against stationary hot zone parts.

5). Physically bumping, shaking, or falling on the grower.

These sources of mechanical perturbation can be prevented by proper machine set up and maintenance.

During the crystal growth development work, there have been occasions when mechanical functions have malfunctioned without causing structure loss. Some examples are:

1). Seed Lift stopped.

2). Crucible Lift stopped.

3). Crucible rotation stopped.

In each case, the malfunctions were corrected within a short period of time - 5 minutes. However, on two separate occasions, the crucible lift stopped for several hours without structure loss problems.

(d). Electrical Considerations

In order to function properly, the crystal grower must maintain the integrity of its electrical controls.

1). The resistance heater must function and control properly through

the temperature sensing device (thermocouple or optical pyrometer).

2). Although it is possible to grow a crystal totally with manual seed lift control, much improved diameter control can be achieved using the Automatic Diameter Control (ADC) System. Optical as well as electrical functions are involved with the ADC.

3). Vacuum pumps are critical to the maintenance of the proper clean argon purge atmosph. . Electrically controlled valves for separate control of both upper (secondary) and lower (primary) vacuum systems is critical to the recharging process.

4). All mechanical functions except for argon flow and coolant water flow are electrically controlled. Therefore, an electrical malfunction in these controls could cause structure loss problems associated with mechanical considerations.

As with mechanical malfunctions, electrical malfunctions have occurred without structure loss problems occuring:

1). Momentary loss of heater power.

2). ADC malfunction.

3). Momentary loss of vacuum pump operation.

Electrical malfunctions can be minimized by proper machine set up and maintenance. However, the incoming plant electricity is dependent on the commercial supplier - (utility company).

(e). Thermal Cracking

Thermal cracking is a condition normally caused by the too rapid cooling of silicon crystals immediately following the growth cycle. Cracks form in the silicon crystal due to the rapid expansion of the solidified silicon when cooled too fast.

When thermal cracking occurs, it usually occurs in the bottom quarter of the crystal. However, thermal cracking has been seen throughout two-thirds

of the crystal when cooling rates were extremely high.

Thermal cracking is usually caused by abrupt removal of a crystal from the melt while it is still at or near to its straight growth diameter. Thermal cracking can also be created by removing a properly tapered crystal from the furnace chamber into the cold pull chamber too rapidly.

Thermal cracking, if present, precludes the ability to cut complete wafers from the portion of the crystal affected. Furthermore, it creates the possibility of blade damage and saw damage.

Thermal cracking is not a problem if normal crystal growth techniques are followed.

4.5.4 Crucible Performance

The devitrification and the apparent dissolution of the vitreous silicon crucible is of concern primarily as it may affect the quality of the ingot material.

A number of questions were raised regarding (1) the maximum lifetime of a crucible in the present mode of operation, (2) the effects of impurities in the glass on the stability of the crucible, and (3) the possibility of contamination of the melt by the crucible (impurities or SiO_2 particles).

The role of the crucible in structure loss is not well understood. In a typical non-recharge run of 12 to 18 hours duration (Figure 44), the inner surface of the crucible usually shows a slight amount of devitrification in the form of small circular spots about 1 mm in diameter randomly distributed. The surface, however, is generally smooth and free of pits or open bubbles.

Severe devitrification (Figure 45) has been observed occasionally after long periods in contact with the melt. The circular devitrified areas grow and become more numerous. Bubbles originally beneath the surface are exposed,

The illustration is not typical, however, of all long recharge runs. In this case, the condition of the crucible was far worse than usually observed.

The visual appearance of crucibles from various commercial vendors varies considerably. Differences in the degree of fusion, the inside surface quality, and the bubble structure are apparent. Chemical purity of all crucibles is good, yet some differences are apparent. The analyses in Table 33 were supplied by the vendors.

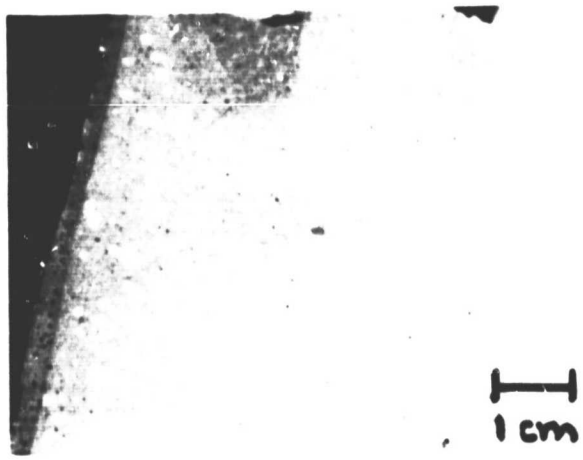

Crucible devitrification after 18 hours
(Inside surface, actual size) ← → 1 cm

Figure 44

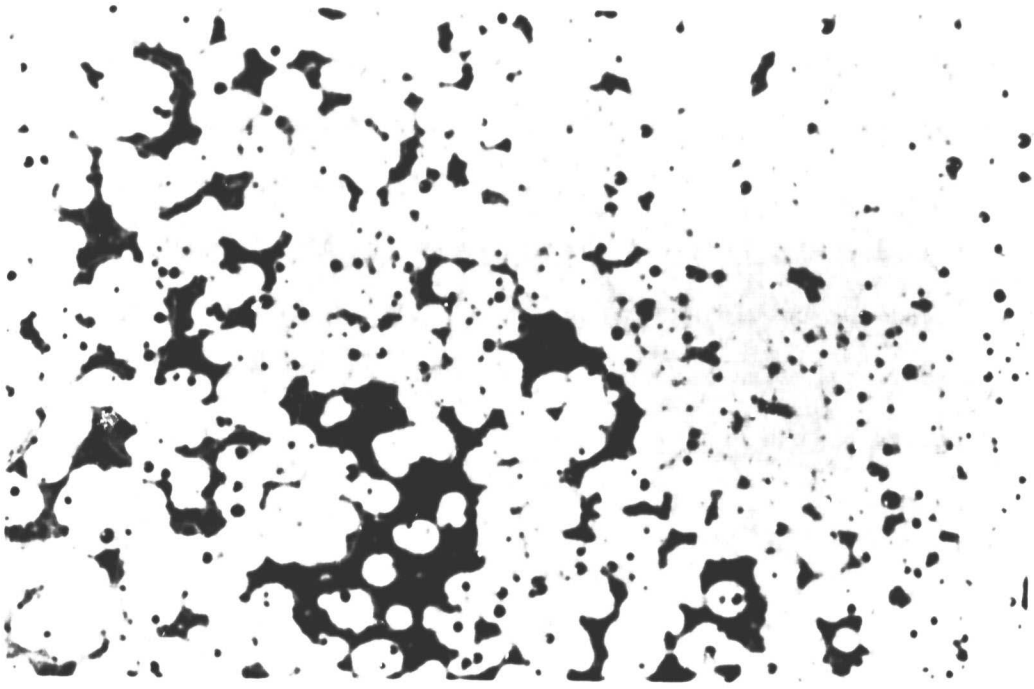

Actual size ← → 1 cm

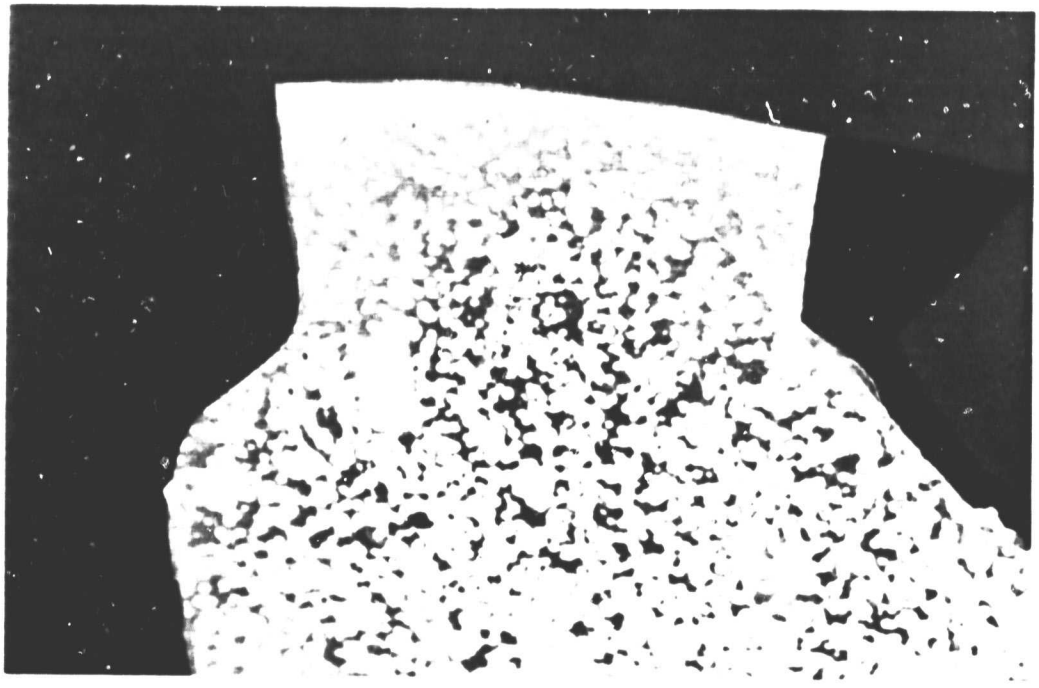

Magnified 3.5X ←—— 1 cm ——→

Unusually severe crucible devitrification

Figure 45

Figure 46 shows a crucible after a typical recharge run. The white layer is the devitrified material which tends to flake off from the glassy silica.

The external portion of the crucible is affected the most, and also that portion which is not in intimate contact with the graphite crucible support exhibits little devitrification. Although much has been written on the devitrification of vitreous silica, it is very difficult at this point to identify the cause as it relates in particular to the CZ process.

CRUCIBLE DEVITRIFICATION
White devitrified SiO_2 forms on outside of
the crucible as a scale

Figure 46

Time and temperature effects were noted during the crystal Growth Development Program. A major portion of the degradation occurs during the melting or recharge cycle when the crucible is subjected to considerably higher temperatures.

The lifetime of the crucible was extrapolated, based on a typical devitrification rate to at least 100 hours.

The statement of work called for investigation of low cost crucibles. Earlier in the program, several crucible manufacturers were contacted. One crucible manufacturer* responded by offering a crucible made from impure sand. This crucible could be obtained at a cost of $90.00 each in small quantities for a 12-inch diameter by 9-inch high crucible. This price could come down perhaps further in quantity purchases.

Chemical analyses of the sand crucible as compared with the high purity quartz crucible are shown in Table 32. It can be seen that the sand crucible had at least an order of magnitude greater impurity content than the crucibles made from natural quartz crystal.

Table 32

Impurity	Quartz Crystal	Sand
AL	20 PPM	200 PPM
Ca	3	50
Ti	2	80
Fe	1	65
Mg	1	8
Na	1	20
K	3	30
Li	1	6

Comparison of Impurity Levels in crucibles made from sand and quartz crystal. Values are in parts per million.

*Quartz Products Corp., Plainfield, N.J.

Four sand crucibles were purchased for evaluation. The first test consisted of establishing the softening point of the crucible. Because of the low purity material, it was expected that the softening point of the crucible might be too low for crystal growth and/or devitrification might proceed too rapidly.

We placed an empty crucible in the furnace and heated the furnace to meltdown temperature. The crucible seemed to withstand these conditions quite well. There was no evidence of sagging or buckling. Approximate temperature was 1500°C for one hour. No devitrification was observed. The crucible fractured during the cool-down cycle.

We then put a small quantity of silicon in a second crucible and attempted to melt it. The furnace was heated to melt-down temperature but the silicon would not melt. We increased the temperature approximately 100° and the silicon still did not melt. We then concluded that there was perhaps something wrong with the control system of the furnace and aborted the run, failing to melt any silicon in the second crucible.

It was then decided to put a full 16 kilogram load into a crucible assuming that the small quantity of silicon was the previous reason for the failure to melt. However, extreme difficulty was experienced in melting the silicon. The furnace had to be raised approximately 200° higher than normal melt-down temperature to achieve any melting at all. This extreme temperature caused the crucible to sag and buckle. The silicon eventually melted, but only after an extra hour had been consumed in melting. Furthermore, a number of pieces of silicon adhered to the side of the crucible which could not be melted off. At this point, the crucible was badly distorted but appeared to be containing the molten silicon and, furthermore, the silicon appeared to be

clean and free of slag or oxide. We therefore, decided to attempt to grow a crystal.

Three attempts at starting a crystal crown were made, none of which succeeded. Zero dislocation structure was lost quickly at approximately 1 inch diameter. It was therefore, decided on the third attempt to continue to pull a dislocated crystal. A 5-inch ingot was pulled which dislocated and quickly went polycrystalline. The crucible maintained its integrity throughout the run without leakage or failure, and we were able to pull most of the silicon from the crucible. The portions of the crucible which were below the melt level were also extremely distorted.

When the crucible was cool and was removed from the furnace, it was observed that it had not actually buckled, but it was swelled. The external surface of the crucible had maintained the original shape of the graphite support, but, in certain areas, it had swelled to a thickness of approximately 3/4 of an inch. The inside surface, which had been in contact with the silicon, remained vitreous and did not appear to be seriously attacked by the silicon. The bulk of the crucible wall, however, was granular and porous.

The crucibles as they were received were much more opaque than the normal crucibles. This indicated that the degree of vitrification or glassiness in the crucible was much less than a normal crucible. It was believed that this lack of vitrification caused a reduction in the thermal conductivity and transmissivity of the crucible, resulting in the problem of melting the silicon. As the swelling of the crucible wall continued, the problem intensified and higher and higher temperatures were required to melt the silicon. If the sand crucible could be fabricated in a more dense, vitrified form, it should perform in a manner similar to that which we are used to.

The vendor of these crucibles, Quartz Products Corporation, was informed of the results and asked to pursue the possibility of making these changes to the crucible.

Crucible devitrification was considered to be a possible cause of structure loss early into the crystal growth development program. Efforts were concentrated on recording observations of crucibles used before and after continuous recharge runs as well as single ingot growth runs.

Results have shown that severe devitrification can degrade the smooth glassy inner surface of the crucible to such an extent that relatively large bubble holes appear on the surface, many being filled with solidified silicon. When this type of devitrification occurs, it is highly probably that solid particles of quartz (SiO_2) are released from the crucible surface into the melt. Most of these particles are held against the walls of the crucible by the centrifugal force of the crucible rotation. However, it is always possible for some particles to somehow be swept out into the melt where they can come in contact with the growth interface, causing the crystal to lose structure. The possibility exists that the faster the growth of the crystal (pull speed), the greater the probability of sucking particles of quartz from the crucible walls into the melt. We have observed during our continuous runs that, when the crucible becomed devitrified to the degree where particles may come off the inner walls of the crucibles, fast pull speeds many times result in structure loss. However, slower pull speeds tend to result in a higher percentage of high quality crystal late in a continuous run when devitrification is marginal. For this reason, it was decided not to attempt fast pull speeds on several of the later 100 kg continuous runs.

Several examples of crucible devitrification are shown in the pictures on the succeeding pages.

Figures 47 and 48 show relatively severe devitrification on the inside

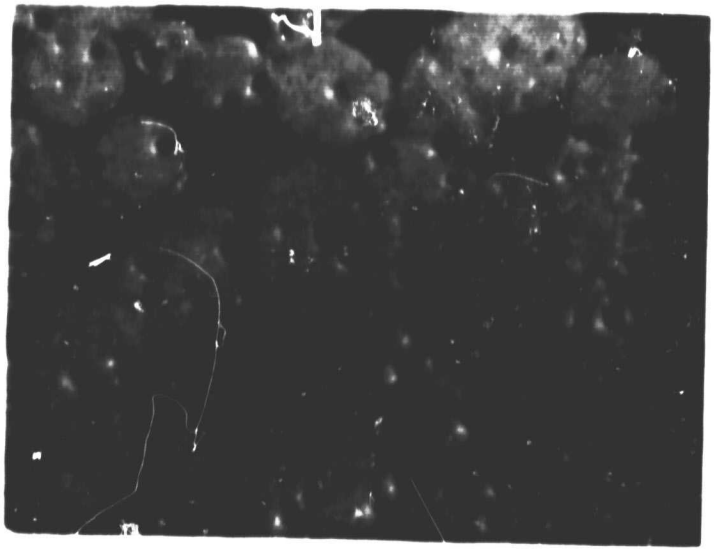

Figure 47

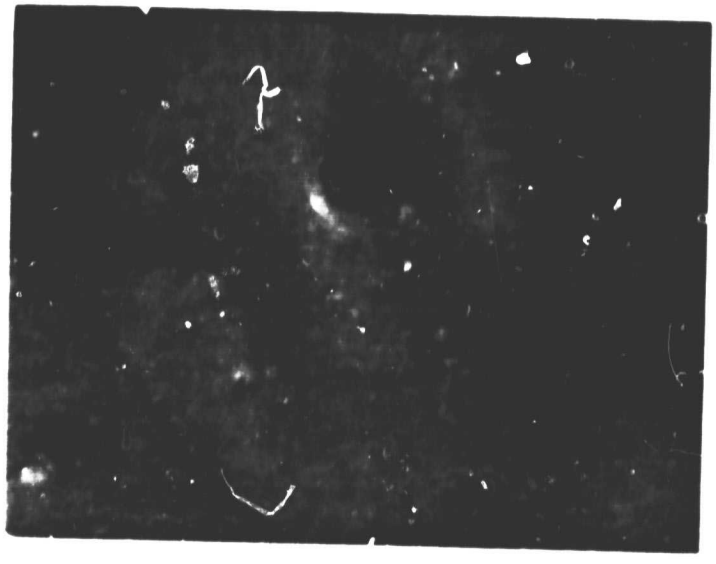

Severe Crucible Devitrification

Figure 48

surface of a crucible after forty four (44) hours of run time. Devitrification is spotty, but covers a majority of the crucible surface below the melt level. Deep bubble holes are visible, several filled with solidified silicon. Figure 48 is a close-up of the same crucible as Figure 47, showing the relative depth of one bubble blow hole.

Figure 49 shows the crucible used in Run No. 47 that failed after approximately fifty (50) hours of run time. The outside of the crucible is shown. It is difficult to tell from the picture that the clear area on the wall of the crucible is a void where the crucible ballooned out on the interior surface of the crucible. Oddly enough, the inner surface of the crucible does not exhibit severe devitrification. Patches of devitrification occupy less than a majority of the inner surface. Moreover, very few open bubble holes are visible (Figure 50). At the time the crucible failed during Run No. 47, 88% of the 60 kg of crystal grown was high quality crystal.

Figure 51 shows the crucible from Run No. 49. The inner surface (melt side) is shown on the left side. The outside surface (graphite side) is shown on the right and a cross section is shown in the middle. As can be seen, the devitrification is more severe on the outside surface of the crucible (thicker and frothy) than on the inner surface. Even though we would classify the inner surface devitrification of this crucible as severe, we were still able to grow high quality crystals at the end of this run after more than eighty hours of continuous run time and more than 100 kg of silicon crystals had been grown. Close examination of the inner surface reveals a fused appearance with a relatively small amount of bubble holes.

Figure 52 shows pieces from the crucible used for Run No. 2*. This crucible was run for a total of 108 hours. Severe devitrification is definitely indicated. The original glassy portion of the crucible has been

C-3

Crucible from Run No. 47
Figure 49

Crucible from Run No. 47 (Inside Surface)

Figure 50

Crucible Used for Run No. 49
Figure 51

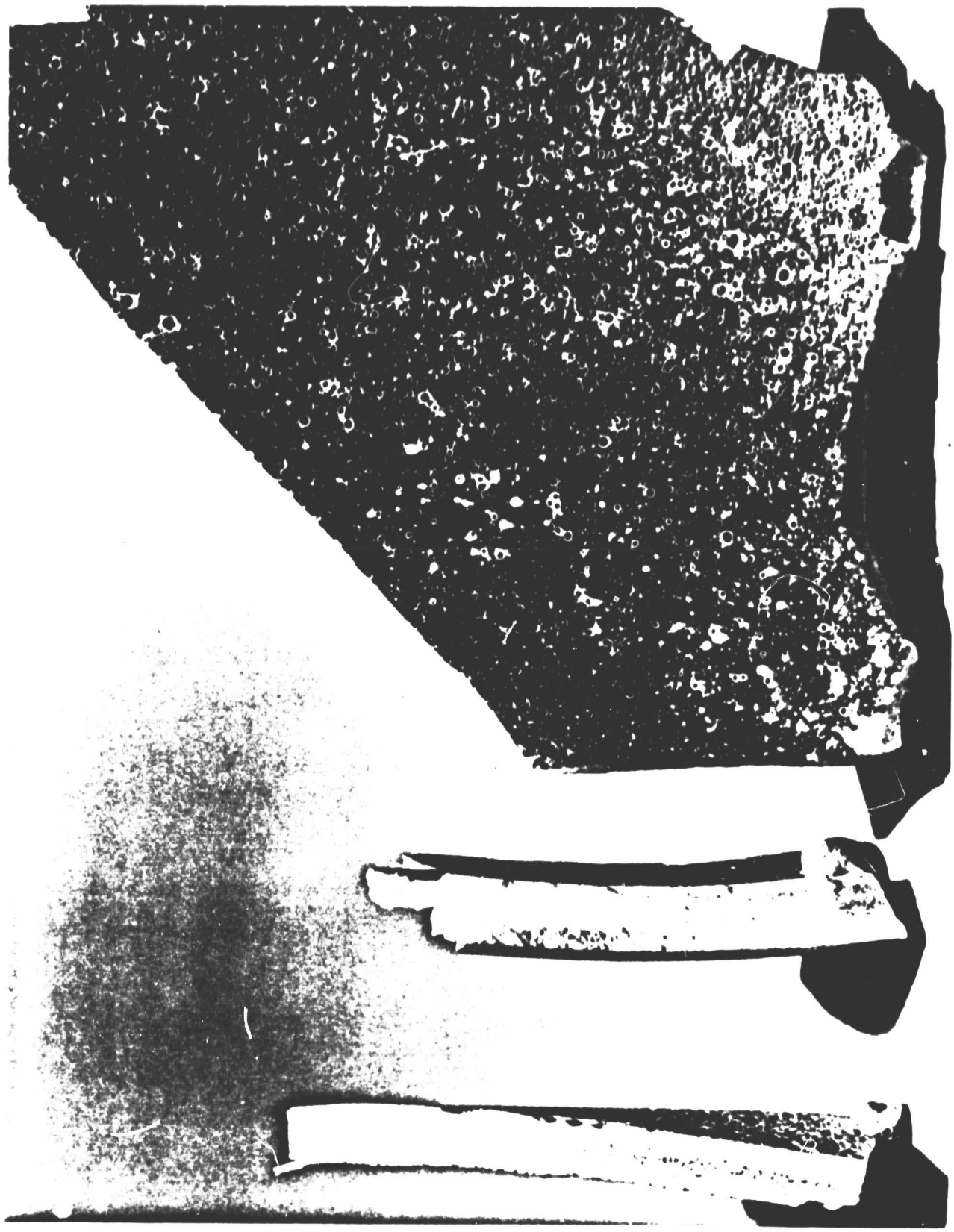

Crucible Used for Run No. 2*
Figure 52

crystallized through nearly three-fourths of its original thickness in certain places. This crucible is very near to a condition of failure. A considerable majority of the devitrification has progress from the exterior surface of the crucible that is in contact with the graphite supporting parts. However, a significant amount of devitrification has originated and progressed from the interior crucible surface that contacts the silicon melt. As previously stated, the mechanism causing this devitrification is not understood satisfactorily. Although quartz has several phases dependent on temperature and pressure, reference materials state that generally High-Quartz changes to Tridymite at approximately 867°C and Tridymite will change to Cristobalite at approximately 1470°C. The softening point of fused quartz is 1667°C. During overly agressive meltdowns (excessively high temperatures) the crucible has been known to soften and sag or deform. Therefore, it can be assumed that crucible temperatures in excess of 1470°C are routinely achieved during meltdowns. The phase changes mentioned above are of a sluggish nature and progress very slowly. However, many elements and compounds have the ability to accelerate the devitrification process. Namely the alkalies, alkali earths, halides and some metals.

The inconsistency in degrees of devitrification along with impurity analysis studies of silicon crystals led to the impurity analysis of new and used crucible samples.

Table 33 lists typical impurity concentrations of fused quartz crucibles (as supplied by the crucible manufactures). Also included in table 33 are impurity analysis results for samples of crucibles taken from Run No. 47 and Run No. 49. From this data, it appears that used crucibles have accumulated impurities during the continuous recharge run. The source of these impurities is not completely understood however, several possibilities exist:

CRUCIBLE IMPURITIES
(Concentration in PPM by Weight)

1 Impurity	2 Amersil	3 Quartz Products	4 General Electric	5 Corning	6 Run #47 Amersil	7 Run #49 Toshiba Cruc.
Al	12	20	28	5	6	7
B	1	NR	1	0.5	0.1	0.4
Ca	4	3	3	1	33	410
Cu	1	NR	1	0.05		
Fe	3	1	4	5	11	12
Li	1	1	0.5	NR	Int	Int
Mg	1	1	1	0.1	6	0.4
K	2	3	3	0.1	35	80
Na	3	1	3	2	66	41
Ti	1	2	2	10	7	16
Cr	NR	NR	3	NR	Int	Int
Zn	NR	NR	2	NR	0.9	5
Mn	NR	NR	2	NR	0.1	0.4
Cl					29	41
Br					9	28
F					20	11
I					6	7
S					2	8
P					6	25
Mo					6	15
Zr					9	0.9
Se					13	32

TABLE 33

1	2	3	4	5	6	7
Impurity	Amersil	Quartz Products	General Electric	Corning	Run #47 Amersil	Run #49 Toshiba Cruc.
Ba					6	35
Pb					2	3
Ge					0.6	6

NR: Not Reported
Int: Interference

Maximum impurities in Fused Quartz (vitreous SiO_2) crucibles provided by vendors. Expressed as parts per million by weight.

TABLE 33 (Cont'd)

1). The silicon raw material.

2). Water or air leaks in the furnace.

3). Improperly cleaned grower interior.

4). The crucible itself.

Samples of new, unused crucibles were sent out for impurity analysis along with used portions of similar crucibles made by the same manufacturer. Table 34 lists the impurity concentrations found in samples of crucibles used for the runs indicated. The seven elements listed are those which have appeared to change the most from impurity levels supplied by the quartz manufacturers. The most noticeable statistics on the chart are the major differences in the impurity levels of new crucibles as opposed to the impurity levels supplied by the respective crucible manufacturers. A complete list of impurity concentrations is presented in Table 35. The discrepancy between the impurity concentrations indicated by the Commercial Testing and Engineering Co. results and purity claims by the crucible manufacturers precipitated special analysis work being performed through one of the crucible manufacturers (Quartz Products Corporation). The results of Quartz Products impurity analysis tests are contained in Table 36.

Duplicate samples of the new and used crucible fragments were sent to Quartz Products. Therefore, results should be directly comparable. The major difference revolved around the testing method:

Quartz Products - Atomic Absorption Spectrophotometer method.

Commercial Testing - Spark Source Mass Spectrography method.

A copy of the return letter enclosed with the Quartz Products results can be found on page 199. This letter contains a brief description of the sample preparation and comments concerning the results.

Commercial Testing and Engineering Company also defends their results and testing procedure as being accurate.

Impurity Concentrations (PPM)

Crucible Samples and Other Related Samples

Sample #	Na	Mg	Ca	K	Fl	Cl	Ba
47-Crucible 12" (Amersil)	66	6	33	35	≃20	29	6
49-Crucible 14" (Toshiba)	41	7	410	80	11	41	35
55-Crucible 14" (Quartz Products)	24	< 0.2	36	52	≃170	9	20
2* Crucible 12" (Quartz Scientific)	57	82	68	220	MC > 0.1%	25	480
New 14" Crucible (Quartz Products)	61	19	14	120	≃270	11	0.9
New 14" Crucible (Toshiba)	20	3	3	24	≤ 1	20	
Run 2* Top of Crucible (cleaned) (Quartz Scientific)	92	4	20	89	≃460	18	≤0.9
Run 55 Hopper Deposit formed during Recharge Cycle after water leak developed (White Powder)	>160	11	21	> 770	≃550	28	*1

TABLE 34

IMPURITY CONCENTRATIONS (PPM)

Sample ID	Na	Mg	Ca	K	Zn	Cu	Fe	Cr	Source Ta	Ca	Ti	Al	P	F	Cl	S	Ba
47-Crucible (Amersil)	66	6	33	35	0.9	2	11	INT.		0.5	7	6	6	≃20	29	2	6
49-Crucible (Toshiba)	41	7	410	80	5	4	12	INT.	2	0.1	16	7	25	11	41	8	35
55-Crucible Q.P.	24	< 0.2	36	52	3	*11	20	INT.			2	9	3	≃170	9	3	20
2* Crucible Q.S. 12"	57	62	68	220	7	*6	150	INT.	<0.4	<0.4	43	150	34	M.C. >0.1%	25	1%	480
New Q.P. Crucible	61	19	14	120	3	*3	13	INT.	<0.2	<0.2	2	9	8	270	11	13	0.9
New Toshiba Crucible	20	3	3	24	1	*0.9	1	INT.	<0.1	<0.1	9	8	3	≤ 1	20	1	*7
2* Crucible Cleaned Top Edge Q.S. 12"	92	4	20	89	2	*9	7	INT.	<0.3	<0.3	10	16	14	≃460	18	2	≤0.9
Hopper Deposit Run #55	>160	11	21	>770	2	*8	12	INT.	<0.1	<0.1	*190	>62	48	≃550	28	9	*1

TABLE 35

IMPURITY CONCENTRATIONS (PPM)

Sample ID	U	Th	Pb	Ce	La	I	Ag	Mo	Nb	Zr	Y	Sr	Rb	Br	Se	As	Ge
47-Crucible (Amersil)	≤0.9	≤1	2	0.8	0.5	6	1	6	2	9	2	0.9	0.3	9	13	0.2	≤0.6
49-Crucible (Toshiba)	≤2	≤3	3	2	1	7	*0.9	15	0.7	0.9	4	13	0.1	28	32	0.2	6
55-Crucible Q.P.	≤1	≤2						0.9	≤1	≤0.5	0.3	0.9		7			
2*-Crucible Q.S. 12"	≤3	≤4		≤0.7				2	2	7	1	7		17			
New Q.P. Crucible	≤1	4						2	*1	*1	*1	0.2		7			
New Toshiba Crucible	≤1	≤1						*4	≤2		1	0.2	≤0.1	1		≤0.1	
2*-Crucible Cleaned Top Edge Q.S. 12"	≤3	≤3						3	≤0.3	5	≤0.3	0.3		28			
Hopper Deposit Run #55	≤0.4	≤0.5	0.5	0.1	0.2		≤0.5	MC >0.1%	0.8	1	≤0.4	≤0.1	≤0.1	14		≤0.3	≤0.1

TABLE 35 (Cont'd)

IMPURITY CONCENTRATIONS (PPM)

Sample ID	Ga	Ni	Co	Mg	V	Sc	B	Li	Nd	Pm	Sn
47-Crucible (Amersil)	0.4	0.5	≤0.2	<0.1	0.4	≤0.2	<0.1	INT.			
49-Crucible (Toshiba)	1	1	0.6	0.4	0.2	≤0.4	0.4	INT.			
55-Crucible Q.P.	0.3	≤1	≤0.3	<0.1	<0.1	≤0.2	*1	1			
2* Crucible Q.S. 12"	1	≤3	≤0.7	0.6	0.2	≤0.5	0.3	1			
New Q.P. Crucible	0.6	≤1	≤0.3	≤0.1	<0.1	0.2	0.5	7			
New Toshiba Crucible	0.5	≤1	≤0.2	<0.1		≤0.2	0.9	0.6			
2* Crucible Cleaned Top Edge Q.S. 12"	≤0.4	≤2	≤0.2	0.2	≤0.1	≤0.4	0.8	0.4			
Hopper Deposit Run #55	0.5	≤4	<0.1	0.1	<0.1	<0.1	0.3	<0.1	0.2	0.1	≤0.1

TABLE 35 (Cont'd)

	TOSHIBA neuf - New (sheet 1 b)	TOSHIBA utilisé - Used (sheet 1 a) Run #49	Q.S.I. utilisé haut du creuset (sheet 2 a) Quartz Specialties top charge	Q.S.I. utilisé bas du creuset (sheet 2 b) Quartz Specialties bottom	Q.S. neuf (sheet 3 a) Quartz Products	Q.S. utilisé (sheet 3 b) Quartz Products Run #55	AMERSIL utilisé (sheet 4 a) Run #47
Lithium	0,6 (0,6)	0,4 -	0,3 (0,4)	0,6 (1,0)	0,7 (7)	0,5 (1)	0,8 (-)
Sodium	1,2 (20)	1,8 (41)	3,7 (92)	1,9 (57)	2,5 (61)	0,8 (24)	9 (66)
Magnésium	0,05 (3)	0,05 (7)	0,1 (4)	0,1 (82)	0,25 (19)	0,2 -	0,3 (6)
Aluminium	12 (8)	12 (7)	21 (16)	130 (150)	20 (9)	26 (9)	22 (6)
Potassium	1,0 (24)	1,5 (80)	3,2 (89)	1,7 (220)	1,9 (120)	0,5 (52)	4,6 (35)
Calcium	0,6 (3)	5,6 (410)	1,3 (20)	20 (68)	1,5 (14)	13 (36)	3,4 (33)
Titane	5 (8)	6 (16)	2 (10)	1 (43)	1,5 (2)	0,6 (2)	1,5 (7)
Chrome	≤ 0,5 (-)	≤ 0,5 -	≤ 0,5 (-)	≤ 0,5 -	≤ 0,5 -	≤ 0,5 -	≤ 0,5 -
Manganèse	≤ 0,3 (<0,1)	≤ 0,3 (0,4)	≤ 0,3 (0,2)	≤ 0,3 0,6	≤ 0,3 (<0,1)	≤ 0,3 (<0,1)	≤ 0,3 (<0,1)
Fer	0,5 (1)	26 (12)	1,1 (7)	66 (150)	1,0 (13)	2 (20)	11 (11)
Cobalt	≤ 0,1 (≤0,2)	≤ 0,1 (0,6)	≤ 0,1 (≤0,2)	≤ 0,1 (≤0,7)	≤ 0,1 (≤ 0,3)	≤ 0,1 (≤ 0,3)	≤ 0,1 (≤0,2)
Nickel	≤ 0,2 (≤ 1)	≤ 0,2 (1)	≤ 0,2 (≤ 2)	≤ 0,2 (≤ 3)	≤ 0,2 (≤ 1)	≤ 0,2 (≤ 1)	≤ 0,2 (0,5)
Cuivre	≤ 0,3 (≤ 0,2)	≤ 0,3 (4)	≤ 0,3 (9)	≤ 0,3 (6)	≤ 0,3 (3)	≤ 0,3 (11)	≤ 0,3 (2)
Zinc	≤ 0,1 (1)	≤ 0,1 (5)	≤ 0,1 (2)	≤ 0,1 (7)	≤ 0,1 (3)	≤ 0,1 (3)	≤ 0,1 (0,9)
Strontium	0,1 (0,2)	0,7 (13)	0,05 (0,3)	1,7 (7)	0,2 (0,2)	0,7 (0,9)	0,4 (0,9)
Cadmium	≤ 0,1 (-)	0,1 -	≤ 0,1 -	≤ 0,1 -	≤ 0,1 -	≤ 0,1 -	≤ 0,1 -
Baryum	0,2 (7)	1,5 (3,5)	0,6 (≤ 0,9)	14 (480)	0,2 (0,9)	2,7 (20)	0,8 (6)
Plomb	0,6 (-)	0,2 (3)	0,4 -	0,1 -	- -	≤ 0,1 -	0,3 (2)

Impurity Analysis Performed by Quartz Products, Inc.

TABLE 36

ANALYSIS OF TRANSPARENT SILICA CRUCIBLES

Translation - 2/27/80

1 - ORIGIN

Samples submitted by Donald Rickard in January, 1980, together with Kayex Corporation report giving the analysis of these crucibles made by Commercial Testing and Engineering Company.

2 - CONTROLS

The samples submitted were fragments of crucibles, each in its own closed plastic packet. Before analysis these pieces were washed in boiling Hydorchloric Acid Solution. They were ground in an agate mortar to a granulometry of less than 50 microns. After rinsing with Hydrofluoric acid, the analysis of the different elements was made by an atomic absorption spectrophotometer. We give (see enclosed table) in each case between parentheses the results from the analysis of CTE. The results are expressed in ppm (reference to weight).

3 - COMMENTARY ON RESULTS

CTE has certainly made their analysis by a physical method (a flash mass spectrometer, emission spectrography). In the absence of a standard, the values obtained are purely qualitative and could present large variations with reference to the actual values.

Our results judged on samples of new crucibles, and in particular on our crucibles, correspond perfectly to those that we have obtained previously.

One can note after use a systematic enrichment of earth alkalies (barium, strontium, calcium), in iron, except for the Quartz & Silice crucibles and in aluminum for the QSI crucibles.

Commercial Testing prepares their samples according to ASTM standards. A brief procedure is listed below as relayed to Kayex by phone.

1. Hand Grind Samples to 200 mesh agate.
2. Mix 1/10 Gm of agate with ultrapure carbon dried in alcohol.

Cleaning Procedure

3. Wash in Acetone
4. Wash in Chloroform
5. Wash in Methanol
6. Etch for 30 seconds to 1 minute in 1:4 Hydrofloric Acid: (Ultrapure acids imported from Germany).
7. Deionized water rinse
8. Ethanol rinse

The following questions are still unanswered:

Are new fused Quartz crucibles consistently as pure as the manufacturers claim?

Are fused Quartz crucibles accumulating significant amounts of impurities during continuous recharge runs, as most results indicate?

If there are impurities present in the silicon melt or furnace atmosphere, are they affecting the silicon crystal that is grown or only being absorbed by the fused quartz crucible?

Further information concerning impurity analysis of silicon samples can be found in Section 5.2 starting on page 237.

A special situation occurred during Run No. 55 which afforded us an opportunity to better learn some of the consequences of a microscopic water leak in the furnace during the growing and recharging process.

During the recharging cycle after the eighth crystal was grown, a

white powdery deposit adhered to the lower portion of the hopper. At the same time, a microscopic (pinhole) water leak was definitely identified in the spectator viewport weld. This powdery substance was included with the other samples for impurity analysis. The results are shown at the bottom of Table 33. The major component was silicon as expected. We would also expect oxygen to be a major component. Also, molybdenum was tested as a major component, which means > than 0.1% concentration. This molybdenum probably came from the hopper from which the powder was scraped. As can be seen, potassium, fluorine, and sodium show high impurity concentrations.

It is felt that the crucible purity plays a major role in the Czochralski crystal growth process. Crystal quality may be affected by the fused quartz crucible especially as a function of time into a continuous recharge run.

The limited crucible analysis data generated during this project indicates that more work and study is needed. Crucible purity should be confirmed without question, also impurity concentrations in used crucibles should be verified.

5.0 Characterization Data and Analysis

5.1 Solar Cell Data

The main source of crystal quality feedback during the Crystal Growth Development program involved solar cell efficiency data - Refer to Section 4.5.3 page 158. It was important to determine what parameters of the crystal growth process would affect solar cell efficiencies, and also to answer questions concerning the effects of the continuous recharging method of Czochralski crystal growth on solar cell efficiencies.

- Would solar cell efficiency be affected by progressively growing more than one crystal from one melt container (crucible)?
- Would solar cell efficiency be affected by growing large diameter (up to 15 cm), high weight (up to 25 kg) crystals?
- What affect does the loss of "zero dislocation (OD)" crystal quality have on solar cell efficiencies?

A complete list of solar cell electrical and efficiency data is included in Table 37. All results were reported by testing samples under AMO conditions. AMI results were determined by calculation from AMO results using a conversion factor of 1.2:1 (AMI:AMO). The relationship between AMO efficiencies and AMI efficiencies did not appear to be totally understood on a practical basis. Therefore, during the project, the AMO to AMI conversion factor was changed from 1:1.4 (AMO:AMI) to the present 1:1.2 (AMO:AMI).

All solar cells in Table 37 were fabricated and tested by Applied Solar Energy, Inc. according to standard(baseline) methods and procedures. In all but one series of cells (Run No. 30) four 2 cm x 2 cm sections were taken from each wafer sample provided by Kayex. Therefore, four individual sets of data were available for each wafer tested. This sampling method was very useful in determining the possible incongruities

within a single large diameter wafer. It also allowed for some insight into the effects of grain size in polycrystalline material on the cell efficiencies.

The "Comments" column of Table 37 has been used to include important information concerning wafer samples and indicates if the wafer sample was polycrystalline (poly).

This section is intended to present data and statistical information concerning solar cell fabrication and testing performed on silicon material grown during continuous recharge runs. General observations, summaries, and conclusions can be found in Section 2.4 of this report.

5.1.1 Single Crystal vs. Polycrystalline Silicon

Table 37 distinguishes between monocrystalline material and polycrystalline material used to fabricate solar cells, in the comments column. To better depict the relationship between monocrystalline material and polycrystalline material used to fabricate solar cells, the graphs in Figures 53 thru 59 have been constructed. Each graph represents the solar cell efficiency results compiled from one specific continuous recharge run (e.g. Figure 53, Run No. 30). Each graph relates the average AMI efficiencies of the four solar cells fabricated from each wafer as a function of total kilograms grown during a continuous recharge run. The symbols (triangles and squares) represent these average values. Monocrystalline material is represented by triangles while polycrystalline material is represented by squares. The range of efficiency values for the four cells fabricated from each wafer is shown by a vertical line running through the symbol representing that wafer sample. If more than one wafer was tested from a crystal, the symbols representing these average efficiency values are connected

SOLAR CELL ELECTRICAL DATA

Sample No.	Comments	Voc mV	Isc mA	Imax mA	Vmax mW	Pmax mW	CFF %	AM0 %	AM1 %	Area cm^2
9-2-T	Avg. values of four cells	542.4	137.5			54.9	74	10.1	12.1	max = 10.3 min = 10.0
9-2-M	Avg. values of four cells	536.6	133.3			51.0	71	9.5	11.4	max = 9.7 min = 9.2
9-2-B	Avg. values of four cells	543.8	135.0			53.3	73	9.9	11.9	max = 10.0 min = 9.8
9-2-B	Avg. values of four cells Dislocated	543.2	135.2			53.7	73	9.9	11.9	max = 10.0 min = 9.8
9-3-T	Avg. values of four cells	537.6	134.0			48.4	67	9.0	10.8	max = 9.5 min = 8.4
9-3-T	Avg. values of four cells Dislocated	537.4	132.5			49.2	69	9.1	10.9	max = 9.9 min = 8.4
9-3-B	Avg. values of four cells Poly	540.7	132.5			50.9	71	9.4	11.3	max = 9.8 min = 8.9
11-1-T	Avg. values of four cells	564.4	134.3			56.3	74	10.4	12.5	max = 10.7 min = 10.2
11-2-T	Avg. values of four cells	546.8	133.9			52.5	72	9.7	11.6	max = 10.2 min = 9.4
11-2-B	Avg. values of four cells	558.3	135.8			54.4	72	10.1	12.1	max = 10.5 min = 9.7
11-3-T	Avg. values of four cells	552.3	137.2			54.9	72	10.2	12.2	max = 10.7 min = 9.8
11-4-T	Avg. values of four cells	549.7	135.2			52.9	71	9.3	11.2	max = 9.6 min = 8.9

TABLE 37

SOLAR CELL ELECTRICAL DATA

Sample No.	Comments	Voc mV	Isc mA	Imax mA	Vmax mW	Pmax mW	CFF %	AM0 %	AM1 %	Area cm^2
11-4-B	Avg. values of four cells	546.6	132.4			50.6	70	9.3	11.2	max = 9.6 min = 8.9
11-4-B	Avg. values of four cells Dislocated	550.7	131.4			52.0	72	9.6	11.5	max = 9.8 min = 9.4
Controls	Avg. values of four cells	567.2	134.8			56.9	74	10.5	12.6	max = 10.8 min = 10.0

TABLE 37 (Cont'd)

SOLAR CELL ELECTRICAL DATA

Sample No.	Comments	Voc mV	Isc mA	Imax mA	Vmax mW	Pmax mW	CFF %	AM0 %	AM1 %	Area cm^2
30-1A-T		582	99.0				75.2	10.5	12.6	3.05
30-1T		593	138.6				74.9	11.4	13.7	
30-1M		593	138.4				75.9	11.5	13.8	
30-1B	*Broken Terminal	553	113.2				72.5	8.4	10.1	
30-2M	Poly	541	109.5				71.6	7.8	9.4	
30-2B	Poly	556	114.7				73.5	8.7	10.4	
30-3T		586	138.5				74.1	11.1	13.3	
30-3M Control (30-4M)	Poly	536	107.0				72.5	7.7	9.2	
30-3B	Poly	555	110.0				72.3	8.2	9.8	
30-4T		590	140.3				74.2	11.3	13.6	
30-4M	Poly	553	115.0				74.4	8.7	10.4	
30-4B	Poly	562	114.5				72.6	8.6	10.3	
30-5T		589	139.5				73.2	11.1	13.3	
30-5M Control (30-2M)	Poly	553	108.3				73.1	8.1	9.7	
30-5B	Poly	552	113.2				67.1	7.8	9.4	

TABLE 37 (Cont'd)

SOLAR CELL ELECTRICAL DATA

Sample No.	Comments	Voc mV	Isc mA	Imax mA	Vmax mW	Pmax mW	CFF %	AM0 %	AM1 %	Area cm^2
30-6T		587	134.7				72.7	10.6	12.7	
30-6M	Poly	529	104.7				72.0	7.4	8.9	
30-6B	Poly	563	119.5				72.3	9.C	10.8	
Controls Run No. 30		553	141.4				72.9	10.5	12.6	
		554	138.6				74.4	10.6	12.7	
		552	139.9				73.2	10.5	12.6	

TABLE 37 (Cont'd)

SOLAR CELL ELECTRICAL DATA

Sample No.	Comments	Voc mV	Isc mA	Imax mA	Vmax mW	Pmax mW	CFF %	AM0 %	AM1 %	Area cm^2
47-1T-1		590	144.1	132.6	485	64.31	75.6	11.9	14.3	
-2		565	143.4	131.0	460	60.26	74.4	11.1	13.3	
-3		590	141.8	124.2	480	59.62	71.3	11.0	13.2	
-4		580	143.9	130.3	480	62.54	74.9	11.6	13.9	
47-3T-1	Thin cell	552	129.1	119.5	450	53.78	75.4	9.9	11.9	
-2	Thin cell	553	130.5	121.3	450	54.59	75.6	10.0	12.0	
-3	Thin cell	545	133.0	113.0	440	49.72	68.5	9.2	11.0	
-4	Thin cell	552	131.4	119.3	450	53.69	74.0	9.9	11.9	
47-3B-1		570	140.5	126.0	470	59.22	73.9	10.9	13.1	
-2		582	142.7	131.5	480	63.12	76.0	11.7	14.0	
-3		586	143.0	131.0	480	62.88	75.0	11.6	13.9	
-4		573	144.1	132.2	470	62.13	75.2	11.5	13.8	
49-1T-1		599	146.1	135.1	485	65.52	74.9	12.1	14.5	
-2		597	144.2	132.2	485	64.12	74.5	11.8	14.2	
-3		596	144.1	124.0	465	57.66	67.1	10.7	12.8	
-4		598	144.2	132.3	485	64.17	74.4	11.9	14.3	

TABLE 37 (Cont'd)

SOLAR CELL ELECTRICAL DATA

Sample No.	Comments	Voc mV	Isc mA	Imax mA	Vmax mW	Pmax mW	CFF %	AM0 %	AM1 %	Area cm^2
49-1B-1		593	140.7	127.1	490	62.28	74.6	11.5	13.8	
-2		593	140.7	127.1	490	62.28	74.6	11.5	13.8	
-3		592	138.2	127.1	490	62.28	76.1	11.5	13.8	
-4		594	140.0	127.1	490	62.28	74.9	11.5	13.8	
49-6T-1		595	142.8	132.0	485	64.02	75.3	11.8	14.2	
-2		593	142.3	129.0	485	62.57	74.1	11.6	13.9	
-3		595	143.1	128.6	485	62.37	73.3	11.5	13.8	
-4		595	140.4	128.0	485	62.08	74.3	11.5	13.8	
49-9T-1		598	143.3	131.2	490	64.29	75.0	11.9	14.3	
-2		593	141.0	120.0	490	58.8	70.3	10.9	13.1	
-3		594	141.5	126.5	490	61.99	73.7	11.5	13.8	
-4		596	142.5	130.0	490	63.7	75.0	11.8	14.2	
49-9B-1		589	138.0	123.0	480	59.04	72.6	10.9	13.1	
-2		589	142.0	128.2	480	61.54	73.6	11.4	13.7	
-3		590	137.3	121.0	480	58.08	71.7	10.7	12.8	
-4		596	139.1	126.1	490	61.79	74.5	11.4	13.7	

TABLE 37 (Cont'd)

SOLAR CELL ELECTRICAL DATA

Sample No.	Comments	Voc mV	Isc mA	Imax mA	Vmax mW	Pmax mW	CFF %	AM0 %	AM1 %	Area cm^2
Control-1 47 & 49		602	143.7	129.3	500	64.65	74.7	11.9	14.3	
-2		600	142.5	129.0	495	63.86	74.6	11.8	14.2	
-3		598	143.0	128.0	480	61.44	71.8	11.4	13.7	
-4		595	143.2	128.5	490	62.97	73.9	11.6	13.9	

TABLE 37 (Cont'd)

SOLAR CELL ELECTRICAL DATA

Sample No.	Comments	Voc mV	Isc mA	Imax. mA	Vmax. mV	Pmax. mW	CFF %	AM0 η %	AM1 η %	Area cm^2
55-2-T_6-1		580	135	123.5	460	57.04	72.6	10.5	12.6	4
-2		580	137.5	125.0	462	57.8	72.4	10.7	12.8	
-3		580	137	126.0	464	58.5	73.6	10.8	13.0	
-4		580	139.5	127.0	465	59.1	73.0	10.9	13.1	
55-2-B-1		575	142.0	114.0	460	52.4	64.0	9.7	11.6	
-2		585	146.0	128.0	485	62.1	72.0	11.5	13.8	
-3		575	141.0	122.0	460	58.9	72.0	10.8	13.0	
-4		585	144.0	127.0	485	61.6	73.0	11.4	13.7	
55-7-T-1		580	136.0	122.0	465	56.7	71.0	10.5	12.6	
-2		581	134.0	123.0	468	58.0	74.0	10.7	12.8	
-3		583	138.0	125.0	473	59.1	73.0	11.0	13.2	
-4		584	137.0	126.0	477	60.1	75.0	11.1	13.3	

TABLE 37 (Cont'd)

SOLAR CELL ELECTRICAL DATA

Sample No.	Comments	Voc mV	Isc mA	Imax. mA	Vmax. mV	Pmax. mW	CFF %	AM0 %	AM1 %	Area cm^2
55-7-B -1	Poly	523	105.0	95.0	418	39.7	72.0	7.3	8.8	
-2	Poly	525	105.5	96.0	420	40.3	72.0	7.4	8.9	
-3	Poly	527	106.0	98.0	421	41.3	73.0	7.6	9.1	
-4	Poly	552	120.0	109.0	440	48.1	72.0	8.9	10.7	
55-10-T -1		580	135.5	124.0	467	58.0	73.0	10.7	12.8	4
-2		580	134.0	125.0	470	58.8	75.0	10.9	13.1	
-3		580	135.5	125.0	471	58.9	74.0	10.9	13.1	
-4		580	135.5	125.0	471	58.9	71.0	10.9	13.1	
55-10-B -1	Poly	539	113.0	101.5	441	45.1	74.0	8.3	10.0	
-2	Poly	540	113.0	102.0	444	45.3	74.0	8.4	10.1	
-3	Poly	551	119.0	108.0	447	48.3	73.0	8.9	10.7	

TABLE 37 (Cont'd)

SOLAR CELL ELECTRICAL DATA

Sample No.	Comments	Voc mV	Isc mA	Imax. mA	Vmax. mV	Pmax. mW	CFF %	AM0 η %	AM1 η %	Area cm^2
2*-1-T_3-1	Not Doped	320	134.0	116.0	185	21.4	49.0	4.0	4.9	
-2	Not Doped	350	135.0	125.0	185	23.12	48.0	4.3	5.2	
-3	Not Doped	320	132.0	113.0	185	20.9	49.0	3.9	4.7	
-4	Not Doped	350	139.0	127.0	190	24.0	49.0	4.4	5.3	
2*-1-B_4-1	Not Doped	357	135.0	110.5	240	26.5	55.0	4.9	5.9	
-2	Not Doped	360	135.5	111.8	250	28.0	57.5	5.2	6.2	
-3	Not Doped	362	136.0	112.0	252	28.2	57.3	5.2	6.2	
-4	Not Doped	368	136.5	113.0	257	29.0	57.8	5.4	6.5	
2*-2-B_3-1		580	141.0	122.0	480	58.6	72.0	10.8	13.0	4
-2		585	142.0	127.0	485	61.6	74.0	10.5	12.6	
-3		580	141.0	128.0	475	60.8	74.0	11.0	13.2	
-4		585	141.0	124.0	480	59.5	72.0	10.0	12.0	

TABLE 37 (Cont'd)

SOLAR CELL ELECTRICAL DATA

Sample No.	Comments	Voc mV	Isc mA	Imax. mA	Vmax. mV	Pmax. mW	CFF %	AM0 η %	AM1 η %	Area cm^2
$2*-4-B_9$ -1	Poly	550	122.2	110.0	450	49.0	73.0	9.1	10.9	
-2	Poly	545	112.0	96.0	450	43.2	70.0	8.0	9.6	
-3	Poly	535	119.0	99.0	450	44.5	69.0	8.2	9.8	
-4	Poly	565	132.0	118.0	465	54.0	72.0	10.0	12.0	
$2*-5-M_4$ Internal Control -1	Actually Sample II $2*-2-B_4$	580	137.0	124.0	475	58.9	74.0	10.9	13.1	
-2		580	142.0	129.0	490	63.2	76.0	11.7	14.0	
-3		580	140.0	126.0	485	60.5	74.0	11.2		
-4		580	143.0	124.0	475	58.9	71.0	10.9	13.1	
$2*-7-T_2$ -1		575	135.0	120.5	458	55.2	70.0	10.2	12.2	
-2		575	137.0	122.0	460	56.0	71.0	10.3	12.4	
-3		576	139.0	123.0	465	57.2	71.0	10.6	12.7	
-4		578	137.0	123.0	465	57.2	72.0	10.6	12.7	

TABLE 37 (Cont'd)

SOLAR CELL ELECTRICAL DATA

Sample No.	Comments	Voc mV	Isc mA	Imax. mA	Vmax. mV	Pmax. mW	CFF %	AM- %	AM1 %	Area cm^2
2*-8-T_4 -1		575	135.0	122.0	444	54.1	69.0	10.0	12.0	4
-2		575	135.0	123.0	447	55.1	70.0	10.2	12.2	
-3		575	136.0	125.0	451	56.3	71.0	10.4	12.5	
-4		575	136.0	126.0	453	57.0	72.0	10.5	12.6	
Control -1		590	138.0	127.0	495	63.1	77.0	11.7	14.0	
-2		590	140.0	128.0	495	63.4	76.0	11.7	14.0	
-3		590	141.0	127.0	495	63.1	75.0	11.7	14.0	

TABLE 37 (Cont'd)

SOLAR CELL ELECTRICAL DATA

Sample No.	Comments	Voc mV	Isc mA	Imax mA	Vmax mW	Pmax mW	CFF %	AM0 %	AM1 %	Area cm^2
60-1-T7-1		585	137.5	124.0	475	58.9	73.2	10.9	13.1	
-2		577	137.8	122.3	475	58.1	73.1	10.7	12.8	
-3		567	135.0	123.5	475	58.7	76.6	10.8	13.0	
-4		562	135.5	126.0	460	58.0	76.1	10.7	12.8	
60-5-B9-1		578	135.5	125.0	475	59.4	75.8	11.0	13.2	
-2		568	135.5	125.0	460	57.5	74.7	10.6	12.7	
-3		567	136.5	127.0	460	58.4	75.5	10.8	13.0	
-4		580	138.0	127.0	475	60.3	75.4	11.2	13.4	
60-7-M14-1	Poly	557	119.7	108.0	450	48.6	72.9	9.0	10.8	
-2	Poly	566	125.0	114.0	460	52.4	74.1	9.7	11.6	
-3	Poly	557	119.7	107.0	450	48.2	72.2	8.9	10.7	
-4	Poly	560	121.0	110.0	460	50.6	74.7	9.4	11.3	
60-8-T3-1		577	130.5	119.0	475	56.5	76.1	10.4	12.5	
60-8-B6-1	Poly	555	112.8	102.0	460	46.9	74.9	8.7	10.4	
-2	Poly	567	122.2	111.0	460	51.1	73.7	9.5	11.4	
-3	Poly	557	120.0	108.0	460	49.7	74.3	9.2	11.0	
-4	Poly	562	119.5	108.0	460	49.7	74.0	9.2	11.0	

TABLE 7 (Cont'd)

SOLAR CELL ELECTRICAL DATA

Sample No.	Comments	Voc mV	Isc mA	Imax mA	Vmax mV	Pmax mW	CFF %	AM0 %	AM1 %	Area cm^2
Control Run No. 60-1		588	144.5	132.0	480	63.4	74.6	11.7	14.0	
-2		589	144.0	133.0	480	63.8	75.3	11.8	14.2	
-3		589	145.0	134.0	480	64.3	75.3	11.9	14.3	
-4		590	145.0	134.0	480	64.3	75.4	11.9	14.3	
62-1T-1		582	135.3			56	68	10.4	12.5	
-2		593	134.9			63	76	11.6	13.9	
-3		590	135.8			58	69	10.8	13.0	
-4		592	136.6			63	73	11.6	13.9	
62-1B-1		588	133.6			56	71	10.4	12.5	
-2		590	134.2			58	72	10.7	12.8	
-3		594	135.3			61	72	11.3	13.6	
-4		590	134.6			58	71	10.7	12.8	
62-2T-1		594	135.0			62	74	11.4	13.7	
-2		598	135.3			62	73	11.5	13.8	
-3	Shunted	570	135.1			*41	51	7.5		
-4		590	135.6			58	69	10.8	13.0	

TABLE 37 (Con'td)

SOLAR CELL ELECTRICAL DATA

Sample No.	Comments	Voc mV	Isc mA	Imax mA	Vmax mW	Pmax mW	CFF %	AM0 %	AM1 %	Area cm^2
62-2B-1		586	134.2			53	66	9.8	11.8	
-2		592	135.4			59	70	10.9	13.1	
-3		592	135.5			58	69	10.8	13.0	
-4		596	134.1			61	75	11.3	13.6	
62-3T-1		598	135.3			63	75	11.7	14.0	
-2		596	136.5			64	73	11.8	14.2	
-3		598	135.7			65	76	12.1	14.5	
-4	Shunted	586	135.6			49	59	9.1		
62-3B-1	Poly	566	130.8			52	74	9.6	11.5	
-2	Poly	578	132.1			55	74	10.2	12.2	
-3	Poly	562	129.4			49	74	9.0	10.8	
-4	Poly	574	130.6			53	75	9.8	11.8	
62-4T-1		588	133.3			54	69	10.1	12.1	
-2		590	136.0			59	69	10.8	13.0	
-3		594	135.2			62	74	11.4	13.7	
-4		592	134.8			59	72	11.0	13.2	

TABLE 37 (Cont'd)

SOLAR CELL ELECTRICAL DATA

Sample No.	Comments	Voc mV	Isc mA	Imax mA	Vmax mW	Pmax mW	CFF %	AM0 %	AM1 %	Area cm^2
62-4B-1		594	134.4			62	76	11.5	13.8	
-2		588	133.6			61	77	11.2	13.4	
-3		594	133.5			61	77	11.3	13.6	
-4		592	134.5			61	75	11.3	13.6	
62-5T-1		596	135.5			61	72	11.3	13.6	
-2	Shunted	580	135.2			47	57	8.7		
-3		592	134.2			55	68	10.3	12.4	
-4		596	135.7			62	73	11.4	13.7	
62-5B-1		594	134.4			61	74	11.2	13.4	
-2		596	135.0			62	75	11.6	13.9	
-3		590	133.9			60	75	11.0	13.2	
-4		586	132.9			55	71	10.2	12.2	
62-7T-1		590	132.9			56	73	10.4	12.5	
-2		596	134.9			62	75	11.6	13.9	
-3		594	134.7			61	74	11.3	13.6	

TABLE 37 (Cont'd)

SOLAR CELL ELECTRICAL DATA

Sample No.	Comments	Voc mV	Isc mA	Imax mA	Vmax mW	Pmax vW	CFF %	AM0 %	AM1 %	Area cm^2
62-7B-1	Poly	574	131.9			53	72	9.7	11.6	
-2	Poly	556	129.7			42	64	7.9	9.5	
-3	Poly	576	131.9			54	73	10.0	12.0	
-4	Poly	554	129.8			46	70	8.6	10.3	
62-8T-1		590	133.6			57	72	10.5	12.6	
-2		596	135.2			64	76	11.8	14.2	
-3	Shunted	582	134.6			47	58	8.6		
-4		586	132.5			52	68	9.6	11.5	
62-8M-1		594	135.0			63	76	11.7	14.0	
-2		596	135.0			63	76	11.7	14.0	
-3		596	134.8			63	75	11.6	13.9	
-4		596	134.5			62	76	11.6	13.9	
62-8B-1	Poly	586	133.0			58	75	10.7	12.8	
-2	Poly	530	125.8			38	73	7.1	8.5	
-3	Poly	568	131.4			52	73	9.7	11.6	
-4	Poly	586	133.0			54	69	9.9	11.9	

TABLE 37 (Cont'd)

SOLAR CELL ELECTRICAL DATA

Sample No.	Comments	Voc mV	Isc mA	Imax mA	Vmax mW	Pmax mW	CFF %	AM0 %	AM1 %	Area cm^2
62-9T-1		594	134.9			62	75	11.5	13.8	
-2		598	135.7			63	74	11.8	14.2	
-3		598	134.9			62	74	11.5	13.8	
-4		596	135.7			62	73	11.5	13.8	
62-9M-1		596	134.6			62	75	11.5	13.8	
-2		596	133.7			62	77	11.5	13.8	
-3		592	133.9			59	74	10.9	13.1	
-4		590	131.6			55	74	10.2	12.2	
62-9B-1	Poly	568	130.0			51	75	9.5	11.4	
-2	Poly	574	131.0			53	75	9.9	11.9	
-3	Poly	570	130.4			52	75	9.6	11.5	
-4	Poly	568	130.1			50	73	9.3	11.2	
Control-1 Run No. 62	Shunted	576	134.5			43	54	8.0		
-2		592	134.1			57	70	10.5	12.6	
-3		592	134.3			60	74	11.2	13.4	
-4		594	133.8			59	74	11.0	13.2	

TABLE 37 (Cont'd)

Poly Range - 10.8→ 8.9
Mono Range - 13.8→ 12.6

▲ Monocrystalline

■ Polycrystalline

SOLAR EFFICIENCY VS. KILOGRAMS GROWN

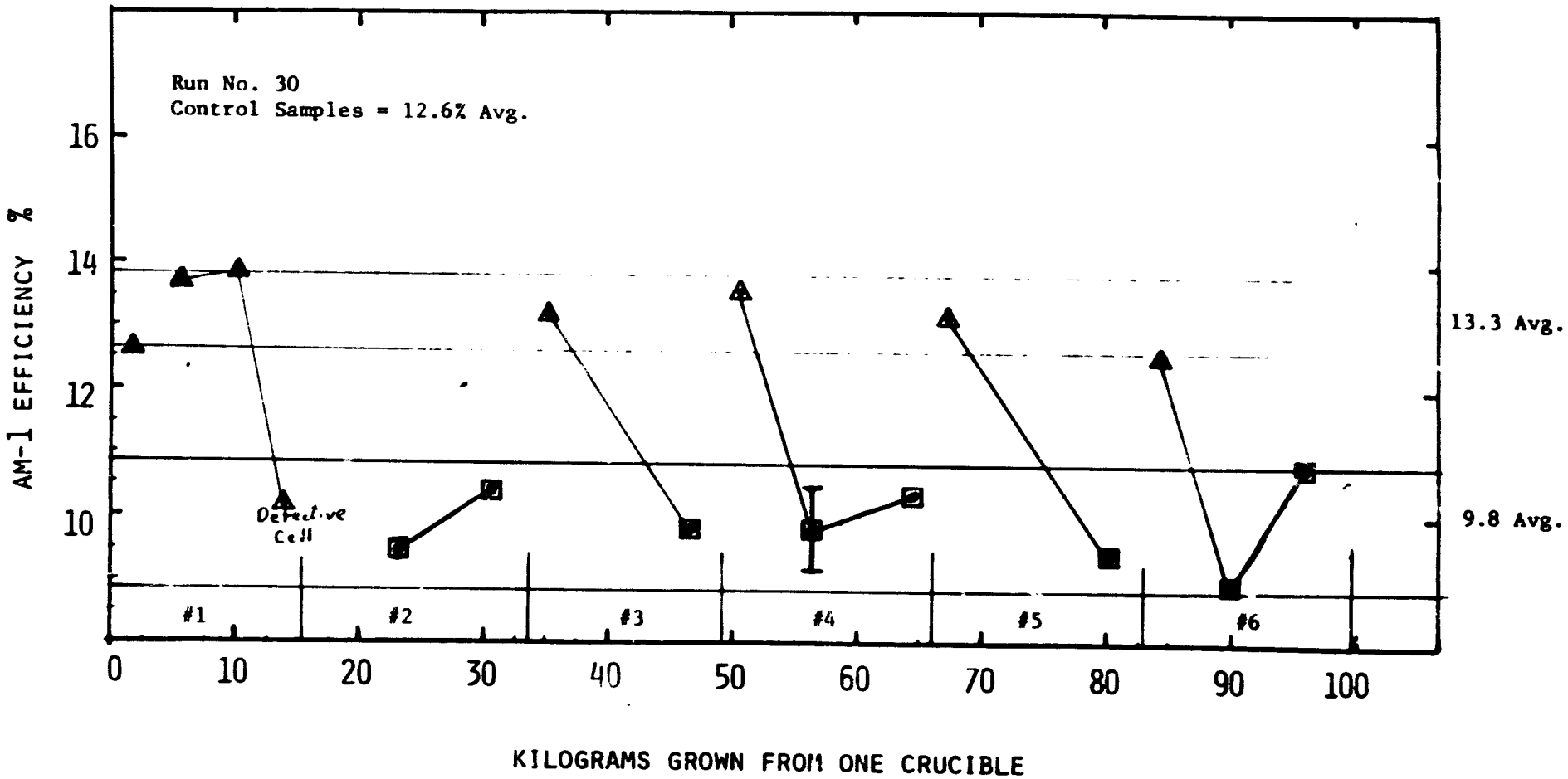

Figure 53

Mono Range - 14.3→ 13.1

▲ Monocrystalline

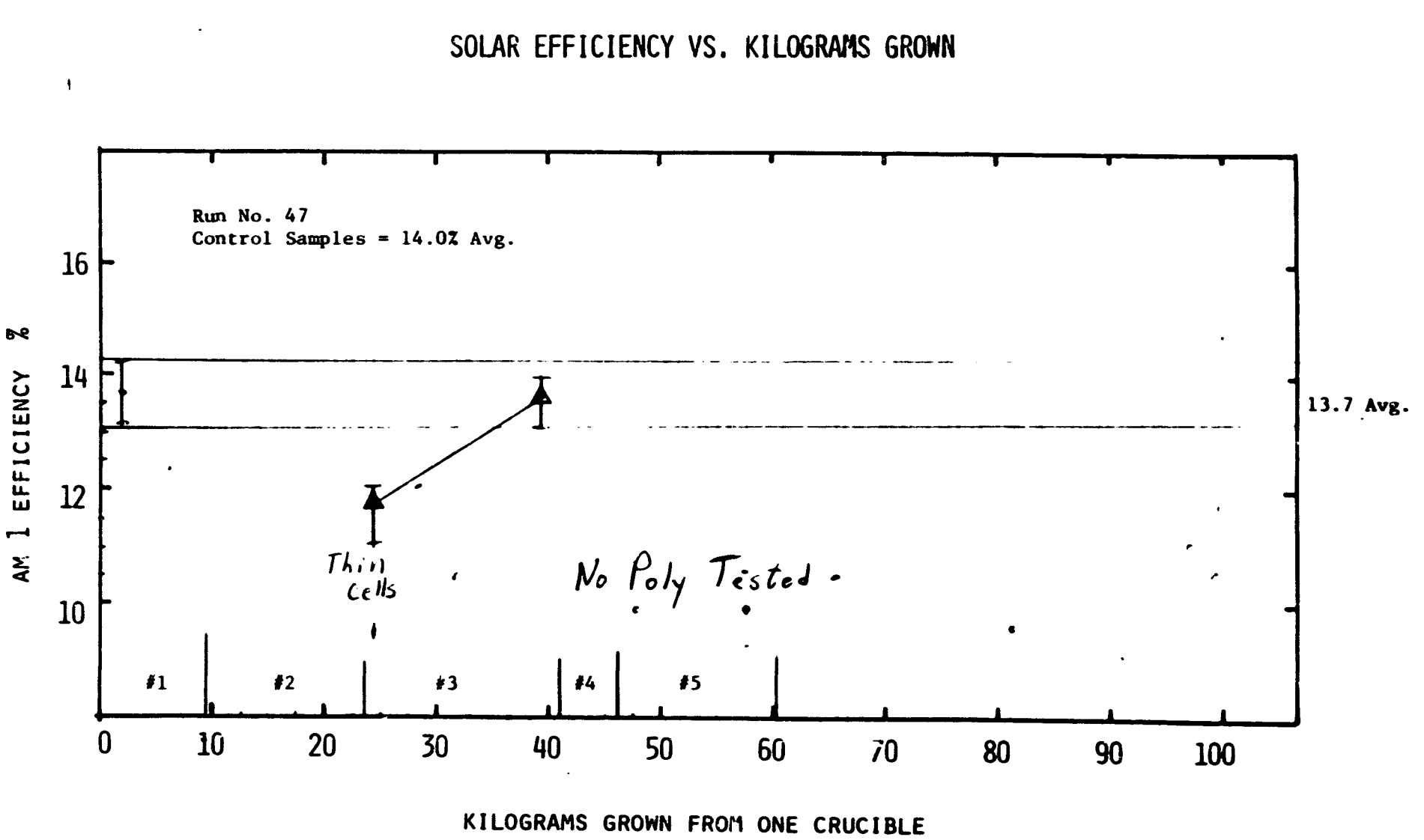

Figure 54

▲ Monocrystalline

Poly Range - No Poly
Mono Range - 14.5 → 12.8

SOLAR EFFICIENCY VS. KILOGRAMS GROWN

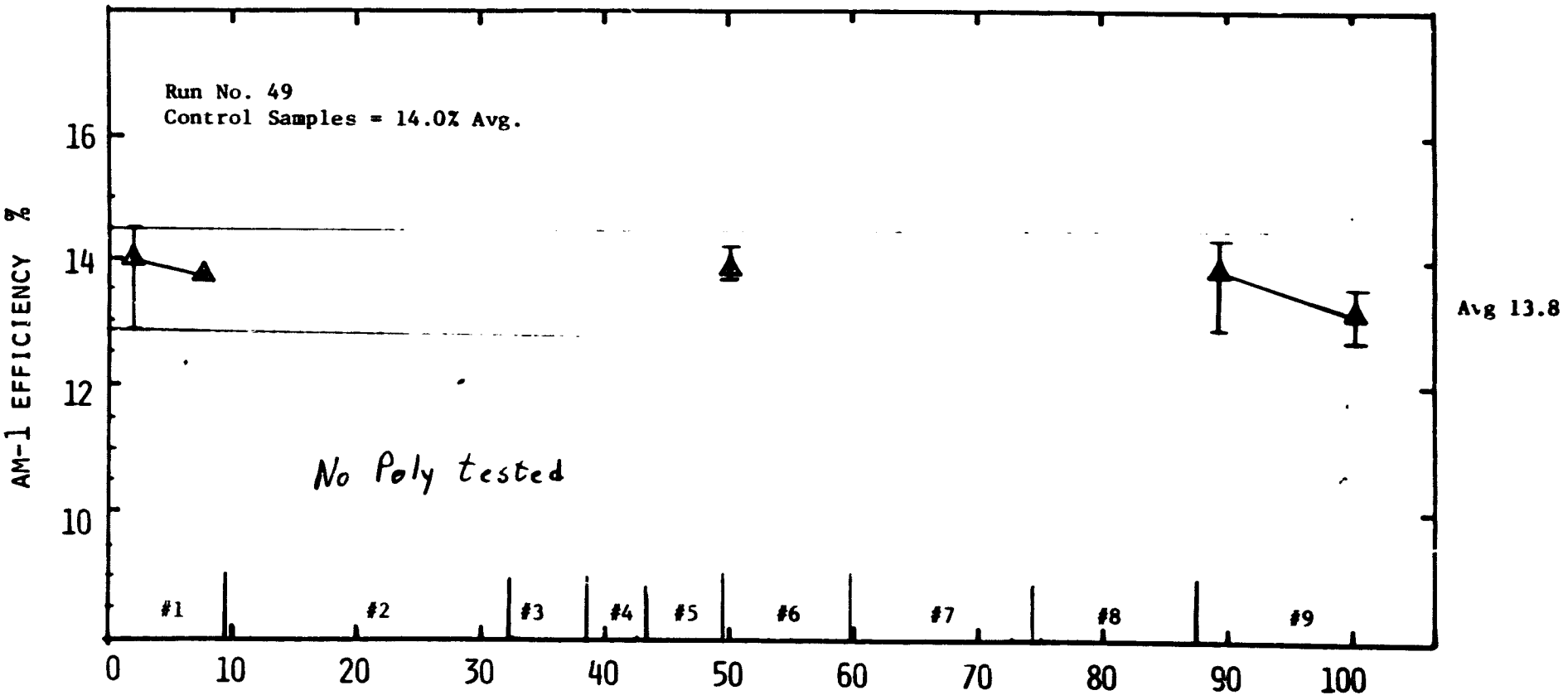

Figure 55

Poly Range - 10.7→ 8.8
Mono Range - 13.8→ 11.6

▲ Monocrystalline

■ Polycrystalline

SOLAR EFFICIENCY VS. KILOGRAMS GROWN

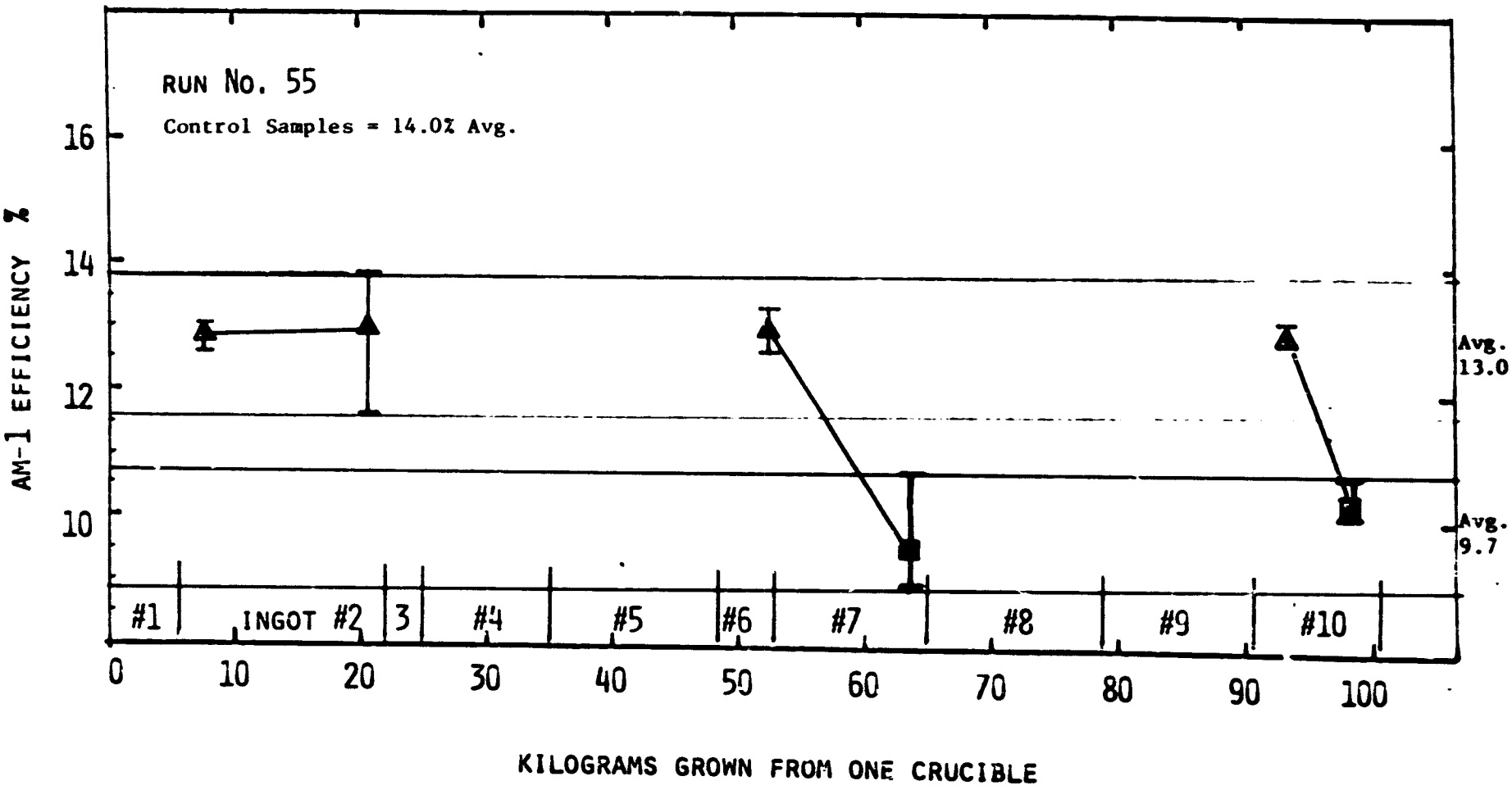

Figure 56

Poly Range - 12.0→ 9.6
Mono Range - 14.0→ 12.0

△ Monocrystalline

◘ Polycrystalline

SOLAR EFFICIENCY VS. KILOGRAMS GROWN

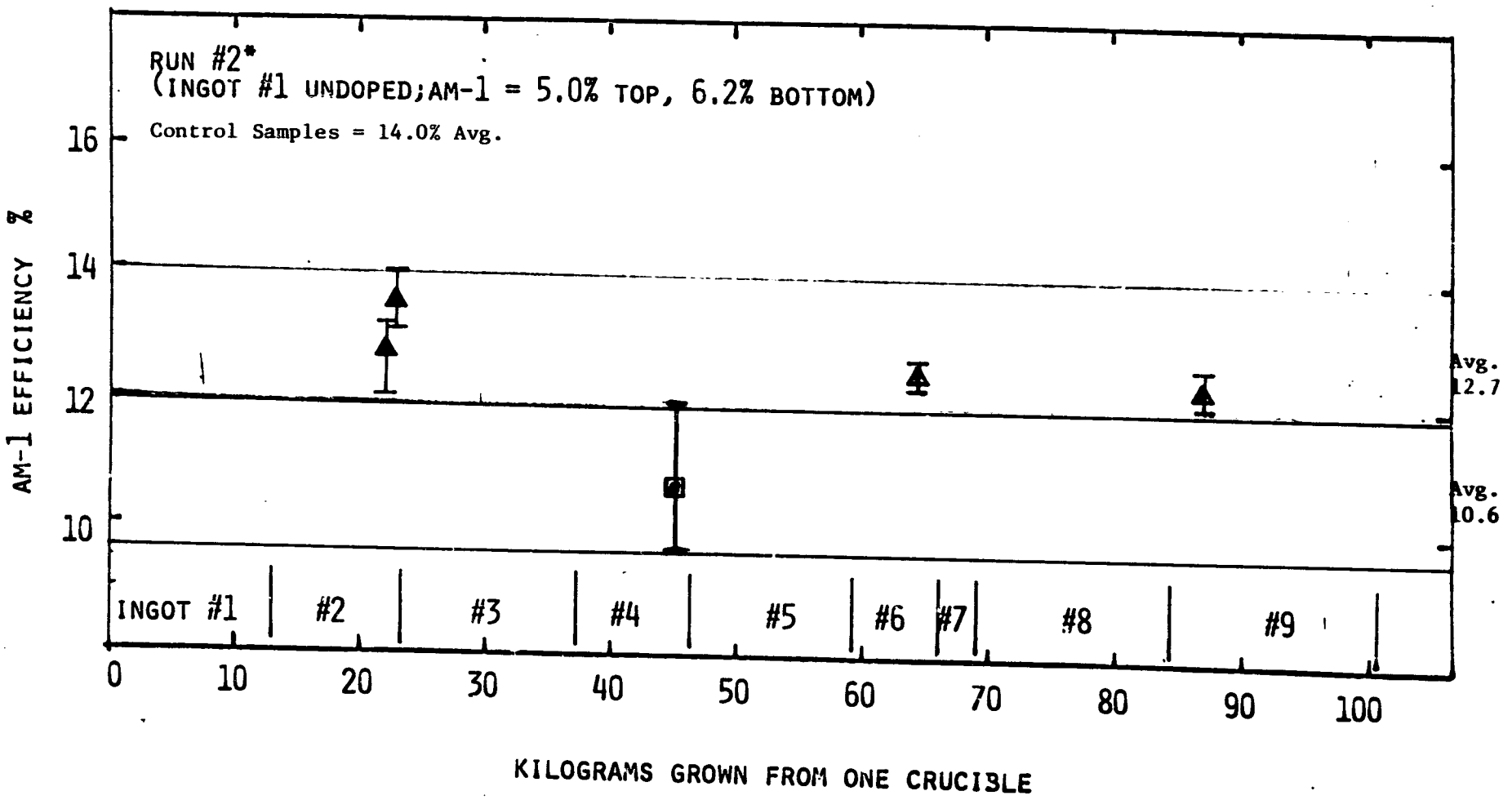

Figure 57

Poly Range - 11.6→ 10.4
Mono Range - 13.4→ 12.5

▲ Monocrystalline

■ Polycrystalline

SOLAR EFFICIENCY VS. KILOGRAMS GROWN

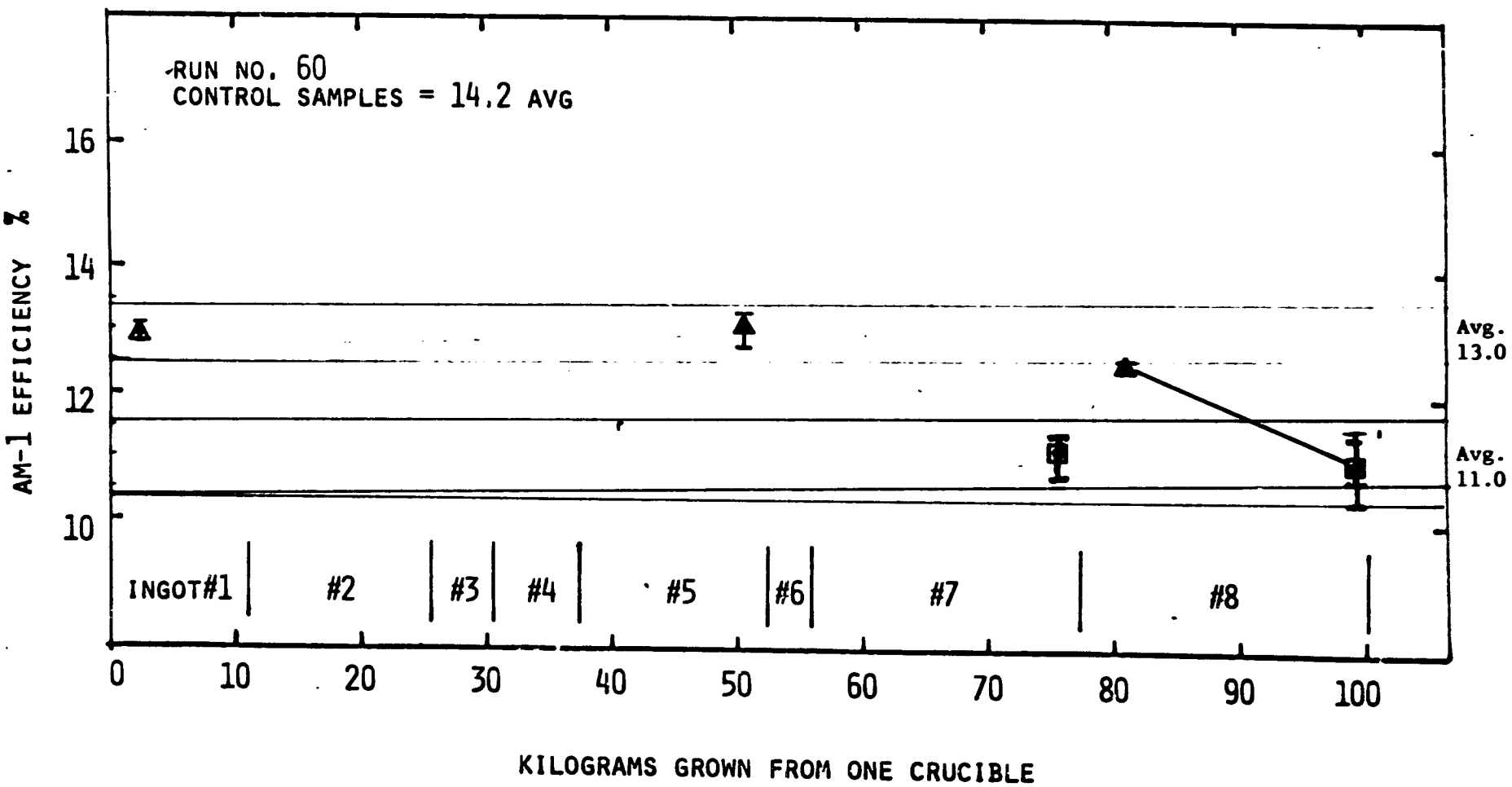

Figure 58

by a straight line. This enables one to see the difference in efficiency values in different parts of the crystal. The horizontal scale has also been divisioned such that each crystal grown during a continuous recharge run is indicated (by number) in relation to the total amount of silicon ingot grown.

It can readily be seen that the average solar cell efficiencies of monocrystalline silicon were significantly higher than the average efficiencies of polycrystalline silicon grown during all continuous recharge runs. The polycrystalline material was generally 15% to 25% lower in AMI efficiency. The wide variations in both average solar cell efficiency and individual cell efficiencies of polycrystalline samples may be attributed to the variations in the grain size present in the sample wafers. Some wafers exhibited very large grain size such that as much as half the wafer was single crystal, whereas the other polycrystalline wafers exhibited a large number of grain boundaries throughout the entire wafer.

The average solar cell efficiencies of monocrystalline material was very near to the average efficiencies of the control samples. Runs No. 30 and No. 62's average efficiencies actually surpassed the control samples average.

The solar cell efficiency data obtained from Run No. 49 revealed another important result:

A significant percentage of Run No. 49 was single crystal material but not of zero dislocation quality. The cells fabricated from single crystal (but not dislocation free) exhibited efficiencies similar to the dislocation free samples tested.

It was not possible to make this same evaluation on all continuous recharge runs since most of the time the crystals developed polycrystalline growth shortly after they lost zero dislocation quality.

5.1.2 Solar Cell Efficiency Performance as a Function of Total Amount Grown During a Continuous Recharge Run

The data contained in Figures 53 thru 59 have led to the conclusion that there is no significant deterioration of solar cell efficiencies from the beginning of a 100 kg continuous recharge run to the end. Specific examples will show a slight variation downwards, while other examples will show a slight variation upwards).

Since Run No. 62 resulted in the most extensive efficiency analysis, it will be used as a representative set of results. Monocrystalline material from the last crystal grown during Run No. 62 actually tested at higher efficiencies than the monocrystalline material from the first crystal grown. For the most part, material from crystals grown after the first crystal show efficiencies at least as good as those of the samples from the first crystal. The major exceptions being polycrystalline material. Solar cells fabricated from the middle of the eighth crystal after approximately eighty (80) kg had been grown resulted in the second highest efficiency average (13.95%) with a surprisingly narrow range of efficiencies (14.0-13.9).

5.1.3 Solar Cell Efficiency Performance as a Function of Growth Time into a Continuous Recharge Run

The graphs used to express AMI Efficiency as a function of total kilograms grown can also be used to relate the effect of time (duration) on AMI efficiencies as a continuous recharge run progresses. Time could replace the horizontal scale variable (kilograms grown) since as time progresses into a continuous recharge run, more silicon and more crystals are grown.

Total run time for all continuous runs is contained in Table 1, page 6. The shortest 100 kg run lasted 79 hours (run No. 30), while the longest 100 kg run lasted 109 hours (Run No. 2*).

The solar cell efficiency results and conclusions would, therefore, be analogous to those stated in section 5.1.2 as they pertain to total amount of silicon grown. Specific continuous recharge runs show a slight decrease in average efficiencies toward the end of a run while other runs show a slight increase. Still, the runs indicate a constant level of efficiency results throughout the run. Here again- the biggest single detriment to high solar cell efficiencies is the loss of monocrystalline type growth with a resultant polycrystalline type growth. It does not matter if it occurs during the growth of the first crystal after less than twelve hours of run time or during the growth of the last crystal after possibly ninety hours of run time.

One other aspect of run time is noticeable when Figures 53 thru 59 are reviewed. It appears as though there may be a greater tendency to realize polycrystalline growth (usually towards the bottom of a crystal) near the end of a continuous recharge run than at the beginning of the run. However, this theory cannot be substantiated for several reasons:

- All crystals grown were not the same length.
- Crystals that lost structure early into a continuous recharge run were tapered and removed from the melt shortly after losing zero dislocation structure.
- If serious structure loss problems occurred late into a continuous recharge run, following the growth of 60-70 kg, the last one or two crystals were grown full size regardless of crystal structure.

Even though the above procedures were generally followed, data and observations concerning structure loss, crucible devitrification and silicon monoxide buildup suggest there may be a relationship between run

time and structure loss. It is felt that more controlled study and investigation is needed in this area.

5.1.4 Solar Cell Efficiency Performance as a Function of Crystal Location

The question--does the solar cell efficiency deteriorate from the start (top) of a crystal to the end (bottom) of a crystal, has been asked many times. It is very difficult to formulate a responsible conclusion based on the limited amount of data available from the solar cell efficiency tests performed under this project. There are crystals that indicate a decrease in average solar cell efficiency from the top to the bottom. However, there are other crystals that indicate an increase in average solar cell efficiency from top to bottom, while other crystals remain fairly constant. Moreover, individual cells fabricated from wafers exhibit both extremes and most of the time overlap no matter what position the sample wafer is taken from the crystal. Here again however, it should be noted that many of the crystal bottoms tested for solar cell efficiencies were polycrystalline material and should not be considered in any comparisons with monocrystalline material.

Figures 53 thru 59 have the horizontal scales proportioned to indicate each crystal that was grown during a continuous recharge run. It is important to remember that the straight lines connecting average efficiency data from the same crystal in no way relate to average efficiencies of material from the crystal since no samples were taken from the crystals in these areas. Another limiting factor is the nonuniformity in crystal length meaning that some crystal bottoms were grown with a relatively small amount of residual melt left in the crucible while other shorter crystal's bottoms were grown with a relatively large amount of residual melt in the crucible.

With all the handicaps to consistent data interpretation, it is still felt that there is no significant deterioration of solar cell

efficiency as a crystal is grown from top to bottom. The major problem, again, stems from loss of monocrystalline structure.

If the limited data on solar cell efficiencies of polycrystalline material is studied, an anomaly is exhibited in the data from Run No. 30 Figure 53. Three examples of significantly increased efficiencies are indicated as polycrystalline growth progresses from the middle of crystals #2, #4, and #6 to the bottoms of these crystals. The normal assumption would predict the reverse. It would be assumed that as polycrystalline growth continues, grain size would become smaller and therefore, lead to lower efficiencies.

A very limited amount of resistivity data was accumulated from continuous recharge runs. However, sufficient samples of crystals grown during the 100 kg continuous recharge runs have been catalcgued and filed so that this type of characterization data could be obtained in the future if necessary. Table 38 presents this data. No conclusions have been formulated as to the effects of resistivity on solar cell efficiency. The contract specifications called for a resistivity range between 1.5 ohm cm and 3.0 ohm cm.

One set of solar cell efficiency results does stand out because of an error in doping procedures. Run No. 2* crystal number 1 was inadvertently not doped Table 37, page 213 and resulted in efficiency levels from 51% (6.2%) to 60% (5.0%) lower than the average monocrystalline efficiency of the total run.

Finally, one Diffusion Length Analysis was performed by Applied Solar Energy, Inc. during the course of the project. The results are indicated in Table 39.

RESISTIVITY RESULTS

Crystal No.	Crystal Position	Resistivity ohm-cm
9-2	Top - OD	5.75
9-2	Middle - OD	6.00
9-2	Bottom - OD	5.6
9-2	Bottom - Dislocated	5.6
9-3	Top - OD	5.2
9-3	Top - Dislocated	5.2
9-3	Bottom - Poly	4.4
11-1	Top - OD	2.99
11-2	Top - OD	2.74
11-2	Bottom - OD	2.57
11-3	Top - OD	3.69
11-4	Top - OD	3.52
11-4	Bottom - OD	3.62
11-4	Bottom - Dislocated	3.62
30-1	Top - OD	2.30
30-1	Middle - OD	1.86
30-1	Bottom - Dislocated	1.82
30-2	Middle - Poly	1.72
30-2	Bottom - Poly	2.94
30-3	Top - OD	2.47
30-3	Bottom - Poly	2.78
30-4	Top - OD	2.34
30-4	Middle - Poly	3.12
30-4	Bottom - Poly	1.95
30-5	Top - OD	2.20
30-5	Bottom - Poly	2.48
30-6	Top - OD	2.16
30-6	Middle - Poly	2.97
30-6	Bottom - Poly	1.90

Table 38

RESISTIVITY RESULTS
(cont)

Crystal No.	Crystal Position	Average Resistivity ohm-cm
49-1	Top	2.67
49-1	Bottom	1.95
49-3	Top	2.12
49-3	Bottom	2.01
49-4	Bottom	2.04
49-5	Top	2.15
49-5	Middle	1.85
49-6	Top	1.80
49-6	Bottom	1.60
49-8	Top	1.83
49-8	Bottom	1.64
49-9	Top	2.06
49-9	Bottom	1.73

1) Resistivity measurements were made without heat treating samples.

2) Average resistivities decrease from top to bottom of crystals.

3) Average resistivities tend to decrease as the continuous run progressed (from the first crystal to the last crystals).

Table 38

RUN NO. 30

DIFFUSION LENGTH MEASUREMENTS

INGOT NO. TOP	DIFFUSION LENGTH (μm)
1	160
3	80
5	70
6	40

Method: Short Circuit Current Response at long (.8-1.0μm)

Cell Thickness: .015" ± .002"

TABLE 39

5.2 Impurity Analysis Data

Impurity analysis was included as a part of the statement of work on the continuation of Phase I of the 954888 contract. Some funding was allocated for this purpose and recommendations were made by JPL as to possible commercial sources to perform the impurity analysis work.

Theoretical calculations predict that impurities will be initially rejected from entering the crystal lattice of the silicon crystal as it is grown in relation to the impurities segregation coefficient. However, over a period of time, as the impurities become more concentrated in the residual melt the impurity levels should increase in the silicon crystal. The first impurity analysis tests did in fact indicate an increase in impurity concentrations as more crystals were grown (Table 40). However, subsequent test results were inconsistent, (and for the most part, make it very difficult to prove the theoretical conclusion).

The charts included in Tables 41 thru 44 interpret the impurity concentrations of the samples indicated in terms of atoms/cm^3 of silicon material. Although 10^{15} or 10^{16} atoms appears to be a very large number, it is a billion times less than the number of atoms of silicon in one cm^3 of pure silicon with virtually no impurities (5×10^{22} atoms/cm^3).

The total impurity concentrations in the crystal samples tested and the residual melt samples tested did not reach the "critical impurity concentration valve, Ce *, for structural breakdown due to constitutional supercooling" [10] (5×10^{19} atoms/cm^3).

Samples of the crucibles used during several of the 100 kg continuous recharge runs were tested for impurity concentrations at the same time the crystal samples and residual melt samples were tested. Results revealed impurity concentrations at least one order of magnitude greater than the samples taken from crystals grown from that crucible, or from

SPARK SOURCE MASS SPECTROSCOPY IMPURITY ANALYSIS
(ATOMS/CM^3) FOR FEEDSTOCK AND SAMPLES OF RUN NUMBER 11

MAJOR IMPURITY	SEGREGATION COEFFICIENT[2]	FEED-STOCK ($\times 10^{15}$)	(INGOT #2) SAMPLE NUMBER (INGOT #4)				
			103	104	105	106	107
			($\times 10^{15}$)				
Ag		7.67	-	-	-	-	-
Al	2.8×10^{-3}	1.53	0.30	1.03	1.54	10.26*	11.36*
Mn	1.3×10^{-5}	5.10	0.26	0.76	0.50	1.01	1.89
Zn	1.0×10^{-5}	1.27	-	0.42	-	-	-
Cu	8.0×10^{-4}	1.95	1.31	2.18	4.36	4.86	9.86
Fe	6.4×10^{-6}	22.20	17.36	24.80	49.59	49.59	50.37
Cr	1.1×10^{-5}	2.39	1.07	2.66	2.66	7.99	8.93
Ti	3.6×10^{-6}	0.86	< 0.58	< 1.16	< 1.45	< 2.60	< 5.76
Mg	3.2×10^{-6}	5.10	1.71	5.69	5.69	11.08*	11.30*
Mo	$\sim 10^{-6}$	-	< 1.15	2.89	2.89	5.77	7.38
Ta		0.15	2.30	4.59	3.06	7.65	8.73
V		-	< 0.05	< 1.54	< 1.54	< 3.08	< 5.69

*Heterogeneous Distribution

TABLE 40

Spark Source Mass Spectroscopy Analysis
(Converted from ppm to Atoms/cm^3)

*Heterogeneous
Int - Interference

Impurity	Segregation Coefficient	Virgin Poly Feed Stock	Sample Number and Description (Atms/cm^3)					
			1-A	30-1-T	30-1-B	30-6-T	30-6-B	30-Residual Melt
Ag							1.17×10^{16}	
Al	2.8×10^{-3}	6.03×10^{15}	4.22×10^{15}	5.43×10^{15}	3.02×10^{15}	4.22×10^{15}	1.81×10^{16}	1.21×10^{17}
Mn	1.3×10^{-5}							7.89×10^{15}
Zn	1×10^{-5}			1.32×10^{16}	*2.63×10^{16}	*5.26×10^{17}	1.32×10^{16}	6.58×10^{16}
Cu	8×10^{-4}						8.46×10^{16}	*2.54×10^{17}
Fe	6.4×10^{-6}	4.24×10^{17}	2.54×10^{17}	*5.09×10^{17}	2.54×10^{17}	3.39×10^{17}	5.09×10^{17}	Int
Cr	1.1×10^{-5}	*8.34×10^{16}	2.5×10^{16}	2.5×10^{17}	6.67×10^{16}	5.00×10^{16}	5.84×10^{16}	4.17×10^{16}
Ti	3.6×10^{-6}	1.13×10^{16}	5.09×10^{15}	1.13×10^{16}	5.66×10^{15}	5.66×10^{15}	2.26×10^{16}	5.66×10^{16}
Mg	3.2×10^{-6}	4.31×10^{15}	8.62×10^{15}	1.29×10^{16}	8.62×10^{15}	1.72×10^{17}	1.72×10^{17}	8.62×10^{16}
Mo	10^{-6}							
Ta				4.42×10^{16}	1.16×10^{17}		1.16×10^{17}	5.53×10^{16}
V								7.05×10^{16}

Table 41

Impurity	Segregation Coefficient	Virgin Poly Feed Stock	Sample Number and Description (Atms/cm^3)					
			1-A	30-1-T	30-1-B	30-6-T	30-6-B	30-Residual Melt
Na		2.54×10^{16}	2.27×10^{16}	1.27×10^{16}	1.78×10^{16}	7.62×10^{16}	1.02×10^{17}	7.62×10^{16}
Ca		4.66×10^{16}	9.32×10^{16}	4.66×10^{15}	4.66×10^{15}	9.32×10^{15}	1.63×10^{16}	3.50×10^{18}
K		5.28×10^{15}	1.32×10^{16}	5.28×10^{14}	5.28×10^{15}	3.96×10^{15}	7.92×10^{15}	1.58×10^{17}
P	0.35	3.19×10^{16}	1.42×10^{16}	3.54×10^{16}	3.19×10^{16}	7.08×10^{16}	2.12×10^{16}	3.19×10^{16}
Cl		1.64×10^{16}	1.09×10^{16}	1.64×10^{16}	1.09×10^{16}	1.09×10^{16}	2.18×10^{16}	2.73×10^{17}
S		1.56×10^{15}	7.78×10^{15}	1.17×10^{15}	1.56×10^{15}	2.33×10^{15}	1.17×10^{15}	3.89×10^{16}
F			3.22×10^{12}	1.07×10^{12}	2.14×10^{12}	1.07×10^{13}	3.22×10^{13}	1.61×10^{15}
B	0.8			1.17×10^{16}				1.31×10^{16}
Co	8×10^{-6}	Int	Int	Int	Int	Int	Int	2.73×10^{16}
Br								8.84×10^{15}
Ba								1.38×10^{16}
Li	0.01	Int	Int	Int	Int	Int	Int	4.63×10^{15}
Ga	8×10^{-3}							3.57×10^{16}
Ge								2.22×10^{16}
Rb								1.08×10^{15}
Cs							1.70×10^{14}	

Table 41

Spark Source Mass Spectroscopy Analysis
(Converted from ppm to Atoms/cm^3)

Impurity	Segregation Coefficient	Sample Number and Description (atms/cm^3)			
		47-1-T	47-3-B	47-Residual Melt	47-Crucible
Ag				5.86×10^{15}	5.86×10^{16}
Al	2.8×10^{-3}	6.03×10^{15}	6.03×10^{15}	6.03×10^{15}	3.62×10^{17}
Mn	1.3×10^{-5}				7.89×10^{15}
Zn	1×10^{-5}		6.58×10^{15}	6.58×10^{15}	5.92×10^{16}
Cu	8.0×10^{-4}		8.46×10^{15}	1.69×10^{17}	1.69×10^{17}
Fe	6.4×10^{-6}	Int	Int	Int	[illegible]
Cr	1.1×10^{-5}	8.34×10^{15}	8.34×10^{15}	8.34×10^{15}	Int
Ti	3.6×10^{-6}		5.66×10^{15}	5.66×10^{15}	3.96×10^{17}
Mg	3.2×10^{-6}	1.29×10^{16}	1.29×10^{16}	1.29×10^{16}	2.59×10^{17}
Mo	10^{-6}			1.92×10^{16}	3.84×10^{17}
Ta		2.77×10^{16}	2.21×10^{16}	1.66×10^{16}	
V					2.82×10^{16}
Na		1.78×10^{17}	2.03×10^{16}	2.54×10^{16}	1.68×10^{18}
Ca		2.33×10^{15}	2.33×10^{15}	2.33×10^{15}	7.69×10^{17}
K		1.32×10^{15}	1.32×10^{15}	1.32×10^{15}	4.62×10^{17}
P	0.35	2.48×10^{16}	2.83×10^{16}	1.42×10^{16}	2.12×10^{17}
Cl		3.82×10^{16}	1.64×10^{16}	3.27×10^{16}	1.58×10^{18}
S		7.78×10^{15}	7.78×10^{15}	3.89×10^{15}	7.78×10^{16}
F		5.36×10^{12}	5.36×10^{12}	5.36×10^{12}	1.07×10^{15}
B	0.8		1.3×10^{16}	1.3×10^{16}	1.3×10^{16}
Co	8.0×10^{-6}	Int	Int	Int	1.82×10^{16}
Br		6.63×10^{15}			1.99×10^{17}
Ba					9.18×10^{16}
Li	0.01	Int	Int	Int	Int
Ga	8.0×10^{-3}				2.04×10^{16}

Table 42

Impurity	Segregation Coefficient	Sample Number and Description (atms/cm^3)			
		47-1-T	47-3-B	47-Residual Melt	47-Crucible
Ge					2.66×10^{16}
Rb		Int	Int	Int	3.24×10^{15}
Cs					4.25×10^{15}
Zr				1.69×10^{16}	3.81×10^{17}
Y		3.73×10^{15}	7.46×10^{15}	3.73×10^{15}	7.46×10^{16}
U					4.26×10^{16}
Th					2.91×10^{16}
Pb					6.6×10^{16}
Ce					2.33×10^{16}
La					1.34×10^{16}
I					1.40×10^{17}
Nb					1.11×10^{17}
Sr		Int	Int	Int	1.61×10^{16}
Se					4.78×10^{17}
As	0.3				9.2×10^{15}
Ni					4.57×10^{16}
Sc					6.7×10^{15}

Table 42

Spark Source Mass Spectroscopy Analysis
(Converted from ppm to Atoms/cm^3)

Impurity	Segregation Coefficient	Sample Number and Description (atms/cm^3)				
		49-1-T	49-5-T	49-9-T	49-9-B	49-Crucible
Ag						*5.27×10^{16}
Al	2.8×10^{-3}	*6.03×10^{15}		6.03×10^{15}	6.03×10^{15}	4.22×10^{17}
Mn	1.3×10^{-5}					3.16×10^{16}
Zn	1×10^{-5}	6.58×10^{15}		1.32×10^{16}		3.29×10^{17}
Cu	8.0×10^{-4}		1.69×10^{16}	5.92×10^{16}	8.46×10^{15}	3.38×10^{17}
Fe	6.4×10^{-6}	Int	Int	Int	Int	1.02×10^{18}
Cr	1.1×10^{-5}	1.67×10^{16}	8.34×10^{15}	1.67×10^{16}	1.67×10^{16}	Int
Ti	3.6×10^{-6}	5.66×10^{15}		5.66×10^{15}	5.66×10^{15}	9.05×10^{17}
Mg	3.2×10^{-6}			2.16×10^{16}	2.16×10^{16}	3.02×10^{17}
Mo	10^{-6}					9.6×10^{17}
Ta			2.21×10^{16}	3.32×10^{16}	3.32×10^{16}	1.11×10^{17}
V						1.41×10^{16}
Na		1.02×10^{16}	1.02×10^{17}	*1.78×10^{17}	2.54×10^{16}	1.04×10^{18}
Ca		2.33×10^{15}	2.33×10^{15}	2.33×10^{15}	2.33×10^{15}	9.55×10^{18}
K		1.32×10^{15}	2.64×10^{15}	*7.92×10^{15}	1.32×10^{15}	1.06×10^{18}
P	0.35	1.42×10^{16}	3.54×10^{15}	2.83×10^{16}	2.83×10^{16}	8.85×10^{17}
Cl		*1.64×10^{16}	*3.27×10^{16}	1.64×10^{16}	*3.81×10^{16}	2.23×10^{18}
S		3.89×10^{15}	3.89×10^{15}	3.89×10^{15}	*7.78×10^{15}	3.11×10^{17}
F				5.36×10^{12}	5.36×10^{12}	5.90×10^{14}
B	0.8	1.30×10^{16}		1.30×10^{16}	1.30×10^{16}	5.20×10^{16}
Co	8.0×10^{-6}	Int	Int	Int	Int	5.45×10^{16}
Br						6.19×10^{17}
Ba						5.36×10^{17}
Li	0.01	Int	Int	Int	Int	Int
Ga	8.0×10^{-3}			5.1×10^{15}		5.1×10^{16}

Table 43

Impurity	Segregation Coefficient	Sample Number and Description (atms/cm^3)				
		49-1-T	49-5-T	49-9-T	49-9-B	49-Crucible
Ge						2.66×10^{17}
Rb		Int	Int	Int	Int	1.08×10^{15}
Cs						8.49×10^{14}
Zr		4.23×10^{15}				3.81×10^{16}
Y		1.12×10^{16}		7.46×10^{15}	1.12×10^{16}	1.49×10^{17}
U						9.46×10^{16}
Th						8.73×10^{16}
Pb						9.9×10^{16}
Ce						5.82×10^{16}
La						2.67×10^{16}
I						1.64×10^{17}
Nb						3.88×10^{1}
Sr						2.33×10^{17}
Se						1.18×10^{18}
As	0.3					9.2×10^{15}
Ni						9.13×10^{16}
Sc						1.34×10^{16}

Table 43

Spark Source Mass Spectroscopy Analysis
(Converted from ppm to Atoms/cm^3)

Impurity	Segregation Coefficient	Sample Number and Description (atms/cm^3)				
		55-1-T	55-10-T	55-10-B	55-Residual Melt	55-Lower Crucible
Ag						
Al	2.8×10^{-3}	*6.03×10^{15}	1.81×10^{16}	6.03×10^{15}	2.41×10^{16}	5.43×10^{17}
Mn	1.3×10^{-5}				*7.89×10^{15}	7.89×10^{15}
Zn	1×10^{-5}		6.58×10^{15}		6.58×10^{15}	1.97×10^{17}
Cu	8.0×10^{-4}	8.46×10^{15}	8.46×10^{15}		6.77×10^{16}	*9.31×10^{17}
Fe	6.4×10^{-6}	5.94×10^{16}	8.48×10^{16}	6.78×10^{16}	5.09×10^{17}	1.70×10^{18}
Cr	1.1×10^{-5}	2.50×10^{16}	3.34×10^{16}	8.34×10^{15}	1.67×10^{17}	Int
Ti	3.6×10^{-6}	5.66×10^{15}	1.13×10^{16}	5.66×10^{15}	1.70×10^{16}	1.13×10^{17}
Mg	3.2×10^{-6}	1.29×10^{16}	8.62×10^{15}	1.29×10^{16}	8.62×10^{15}	
Mo	10^{-6}				3.2×10^{16}	5.76×10^{16}
Ta		2.77×10^{16}	*5.53×10^{16}	*2.77×10^{17}	2.21×10^{16}	
V					7.05×10^{15}	7.05×10^{15}
Na		2.29×10^{16}	1.02×10^{16}	1.02×10^{17}	1.78×10^{16}	6.1×10^{17}
Ca		2.33×10^{15}	*6.99×10^{15}	2.33×10^{15}	*6.99×10^{15}	8.39×10^{17}
K		1.32×10^{15}	1.32×10^{15}	7.92×10^{15}	1.32×10^{15}	6.86×10^{17}
P	0.35	2.83×10^{16}	1.42×10^{16}	2.83×10^{16}	2.83×10^{16}	1.06×10^{17}
Cl		1.09×10^{16}	1.09×10^{16}	*3.82×10^{16}	3.82×10^{16}	4.91×10^{17}
S						1.17×10^{17}
F		5.36×10^{12}	5.36×10^{12}	5.36×10^{12}		9.11×10^{15}
B	0.8		1.3×10^{16}	2.6×10^{17}	1.3×10^{16}	*1.3×10^{17}
Co	8.0×10^{-6}	Int	Int	Int	Int	2.73×10^{16}
Br		4.42×10^{15}	2.21×10^{15}		1.33×10^{16}	1.55×10^{17}
Ba					3.06×10^{16}	3.06×10^{17}
Li	0.01	Int	Int	Int	Int	4.63×10^{16}
Ga	8.0×10^{-3}					1.53×10^{16}

Table 44

Impurity	Segregation Coefficient	Sample Number and Description (atms/cm^3)				
		55-1-T	55-10-T	55-10-B	55-Residual Melt	55-Lower Crucible
Ge						
Rb		Int	Int	Int	Int	
Cs						
Zr						2.12×10^{16}
Y		Int	Int	Int	Int	1.12×10^{16}
U						4.73×10^{16}
Th						5.82×10^{16}
Pb						
Ce						
La						
I						
Nb					5.54×10^{16}	5.54×10^{16}
Sr		Int	Int	Int	Int	1.61×10^{1}
Se						
As	0.3					
Ni		1.83×10^{17}	1.83×10^{17}	9.13×10^{16}	5.48×10^{17}	9.13×10^{16}
Sc						6.7×10^{15}

Table 44

the residual melt sample retrieved from the crucible at the end of the 100 kg continuous run. For that reason, it has been theorized that the crucible may be acting as a getterer for melt impurities and therefore preventing significant increases in impurity concentrations in the silicon crystals. (Refer to Section 4.5.4 for more details on crucible impurities).

5.2.1 Crystal Ingots

Representative samples taken from silicon crystal ingots grown during continuous recharge runs were submitted to a commercial testing service for determination of trace element concentrations. Tables 41 thru 44 contain the results of these analysis.

Interpretation of these results was undertaken using only data which was felt to be relatively consistent. These interpretations are stated below.

1). Except for Run No. 30, the data does not indicate any consistent trend of increasing or decreasing impurity concentration throughout a continuous recharge run.

2). The residual melts tested seemed to show higher concentrations of many of the trace element impurities when compared to crystal samples, with the exception of Run No. 47.

3). The fused quartz crucibles used during continuous recharge runs not only exhibited a larger number of measurable quantities of trace elements but for the most part indicated a one or two power higher concentration level than the crystals grown from the crucible and the residual melt from that crucible.

4). The total trace element impurity concentrations in the crystal samples and the residual melt samples are less than the "critical impurity concentration value, for structural breakdown due to constitutional supercooling (5×10^{19} atoms/cm^3). [10]

5.2.2 Crucible Samples

Trace element impurity levels have been higher in the crucible samples tested than in the crystals grown from the crucible in every case. Furthermore, impurity concentrations, for the most part (over 90% of the elements indicated), have been higher in the fused quartz crucible than in the residual melt samples tested. Refer to Tables 41 thru 44 and Section 4.5.4 for impurity analysis results.

Table 34,page 194 tends to indicate that differences in impurity concentration occur in new crucibles as well as samples taken from crucibles used during continuous recharge runs.

The data available is extremely limited and has been challenged by one fused quartz crucible manufacturer (Refer to Section 4.5.4). Therefore, it is felt that an in depth discussion of the analysis and data is not warranted at this time.

Further analysis of crucible samples is necessary to more fully define the parameters necessary to maintain acceptable purity levels within the total furnace environment.

5.2.3 Plans and Recommendations

Spark Source Mass Spectroscopy analysis for trace elements is rather expensive if done commercially (approximately $240 per sample) therefore, sample selection must be very critical in order to obtain data that will enable correct interpretation of each run.

It is felt that impurity analysis can and should be used to further the understanding of the Czochralski crystal growth process. This analysis should be in the form of trace elements, carbon and oxygen concentrations and analysis of the gaseous environment within the furnace.

6.0 Economic Analysis and Model

Throughout the 954888 project, periodic updating of cost projections, economic models and Samics/IPEG economic analyses were performed. Initial economic models and cost projections were augmented by continuing process development and crystal growth runs. Time cycles have been revised, growth and recharging methods have been changed or modified. In each case, the intent was always the same: to produce the maximum amount of high quality silicon ingot in the least amount of time.

A general explanation of the system used to define, compare and evaluate economic analyses and cost projections is contained in section 2.3 starting on page 46. The two basic units of measure described in section 2.3 are throughput in kilograms of crystal grown per hour of run time (kg/hr), and add-on cost per kilogram of crystal grown ($/kg). The add-on cost relates to the expense incurred when the polycrystalline silicon is melted and transformed into a single crystal ingot.

From the throughput and add-on cost data, other calculations can be made (with certain assumptions relating to slicing), for number of crystal growers required in a production facility to produce silicon sheet at a given rate.

It should be noted that all cost data contained in this report are projections. All process development work, including continuous recharge growth runs was performed under developmental and/or prototype conditions. Later stages of the Phase I program and the Phase II program was intended to duplicate the anticipated production type process procedure as closely as possible. This was done using one crystal grower and not three. The time cycles and cost parameters were then extrapolated for three crystal growers per operator.

6.1 Summary of Cost Projections

The first formal attempts at cost projections and formulations of economic models was completed by Kayex in February, 1978. The data input for these initial economic models was generated by the Hamco Division's knowledge of the present crystal growing techniques and conditions. Crystal growing standards, along with other standards (such as slicing conditions) were developed based on input of the silicon growth and processing industry. These first economic models were broken down into four categories:

1). Batch #1 - Batch type growth using a 12" x 9" crucible and growing 10 cm diameter crystals.

2). Batch #2 - Batch type growth using a 12" x 9" crucible and growing 12.5 cm diameter crystals.

3). Continuous CZ #1 - Continuous recharge method growing five (5) 20 kg crystals (10 cm in diameter) from one 12" x 9" crucible.

4). Continuous CZ #2 - Continuous recharge method growing three (3) 33.3*kg crystals (12.5 cm in diameter) from one 14" x 10½" crucible.

The details of each of these four economic models can be found in the "Fifth Monthly Progress Report" February 1-28, 1978 - Continuous Czochralski Growth, Contract #954888.

The details and final cost projections of these four economic models will not be discussed here for they would only tend to confuse the reader when Samics/IPEG cost projections are introduced. Several key assumptions made during the formulation of these four economic models were inconsistent with the Samics/IPEG guidelines that were used for future cost calculations and economic modeling.

* The first crystal was actually 34.4 kg.

The first cost projections (based or SAMICS/IPEG guidelines) were completed in March of 1978. The same four CZ growth methods were used to formulate the cost projections and economic models. The assumptions, CZ Growth Methods (Table 45), process cycle time for CZ #1, input data and economic model discussion for the CZ #1 growth method are included on pages 252 thru 255. Applying the SAMICS/IPEG model to the input data yielded an add-on cost of $19.30 per kg (in 1975 dollars). *If converted into today's dollar value (1980), the add-on cost would be $27.02 per kg.

Although the add-on cost arrived at for the CZ #1 growth method appeared to meet the D.O.E.-J.P.L. cost goals for 1980 and 1982, it did not meet the cost goals for 1986. Therefore, a second continuous recharge growth method was analyzed (CZ No. 2). This growth method allowed for the growth of 134 kilograms of silicon ingot 12.5 cm in diameter. Four ingots were to be grown from one 14" x 10½" fused quartz crucible (Table 46). The SAMICS/IPEG input data and cost calculations for CZ No. 1 and Cz No. 2 are contained in Table 47.

The growth of four 33.5 kg, 12.5 cm diameter crystals from one 14" x 10½" crucible (CZ #2) projected a decrease in the add-on cost to $15.07/$m^2$** in 1975 dollars or ($21.10/m^2 in 1980 dollars). Although the $15.07/$m^2$ add-on cost was less than the IPEG price goal for P wafers in 1986, it allowed for only $3.13/$m^2$ for slicing the silicon crystal ingots.

* Starting in April of 1980 all cost calculations and SAMICS/IPEG analysis was to be completed in 1980 dollars. In order to directly compare 1975 dollars to 1980 dollars, a conversion factor of 1.4:1 was indicated by J.P.L.

**1980 J.P.L. cost goals assume the 1 kilogram of silicon ingot can be sliced into wafers to produce 1 square meter of surface area.

ASSUMPTIONS

Cycle Time = 74.9 hrs

Machine Utilization = 90%

Cycles/yr = (345 days/yr) (24 hr/day) (.90)/74.9 hrs/cycle = 99.5 cycles/yr

Direct Labor - One operator runs three machines. This equivalent to 4 people/yr continuous operation.

4 people/3 machines = 1-1/3 man x yr/machine

Slicing Yield

1978 = 1.77 kg/m^2 (wafer + kerf = .076 cm)

1982 and 1986 = 1.0 kg/m^2 (wafer + kerf = .043 cm)

CZ GROWTH METHODS

Conditions	Batch #1	Batch #2	Continuous #1	Continuous #2
Crucible Size (in)	12 x 9 h	12 x 9 h	12 x 9 h	14 x 10½h
Crystal Diameter (cm)	10	12.5	10	12.5
Growth Rate (cm/hr)	10	10	10	10
Total Poly Melted (kg)	18	18	105	110
Total Crystal Pulled (kg)	14.4	14.4	100	101
Pulley Yield (%)	80	80	95	92
Usable After Grinding (kg)	12.6	12.6	87.5	88.3
Ground Crystal Yield (%)	70	70	83	80
No. Crystals/Crucible	1	1	5	3

Table 45

INPUT DATA (For Cont. CZ#1)

The input data are in 1978 dollars. The SAMICS/IPEG model has been followed with the exception of treatment of the poly raw material. This has been left out of the calculation in order to arrive at a CZ add-on cost. Ultimately the CZ add-on cost should be combined with the slicing cost, with the assignment of appropriate material plus overhead costs for the poly silicon, to arrive at the "WAFERCO" cost for comparison with the SAMICS goals.

1.	Direct Equipment Initial Capital Cost EQPT	$150,000
2.	Direct Manufacturing Floor Space (Type A) SQFT	100
3.	Annual Direct Labor Salaries	
	Production Operator (B3752D)	
	(1.33 PRSN x YRS) ($9,400) (1.08) (1.08)	14,582
	Elect. Technician (B3704D)	
	(0.1 PRSN x YRS) ($11,000) (1.08) (1.08)	1,283
	Inspector (B3720D)	
	(0.1 PRSN x YRS) ($8,250) (1.08) (1.08)	962
	Total DLAB	$ 16,827
4.	Directly Used Materials & Supplies	
	Cycles/Yr = 99.5	
	Hours/Cycle = 74.9	
	P Poly (kg/yr)	10,447 kg
	Crucibles @ $200 ea.	$ 19,900
	Seeds $5/cycle	498
	Dopant (not costed)	---
	Argon* (E1112D) 100 ft^3/cycle-fr @.014/ft^3	11,476
	Miscellaneous including graphite usage	19,264
	Total Material, excluding poly MATS-1	$ 51,138

5. Direct Process Usage of Utilities

Electricity (C1032B)

(50 kw) ($.027 x 1.12) (72.4 hr/cycle)

(99.5 cycles/yr) = $ 10,806

Cooling Water (C1128D)

(50 kw) (.00566 x 1.15) (73 hrs/cycle)

(99.5 cycles/yr) = 2,361

UTIL $ 13,167

6. Annual Production

Poly melted x yield

105 (kg/cycle) (99.5 cycles/yr) (.83) = QUAN 8,706 kg

* Includes 13% inflation rate per SAMICS

IPEG PRICE CALCULATION

Price ~ $(C_1 *EQPT) + (C_2 *SQFT) + (C_3 *DLAB) +$

$(C_4 *MATS) + (C_5 *UTIL)/QUAN$

in which C_1 = $0.49/yr per dollar of EQPT

C_2 = $97/yr per ft^2 of SQFT

C_3 = $2.1/yr per dollar of DLAB

C_4 = $1.3/yr per dollar of MATS

C_5 = $1.3/yr per dollar of UTIL

In 1978 dollars:

CZ add-on Price = $ 23.22/kg*

In 1975 dollars:

CZ add-on Price = $ 19.30/kg*

*Price does not include poly or its overhead constant

ECONOMIC MODEL DISCUSSION AND CONCLUSIONS

Using the IPEG add-on cost for continuous CZ#1, one can calculate the margin available for slicing for 1978 through 1986 if slicing yields are assumed as follows:

Year	Slice Yield
1978	1.77 kg/m^2
1982	1.0 kg/m^2
1986	1.0 kg/m^2

Year	IPEG Price (1975 $) Goal - P Wafers	CZ Add-on Cost	Margin left for Slicing
1978	$381/$m^2$	$ 34.16/m^2	$ 347/m^2
1982	128	19.30	$ 109
1986	18.2	19.30	($-1.1)

CZ GROWTH METHODS

Conditions	Continuous No. 1	Continuous No. 2
Crucible Size (in.)	12 x 9 h	14 x 10-1/2 h
Crystal Diameter (cm)	10	12.5
Growth Rate (cm/hr)	10	10
Total Poly Melted (kg)	105	143.3
Total Crystal Pulled (kg)	100	134
Pulled Yield	95	94
Usable After Grinding (kg)	87.5	117
Ground Crystal Yield (%)	83	81.5
No. Crystals/Crucible	5	4

TABLE 46

SAMICS/IPEG INPUT DATA AND COST CALCULATION FOR CZ NO. 1 AND CZ NO. 2

Conditions: (Per Cycle)	CONTINUOUS CZ NO. 1	CONTINUOUS CZ NO. 2
Total Si Melted (kg)	105	143.3
Crystal Weight (kg)	20	33.4
No. of Crystals/Crucible	5	4
Diameter of Crystal (cm)	10	12.5
Growth Rate (cm/hr)	10	10
Cycle Time (hrs)	75.4	75.1
Crucible Size	12" x 9" high	14" x 10-1/2" high
Yield (%)	83	81.5
Input Data (1975 $)		
Capital Equipment Cost (EQPT)	$124,700	$124,700
Manufacturing Floor Space (SQFT)	100	100
Annual Direct Labor Salaries		
Prod. Operator (1.33 prsn x yrs)	$ 11,572	$ 11,572
Elect. Tech. (0.33 prsn/yrs)	$ 1,018	$ 1,018
Inspector (.1 prsn/yrs)	$ 763	$ 763
Total (DLAB)	$ 13,353	$ 13,353
Direct Used Material and Supplies		
85% Usage per year		
Cycles/yr; hrs/cycle	98.7; 75.4	99.1; 75.1
Poly - kg/yr (charged)	10,363 kg	14,201 kg
Seed ($4.16/cycle)	$ 410	$ 412
Dopant (not costed)	---	---
Argon (100 ft^3/cycle - hr @ $0.014/$ft^3$)	$ 9,563	$ 9,563
Crucibles - $166/12"; $208/14"	$ 16,384	$ 20,613
Miscellaneous (including graphite $2.25/cycle-hr (12"); $2.50/cycle-hr (14"))	$ 16,753	$ 18,615
Material Total (MATS)	$ 43,110	$ 49,203
Utilities (Process)		
Electricity (C10328) (50 kw)($.025/kw) (cycle time-3 hr)(#cycles)	$ 8,932	$ 8,932
Cooling Water (C11280) (50 kw)($.00528/kw)(cycle time-2 hr)(#cycles)	$ 1,912	$ 1,912
Utilities Total (UTIL)	$ 10,844	$ 10,844

TABLE 47

	CONTINUOUS CZ NO. 1	CONTINUOUS CZ NO. 2
IPEG PRICE		
C_1 *EQPT = \$0.489/yr-dollar *EQPT	$ 60,978	$ 60,978
C_2 *SQFT = \$96.9/yr-ft^2 *SQFT	9,690	9,690
C_3 *DLAB = \$2.133/yr-dollar *DLAB	28,482	28,482
C_4 *MATS = \$1.255/yr-dollar *MATS	54,103	61,750
C_5 *UTIL = \$1.255/yr-dollar *UTIL	13,609	13,609
TOTAL	\$166,862	\$174,509
QUAN (total charge x % yield)(kg)	8,602 kg	11,574 kg
Throughput	1.12 kg/hr	1.56 kg/hr
ADD-ON COST (\$/kg or \$/m^2) (assume 1 kg → 1 m^2)	\$19.40	\$15.07

TABLE 47

In order to formulate cost projections for CZ No. 1 and CZ No. 2, it was necessary to project process cycle times (Table 48). These initial cycle times were arrived at by using crystal diameter and growth rate goals of the project along with estimated times for growth preparation, hot fill and recharge cycles and shut down cycles. Total cycle time for CZ No. 1 and Cz No. 2 were projected to be similar. CZ No. 2 produces considerably more crystal in the same run time because the crystal diameter goal (5") is larger than CZ No. 1 goal (4") while the growth rate remains the same at 10 cm/hr. The resulting significant increase in throughput is the largest single factor in reducing the CZ add-on cost. The calculations illustrate the economy of increasing the throughput by an increase in crystal diameter. The cost per meter^2 indicated assumes that one kg of ingot will produce one square meter of silicon sheet.

In December of 1978, following process development work involving hot filling experiments, recharging and several continuous recharge runs, the initial cost projections and economic models were updated.

In addition to the update of CZ No. 1 and CZ No. 2 two new economic models were developed for the purpose of economic analysis and comparison between the present technology (CZ #1) and those technologies required for 1986 or later (Table 6, page 48).

The circled items in Table 6 are the major differences among the four methods, thus, the crucible size increases from 12 x 9 inch to 15 x 12, the diameter from 10 to 17.8 cm, and a modest increase in growth rate for CZ #4. The other criteria assumed were that (1) the cycle time would be approximately the same, that is, approximately 75-80 hours based on the predicted life of the crucible, and (2) that the yields achievable would be a relatively constant 81-84%. The other figures are calculated from these predetermined conditions.

PROCESS CYCLE TIME

OPERATION	CZ NO. 1 (MIN.)	CZ NO. 2 (MIN.)
1. Preparation	180	240
Load Poly	45	45
Close Furnace	5	5
Pump Down	10	10
Melt	120	180
2. Hot Fill/Growth Cycle	765	895
Position Poly	5	5
Lower Poly	5	5
Melt Poly	60	120
Retract Poly*	5*	5*
Lower Seed*	15*	15*
Stabilize Temperature	40	40
Seed Growth	30	30
Crown Growth	60	60
Straight Growth	525	575
Taper End	40	60
3. Recharge/Growth Cycles	3460 (4 cycles)	3210 (3 cycles)
Cool Crystal	30	45
Remove Crystal	10	10
Position Poly	5	5
Lower Poly	5	5
Melt Poly	120	220
Retract Poly*	5*	5*
Lower Seed*	15*	15*
Stabilize Temperature	40	60
Seed Growth	30	30
Crown Growth	60	60
Straight Growth	525	575
Taper End	40	60
4. Shut Down Cycle	120	160
Cool Furnace	60	80
Remove Crystal**	10**	10**
Clean, Set Up	60	80
Total Time (Min.)	4525	4505
(Hr.)	75.4	75.1

*Completed during stabilization of melt temperature.
**Completed during furnace cooling time.

TABLE 48

The add-on costs are expressed in 1975 dollars per meter^2 and the IPEG equation was used to calculate these costs. The costs in 1980 dollars are included below the 1975 dollar costs.

At this time, an analysis was also performed relating the effect of number of crystals grown per crucible on the CZ add-on cost (Figure 17, page 49).

Putting the number of crystals per crucible into the IPEG equation as a variable (from 1-5), it can be seen that the cost per Kg diminishes rapidly by growing two ingots instead of one. The cost reduction for additional ingots becomes less and less significant as more crystals are grown.

The arrows indicate(Figure No. 17),the point where a quantity of 100 kg is reached for a given method.

Except perhaps in the case of CZ No. 4, it would appear that production of more than 100 kg from a crucible has a marginal effect in reducing the cost per kg.

The advisability of growing more ingots must be weighed against the expected yields and the risks associated with longer runs.

Also, when 100 kg is produced, the crucible is no longer the major cost item; rather, the materials used and the cost items related to time become significant, such as labor, equipment, and utilities.

The data indicated that once the 100 kg capability was achieved, efforts should be directed toward other cost reducing possibilities such as increased growth rates. The effect of increased growth rate on CZ costs is shown in Figure 60. If the growth rate is increased from 10 to 12 cm/hr, then cost will be reduced from $19.24 to $17.70 for CZ No. 1.

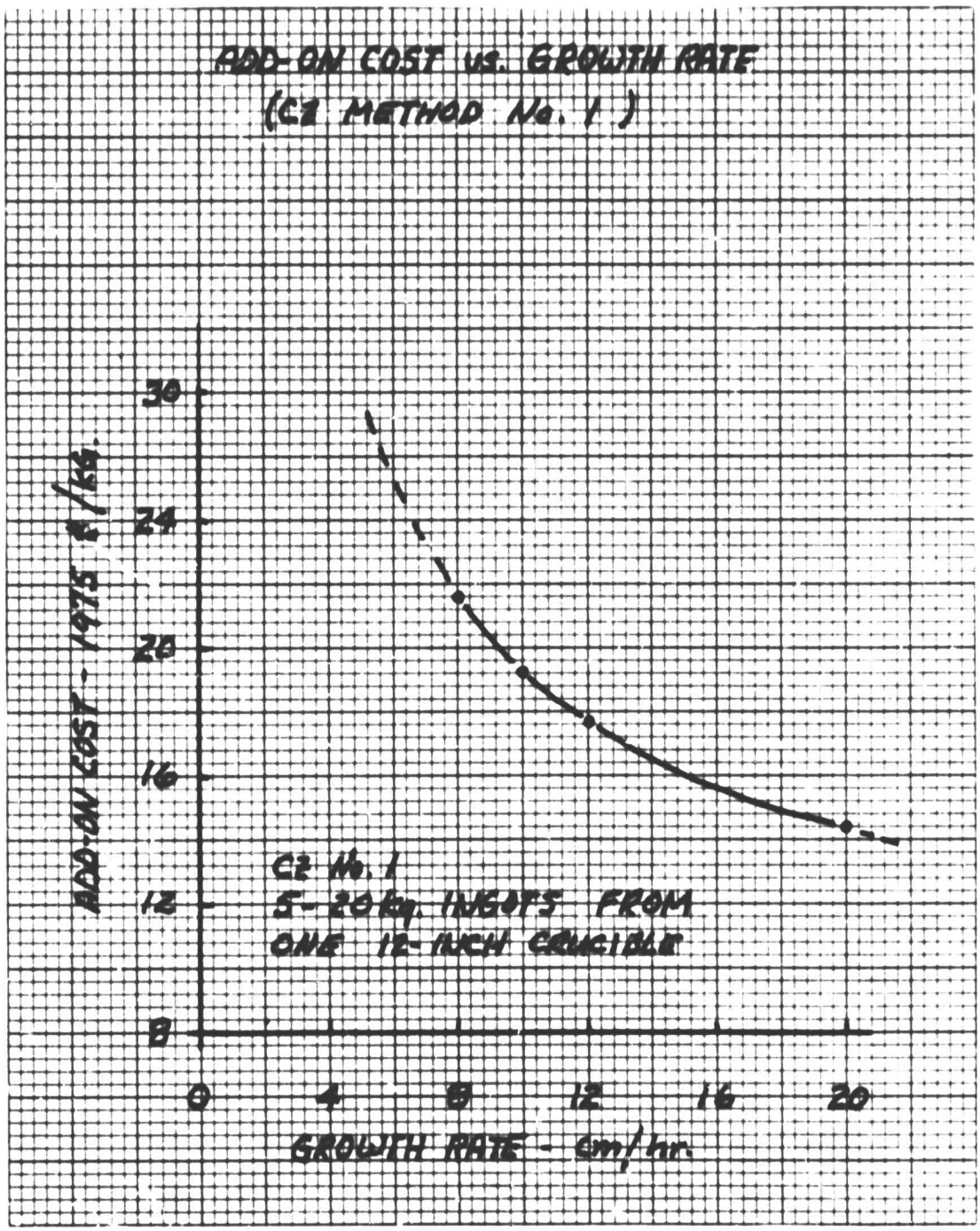
ADD-ON COST vs. GROWTH RATE
(C2 METHOD No. 1)
ADD-ON COST - 1975 $/kg.
30
24
20
16
12
8
C2 No. 1
5-20 kg. INGOTS FROM
ONE 12-INCH CRUCIBLE
0
4
8
12
16
20
GROWTH RATE - cm/hr.

Figure 60

Following the first two 100 kg continuous recharge runs using 12" x 9" crucibles, a change over to 14" x 10½" crucibles was made. The 954888 contract extension required five more 100 kg continuous recharge runs. Those runs were to be performed using 14" x 10½" crucibles. Therefore, an economic analysis and cost projection of the growth of 100 kg of silicon ingot from one 14" x 10½" crucible was prepared.

This new cost update was referred to as (CZ No. 2*) so that it could be differentiated from the original CZ No. 2 which assumed the growth of three 33.5 kg crystals from one 14" x 10½" crucible (Table 46). The new CZ No. 2* allowed for the growth of four 25 kg crystals from one 14" x 10½" crucible.

Table 49 presents a general time cycle projection for the initial Cz No. 2* growth method along with the SAMICS/IPEG add-on cost calculated from the time cycle projection. This initial cost projection was formulated in August of 1979. Table 49 also includes a general breakdown of the actual time cycles for Runs No. 49 and No. 55, both 100 kg continuous recharge runs. From these two 100 kg runs, a new updated cost projection was formulated in December, 1979. It can readily be seen that actual continuous recharge run times were considerably longer than the projected run times and time cycles. The reasons for the longer run time can be seen in the table. Run No. 49 resulted in nine crystals being grown and Run No. 55 resulted in ten crystals being grown. More than five crystals were grown during these runs so that a high percentage of monocrystalline material could be produced. This had a significant impact on the growth preparation time required during each run. This increase in the number of crystals grown also impacted on the number of recharge cycles required for each run and therefore should have increased the recharge time correspondingly. However, due to the use of the chunk recharging method - as opposed to the rod recharging method - the recharge cycle time was actually less than projected (for twice as many recharge cycles).

COST UPDATE FOR CZ NO.2 *

Operation	Projected Time (Hr)	Actual Time Run #49 (Hr)	Actual Time Run #55 (Hr)	Updated Projection(Hr)
Melt Down	4 (7.0%)*	2 (2.3%)	1.8 (2.0%)	3 (5.3%)*
Growing Preparation				
1) Stabilize Temperature	10.6 (18.4%)	23 (26.7%)	36.5 (40.1%)	14.6 (25.6%)
2) Growing Seed	(4 ingots)	(9 ingots)	(10 ingots)	(4 ingots)
3) Crown Growth				
4) Melt Backs				
Ingot Growing	30.4 (52.9%)	50 (58.1%)	43.9 (48.3%)	30.4 (53.3%)
(Straight Section)	(10 cm/hr)	(7.0 cm/hr)	(7.2 cm/hr)	(10 cm/hr)
Recharge Cycle (Lump Only)				
1) Removal of Crystal	12.5 (21.7%)	11 (12.8%)	8.5 (9.4%)	9.0 (15.8%)
2) Load Hopper	(3 times)	(5 times)	(6 times)	(3 times)
3) Hot Fill				
4) Melt Down	---	---	---	---
Total Time	57.5	86	91	57
Add-On CZ Cost (1980 Dollars)	(23.90)**	(33.32)	(34.97)	(23.76)**

CZ No. 2: 14" Crucible; 100 kg; 13.3 cm diameter; 10 cm/hr

*Includes Melt Down Preparation

** Includes 2-1/2 hours for shut down cycle

Table 49

The straight growth rate during Runs No. 49 and No. 55 was lower than projected and therefore, also impacted on the total run time.

The updated projection looks at the actual time cycles in relation to the original projected time cycles for CZ No. 2*, and attempts to better define these time cycles and the resultant CZ add-on cost ($23.76/kg) for the CZ No. 2* growth method.

After two 100 kg continuous recharge runs using 14" x 10½" crucibles the updated cost projection agreed quite closely to the original projection for CZ No. 2* ($23.90/kg).

Cost projection updates during the second half of 1979 centered around the growth of 100 kg of silicon ingots. Prior to the completion of Phase I of the 954888 contract, J.P.L. requested that Kayex submit a proposal for a three month extension to the 954888 contract (Phase II). This contract extension involved the growth of 150 kg of silicon ingot from one 14" x 10½" crucible. This increase to 150 kg of silicon represented a 50% increase in the quantity produced. Projected crucible lifetime necessitated a revision in the growth parameters acceptable for the growth of 100 kg of silicon. Phase II, therefore, required the growth of 15 cm diameter ingots rather than the 12.7 cm diameter ingots grown during Phase I of the contract.

Table 50 lists the conditions of this new CZ Growth method referred to as CZ No. 3*. This new CZ No. 3*should not be confused with the CZ No. 3 method previously formulated in December, 1978.

CZ No. 3* Growth Method

Conditions

Crucible Size (in.)	14 x 10.5
Crystal Diameter (cm)	15
Growth Rate (cm/hr)	10
Total Poly Melted (kg)	155
Ingot Size (kg)	25
No. Ingots/Crucible	6
Total Crystal Pulled(Kg)	150
Pulled Yield (%)	96.8
Usable After Grinding (Kg)	128
Ground Crystal Yield (%)	80

Table 50

The initial SAMICS/IPEG cost calculations indicated an add-on cost of $15.62 per kilogram of usable silicon in 1980 dollars. This analysis was based on a total cycle time of 58½ hours. The projected add-on cost for CZ No. 3* represented a 34.2% decrease from the projected add on cost for the production of 100 kg of silicon (CZ No. 2*).

An updated SAMICS/IPEG cost analysis was performed following the first two 150 kg continuous recharge growth runs. This analysis resulted in a slightly higher add-on cost than initially projected due to a revision of the cycle times for CZ No. 3*. Therefore, the final projected add-on cost for the CZ No. 3* growth method was $16.14 per kilogram of usable silicon for solar cell manufacture. Details of the SAMICS/IPEG input data and cost

calculations can be seen in Section 6.2.

The add-on costs projected for CZ No. 3* do not include the costs necessary to slice the crystal ingots into wafers. Also, the projected add-on costs do not include the cost of the polycrystalline silicon used to produce the monocrystalline silicon.

A chronological summary of cost projections can be seen on page 267. Table 51.

6.2 Cost Components of Convential CZ Growth vs. CZ No. 3*

At the completion of phase II of the 954888 contract a comparison of the SAMICS/IPEG cost components was investigated. The results of the comparison is included in Table 52 and 53.

Two methods of conventional (Batch Type) CZ growth were considered in Table 52. Batch #1 assumes the growth of one 10 cm diameter crystal per crucible. The crucibles used for the Batch #1 process are 12" x 9". Batch #2, assumes the growth of one 12.5 cm diameter crystal from one 14" x 10½" crucible.

The projected cost for each component is followed by the percentage of the total cost which it represents. The materials component has been broken down further to point out the cost factor attributed to the crucible as well as other items that make up the materials component.

It should be noted that the cost components for the conventional (batch) CZ growth have used the SAMICS/IPEG guidelines so that they can be compared directly to the cost components for continuous recharge type CZ growth. Therefore, these cost figures may or may not agree with costs experienced by commercial producers of silicon.

Table 53 presents the SAMICS/IPEG cost components for CZ No. 3* type continuous recharge crystal growth. Two projections are included; one (Ideal*) assumes that optimum crystal growth conditions exist and that no problems

SUMMARY OF COST PROJECTIONS

	Batch	Cont. #1	Cont #2	Cont #3*
Crucible Size (in)	12 D x 9 H	12 D x 9 H	14 x 10.5	14 x 10.5
Ingot Diameter (cm)	10	10	13	15
Growth Rate (cm/hr)	7.6	10	10	10
Ingot Size (kg)	14.4	20	25	25
No. Ingots/Crucible	1	5	4	6
Total Pulled (kg)	14.4	100	100	150
Yield, Usable (%)	70	83	81	80
CZ Add-On 1980 $/kg	$52	$27	$23	$16.1
With $14 poly	$71	$47	$43	$36.1
$/watt	$.50	$.34	$.31	$.25
When Reported	Apr. '78	Apr. '79	Dec. '79	Apr. '80

All Costs are expressed in 1980 dollars.

Table 51

SAMICS/IPEG COST COMPONENTS OF

CONVENTIONAL BATCH CZ GROWTH

	BATCH #1[1]	BATCH #2[2]
Equipment x $0.489 = EQPT	$ 71,150 (25.6%)	$ 71,150 (23.8%)
Area x $96.9 = SQFT	9,690 (3.5%)	9,690 (3.2%)
Direct Labor x $2.133 = DLAB	50,637 (18.3%)	50,637 (16.9%)
Utilities = 1.255 = UTIL	17,240 (6.2%)	22,530 (7.5%)
Materials x 1.?55 = MATS		
Seeds	5,399 (1.9%)	3,941 (1.3%)
Argon	26,078 (9.4%)	25,891 (8.7%)
Crucibles	67,488 (24.4%)	82,755 (27.7%)
Graphite & Misc.	29,420 (10.6%)	32,689 (10.9%)
(Sub-Total, MATS)	(128,385)(46.3%)	(145,276)(48.6%)
TOTAL ANNUAI COST	$277,101 (100%)	$299,282 (100%)
Add-on Cost per kg	$ 51.12	$ 42.19

1) 12-inch diameter crucible (see details of other assumptions in Table 54)

2) 14-inch diameter crucible (see details of other assumptions in Table 54)

Table 52

SAMICS/IPEG COST COMPONENTS OF

CONTINUOUS CZ GROWTH

	IDEAL*		CONSERVATIVE*	
Equipment x $0.489 = EQPT	$71,150	(28.4%)	$ 71,150	(29.6%)
Area x $96.9 = SQFT	9,690	(3.9%)	9,690	(4.0%)
Direct Labor x $2.133 = DLAB	50,637	(20.2%)	50,637	(21.1%)
Utilities x $1.255 = UTIL	23,471	(914%)	23,773	(9.9%)
Materials x $1.255 = MATS				
Seeds	3.143	(1.3%)	2,179	(0.9%)
Argon	26,728	(10.7%)	27,127	(11.3%)
Crucibles	32,996	(13.2%)	22,876	(9.5%)
Graphite, Misc.	32,689	(13.0%)	32,689	(13.6%)
(Sub-Total, MATS)	(95,556)	(38.2%)	(84,871)	(35.3%)
TOTAL ANNUAL COST	$250,504	(100%)	$ 240,121	(100%)
Add-on Cost per kg	$16.14		$22.31	

See Table 55 for assumptions made for these calculations.

Table 53

are experienced, while the second (conservative*) allows for a moderate amount of time delays brought about by possible problems associated with CZ crystal growth.

A detailed SAMICS/IPEG cost analysis for Batch #1, Batch #2, continuous CZ #3 (Ideal) and continuous CZ #3 (conservative) are included in Table 54 and Table 55.

The final analysis indicates that the CZ No. 3 method, for production of low cost monocrystalline silicon for use in solar cells, can lower the cost of this silicon from 62% to 68% in comparison to conventional batch type CZ crystal growth.

	Batch #1	Batch #2
Input Data ($1980)		
Capital Equipment Cost (EQPT)	$145,500	$ 145,500
Manufacturing Floor Space (SQFT)	100	100
Annual Direct Salaries		
Prod. Operator (1.33 persons/yr)	17,503	17,503
Elect. Tech. (0.33 persons/yr)	5,082	5,082
Inspector (0.1 persons/yr)	1,155	1,155
Total DLAB	23,740	23,740
Direct Used Materials & Supplies		
85% Usage per year		
Cycles/yr; Hrs/Cycle	430.2; 17.3	314; 23.7
Poly kg/yr charged	7,743.6	9,420
Seed ($10/cycle)	4,302	3,140
Dopant (not costed)		
Argon (150 ft^3/cycle hr @ $0.02/$ft^3$)	20,779	20.630
Crucibles ($125/12"; $210/14")	53,775	65,940
Miscellaneous (inc. graphite)		
$3.15/cycle hr (12");		
$3.50/cycle hr (14")	23,442	26,047
Materials Total (MATS)	$ 102,298	$ 115,757
Utilities (Process)		
Electricity		
(65 kw @ $0.035/kw)(cycle time - 3.2 hrs)		
(# cycles)	14,485	14,644

Table 54

	Batch #1	Batch #2
Cooling water		
(65 kw @ $0.0074/kw) (cycle time - 1.8 hrs)		
(# cycles)	3,373	3,308
Utilities Total (UTIL)	17,858	17,952
IPEG PRICE		
C_1 EQPT = $0.489/yr = $EQPT	71,150	71,150
C_2 SQFT = $96.9/yr = $SQFT	9,690	9,690
C_3 DLAB = $2.133/yr = $DLAB	50,637	50,637
C_4 MATS = $1.255/yr = $MATS	128,384	145,275
C_5 UTIL = $1.255/yr = $UTIL	22,412	22,530
Annual Cost	$282,273	$299,282
QUAN (Total charge x % yield) (kg)	5,420.5 kg	7,093 kg
Throughput	0.728 kg/hr	0.953 kg/hr
Add on Cost ($/kg or $/M^2)	$52.08	$42.19

*All costs expressed in 1980 Dollars

Table 54 (Cont'd)

	Ideal	Conservative
Total Si Melted	155	155
Crystal wt. (kg)	25	25
No. Crystals/Crucible	6	6
Diameter of Crystal (cms)	15.0	15.0
Growth Rate (cms/hr)	10	7
Cycle Time (hrs)	59.4	85.7
Crucible Size (ins)	14" x 10-1/2"	14" x 10-1/2"
Yield (%)	80.0	80.0
INPUT DATA ($1980)		
Capital Equipment Cost (EQPT)	$145,500	$ 145,500
Manufacturing Floor Space (SQFT)	100	100
Annual Direct Salaries		
Prod. Operator (1.33 persons/yr)	17,503	17,503
Elect. Tech. (0.33 persons/yr)	5,082	5,082
Inspector (0.1 persons/yr)	1,155	1,155
Total DLAB	23,740	23,740
Direct Used Materials & Supplies		
85% Usage per year		
Cycles/yr; Hrs/cycle	125.2; 59.4	86.8; 85.7
Poly kg/yr charged	19,406	13,454
Seed ($20 ea) (1/cycle)	2,504	1,736
Dopant (not costed)		
Argon (150 ft^3/cycle hr @ $ 0.02/ft^3)	21,297	21,615
Crucibles (210/14")	26,292	18,228
Miscellaneous (inc. graphite)		
@ $3.50/cycle hr)	26,047	26,047
Materials Total (MATS)	76,140	5?,626

Table 55

	Ideal	Conservative
Utilities (Process)		
Electricity		
(65 kw @ $0.035/kw) (cycle time - 2.7 hrs)		
(# cycles)	16,150	16,390
Cooling Water		
(65 kw @ $0.00528/kw)(cycle time)		
(# cycles)	2,552	2,553
Utilities Total (UTIL)	18,702	18,943
IPEG Price		
C_1 EQPT = $0.489/yr = $EQPT	71,150	71,150
C_2 SQFT = $96.9/yr = $SQFT	9,690	9,690
C_3 DLAB = $2.133/yr = $DLAB	50,637	50,637
C_4 MATS = $ 1.255/yr = $MATS	95,556	84,871
C_5 UTIL = $1.255/yr = $UTIL	23,471	23,773
Annual Cost	$250,504	$240,121
QUAN (total charge x % yield) (kg)	15,525 kg	10,763.2 kg
Throughput	2.086 kg/hr	1.446 kg/hr
Add on Cost ($/kg or $/$M^2$) (Assume 1 kg = 1 M^2)	$16.14	$22.31

Table 55 (cont'd)

7.0 REFERENCES

1. Lane, R. L. and Johnson, C. M., Kayex Corporation. "Fifteenth Project Integration Meeting Report", Presented April 1, 1980, Low Cost Silicon Solar Array Project DOE/JPL, Contract No. 954888, April 1, 1980.

2. Exhibit A to Letter Contract No. 954888 - Modification No. 1, September 8, 1977. Kayex Corporation.

3. Contract No. 954888 - Modification No. 8 between the Jet Propulsion Laboratory and Kayex Corporation, December 7, 1979.

4. Kayex Corporation First Quarter Stockholders Report, January thru March, 1980.

5. Runyan, W. R. Silicon Semiconductor Technology. McGraw-Hill, 1965.

6. Lane, R. L. and Johnson, C. M. Op. Cit.

7. Lane, R. L., Kayex Corporation. "Quarterly Progress Report for Quarter Ending December 31, 1978". Low Cost Silicon Solar Array Project DOE/JPL, Contract No. 954888, December, 1978.

8. Yoo, H., Applied Solar Energy Corporation. Fourteenth and Fifteenth Project Integration Meetings Report - December 5, 1979 and April 2, 1980. Low Cost Silicon Solar Array Project DOE/JPL, Contract No. 955089.

   Minahan, J. A., Spectrolab, Inc. Fourteenth and Fifteenth Project Integration Meetings Report - December 5, 1979 and April 2, 1980. Low Cost Silicon Solar Array Project DOE/JPL, Contract No. 955055.

9. Schmid, F., Khattak, C. P., Digges, T. G., Jr., and Kaufman, L. Journal of the Electrochemical Society: Electrochemical Science and Technology, Vol. 126, No. 6935, June, 1979.

10. Lane, R. L. and Kachare, A. H. "A Novel Czochralski Grower for Low-Cost Production of 100 kg of Silicon Crystal from One Crucible". Presented at The American Ceramic Society 1979 Joint Fall Meeting on Energy Conversion and Electronic Ceramics, September 17, 1979.

11. Lane, R. L., Kayex Corporation. "Quarterly Progress Report for Quarter Ending March 31, 1978", Low Cost Silicon Solar Array Project DOE/JPL, Contract No. 954888, March, 1978.

APPENDIX A

STRUCTURE LOSS IN CZ SILICON CRYSTAL GROWTH

1.0 INTRODUCTION

Silicon single crystals are grown in high purity vitreous silica (commonly called fused quartz) crucibles, in a CZ furnace having an inert atmosphere to prevent oxidation of the silicon. The technology has advanced to the point where large single crystal ingots can be grown with relative ease having no dislocations discernible by etch-pit count. The only defects present in such a crystal are point defects brought about by the thermal equilibrium vacancies or by impurities in the lattice.

By structure loss is meant the loss of this zero dislocation (O-D) structure. When an O-D crystal loses structure, the shock is nearly always severe enough to subsequently cause twinning and eventually polycrystalline growth.

It is considered highly desirable in CZ growth to produce O-D crystals, because the growth is stable and easily controlled, and the resulting material produces the highest efficiency solar cells.

Attempts to grow 100 kilograms of high quality CZ ingots by the "continuous" process (e.g. growth with periodic melt replenishment) have been limited to about 50 kilograms by structure loss problems, and at this point it is not clear what mechanisms are causing the problem, although there are a number of known structure loss mechanisms.

2.0 CAUSES OF STRUCTURE LOSS

Structure loss mechanisms can be categorized into three general areas, (1) mechanical or equipment perturbation such as vibration or shock, (2) thermal perturbation, and (3) melt contamination, especially particulate contamination.

2.1 MECHANICAL PERTURBATIONS

Loss of structure by mechanical upset to the growth process can be caused by poorly working mechanisms, improper design or construction of the grower, or the effects of external shock or vibration on the equipment. Although this is occasionally observed, it is not considered to be a problem with the growth runs on the project. Proper maintenance of the equipment is the best way to avoid mechanical problems.

2.2 THERMAL PERTURBATIONS

Large thermal changes are likely to cause structure loss as they affect the profile of the crystal growth front and the growth rate. Suitable design and maintenance of the hot zone and control systems is sufficient to avoid structure loss by this mechanism. Thermal upset can also be caused by argon flow rate changes, cooling water flow or temperature changes, and, of course, a momentary power loss. Thermal problems are not believed to represent a problem for continuous CZ.

2.3.0 MELT CONTAMINATION

It is well established that a foreign particle in the silicon melt will cause at least the loss of O-D structure, and most likely will cause twinning or polycrystalline growth. Silicon monoxide and quartz particles cause loss of structure, the effect being easily observed by the operator. Silicon carbide particles behave in a similar way in EFG growth. The possibility exists, in CZ growth, that SiO, SiO_2, or SiC could enter the melt. Thus, all are possible causes of structure loss and should be investigated.

2.3.1 Silicon Monoxide (SiO) - This material is formed by vaporization from the melt and subsequent condensation as a submicron powder on cooler surfaces in the furnace. The oxygen that is required for its formation

comes from the crucible or from other sources such as air or water leaks, or impure argon. Although considerably more care must be taken on recharge runs to have a leak-tight system, it is believed that normal SiO deposition as a result of this reaction between liquid silicon and the crucible can be tolerated. Gas turbulence in the furnace must be minimized to prevent dislodging particles from the inner walls. To some extent, gas flow can be controlled in the furnace, directing the deposits to areas that are away from the growth region.

2.3.2 Silica (SiO_2) - Occasionally, silica particles are seen floating on the melt. These are probably due to chips from the crucible produced during the loading or melt-down. Silica is distinguishable from silicon monoxide because it does not evaporate, and the operator waits until the particle lodges against the wall of the crucible before starting a crystal.

Assuming proper care is exercised in loading the crucible and that the crucibles are high quality, then visible silica particles appearing on the melt initially should be very rare.

During long runs, however, microscopic particles of silica may be released from the crucible, which could float to the surface and destroy the crystal structure. Defects in the inner wall of the crucible such as unfused areas, pinholes, blisters or gas bubbles near the surface are potentially sources of particles.

The crucible is also subject to crystallization from the glassy form of SiO_2 to quartz by a process generally called devitrification. This occurs at high temperature and is accelerated (or catalyzed) by alkalis, alkaline earths, halides, and, to a lesser extent, a number of

other metallic ionic species. A small amount of devitrification is often observed on the inner surface of crucible walls with no apparent deleterious effect. If devitrification is severe, however, it seems plausible that quartz particles could be released into the melt. There is no direct evidence of this mechanism. However, the degree of crucible devitrification is not predictable and occasionally severe. More investigative work should be done.

2.3.3 Silicon Carbide (SiC) - Little is known about carbon control in CZ melts. Carbon contamination in CZ furnaces occurs, but the mechanism of its production is not clear, and the level of contamination is below saturation in semiconductor grade wafers.

Silicon carbide "scum" can be produced easily in the crystal grower by the use of improperly "baked out" graphite parts. Presumably, vaporized hydrocarbons from the graphitization process react with the melt surface.

In investigating this mechanism, consideration should be given primarily to the crucible as a source of oxygen. Oxygen is then transported to the graphite via direct contact or via SiO production and deposition on the graphite. The carbon monoxide produced would diffuse back to the melt surface.

If the production of CO is unavoidable, the control of gas flow in the furnace should minimize melt contamination by controlling both the transport of SiO and CO.

If there is a CO or CO_2 phase present in the furnace atmosphere due to oxygen from chamber leaks or from the crucible, then gaseous transport of carbon to the melt would appear to be feasible. In long

recharge runs, saturation could occur, leading to precipitation of SiC particles at the growth interface in the supercooled region.

3.0 CONCLUSION

The important structure loss mechanisms, in order of decreasing probability appear at present to be as follows:

(1) Silicon carbide precipitation from the melt.

(2) Release of particles from the crucible.

(3) Silicon monoxide particles falling in the melt.

(4) All other processes, e.g. mechanical, thermal, leaks, etc.

APPENDIX B

COMPARISON OF LUMP VS ROD RECHARGING

	ROD	LUMP
Recharge Time	Relatively slow - about 4 hours to recharge because rod must be heated slowly at first.	Faster than rod. 18-22 kg can be recharged to seed dip in 2 hours.
Contamination of Melt	None, except for handling rods.	Lumps contact metal feeding mechanism. To date, we have seen no contamination of hopper material in crystal impurity analysis.
Effect on Crucible	The biggest single disadvantage to the poly rod method. High heater temperatures necessary to keep the center of the melt hot enough to melt the poly rod tend to increase devitrification of the crucible, thus decreasing the crucible life.	Crucible temperature remains lower, prolonging the life of the crucible. Particles may stick to crucible wall.
Convenience	Rod must be notched to hold it.	Convenient. Hopper can remain in furnace during the entire run. Simply load hopper with bagged silicon.
Capacity of Recharge Mechanism	20 kg rods (18-20 kg recharge capacity).	18 kg per cycle. Unlimited number of cycles.
Miscellaneous	5-inch diameter poly rods are not crack free. The possibility always exists of a rod breaking apart and falling into the crucible. From experience, it appears that partial rods being used over increases the possibility of the rod breaking apart considerably. Therefore, it is felt that partial rods left over should not be reused for recharging.	No thermal cracking problems with the hopper.